UNIVERSITY OF BIRMINGHAM

REGULATION OF CD4$^+$ T CELL *Il10* TRANSCRIPTION AND TCR SIGNAL STRENGTH IN TOLERANCE AND CANCER

By

DAVID ARTHUR JOHN LECKY

A thesis submitted to the University of Birmingham for the degree of

DOCTOR OF PHILOSOPHY

Institute of Immunity and Immunotherapy

College of Medical and Dental Sciences

University of Birmingham

Edgbaston

B15 2TT

June 2024

ABSTRACT

T cells secrete IFNγ, which has a key role in activating macrophages and enhancing antigen presentation through increasing MHC class I and II expression. The inflammatory response is counteracted by negative regulators of the immune system, which limit damage to self by excessive immune responses, including via $FOXP3^+$ $CD4^+$ Tregs and Type 1 Regulatory $CD4^+$ T cells (Tr1 cells). These induce negative regulation through PD-1, CTLA-4 and TIGIT, for example, but also through expression of immunosuppressive cytokines such as interleukin-10.

Previously published data showed that immunisation with modified myelin basic protein ([4Y]-MBP) peptide to transgenic Tg4 T cell Receptor (TCR) mice that specifically and uniquely recognise MBP led to rapid induction of *Il10* transcription in a $CD4^+$ T cell subset. Here we sought to define and modulate *Il10*$^+$ T cell early development.

We found that a high dose of [4Y]-MBP peptide rapidly induced a Tr1-like phenotype in *Il10* expressing $CD4^+$ T cells, and that emergence of Tr1-like cells was preceded by *Ifng* transcription. Via APCs, anti-IFNγ strongly reduced $CD4^+$ *Il10* transcription, strong TCR signalling, and Tr1-like markers, an effect that was additive with anti-IL-27. In complementary experiments, we explored the role of IFNγ in modulating T cell *Il10* transcription during an anti-tumour immune response. Anti-IFNγ increased tumour burden in mice, reducing their survival, which was associated with reduced $CD4^+$ T cell *Il10* transcription and TCR signalling strength. Changes in *FoxP3*$^+$ Treg *Il10* transcription through IFNγ neutralisation correlated with reduced activation of tumour associated macrophages. These data reveal a regulatory feedback role for IFNγ and TCR signalling strength in modulating *Il10* transcription in two distinct subsets of regulatory T cells under a variety of immune environments.

ACKNOWLEDGEMENTS

Firstly, I would like to thank the Wellcome Trust for providing the funding for my programme and research. To the MIDAS Programme team – Steve Watson, Robin May, Graham Wallace, Eva-Marie Frickel, and Vikki Harrison – thank you for your continuous support, and especially for letting me go off-piste with my project choice.

To the Bending Group – David Bending, Lozan Sheriff, Alastair Copland, Tom Elliot, Emma Jennings, Lizzie Jinks, Sophie Rouvray, and Lorna George – without whom none of this would be done via endless team tissue preps and BMSU trips, thank you. David, thank you for taking me under your wing. I am very grateful for all the time and energy you have given me. And yes, that includes the COVID year when we were basically the only person the other saw outside our households.

An especially important thank you to the Flow Cytometry Services team, in particular Adriana Flores-Langarica, Guillaume Desanti and Ferdus Sheik, as well as the BMSU, without whom none of this work would have been done. I know that's said a lot, but it's true here.

To the Fellows Labs, your advice and feedback through supervisory meetings, fortnightly Flabbies and even the odd trip to the pub has been invaluable. Thank you.

I don't think any MIDAS Cohort has been as lucky as ours – Abbey Lightfoot, Lisa Scarfe, Poppy Nathan, Rachel Lamerton, and Sofia Hain. Lifelong friendships have been made. We truly are the *crème de la crème*.

To my friends who I have no professional attachment to – Gillian Mackie, Tristan Kennedy, Abbie Chadwick, Ruby Persaud, Beth Kennedy – thank you for sharing your times with me, both bad and good. You, and the others above and below, have helped

me through some difficulties for which I will be eternally grateful and will never forget your kindness and openness. Never has a completely *100%* soundproof booth been used to workshop so many excellent bits.

To my family – Jonathon, Yvonne, Mark, Christie, Andy, Karina, Rae, Martin & Isley – you are a constant source of joy and inspiration, and I love you all very much. Mum & Dad, there's finally a doctor in the family so can we please drop the subject now? Thanks. Without your encouragement to read and study, who knows where I'd be? I'm putting it down to a reading light you got me for Christmas circa 2002.

Deanna. You've helped me so much over the past four years and half the time you've not even been doing it on purpose, it's just you being yourself. You've been there thick and thin, putting up with a lot of waxing and waning but it could have been done without you. Thank you for your enduring love and support – we are an excellent team and I look forward to collaborating with you again in the future.

CONTENTS

LIST OF FIGURES

LIST OF TABLES

LIST OF ABBREVIATIONS

Table 0-1: Abbreviations

Abbreviation	Meaning
Ac1-9 [4Y]-MBP	Acetylated N-terminal region of MBP, with native lysine at position 4 substituted for tyrosine (ASQ**Y**RPSQR)
AHR	Aryl Hydrocarbon Receptor
APC	Antigen presenting cell
CDR	Complementarity-Determining Region
CFA	Complete Freud's Adjuvant
CTLA-4 / *Ctla4* / CD152	Cytotoxic T Lymphocyte Associated Protein 4
DEG	Differentially Expressed Genes
EAE	Experimental Autoimmune Encephalomyelitis
EDI	Escalating Dose Immunotherapy
FACS	Flow Assisted Cell Sorting
FOXP3 / *FoxP3*	Forkhead box P3
Timer	Fast Timer
GFP	Green Fluorescent Protein
GITR / CD357	Glucocorticoid-induced TNFR-related protein
hNGFR	Human Nerve Growth Factor Receptor
ICOS / CD278	Inducible Co-Stimulator of T cells
IFNγ / *Ifng*	Interferon gamma
IL-2Rα / CD25	Interleukin-2 Receptor alpha chain
IL-10 / *Il10*	Interleukin-10
IL-17A /*Il17a*	Interleukin-17A
IL-27	Interleukin-27
ITAM	Immunoreceptor Tyrosine-based Activation Motifs
LAG3 / CD223	Lymphocyte Activation Gene 3
Lck	Lymphocyte-specific protein tyrosine kinase
mAb	Monoclonal antibody
MBP	Myelin Basic Protein
MHC	Major Histocompatibility Complex
NFAT	Nuclear Factor of Activated T cells
NK	Natural Killer
Nr4a3 / Nor1	Nuclear Receptor 4a3 / Neuron-derived Orphan Receptor 1
OX40 / TNFRSF4 / CD134	Tumour Necrosis Factor Receptor Superfamily, member 4
PCA	Principal Component Analysis
PD-1	Programmed Cell Death protein 1
PVR / CD155	Poliovirus Receptor
SCH	Spinal Cord Homogenate
rmIFNγ	Recombinant Murine IFNγ
RNA	Ribonucleic Acid

RNA-seq	RNA Sequencing
TAM	Tumour Associated Macrophages
TCR	T cell Receptor
TIGIT	T cell Immunoreceptor with Ig and ITIM Domains
TIL	Tumour Infiltrating Lymphocyte
Tocky	**T**imer **o**f T **c**ell **k**inetics and activit**y**
Tr1	Type-1 Regulatory T cell
Treg	Regulatory T cell – specifically $FOXP3^{+}$ regulatory T cells
YFP	Yellow Fluorescent Protein

PUBLICATIONS CONTRIBUTED TO DURING THESIS

Antigen and checkpoint receptor engagement recalibrates T cell receptor signal strength, 2021. Thomas A.E. Elliot, Emma K. Jennings, David A.J. Lecky, Natasha Thawait, Adriana Flores-Langarica, Alastair Copland, Kendle M. Maslowski, David C. Wraith, and David Bending, *Immunity*, Vol. 54 Issue 11 Pages 2481-2496 e6 DOI: 10.1016/j.immuni.2021.08.020

Application of dual Nr4a1-GFP Nr4a3-Tocky reporter mice to study T cell receptor signalling by flow cytometry, 2021. Emma K. Jennings, David A.J. Lecky, Masahiro Ono, and David Bending, *Star Protocol,* Vol. 2 Issue 1 Pages 100284 DOI: 10.1016/j.xpro.2020.100284

Long-term antibiotic exposure promotes mortality after systemic fungal infection by driving lymphocyte dysfunction and systemic escape of commensal bacteria, 2022. Rebecca A. Drummond, Jigar V. Desai, Emily E. Ricotta, Muthulekha Swamydas, Clay Deming, Sean Conlan, Mariam Quinones, Veronika Matei-Rascu, Lozan Sherif, David Lecky, Chyi-Chia R. Lee, Nathaniel M. Green, Nicholas Collins, Adrian M. Zelazny, D Rebecca Prevots, David Bending, David Withers, Yasmine Belkaid, Julia A. Segre, and Michail S. Lionakis, *Cell Host Microbe*, Vol. 30 Issue 7 Pages 1020-1033 e6 DOI: 10.1016/j.chom.2022.04.013

Nur77-Tempo mice reveal T cell steady state antigen recognition, 2022. Thomas A.E. Elliot, Emma K. Jennings, David A.J. Lecky, Sophie Rouvray, Gillian M. Mackie, Lisa Scarfe, Lozan Sheriff, Masahiro Ono, Kendle M. Maslowski, and David Bending, *Discovery Immunology*, Vol. 1 Issue 1 Pages 001-009 DOI: 10.1093/discim/kyac009

T-cell response to checkpoint blockade immunotherapies: from fundamental mechanisms to treatment signatures, 2023. Thomas A.E. Elliot, David A.J. Lecky, and David Bending, *Essays in Biochemistry*, Vol. 67 Issue 6 Pages 967-977 DOI: 10.1042/EBC20220247

***Salmonella* cancer therapy metabolically disrupts tumours at the collateral cost of T cell immunity**, 2023. Alastair Copland, Gillian M. Mackie, Lisa Scarfe, David A.J. Lecky, Nancy Gudgeon, Riahne McQuade, Masahiro Ono, Manja Barthel, Wolf-Dietrich Hardt, Hiroshi Ohno, Sarah Dimeloe, David Bending, and Kendle M. Maslowski, *bioRxiv*, preprint DOI: 10.1101/2023.01.12.523780

Lag3 and PD-L1 govern T cell receptor signal duration in adaptively tolerised CD4^{+} T cells, 2024. Lozan Sheriff, Alastair Copland, David A.J. Lecky, Reygn Done, Lorna S. George, Emma K. Jennings, Sophie Rouvray, Thomas A.E. Elliot, Elizabeth S. Jinks, Lalit Pallan, and David Bending, *bioRxiv*, preprint DOI: 10.1101/2024.06.06.59776

Interferon-γ and IL-27 positively regulate type 1 regulatory T-cell development during adaptive tolerance, 2024. David A.J. Lecky, Lozan Sheriff, Sophie T. Rouvray, Lorna S. George, Rebecca A. Drummond, David C. Wraith, David Bending, *bioRxiv*, preprint DOI: 10.1101/2024.06.21.598825

Chapter 1 : Introduction

1.1 T cell Differentiation

Jacques Miller first described the necessity of the thymus in skin graft rejection in 1961 [1], demonstrating how immediate removal of a neonatal murine thymus leads to tolerance of allogenic skin grafts compared to intact mice, but with reduced white cell counts and a deficiency in plasma cells and germinal centres. This was one of the first descriptions of thymus function, showing that it was not, as was widely believed at the time, a vestigial organ. In the 60 years since, much has been discovered about the thymus and T cells' ever increasing and diversifying functions.

1.1.1 Thymic Development

Haematopoietic stem cells in the bone marrow differentiate into lymphoid progenitor cells that migrate to the thymus where they undergo clearly defined maturation stages [2]. In the thymic cortex, developing thymocytes are double negative, lacking both CD8 and CD4 expression [3]. These surface glycoproteins co-receptors denote their broader function and dictate the ability of their T cell receptor (TCR) complex to bind a particular peptide presenting ligand once it matures – major histocompatibility complex (MHC) class I or II [4]. Instead of CD8 or CD4, thymocytes are initially defined as $CD44^+$ $CD25^-$, before gaining CD25 (the IL-2 receptor alpha chain) expression in the first stage of thymic development [5]. Then, they lose CD44 expression and the TCRβ chain is rearranged (beta-selection) [6]. Thymocytes that have successfully rearranged their β chain locus pair with a pre-TCRα chain [7]. This pre-TCR complexes with CD3, and CD25 expression is lost. Cells which do not successfully rearrange their β chain locus die by apoptosis. The pre-TCR : CD3 complex leads to survival, proliferation, cessation of TCRβ chain loci rearrangement, and joint CD4 and CD8 expression to become double positive (DP) T cells [8].

DP T cells then undergo TCRα rearrangement to produce a complete αβ TCR, whereafter they undergo positive selection in the thymic cortex, interacting with MHC classes I or II bearing self-antigen [9]. DP T cells that engage with self-antigen presented by MHC on cortical thymic epithelial cells (cTECs) survive if the interaction is of appropriate affinity, but those that form weaker interactions die by apoptosis.

Following this stage, DP T cells migrate to the thymic medulla where they undergo negative selection [10]. Professional antigen presenting cells (APCs) such as dendritic cells and medullary thymic epithelial cells (mTECs) express self-antigen bound MHC. If a DP T cell interacts too strongly with the presented self-antigen, it apoptoses [11]. If a DP T cell survives, either the CD4 or CD8 coreceptor is downregulated, producing single positive CD8 or CD4 T cells that enter the periphery. These circulate in the periphery as naïve T cells between secondary lymphoid tissues including the lymph nodes, Peyer's patches, tonsils, and the spleen, waiting until they encounter their cognate antigen. Naïve T cells express CD62L (L-selectin) and CCR7, but lack CD25, CD44, and CD69. However, naïve T cells are not a homogenous population – they still differ in phenotype, function, behaviour, and differentiation outcome [12]. Not every naïve T cell, for example, can become a regulatory T cell (Treg) following activation.

T cells reactive towards ubiquitously expressed antigens are likely to be deleted, but those reactive with tissue-restricted antigens are the primary source of Treg generation [13, 14]. During negative selection, self-reactive thymocytes are either deleted or differentiated into Tregs [15], and $CD4^+$ $CD8^-$ progenitor Tregs arise. Thymic Treg development is thought to be a two-step process; firstly, strong TCR stimulation in developing $CD4^+$ $CD8^-$ thymocytes causing upregulation of IL-2, GITR, OX40 and TNFR2, followed by cytokine dependent conversion of progenitor Tregs to mature

Tregs - cytokines such as IL-2 and IL-15, that share the cytokine receptor common gamma subunit, can induce FoxP3 expression in this population. [16, 17] mTECs mediate negative selection of autoreactive thymocytes or their differentiation to FoxP3$^+$ CD25$^+$ Tregs [18-20]. Peptide presentation by mTECs differs between perinatal and adult mice, leading to the generation of a distinct, age-dependent TCR repertoire on Tregs [21]. Tregs recognise high affinity self-antigens via their TCR, leading to increasing signal intensity [22] and receive stronger TCR signals than conventional T (Tconv) cells during thymic development [23]. Stronger TCR signals are associated with Treg specific induction of epigenetic changes and gene expression patterns [24].

Tissue specific antigens are induced in mTECs by Autoimmune Regulator (Aire), a transcription factor and subsequently presented to developing thymocytes at low frequencies. Without Aire, T cell clones that would differentiate into Tregs instead differentiate into Tconv cells [25]. These Tconv go on to induce autoimmune diseases. Bone marrow-derived APCs also participate in thymic development of Tregs from certain TCR clones in the medulla, in an Aire-independent mechanism [26]

1.1.2 T cell Activation

At sites of harm such as infection or injury, specialist APCs, such as dendritic cells (DCs), recognise inflammatory signals like pathogen-associated molecular patterns (PAMPs) including lipopolysaccharide and peptidoglycan via their Toll-like receptors (TLRs). Immature DCs that engulf, digest, and process recognised pathogens intracellularly then present derived antigens on their MHC and migrate to secondary lymphoid tissues as mature DCs, where they interact with naïve T cells [27]. Although B cells and macrophages are also APCs, DCs constitutively express MHC class II

(MHCII) [28]. DCs can also take up extracellular material in a receptor-independent manner.

For T cell activation to occur, there are three major stages: 1) activation, 2) survival, and 3) differentiation (fig. 1-1) [29]. The activation signal occurs when an appropriate and specific cognate antigen bound to MHC class I (expressed ubiquitously) or II binds the TCR complex, and initiates TCR signalling. Peptide bearing MHC (pMHC) I specifically binds CD8-TCR complexes, and pMHC II binds CD4-TCR. Co-stimulation signals include CD80 (B7-1) or CD86 (B7-2) on DCs binding to CD28 on T cells, or ICOS ligand (ICOS-L) on B cells to ICOS on T cells. Unlike CD28, ICOS is induced by T cell activation, so is not interchangeable with CD28 for naïve T cell activation but can serve as signal 2 for reactivation [30, 31]. $CD4^+$ T cells require professional APCs for the first and second signal. The survival signal modifies the activation signal, allowing activation to continue. Without co-stimulation (often referred to as signal 2), T cells become anergic [32]. The induction of anergy is a mechanism to limit inappropriate responses to self-antigen, and once a T cell becomes anergic, it is unlikely to activate, even if both signals are given. Finally, the differentiation signal comes from cytokines and other co-stimulatory and co-inhibitory receptor signals from the antigen presenting cell or other cells present in the environment, wherein the proliferating T cell clones have their function/subset directed partially by the combination of cytokines they encounter during activation. For examples, autocrine or paracrine sources of IL-2 binds CD25, inducing proliferation [33, 34]. T cells are no longer considered naïve when they have been exposed to an antigen they recognise and several differentiated T cell subsets do not require CD28 co-stimulation to reactivate, they may also use ICOS, for example.

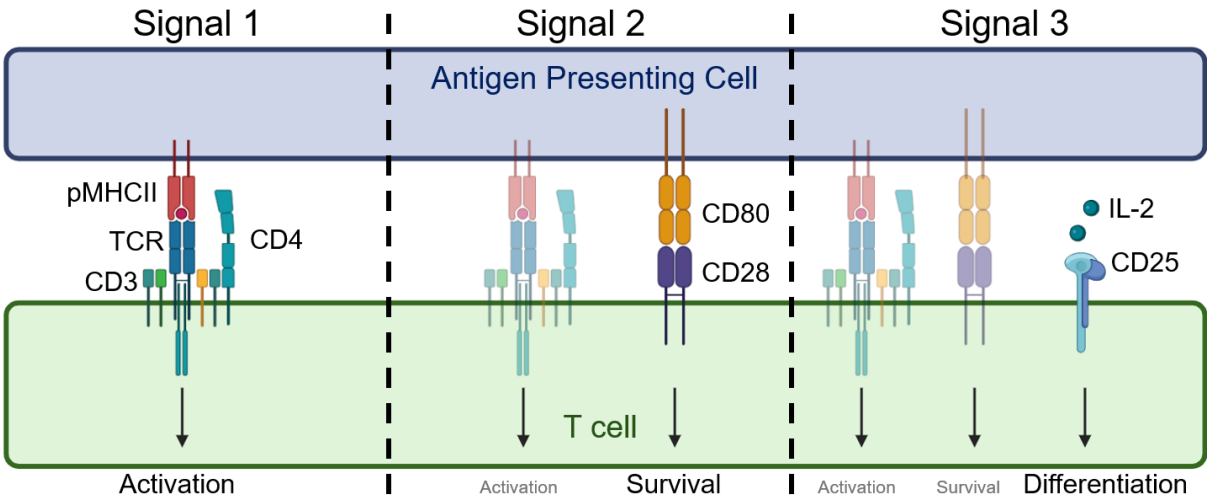

Figure 1-1: T cell activation signals.
Naïve T cells require three signals to activate: activation, survival and differentiation. Firstly, peptide-bearing MHC class II (pMHCII) forms a complex with the specific TCR for that peptide sequence. Downstream signalling is initiated through TCR complex subunits CD4 and CD3. Secondly, a survival signal is received by the T cell from the antigen presenting cell (APC) – CD80 (B7-1) on an APC is presented to CD28 on a T cell. The second signal modifies the first, allowing activation to continue or the T cell becomes anergic. Thirdly, the differentiation signal from cytokines released by the T cell, APC and/or other nearby cells. In the example above, IL-2 binds CD25, which induces proliferation of the newly activated T cells.

1.1.3 T cell Subsets and Functions

Following activation, T cells undergo clonal expansion and differentiation into specialist subsets. The two major T cell subsets are $CD4^+$ and $CD8^+$ T cells, often labelled helper, and cytotoxic T cells respectively. Whilst $CD4^+$ and $CD8^+$ T cells have differing effector functions, both have a memory subset that can be further subdivided into central memory (TCM – $CD45RO^+$ $CCR7^+$ $CD62L^+$ $CD44^{Int/Hi}$) found in the lymph nodes, effector memory (TEM – $CD45RO^+$ $CCR7^-$ $CD62L^-$ $CD44^{Int/Hi}$) found in circulation, and tissue resident memory (TRM – $CD69^+$ $CD49a^+$ $CD103^+$).

1.1.3.1 $CD8^+$ Cytotoxic T cells

$CD8^+$ T cells are key in defending against pathogens, such as viruses and bacteria, and in tumour surveillance. Once activated, $CD8^+$ T cells utilise three methods to kill

infected or malignant cells. The first method is the release of Tumour Necrosis Factor alpha (TNFα) and Interferon gamma (IFNγ) upon antigen recognition, which enhance both innate and adaptive immunity by promoting proliferation, inflammation, and apoptosis [35, 36]. Secondly, they release cytotoxic granules such as perforin, granzymes and granulysin, directly attacking target cells [37]. Perforin forms a pore in a target cell membrane, allowing granzymes to enter and induce a caspase cascade, causing it to release its contents (apoptosis). Thirdly, $CD8^+$ T cells induce destruction of infected cells via Fas : FasL binding. Again, this utilises a caspase cascade by $CD8^+$ T cell bound FasL initiating Fas trimerization and inducing signalling [38].

1.1.3.2 $CD4^+$ Helper T cell Effector Subsets

As implied, $CD4^+$ T cells help other immune cells by releasing cytokines that induce differing functions. B cell activation, for example, requires $CD4^+$ T cells for activation, differentiation, and germinal centre formation. As well as several smaller subsets, $CD4^+$ T cells differentiate into two major effector subsets: Th1 and Th2. Th1 cells are induced by IFNγ and IL-12 exposure, characterised by expression of the transcription factor Tbet, and further production of IFNγ. In producing an inflammatory response, Th1 cells are key in defending against intracellular bacteria, viruses, and cancer by increasing macrophage killing efficacy and $CD8^+$ T cell proliferation.

Th2 cells are induced by IL-4 and IL-33 and are characterised by the transcription factor GATA3 and secrete IL-10 (interleukin-10), IL-5, and IL-4. Th2 cells stimulate the humoral immune response, inducing antibody class switching and increasing antibody production, thereby promoting neutralisation of recognised pathogenic factors. Primarily, they mediate anti-parasitic and allergy responses. Th17 cells are a smaller subset, induced by Transforming Growth Factor β (TGFβ), IL-6 and IL-23, expressing

the RORγt transcription factor, and secreting IL-17 (its namesake) and IL-6. Th17 cells are present at mucosal barriers and defend against gut-derived pathogens and are capable of transdifferentiating into Th1 cells or peripheral Tregs [39, 40]. T follicular helper (Tfh) cells are defined by transcription factor Bcl6 expression, secretion of IL-21 and IL-4, and are induced by IL-6 and IL-21. They assist B cells activation and stimulate production of antibodies by providing secondary signals following B cell pMHCII : TCR complex interaction.

1.2 T cell Receptor

The TCR is a protein complex exclusively found on the surface of T cells that recognises antigen fragments bound to MHC. Any given T cell express many TCRs on their cell surface, all recognising the same antigen, and post-activation there may be many clones all recognising the same antigen, but different subsets will have differing functions upon antigen recognition.

1.2.1 T cell Receptor Complex Structure & Expression

The TCR “proper” is a heterodimer, most often composed of one alpha (α) and one beta (β) chain making up 95 % of TCRs. Around 5 % are instead composed of one gamma (γ) and a delta (δ) chain. The two TCR chains are linked by disulphide bonds and anchored in the T cell membrane in complex with invariant CD3 chains (one CD3γ, one CD3δ and two CD3ε) along with the CD3ζ chain (CD247). TCRα and TCRβ chains have both variable and constant domains. The variable domains bind to the peptide-MHC complex whereas the constant domains are proximal to the cell membrane.

T cell receptor α, β, γ and δ chains recombine their chains to produce a desired whole TCR that can bind a unique antigen. Much like B cell receptors or antibodies, V(D)J

recombination, which occurs in the thymus for T cells, is fundamentally important to generating diverse antigen receptor repertoires (fig. 1-2). Crucially, the major distinction between TCRs and BCRs is that the TCR binds peptide fragments processed on MHC, whereas the BCR recognises antigen in its native conformation. TCR chains contain a variable (V) terminal region, dictated by V(D)J recombination, and a constant (C) region. Recombination activating genes (RAGs)-1 and -2 form a RAG complex, which binds to recombination signal sequences (RSS, which direct recombination) and initiate V(D)J recombination [41]. TCRα chains contain V and J gene segments, whereas the β chain contains D segments, as well as V and J. D-to-J (diversity to joining) first occurs in the TCRβ chain, where the $D_\beta 1$ or $D_\beta 2$ gene segment is joined to one of multiple $J_\beta 1$ or $J_\beta 2$ segments respectively. This is followed by V_β-to-$D_\beta J_\beta$ rearrangement. All the gene segments between those in the newly formed complex are subsequently deleted, and the primary $V_\beta D_\beta J_\beta$ incorporates the constant β gene region. Any intervening sequence is spliced out, and translation of the full TCRβ can occur. TCRα chain follows, except lacking a D segment as part of their recombination.

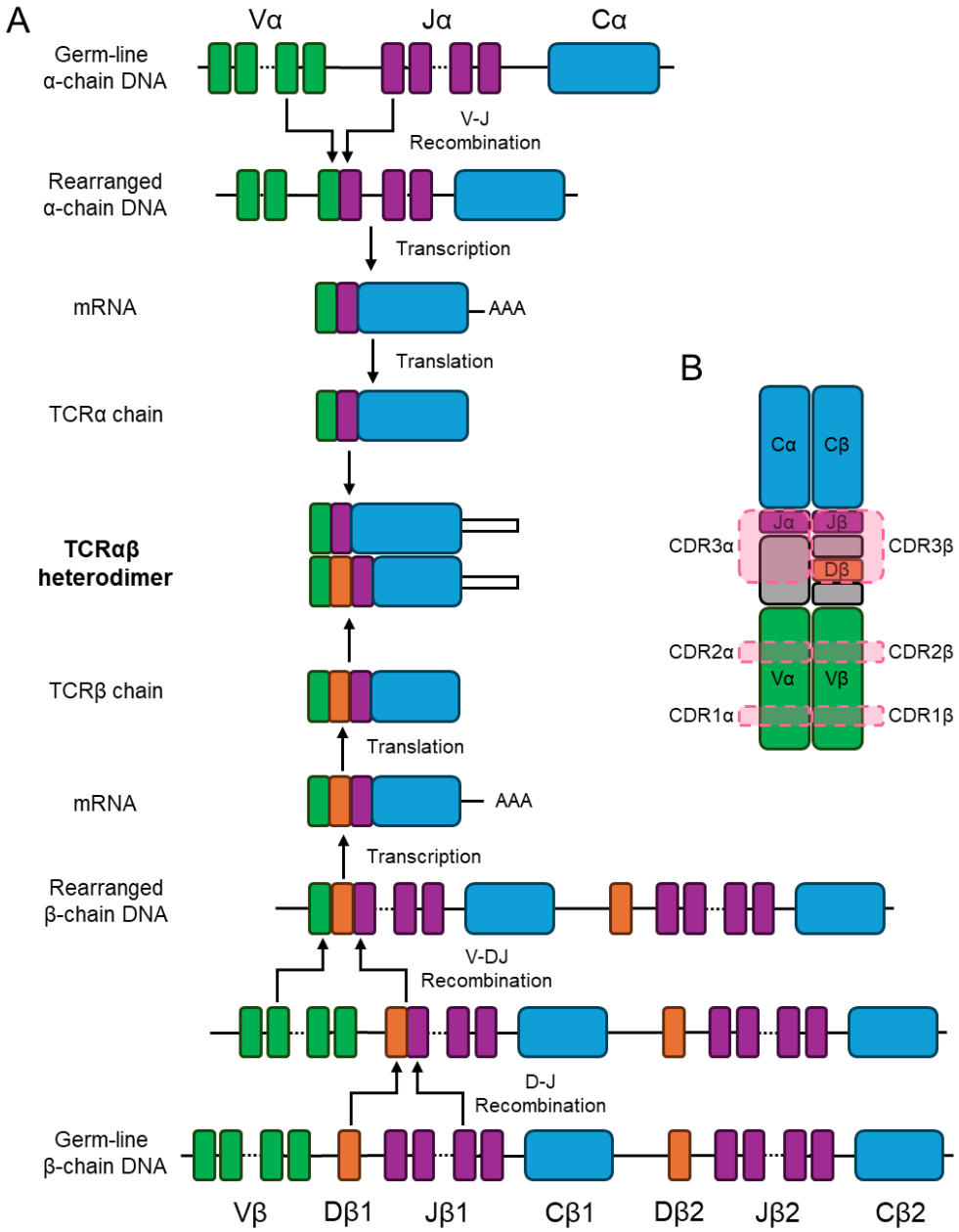

Figure 1-2: V(D)J Recombination of T cell Receptor αβ chains.
TCRs are composed of two chains, and a diverse and robust repertoire depends on the adaptability of the chain sequences through V (Variability) D (Diversity) J (Joining) recombination by RAG enzyme complexes. **(A)** β chains undergo an initial Dβ-Jβ recombination step from either β1 or β2 gene sets. Then, both αβ chains undergo V-(D)J recombination and combine with a constant (C) region, before transcription and translation, where the chains homodimerise as a cell surface protein. **(B)** Complementarity Determining Regions (CDRs) are defined completely by the variability regions for CDR1 and CDR2 for both αβ chains, and by J chains with random addition and deletion of polynucleotides between randomly selected genes for CDR3 for α chain. The β chain exclusive D region contributes to CDR3.

1.2.2 Peptide Binding

Variable domains have complementarity-determining regions (CDRs) that are hypervariable with separate functions in the TCR : pMHC binding. CDR1 interacts with peptide C-terminal and N-terminal in the β and α chain respectively, CDR2 recognises MHC, and CDR3, the most variable, contains the principal peptide binding residues. The intensity of TCR signalling is inherently related to the T cell activation status and determined by other factors such as phenotype and co-stimulation. For example, Tregs with TCRs displaying similar specificity to the same antigen also have similar transcription profiles when under differing signal intensities [42].

1.2.3 Signalling

TCR ligation is key to canonical signal transduction and activation in T cells. An antigen is presented on MHC I or II, binding the TCR and the coreceptors CD8 or CD4 respectively and initiating downstream signalling (CD4 and MHCII in the example shown in fig. 1-3). For a potent response to an antigen, it must be presented on MHC. Additional coreceptors like CD28 and ICOS are also bound and signal simultaneously to ensure T cell activation and avoid anergy.

LCK (lymphocyte-specific protein tyrosine kinase) associates with CD8 and CD4 coreceptors intracellularly. It phosphorylates the CD3 coreceptor complex (CD3γ/δ/ε) and ζ-chains of the TCR. This phosphorylation recruits and activates Zeta-chain-associated protein kinase 70 (Zap70). pZap70 phosphorylates Linker of Activated T cells (LAT), leading to recruitment of phospholipase C-γ1 (PLC-γ1) and other Src homology domain containing proteins including VAV1, GRB2, GADS (GRAP2), and SLP76 (LCP2). ITK, also activated by LCK, also activates PLCγ1. VAV1 activates

Mitogen-activated protein kinases (MAPK) signalling leading to transcription factor Jun and Fos activation and actin polymerisation.

Activated PLC-γ1 hydrolyses phosphatidylinositol 4,5-bisphosphate (PIP_2) to inositol 1,4,5-triphosphate (IP_3) and diacylglycerol (DAG). IP_3 initiates release of Ca^{2+} from intracellular stores such as the endoplasmic reticulum via IP_3 Receptor (IP_3R) binding, as DAG activates Protein Kinase C delta (PKCθ) and Ras guanyl nucleotide-releasing protein (RasGRP). Ca^{2+} leads to dephosphorylation of phosphorylated Nuclear Factor of Activated T cells (pNFAT), allowing transcription factor NFAT to enter the nucleus and initiate gene transcription, whilst RasGRP activates Extracellular signal-regulated kinase (ERK) signalling and activation of the Activator Protein (AP-1) family of transcription factors.

In addition to downstream TCR complex signalling, CD80 or CD86 presented by an APC binds CD28 on the T cell surface. The CD28 intracellular domain recruits Phosphoinositide-3 kinases (PI3Ks), which phosphorylate PIP_2 to phosphatidylinositol 3,4,5-trisphosphate (PIP_3), activating 3-phosphoinositide-dependent protein kinase 1 (PDK1) that leads to downstream activation of PKCθ and the Akt (Protein kinase B/PKB)-mTOR (mammalian Target of Rapamycin) pathway via Akt phosphorylation. PKCθ signalling, initiated by both TCR and co-stimulation, leads to NF-κB (Nuclear Factor kappa-light-chain-enhancer of Activated B cells) signalling via the IkB kinase (IKK) pathway. Akt-mTOR signalling leads to survival via a reduction in apoptosis and permitting proliferation through increased ribosome biogenesis and protein translation.

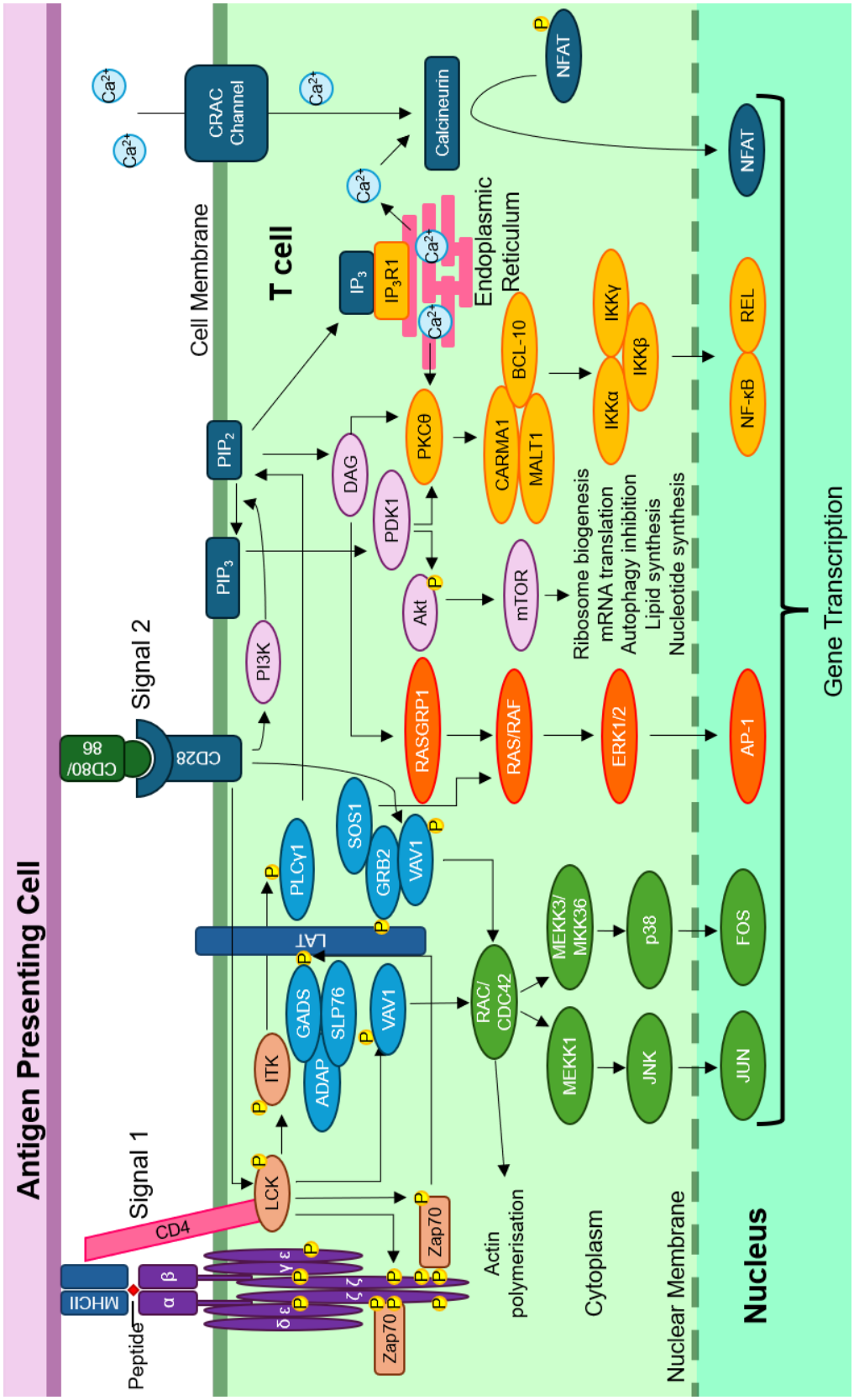

Figure 1-3: T cell Receptor and CD28 Co-stimulation Signalling Pathways in a CD4⁺ T cell. Adapted from [43, 44]

1.3 Regulatory T cells

Largely, the non-exhaustive list of effector subsets in section 1.1.3 described above activate target cells to generate a response against a pathogen, or directly attack a target. Regulatory T cells, however, suppress immune responses as opposed to activating them. They suppress activation, proliferation, and T cell cytokine production, and in doing so tolerise self [45], food [46] and commensal [47] antigens, thereby limiting excessive immune responses, regulating placental immunity [48], maintaining homeostasis and mediating regeneration of tissues [49-52]. Whilst thymic or natural Tregs (tTregs) are not derived from naïve T cells, but directly differentiated in the thymus, a select few naïve $CD4^+$ T cells in the periphery are also capable of becoming regulatory. tTregs and adaptive or pTregs both express master gene regulating transcription factor FOXP3 [53-55] and produce TGFβ and IL-10 [56-58]. Naïve $CD4^+$ T cells may also become peripherally induced type 1 regulatory T cells, which are $FOXP3^-$, instead expressing cMaf, and secreting IL-10.

1.3.1 Treg Phenotype

Natural, thymus-derived Tregs are defined by lineage-specific and constitutive expression of FoxP3 and CD25 (IL2Rα), as well as CTLA-4. CD25 and its ligand IL-2 is essential for differentiation and proliferation of Tregs [59]; systemic autoimmunity in IL2Rα or IL2Rβ deficient mice is rescued by adoptive transfer of $CD4^+$ $CD25^+$ cells from wild-type mice [60]. Mice deficient for IL-2 expression also have reduced $CD4^+$ $CD25^+$ T cells [61]. pTregs are found in barrier tissues, and are generated when naïve T cells are activated in the presence of TGFβ and IL-2, without pro-inflammatory IL-6 [62]. Tregs that share specificity but differ in TCR affinity display different suppressive mechanisms: high affinity receptors express TCR-dependent mediators i.e. IL-10,

GITR, TIGIT and CTLA-4, whereas low affinity TCRs express more Ebi3 (IL-27B subunit), responsible for IL-27 and IL-35 mediated suppression [63-65].

1.3.2 Treg Immunosuppressive Function

Functional heterogeneity of Tregs reflects the broad swath of suppressive mechanisms they use to control various immune responses. These include contact, humoral, antigen-specific, or non-specific. Most immune cells are regulated by Treg immunosuppressive mechanisms, such as B cells, macrophages and dendritic cells [66]. Functionally, pTregs and tTregs appear to be equivalent, but have distinct TCR repertoires. tTregs are mostly self-recognising, whilst pTregs are biased to recognising non-self-antigens with high affinity [63].

Antigen-specific suppression is caused by direct Treg-APC interaction, due to recognition of the specific antigen bound to pMHCII by the Treg TCR. These mechanisms interfere with antigen presentation, induce anergy, or trigger pTreg induction. Mechanisms include inducing a tolerogenic APC or rendering it unable to present specific antigen. An example of this suppression includes DCs expressing CD80/86 co-stimulatory receptors binding immune checkpoint CTLA-4 in Tregs, removing CD80/86 by endocytosis [67]. CTLA-4 can mediate an increase in indoleamine-2,3-dioxygenase (IDO) expression in DCs, lowering tryptophan concentrations below what is necessary for effector T cells to proliferate [68].

CD39 and CD73 expression on Tregs degrade ATP to adenosine. This antigen-non-specific mechanism increases adenosine concentrations in the microenvironment, inhibiting antigen presentation and suppressing the proliferation activated effector T cells [69]. Treg production of TGFβ, IL-10 and IL-35 is another antigen independent

method of immunosuppression, and their collective function is very broad. This includes suppression of T and B cell activation and proliferation and induces pTreg and Breg (regulatory B cell) formation [70-73]. TGFβ and IL-10 inhibit antigenic presentation to stimulate tolerogenic DC generation, in turn enabling pTreg induction [74-78].

Further methods of Treg suppression include impairing Ca^{2+}-dependent NFAT and NF-κB transcription factor function in effector T cells via Ca^{2+} supply disruption [73, 79], perforin-dependent cytotoxicity [80], and reduction of environmental cytokines. These include IL-2 [81] and Treg TNF-related apoptosis-inducing ligand (TRAIL) expression, which interacts with Death receptor 5 (DR5) to induce apoptosis via caspase-8 in effector T cells [82, 83].

Treg suppression of effector T cells have been suggested to target specific effectors associated with transcription factor expression. Tbet expression in Tregs in associated with TIGIT expression, which may increase IL-10 and decrease IL-12 when bound to its cognate ligand, CD155, on dendritic cells, thus suppressing Tbet expressing Th1 cells [84, 85]. IFNγ activates STAT1, inducing Tbet expression in Tregs and subsequently CXCR3, which causes Tregs to migrate to Th1-mediated inflammation sites [86]. Tbet and TIGIT expressing Tregs have demonstrated selective inhibition of Th1 and Th17 mediated immune responses [87, 88]. Tbet expression is lower in Tregs than Th1 cells, and high FoxP3 expression is TCR-dependent: FoxP3 suppresses Tbet dependent proinflammatory gene expression, and prevents Tregs from transforming into Th1 cells [89]. TCR and IFNγ, therefore, determine functional maturation and homeostasis of Tregs in the Th1-mediated immune response. STAT3 expression,

related to Th17 responses, enables expression of *Il10, Ebi3, Gzmb,* and *Prf1* in mice [90].

1.3.3 Treg Homeostatic Function

The roles of Tregs in homeostasis depend on their maturity and tissue distribution. Lymph node produced IL-7, mediated by JAK3/STAT5 and PI3K/Akt signalling pathways, is vital for tTregs in circulation between secondary lymphoid organs [91], enabling survival and proliferation through Bcl2 and Ki67 expression. In humans, thymopoiesis has a low impact on tTreg population maintenance, confirmed by the minimal effects of the thymus shrinking with age and early thymectomy of tTreg populations in adults, despite loss of thymic output and tTreg decrease post-thymectomy [92]. Compensatory proliferation of pTregs maintains the tTreg population. Memory Tregs are long-lived and emerge after preventing or resolving primary inflammation. Their suppressive effects are even stronger when induced by secondary contact with a recognised antigen [93]. Differentiation of memory Tregs required IL-2, whereas maintenance required only IL-7, and appropriately these cells are $CD25^+$ $CD127^+$ (IL-2R and IL-7R respectively) [94]. They also express anti-apoptotic factors Bcl2 and Mcl1, whilst non-memory i.e. effector Tregs actively proliferate and apoptose comparatively easily because of low Bcl2 and Mcl1 expression [95]. Effector Treg homeostasis relies on strong TCR signalling to enable expression of effector specific genes [96].

The mechanisms of Tregs involvement in tissue-specific repair of muscle, bone, lung, skin and central nervous system (CNS) vary from tissue to tissue [97]. The combined DC-mediated effects of Treg tonic TCR signalling via recognising self-pMHCII [98, 99], co-stimulatory signalling by CD28 : CD80/86 [100, 101] and humoral factors such as

IL-2 [102, 103] are observed in T zone niches of secondary lymphoid organs. Treg distribution in niches is tissue-specific, enabled by affinity to the matching peptide [104, 105]. Tregs can acquire chemotactic receptors upon maturation [106] and upon migrating to lymph nodes, where autoreactive T cells are primed, they seem to mediate induction and suppression of tissue-specific responses [107].

Highly suppressive Tregs in secondary lymphoid organs are localised in separate clusters and are surrounded by autoreactive lymphocytes, mostly activated $CD4^+$ T cells expressing high amounts of IL-2 [108]. The cluster centre is occupied by mature DCs, expressing high amounts of MHCII and co-stimulatory markers. Tregs closer to the cluster centre express more STAT5, CTLA-4 and CD73. Within the cluster, effector T cells trigger Tregs to compensate, leading to loss of TCR signalling which deforms the cluster, suppressing Treg function and leading to excessive effector activation. Maintenance of self-tolerance is an active process using subtle regulatory mechanisms in the periphery. Antigen specific DC population depletion causes a terminal reduction in specific Treg clones [109, 110], as does disruption of CD28 : CD80/86 interactions [111-113].

1.3.4 Type 1 Regulatory T Cells

Whilst ($FoxP3^+$) Tregs mediate self-tolerance, Tr1 cells contribute to peripheral tolerance, and self-tolerance to a lesser proportion. $FoxP3^-$ Tr1 cells are induced peripherally and limit response to antigens, both non-self and self. Tr1 cells were first discovered when a severe combined immunodeficiency (SCID) patient received a mismatched allogenic foetal liver and thymus transplant but subsequently developed stable mixed chimerism [114, 115]. The patient showed high levels of IL-10 in their serum and T cell clones produced substantial IL-10 and very little IL-2 rapidly following

TCR stimulation. Tr1 cells are present in the circulation and reside in healthy colon and tonsils [116-119]. A population has also been identified in human decidual tissue, suggesting a role for Tr1 cells in foetal-maternal tolerance [120].

Tr1 produce high IL-10 and TGFβ, variable IFNγ (similar to naïve T cells) and little to no IL-2 or IL-4 [121]. They require IL-10 to function [122]. The Tr1 cell cytokine profile is distinct from Th1 and Th2 cells and as such, Tr1 cells proliferate poorly when exposed to recognised antigen, but this is rescued by IL-2, and they proliferate in response to IL-15 also [123]. Tr1 IL-10 secretion directly limits T cell responses, and indirectly by limiting antigen presentation on APCs [124-127]. Through their cytotoxic ability, Tr1 cells potentially contribute to tolerance via APC killing [128-131], and use PD-1/PD-L1 and CTLA-4 to suppress immune responses [132], in addition to regulation via B cell antibody production [119, 133].

IL-10$^+$ CTLA-4$^+$ Th2 cells can arise in mice, but are distinct from Tr1 cells as the Th2 cells express large amounts of IL-4, IL-5 and IL-13 [134]. IL-10 and IFNγ co-expression has been used to identify Tr1, Tr1-like cells, and IL-10$^+$ Th1 cells, making it less than ideal for specifically phenotyping Tr1 cells. IL-10$^+$ Th1 cells highly express *Tbx21* and *Egr2* but low *Gata3* [135], but Tr1 cells from healthy donors expressed elevated *GATA3* expression compared to CD4$^+$ memory T cells with no change in *TBX21* or *EGR2* [136]. Transcriptomic analyses performed on Tr1 clones revealed that CD49b and LAG3 (an MHCII-binding inhibitory surface receptor with greater affinity than CD4 [137]) were uniquely co-expressed by Tr1 cells, and that they were the major subset of human and murine CD4$^+$ T cell IL-10 producers, compared to single positive LAG3 cells *in vitro* [116]. Human intestinal Tr1 cells co-express PD-1 and CCR5, and all murine Tr1 cells

express LAG3, CD49b, PD-1 and CCR5, and can reliably be used to identify the subset [117].

Other markers can also assist in identifying Tr1 cells, such as CD226 [130], TIM-3, TIGIT and CTLA-4 [118]. CD226, TIM-3 and TIGIT have roles in Tr1 mediated suppression, consistent with FoxP3$^+$ Tregs which have increased suppressive ability when expressing LAG3 or TIM-3 [138, 139]. However, many of these markers can be induced transiently, with cells temporarily adopting a suppressive state [140]. Transcription factors cMaf and BLIMP1 have been demonstrated as essential for Tr1 cell differentiation and function in mice [141, 142], however a lineage-defining transcription factor eludes the field [143].

Tr1 cells are peripherally induced and antigen-experienced [144], and generation *in vivo* occurs through various mechanisms. These involve antigen presentation (both self and persistent foreign) with signalling from APC [128, 144-148]. IL10-producing APCs may promote Tr1 development; during viral infection; IL-10 expressing monocytes have inducted protective Tr1-like cells [149]. Other IL-10$^+$ APCs like dendritic cells (DC-10s) [150], scavenger asialoglycoprotein receptor (ASGPR) expressing APCs [147] and macrophages [151] promote Tr1 cell differentiation *in vivo*. They can also differentiate based on non-classical co-stimulation such as CD2, CD55, ICOS or PD-L1 [152-155], but the extent is uncertain. CD46 co-stimulation has been described as inducing Tr1-like cells, however, these may be IL-10$^+$ Th1 cells [156-158].

Tr1 cell function induced via PD-L1 co-stimulation requires IFNγ [159]. IL-27 and TGFβ regulate IL-10 and promotes Tr1 cell differentiation in mice [160, 161]. IL-27 has been reported to have only a modest effect on human CD4$^+$ T cell IL-10 production [162],

however it also promoted IL-10 production through overexpression of EOMES [129], a transcription factor. Currently, data does not suggest that TGFβ signalling has a role in Tr1 cell differentiation [163].

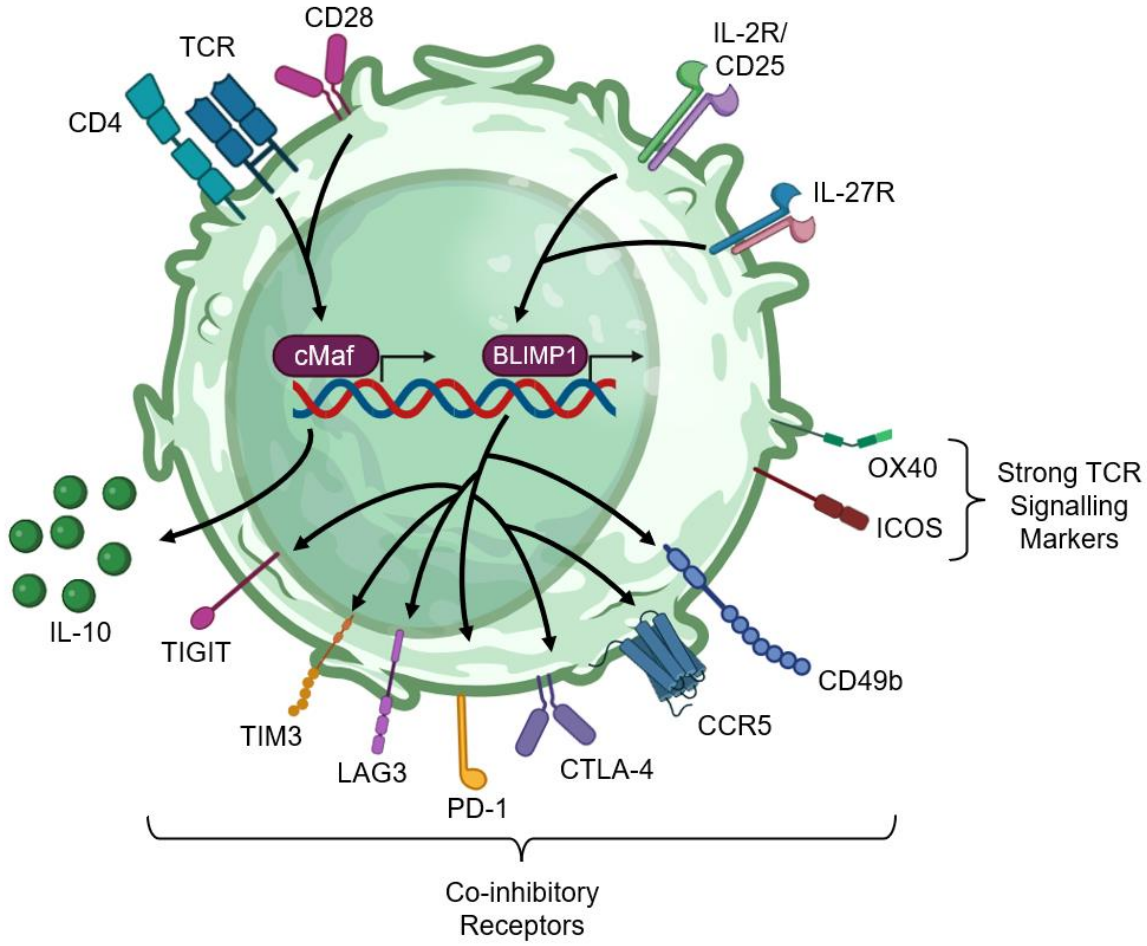

Figure 1-4: Tr1 cell markers and induction pathways.
A key feature of Tr1 cells is high secretion of IL-10, induced by transcription factor cMaf initiated by TCR complex and co-stimulation signalling (signals1 and 2). Downstream effects of IL-10 limit innate and adaptive immune responses. BLIMP1, initiated by cytokine receptors such as IL-2R (CD25) and IL-27R drive expression of co-inhibitory receptors including CTLA-4, Lag3, TIM3 and TIGIT (which bind CD80/86, MHCII, CEACAM1 and Galectin-9, and CD155 respectively), as well as CD49b, CCR5, and CD49b. There has been crosstalk to suggest BLIMP1 also induces *Il10*, and the transcription factors above do not exclusively induce co-inhibitory receptors, as downstream TCR signalling also induces them, as well as activation markers and markers of strong TCR signalling OX40 and ICOS. Tr1 cells lack a lineage defining marker, and there is a lack of consensus on a definitive phenotype.

1.4 Interleukin-10

A key player in immune responses is the highly conserved cytokine IL-10, which is the hallmark cytokine of Tr1 cells. Initially known as Cytokine Synthesis Inhibitory Factor (CSIF), IL-10 is a pro-tolerance cytokine with roles in infection, hypersensitivity, autoimmunity, and cancer. Described as anti-inflammatory and/or pro-regulatory, IL-10 is an essential negative regulator of both innate and adaptive immune responses towards antigen-mediated stimulus. Its role as an anti-inflammatory cytokine prevents excessive inflammatory responses to limit host tissue damage, maintain commensal populations, and limit recognition of self-antigen as pathogenic [164-166]. In an example of its importance, IL-10 deficient mice often exhibit lethal pathogenic inflammation, however, responses towards infection are enhanced or unaffected [167-170].

Nearly all white blood cells, including T & B cells, DCs, γδ T cells, Natural Killer cells (NK cells), Mast cells, Neutrophils, Eosinophils, and Keratinocytes produce anti-inflammatory IL-10. IL-10 has a short half-life and short range of activity, therefore, having many cell types with the ability to produce IL-10 could be necessary to ensure rapid availability at different, diverse niches throughout the body. Additionally, it could be important to compartmentalise IL-10 action to prevent adverse inflammatory effects. The significance and complexity of IL-10 regulation is emphasised by the evolution of pervasive, body-wide sources of IL-10, but why is poorly understood. Special roles for different cell types in mediating IL-10 function has not been ruled out [171].

1.4.1 Structure

This pleiotropic, immunoregulatory cytokine is biologically functional as a 36kD homodimer encoded by the *Il10* gene on chromosome 1 in both humans and mice [172]. The IL-10 monomers are each 160 amino acids long and held together by two disulphide bridges. These bridges maintain structural integrity and are required for biological activity [173].

1.4.2 Binding

IL-10 binds solely to a hetero-tetrameric surface receptor, composed of two IL-10Rα (IL-10 Receptor alpha) and two IL-10Rβ (beta) subunits, wherein IL-10Rα binds IL-10 with high affinity and IL-10Rβ is the accessory signalling subunit [174-176]. IL-10Rα and IL-10Rβ are transmembrane glycoproteins with differing intracellular domains, in both length and amino acid sequence, associated with JAK1 and TYK2 (Tyrosine-protein Kinase) respectively [177]. IL-10 binds IL-10Rα followed by IL-10Rβ to the IL-10:IL-10Rα complex [176, 178, 179]. IL-10Rβ has widespread expression amongst different cell types, but IL-10Rα is restricted to immune cells, being particularly high on monocytes and macrophages [174, 175, 180-182]. Murine IL-10R complex can bind both human and murine IL-10, whilst human IL-10R can only bind human IL-10 [183].

1.4.3 Signalling

IL-10R binding leads to JAK-STAT (Janus Associated Kinase, Signal Transducer and Activator of Transcription) and AKT (Protein Kinase B) signalling cascades, mostly through STAT3, but also STAT1 and STAT5 to a lesser extent [184, 185]. Interestingly, IL-10R does not contain STAT1 binding sites, suggesting downstream recruitment of STAT1 or formation of STAT1:STAT3 heterodimers [186, 187]. IL-10Rβ recruits and phosphorylates receptor-associated TYK2 and JAK1 to activate them [188, 189]. This

leads to STAT3 phosphorylation and then phosprylated-STAT3 (pSTAT3) dimer formation, which binds target gene promoters and induces RNA transcription [186, 190]. The pSTAT1/pSTAT3 ratio is increased in the presence of IFNγ [191]. In different cancer models, STAT3 is constitutively active, suggested to be mediated by Epidermal Growth Factor Receptor (EGFR) [192-194]. The strength of IL-10 suppressive signalling is dependent on the timing of IL-10 expression and the activity can be diminished during inflammatory responses. IL-10 suppressed cytokine production more effectively when given before Lipopolysaccharide (LPS) in experimental endotoxemia, but not after [195]. Also, IL-10 activity was diminished during the initial stages of chronic infection with LP-BM5 retrovirus [196].

1.4.4 Expression

IL-10 can be produced by almost all innate and adaptive leukocytes, but it is mainly synthesised and secreted by monocytes, as well as activated lymphocytes, such as Th2 cells, Tregs, and DCs [197-199]. All T helper subsets can produce IL-10 to mitigate hyperactive immune responses [200]. Effector Treg secreted IL-10 is an antagonist of IL-12 production during toxoplasmosis [201]. Expression of IL-10R is higher on memory $CD4^+$ T cells than naïve [202].

IL-10 expression can also be regulated during transcription by epigenetic changes, such as histone modification, and post-transcriptional, as *Il10* mRNA contains destabilising AUUA repeated in the 3'UTR, facilitating mRNA degradation by tristetraprolin [203-205]. IL-10 may be constitutively transcribed and then regulated post-transcriptionally to shorten signal response times.

1.4.5 Relationship with Interleukin-27

IL-27 is an immunoregulatory cytokine that induces IL-10 and is a potent antagonist of inflammation. Type I and II Interferon signalling, as well as NF-κB-mediated CD40, 4-1BBL and TLR signalling initiate unique subunit IL-27-p28 transcription [206-212]. Myeloid cells (macrophages, monocytes, dendritic cells) are considered the dominant producers of IL-27, but plasma cells, endothelial cells & epithelial cells can also express it [213].

IL-27 regulates the immune response through several mechanisms, including by inhibiting differentiation of effector T cell subsets, induction of co-inhibitory genes to promote T cell exhaustion, and polarisation of $FoxP3^+$ Tregs to a $Tbet^+$ subset that specialises in controlling Th1 immunity [214-218]. IL-27 directly modifies $CD4^+$ and $CD8^+$ effector T cell function. IL-6 and IL-27, with both CD3 and CD28 stimulation, is sufficient to induce IL-10 in $CD4^+$ and $CD8^+$ T cells. This expression is STAT1 dependent [219]. IL-27 can differentiate naïve T cells into Tr1 cells ($FoxP3^-$) IL-10-producing sub-population that suppress inflammation, autoimmune reactions and graft versus host disease (GVHD) largely via IL-10 [220].

Furthermore, IL-27 can induce IL-10 production from a wider range of cell types, including Th1, Th2, Th17 and Treg cells [160, 221-223]. *Il27*$ra^{-/-}$ T cells are defective in producing IL-10 [219], and suffer lethal immunopathology reminiscent of *il10*$^{-/-}$ [216]. STAT1 and STAT3 mediate downstream signalling of the IL-27 receptor [223]. STAT3 activation, but not STAT1, can enhance IL-10 expression [224].

TGFβ is essential for Treg differentiation, and production of IL-10 by Tregs [225]. Naïve CD4+ T cells activated in vitro (e.g., via anti-CD3 and anti-CD28 stimulatory antibodies)

in the presence of TGFβ become Tregs, which are termed induced Tregs (iTregs) to distinguish them from 'natural' Tregs that largely differentiate in the thymus. TGFβ expression by Tregs is an important effector mechanism for immune suppression in addition to their production of IL-10 [226]. Whilst TGFβ and IL-6 are known differentiation factors for Th17 cells, in the absence of the cytokine IL-23 these culture conditions favour the differentiation of an IL-10^{+} Th17 cell phenotype that can attenuate pathology [227]. Therefore, whilst both IL-27 and TGFβ signalling pathways can promote T cell IL-10 production, these are most likely dependent on the overall cytokine milieu and cellular differentiation states [228].

1.5 Function and Regulation of IL-10

1.5.1 IL-10 Function

IL-10 inhibits adaptive and innate immune responses both directly and indirectly, by inhibiting pro-inflammatory cytokines, cell proliferation, and antigen presentation [229-232] and acts as an inhibitor of negative feedback due to excessive T cell responses [233].

1.5.1.1 Cytokine Inhibition

IL-10 suppresses dendritic cell function through inhibition of IL-12 expression, and through suppression of IFNγ-induced gene transcription, such as CXCL10 and ISG-54, and STAT1 phosphorylation to directly counter IFNγ [231, 234]. IL-10 inhibits production of pro-inflammatory mediators triggered by TLR signalling through inhibition of MYD88 (Myeloid Differentiation Response 88) translation and ubiquitination [235, 236]. TLRs recognise conserved sequences from pathogens that activate innate immune cells, such as DCs and macrophages. Part of the anti-inflammatory function

of IL-10 is inhibition of pro-inflammatory cytokines, such as IL-1α, IL-1β, IL-6, IL-8, TNFα, GM-CSF and G-CSF synthesis [237]. APCs such as dendritic cells and macrophages, are the main targets of IL-10.

1.5.1.2 Stimulation of Immune Subsets

IL-10 is viewed as stimulatory for the humoral immune response, as opposed to its inhibitory function in T cells. IL-10 promotes B cell differentiation, survival, and antibody production [238]. Stimulatory IL-10 is implicated in several autoimmune diseases, including the developments of Systemic Lupus Erythematosus (SLE) and MS by increasing the production of autoantibodies, correlations with relapse and [239, 240].

1.5.1.3 Cell Proliferation

IL-10 inhibits proliferation in T lymphocytes by inducing antigen-specific T cell anergy in $CD4^+$ and $CD8^+$ T cells [241, 242], and suppression of Th1 cell differentiation through inhibition of IL-2 & IFNγ. Inhibiting NF-κB translocation to the nucleus and DNA binding is a key function of IL-10 signalling [243]. In T cells, NF-κB upregulates genes involved in maturation, proliferation, and development [244]. Through inhibition of IL-12 and IL-23 production, IL-10 effectively reduces $CD4^+$ T cell differentiation [245, 246], directly inhibits Th cell function and stimulates other immune cell subtypes, including Tregs and $CD8^+$ T cells [247-252].

1.5.1.4 Induction of Tolerance

Murine colitis is mediated by activation and differentiation of effector T cells [253]. Tregs are critical in the prevention of spontaneous or experimentally induced colitis. Mutations in IL-10 or IL-10R lead to early onset Inflammatory Bowel Disease (IBD) in humans and spontaneous colitis in mice, indicative of the necessary tolerogenic

function of IL-10 for normal bowel function and maintenance of peripheral tolerance [253-255].

Intestinal IL-10 producing macrophages induce Tregs in different colitis models [256-258]. Genetic deficiency in MyD88, an essential downstream adapter for TLR signalling, blocks colitis in IL-10-deficient mice, indicating that recognition of PAMPs by TLRs is needed for IL-10 release [259, 260]. IL-10 production by macrophages is required for preventing experimental colitis in a model that is induced by T cell adoptive transfer [258], but myeloid cell derived IL-10 does not appear to play a role in spontaneous colitis [261, 262], However, when IL-10 is specifically deleted in Treg then these mice go on to develop spontaneous colitis, demonstrating that colonic Treg production of IL-10 is essential for maintaining gut immune homeostasis [263]. During infection, excessive IL-10 can result in decreased DC function, reduced effector response and consequently increased microbial replication [264, 265].

IL-10 deletion from T cells leads to decreased survival, weight loss and increased IFNγ and TNFα, as well as other inflammatory cytokines [266]. In TCR-restricted murine models, repeated administration of autoreactive myelin basic protein (MBP) peptides over several weeks induces tolerance through induction of IL-10 secreting $CD4^+$ $FoxP3^-$ T cells in the experimental autoimmune encephalomyelitis (EAE) model of multiple sclerosis (MS) [267-271].

1.5.1.5 Experimental Autoimmune Encephalomyelitis and Peptide Immuno-therapy

Tolerance can be broken and EAE induced by inoculation of H-2u haplotype mice, which is reactive to MBP, with spinal cord homogenate (SCH) in combination with

Complete Freud's Adjuvant (CFA) containing heat-killed *Mycobacterium tuberculosis* and pertussis toxin, triggering $CD4^+$ T cells to lead a response against neural tissues [272]. This EAE model was later used to generate the Tg4-TCR transgenic mouse after isolating an encephalitogenic TCR from H-2u mice [268]. Tg4 mice express a Vβ8.2 transgene that recognises the immunodominant epitope of MBP – the acetylated N-terminal peptide also referred to as Ac1-9.

Whilst the native Ac1-9 MBP has low affinity with class II ($I\text{-}A^U$) and lies below the threshold of tolerance, this can be altered through modification of the principal anchor residue; lysine at the 4^{th} (4K) position. Being non-hydrophobic and of smaller size, it fits poorly into the major hydrophobic pocket of $I\text{-}A^U$, a restriction element of MHCII [273]. Mutated peptide analogues that swap 4K for alanine or valine increase affinity, but tyrosine (4Y) demonstrated much stronger affinity than others tested [268]. The higher affinity peptide allows the autoreactive Tg4-TCR to recognise the MBP peptide and mount a stronger tolerogenic response against it, judged by CD69 upregulation, clonal deletion of DP thymocytes, and TCR modulation by $CD4^+$ thymocytes. Repeated administration of high affinity peptide leads to a shift in cytokine secretion away from IL-2, IL-2 and IFNγ to IL-10, but not TGFβ, also reducing $CD4^+$ T cell proliferation capacity [267, 274]. These $IL\text{-}10^+$ $CD4^+$ T cells suppressed proliferating responder cells, and were found to be FoxP3 negative and originated from Th1 cells [135, 269, 275]

Using the Tg4 model in a ten day intranasal administration of 100 µg peptide, lower affinity encephalitogenic [4A] or [4K]-MBP conferred partial protection against EAE, induced three days after the final dose. However higher affinity peptide [4Y]-MBP provided complete protection [272]. It induced the strongest $IL\text{-}10^+$ Treg generation,

and following an *in vitro* recall response, expressed IFNγ. Escalating Dose Immunotherapy (EDI) uses increasing doses of self-antigen to induce tolerance via a subcutaneous (non-mucosal) route [276], opposed to intra-nasal [270].

IL-10 induction is associated with efficacious peptide immunotherapy in human and murine cancers [277-280].

1.5.1.6 Modified IL-10 as Disease Treatment

Tumours in mouse models treated with IL-10 or engineered to express IL-10 show rapid tumour rejection [281]. Similarly, PEGylated IL-10 (peg-IL-10, Pegilodecakin) treatment leads to tumour rejection [282, 283]. This study noted an increase in granzyme B and IFNγ, and a three-fold increase in oligoclonal tumour-infiltrating cytotoxic $CD8^+$ T cells. Peg-IL-10 had no effect on $IL10R^{-/-}$ mice, and STAT1 was active in tumour cytotoxic $CD8^+$ T cells, but not lymph node cytotoxic $CD8^+$ T cells. This has been supported by other studies, one of which found decreased VEGF and MMP-9 mRNA [284-286]. Pegilodecakin treated patients showed increased cell number and more activated $LAG3^+$ $PD\text{-}1^+$ $CD8^+$ T cells in circulation, further increased by treatment combined with anti-PD-1. Median overall and progression-free survival were more favourable in melanoma patients who were not PD-1 refractory compared with those who were [287]. Pegilodecakin and anti-PD-1 combination therapy showed favourable response as second-line therapy in patients with non-small-cell lung cancer and renal cell carcinoma in comparison with previous studies with anti-PD-1 monotherapy [288, 289]. Systemic administration of pegilodecakin can lead to adverse side effects, like use of rIL-10 leading to stimulated B cells and promotion of autoimmune disease [290-292].

Recombinant IL-10 has been suggested to treat autoimmune diseases, however many clinical trials offered unencouraging results. Psoriasis is one of few examples of autoimmune diseases in which IL-10 treatment has shown encouraging results [293]. IL-10 and IL-10R deficient mice and humans develop cancer and inflammatory bowel disease, suggesting that they are key in preventing these diseases [294, 295]. B cell lymphomas in IL-10R-deficient children lack cytotoxic T cell infiltration. With a complex network of cells acting as producers and receivers of IL-10, in a highly regulated and compartmentalised system it is unlikely that infusing rIL-10 into a patient will resolve disease [171]. IL-10 can be produced by tumour cells, including melanoma [296], and there is evidence that suggests IL-10 expression in tumours contributes to tumour escape mechanisms and protects the tumour from immune surveillance, thereby perpetuating disease, however the IL-10:tumour dynamic is very complicated [297-299]. IL-10 can enhance antitumour immunity in certain cancers [283, 287, 300-303]. Elevation of IL-10 in tumour models leads to T cell mediated tumour rejection [183]. IL-10 promotes anti-tumour immunity in multiple murine tumour models [301, 304, 305].

An IL-10 fusion protein (IL-10-Fc) with an extended half-life, was able to potently enhance expansion of immunotherapy-unresponsive, exhausted tumour-infiltrating, tumour-killing effector $CD8^+$ T cells [300]. Treatment with IL-10-Fc promoted oxidative phosphorylation. $CD8^+$ Tumour Infiltrating Lymphocytes (TILs) under persistent antigen stimulation and metabolic stress, such as in the TME, accumulate dysfunctional mitochondria, which leads to a reduced proliferative capacity and effector function. Impaired mitochondrial oxidative phosphorylation drives T cell exhaustion [306-308].

A cetuximab-IL-10 fusion protein (CmAb-$(IL\text{-}10)_2$) prevented DC-mediated $CD8^+$ TIL apoptosis through regulation of IFNγ production [302]. Combination with Immune Checkpoint Blockade (ICB) significantly improved anti-tumour effects in advanced murine tumours compared to monotherapy. Despite anti-PD-1/PD-L1 immunotherapy to inhibit apoptosis, Qiao et al suggest that since ICB significantly increases IFNγ expression by TILs, further prevention of T cell apoptosis by CmAb-$(IL\text{-}10)_2$ is likely due to IFNγ production by $CD8^+$ TILs [309-311].

Expansion of tumour-specific $CD8^+$ T cells and their activation is necessary for the long-term success and durability of immune-oncology strategies [312-314]. A half-life extended IL-10 fusion protein (IL-10-Fc) has shown direct expansion of terminally exhausted $CD8^+$ TILs in the B16F10 model, leading to increased effector function, independent of progenitor exhausted $CD8^+$ TILs, through metabolic reprogramming [300]. This therapy eradicated solid tumours when combined with ICB or adoptive T cell transfer, suggesting a combined treatment approach could enhance efficacy and response rates [303, 315]. IL-10, and its PEGylated form, activate cytotoxicity and proliferation in $CD8^+$ T cells [282, 301].

1.5.2 IL-10 Regulation

1.5.2.1 Transcription Factors

cMaf, NFIL3 and PRDM1 are positive regulators of IL-10 expression. Their expression is highly upregulated EDI [276]. Bhlhe40, which does not interfere in Tr1 differentiation, is a negative regulator, and potent inhibitor, of IL- 10 whilst increasing IFNγ secretion in naïve $CD4^+$ T cells [136]. Cebpb is required for *Il10* production in Tr1 cells and induces *Il10* in M2 macrophages [142, 316].

1.5.2.2 Co-Inhibtory Molecules

LAG3, TIM-3 and TIGIT expression is highly upregulated during EDI, whilst PD-1 expression is largely unchanged I. PD-L1 blockade during murine infection enhanced effector Treg function and IL-10 expression [317]. Irf8 is a negative regulator of IL-10 expression and function, at both protein and transcript level [142].

1.5.2.3 IL-10 & TCR Signalling

Binding of the TCR complex to a cognate peptide bound to MHC (pMHC) triggers a signalling cascade that leads to the activation of NFAT, AP-1, and NF-κB, which are the major downstream transcription factors controlling T cell activation. NFAT1 is known to dimerise with AP-1 and other transcriptional factors to promote cytokine gene transcription [318]. NFAT1 has been shown to bind the *Il10* promoter in Th2 cells and to fourth intron of *Il10* in Th1 cell lines [319]. Analysis of branches of TCR signalling has highlighted that ERK, an important MAP kinase that leads to AP-1 upregulation, can positively regulate IL-10 expression in $CD4^+$ T helper cells [320]. IL-10 production in $CD8^+$ T cells in a model of coronavirus induced encephalitis [321]. Analysis of different T helper subsets have shown that for Th1 cells they also require IL-12 induced STAT4 (which is also critical for Th1 production of IFNγ) signalling to produce IL-10 [320] whereas Th2 cells require the IL-4:STAT6:GATA3 axis [322]. In addition, IRF4, an important transcription factor activated by strong TCR signalling, positively regulates IL-10 expression in Th2 cells and directly binds to the *Il10* promoter [323]. IRF4 can also dimerise with NFAT1 and this complex has been shown to be able to bind to Conserved Non-coding Sequence (CNS)-9 (a locus in the *Il10* gene), leading to sharply enhanced *Il10* transcription [324].

Strong TCR signalling (i.e., an antigen that strongly adheres to the TCR) has been demonstrated to cause rapid upregulation of IL-10 in $CD4^+$ T cells [325], in both tolerance and cancer settings, indicating regulatory function. However, the exact mechanism of IL-10 induction from strong stimulus is unknown, nor the subset of cells that expresses IL-10 in rapid response to a strong stimulus. This thesis sought to understand the regulation of IL-10 in tolerance and cancer settings, and the role TCR signalling and other factors such as cytokines have in its expression.

1.6 Aims

This project aims to understand the role of strong TCR signalling in driving IL-10 expression and how it is controlled in T cell responses during cancer and tolerance. This includes identification of early T cell phenotypic biomarkers (IFNγ, LAG3, PD1, and IL-10) *in vivo* to gain insight into regulators of checkpoint expression. IL-10 and IFNγ have a complex role in recognition of self and non-self, in that antigen recognition, e.g. of tumour or self-antigens, by T cells leads to IFNγ and IL-10 production. This upregulates immune checkpoint receptor ligands on tumour cells to stimulate a checkpoint receptor (e.g. PD1) on immune cells, downregulating the immune response directed towards tumours. However, it remains less clear what role the IL-10 : IFNγ axis plays in controlling T cell intrinsic expression of negative regulators. Therefore, given that IFNγ is a potent effector cytokine in driving anti-tumour immunity and IL-10 drives tolerance of perceived pathogens, understanding how they regulate immune checkpoints will be key for future optimisation of immunotherapies.

Immunotherapies such as anti-PD-1 lead to increased T cell IFNγ expression in tumours. Whilst IFNγ has important anti-tumour functions on tumour cells and other immune cells our pilot data suggested feedback signalling on T cells may paradoxically boost the expression of negative regulators such as LAG3 and IL-10.

Pilot data has shown that IL-10, LAG3 and PD1 likely exert distinct time-dependent roles in controlling T cell activation and that T cell expression of IL-10 and LAG3 is dependent on IFNγ and TCR signalling strength. In this project we hypothesise that the increased T cell IL-10 and IFNγ expression in mouse model responses to strong

TCR signalling drives regulatory pathways to limit inflammation in tolerogenic and oncogenic environments.

This thesis will address three main aims:

1) Define the development of *in vivo* T cell *Il10* transcriptional response and kinetics of checkpoint and cytokine expression in response to an accelerated adaptive tolerance model,

2) Modulate the development of these early *Il10* transcriptional responses to the same strong TCR stimulation model and,

3) Investigate whether modulation of pro-inflammatory IFNγ affects T cell responses including *Il10* transcription, and tumour outcomes with regards to immunotherapy.

Chapter 2 : Materials & Methods

2.1 Mice

Tg4 *Nr4a3*-Tocky *Il10*-GFP and *FoxP3*-Tocky mice were used as previously described [325, 326]. *Nr4a3*-Tocky Great (*Ifng*-YFP) Smart-17A (*Il17a*-hNGFR) mice [327], generated as previously described [325], were mated to Tiger (*Il10*-GFP) mice [328] to generate *Nr4a3*-Tocky Tiger (*Il10*-GFP) Great (*Ifng*-YFP) Smart-17A (*Il17a*-hNGFR). *Nr4a3*-Tocky Tg4 Tiger (*Il10*-GFP) were mated to Great (*Ifng*-YFP) Smart-17A (*Il17a*-hNGFR) to generate *Nr4a3*-Tocky Tg4 Tiger (*Il10*-GFP) Great (*Ifng*-YFP) Smart-17A (*Il17a*-hNGFR) mice (table 2-1). All animal experiments were approved by the local animal welfare and ethical review body and authorised under the authority of Home Office licenses P18A892E0A, PP9984349 and PP3965017 (held by Dr David Bending). Animals were housed in specific pathogen-free conditions. Both male and female mice were used, and littermates of the same sex were randomly assigned to experimental groups. *Nr4a3*-Tocky mice were originally obtained under MTA from Dr Masahiro Ono, Imperial College London, UK. Only modified variants of the *Nr4a3*-Tocky line were used in this thesis.

In *Nr4a3*-Timer mice, the first coding exon of *Nr4a3* in BAC RP23-122N18 was replaced with the transgene cassette containing the *Timer* (*Fast-Timer)* gene [329], a poly-A tail and a floxed neomycin resistance gene (*neo)* [326]. Purified BACs were microinjected into the pronucleus of embryos from C57BL/6 mice. The *Nr4a3*-Timer BAC transgene initiates Timer production through NFAT binding to an *Nr4a3* promoter region.

2.2 $CD4^+$ T cell Isolation and Culture

Naïve $CD4^+$ T cells were isolated using MoJo magnetic bead negative selection kits (BioLegend) according to the manufacturer's instructions. Naïve T cells were then cultured on 96-well flat bottom plates (Corning), which were pre-coated with 1 µg/mL anti-CD3 and 5 µg/mL anti-CD28, in 10 % FBS (v/v) RPMI containing 1 % penicillin/streptomycin (Life Technologies) at 37 °C and 5 % CO_2 for the indicated time points in the presence of recombinant murine IFNγ (BioLegend).

2.3 Immunisations

Tg4 Tiger, Tg4 *Nr4a3*-Tocky Tiger, Tg4 *Nr4a3*-Tocky Tiger Great Smart mice were immunized through subcutaneous injection of [4Y]-MBP peptide (doses stated in figure legends and results) in a total volume of 200 µL PBS into the flank. Mice were then euthanised at the indicated time points, and spleens removed to analyse systemic T cell responses.

2.4 *In vivo* Antibody Treatments

For *in vivo* blockade experiments, *in vivo* grade anti-PD-L1 (clone MIH5[330], rat IgG2a, obtained under MTA from Prof Miyuki Azuma), *in vivo* grade anti-IL-27 (clone MM27.7B1, rat IgG2a), or *in vivo* grade anti-IFNγ (clone XMG1.2, kind gift from Prof Anne Cooke, University of Cambridge, rat IgG1) were administered through intraperitoneal injection on hours or days indicated in figure legends. For anti-IFNγ experiments, an isotype control group was used consisting of rat IgG1 (clone MAC221, kind gift from Prof Anne Cooke, University of Cambridge), for anti-PD-L1 and anti-IL-27 experiments, an isotype control group was used consisting of rat IgG2a (clone MAC 219, kind gift from Prof Anne Cooke, University of Cambridge). In combinatorial

Strain Name	Modifications
C57BL/6	None, genetic background stock
Tiger	IL10-IRES-GFP knock-in reporter mice
Tg4 Tiger	Tg4 TCR transgenic (specific for MBP peptide) crossed with IL10-IRES-GFP knock-in reporter mice
Nr4a3-Tocky Tg4 Tiger	BAC containing Nr4a3 gene modified to swap first coding exon for Timer Fast (Timer) protein Tg4 TCR transgenic (specific for MBP peptide) crossed with IL10-IRES-GFP knock--in reporter mice
Nr4a3-Tocky Tg4 Tiger Great Smart 17A	BAC containing Nr4a3 gene modified to swap first coding exon for Timer Fast (Timer) protein, crossed with 1) mice homozygous for IFNγ-IRES-YFP and IL17A-IRES-HNGFR knock-ins and 2) Tg4 TCR transgenic (specific for MBP peptide) crossed with IL10-IRES-GFP knock-in reporter mice
Nr4a3-Tocky Tiger Great Smart 17A	BAC containing Nr4a3 gene modified to swap first coding exon for Timer Fast protein, crossed with 1) mice homozygous for IFNγ-IRES-YFP and IL17A-IRES-HNGFR knock-ins and 2) IL10-IRES-GFP knock-in reporter mice
FoxP3-Tocky Tiger	BAC containing FoxP3 gene modified to swap first coding exon for Timer Fast (Timer) protein crossed with IL10-IRES-GFP knock-in reporter mice
IFNgRfl/fl	IFNγR floxed
CD4-Cre IFNgRfl/fl	CD4-cre BAC transgene crossed on to the IFNγR floxed line

Table 2-1 Transgenic Mouse Strains

experiments an isotype pool of rat IgG1 and rat IgG2a was used as a control with addition of the appropriate isotype to single treatment controls.

2.5 Tissue Preparation for Flow Cytometry and Cell Sorting

For analysis of splenic lymphocyte and macrophage populations spleens were dissociated using scissors in 1.2 mL of digestion media containing 1 mg/mL collagenase D (Merck Life Sciences) and 0.1 mg/mL DNase I (Merck Life Sciences) in 1 % FBS (v/v) RPMI. Samples were then incubated for 20-25 min at 37 °C in a thermo-shaker. Digestion mixture was then passed through a 70 µm filter (BD Biosciences) and washed with 30 mL ice cold media (10 % FBS RPMI). Digested cells were washed once and stained in 96-well U-bottom plates (Corning) in FACS buffer (PBS 1 % v/v FBS). Analysis was performed on a BD LSR Fortessa X-20 instrument. The blue form of the Timer protein (Timer Blue or Timer Blue) was detected in the blue (450/40 nm) channel excited off the 405 nm laser. The red form of the Timer protein (Timer Red or Timer Red) was detected in the mCherry (610/20 nm) channel excited off the 561 nm laser. A fixable eFluor780-flurescent viability dye (eBioscience) was used for all experiments. GFP was detected in the FITC (530/30 nm) channel excited off the 488 nm laser. In dual reporter (*Il10*-GFP and *Ifng*-YFP) experiments, a custom detector configuration detected GFP in the 510/20 nm channel on a 495 long pass and YFP in the 542/27 channel on a 525 long pass. Directly conjugated antibodies used in these experiments are listed below. For intracellular staining of FoxP3, the FoxP3 transcription factor staining buffer kit was used (eBioscience). For cell sorting, single cell suspensions from biological replicate mice were generated. Cells were sorted on a FACS ARIA FUSION cell sorter.

2.6 Spectral Cytometry

Cells were prepared as in 2.5 Flow cytometry and cell sorting, except the cells were stained in Brilliant Stain Buffer (BD Biosciences) and analysis was performed on a Sony ID7000 spectral cytometer. Spectral cytometers detect and record the entire emission spectrum of a sample, using a patented algorithm to deconvolute (unmix) the spectrum into individual fluorochromes and dyes using accurately recorded single controls. The specificity of these controls is paramount to the appropriate deconvolution of a sample's spectrum, as the instrument is so sensitive that it can simultaneously detect, for example, FITC, GFP and YFP within the same sample, which is not normally possible on a conventional cytometer with standard configurations.

Controls were generated using Invitrogen UltraComp ebeads compensation beads, cells from unimmunised mice, and reporters from immunised mice. Non-tandem dyes were generated once per antigen and uploaded to the machine software (i.e., CD4-APC, CD4-BUV395, CD8-APC etc). Tandem dyes, such as PE-Cy7, PerCP-Cy5.5 and BUV737 were freshly generated for each use, due to associated fluorochrome degradation. Unimmunised Tg4 murine splenocytes were to establish an unstained baseline spectral emission used for autofluorescence controls. Reporter controls were generated by administering a high dose (4 mg/kg) of [4Y]-MBP peptide to Tg4 Tiger or Tg4 Nr4a3-Tocky mice before mice were euthanised and splenocytes harvested. For a Timer Blue or Timer Red single from Nr4a3-Tocky mice, spleens were harvested at 4 and 24 hr respectively to generate a clear single. Single colour references for GFP, Timer Red and Timer Blue were generated by Dr David Bending.

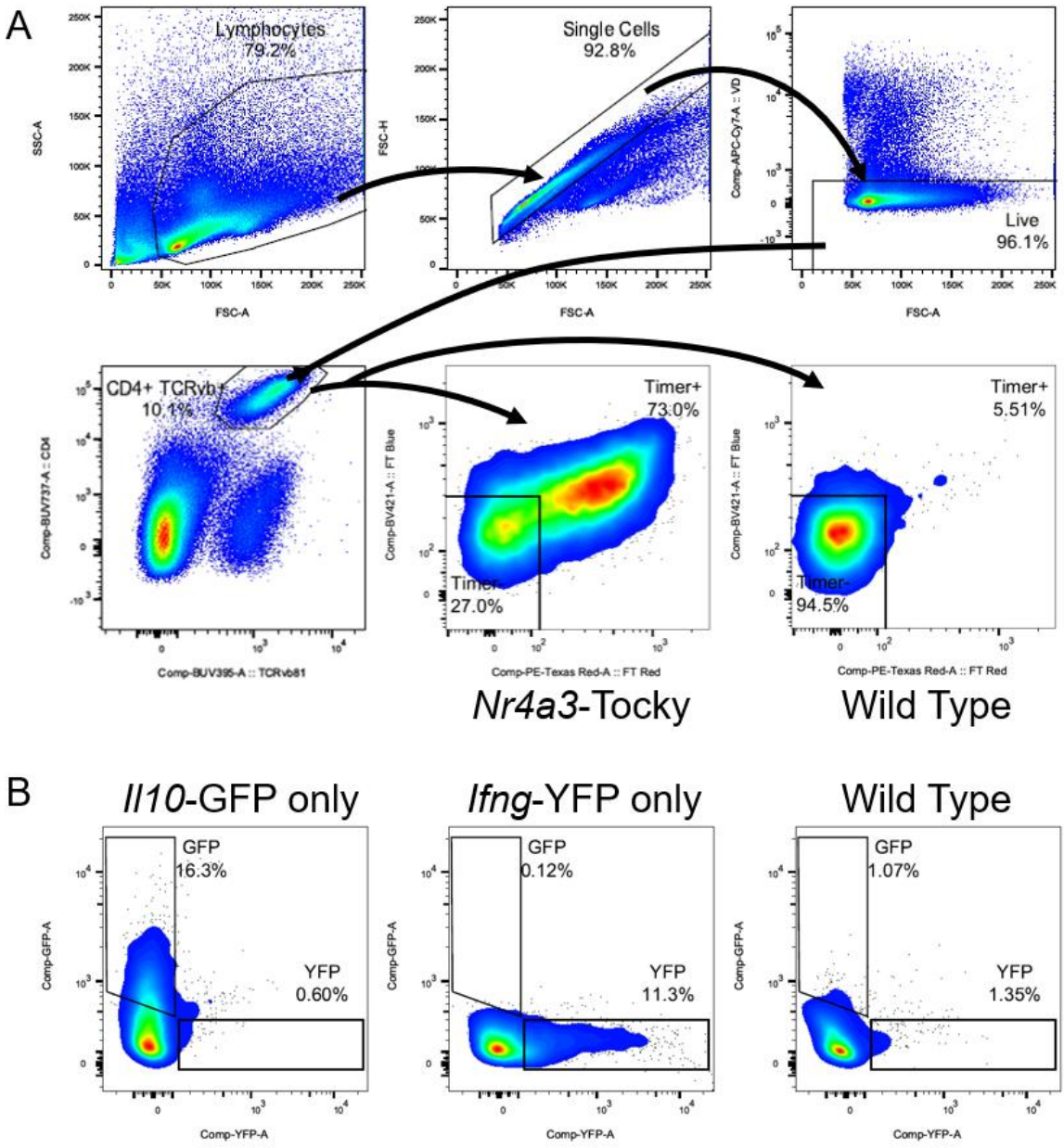

Figure 2-1: Gating strategy for CD4⁺ *Nr4a3*-Timer⁺ T cells
(A) Lymphocytes were broadly defined through Forward and Side scatter area before elimination of doublets etc. and retention of singlets through Forward scatter area and height. These were then determined to be live via non-uptake of viability dye efluor780 fixable viability dye, detected by the APC-Cy7 channel. Live splenocytes were then assessed for dual CD4 and TCRvβ8.1/2 expression before selection for Timer⁺ (i.e. *Nr4a3* or *Foxp3*). A gate was drawn over the Timer⁻, which was subsequently inverted, retaining the Timer⁺ (including Blue⁺ Red⁻, Blue⁻ Red⁺ and Red⁺ Blue⁺). *Nr4a3*, expressed downstream of TCR signalling, is used as a proxy of TCR specific activation. A wild type (reporter negative mouse) has been included to demonstrate gating Timer⁺ cells. **(B)** Single cytokine reporters *Il10*-GFP and *Ifng*-YFP shown against a wild type to demonstrate how GFP⁺ or YFP⁺ gates are drawn from Timer⁺ cells.

2.7 Enzyme-Linked Immuno-Sorbent Assay (ELISA)

Supernatants from *in vitro* assay cultures were collected after 24 hr and extracellular IL-10 was measured using R&D Systems Mouse IL-10 DuoSet ELISA kit according to instructions. All steps carried out at room temperature and adhesive seals were applied for each incubation step. IL-10 capture antibody at 4 µg/mL was bound to a 96-well U-bottom plate overnight with 100 µL per well and then washed with 400 µL Wash Buffer and aspirated thrice. Wells were then blocked with 300 µL Reagent Diluent and incubated for 1 hr before repeating the wash steps. 100 µL of sample or standard in Reagent Diluent were added to each well and incubated for 2 hr before repeating the wash steps. Samples were diluted in PBS if necessary. 100 µL of Detection Antibody at 250 ng/mL was then added to each well and incubated for 2 hrs before repeating the wash steps. 100 µL of Streptavidin-HRP (at working concentration) was added to each well and incubated for 20 minutes in the dark before repeating the wash steps. 100 µL of Substrate Solution was added to each well and incubated for 20 minutes in the dark. 50 µL of Stop Solution was added to each well and incubated for 20 minutes in the dark before repeating the wash steps. Optical density measured at 450nm by a microplate reader. Reads generated were conferred a concentration based on the interpolated standard curve, which was generated per plate.

2.8 Macrophage and T cell Co-cultures

Tg4 *Nr4a3*-Tocky Tiger (*Il10*-GFP) mice were immunized through subcutaneous injection of 4 mg/kg [4Y]-MBP peptide in a total volume of 200 µL PBS into the flank s.c. and administered with 1 mg of anti-IFNγ antibody (clone XMG.12) i.p. After 12 hr, spleens were digested as described earlier and splenocytes stained for anti-CD11b-

APC, anti-F4/80 BUV395 and eFluor780-flurescent viability dye. Live macrophages were (identified as $CD11b^{+}F4/80^{+}$) were flow sorted on a FACS ARIA FUSION machine. $CD4^{+}$ T cells were sorted from an unimmunised donor Tg4 *Nr4a3*-Tocky Tiger mouse. 50,000 macrophages were cultured with 150,000 $CD4^{+}$ T cells (3:1 ratio of T cell to Macrophages) in 96-well U-bottom plates in 0.2% tissue culture grade 2-mercaptoethanol (Gibco), with either media alone or addition of 0.4 µM [4Y]-MBP for 18 h before analysis of T cells by flow cytometry.

2.9 *In vivo* NK cell Depletion

For *in vivo* depletion of $NK1.1^{+}$ cells, 200 µg of *in vivo* grade anti-NK1.1 (clone PK136), a depleting antibody, or isotype control IgG2a (clone C1.18.4) was administered through intraperitoneal injection in 200 µL PBS. 48 hr later, mice were immunised as described above with 4mg/kg [4Y]-MBP, before the animals were culled and tissue harvested 24 hr post-immunisation.

2.10 *In vitro* Restimulation of Antigen Experienced T cells (Hybrid model)

For the hybrid tolerance model, Tg4 Nr4a3-Tocky Il10-GFP mice were immunized through subcutaneous injection of 4 mg/kg [4Y]-MBP peptide. 24 hr later mice were euthanised and spleens were removed and digested as described above. Digested cells were washed once and 5×10^5 splenocytes cultured for 24 hr in 96-well U-bottom plates in a final volume of 200 µL RPMI 1640 containing 10% FCS and penicillin/streptomycin (Life Technologies) and 55 µM tissue-culture grade 2-mercaptoethanol (Gibco) for the stated time periods in the presence of a range of [4Y]-MBP peptide concentrations. Agonist antibodies (agICOS), antagonist antibodies (anti-

IFNγ, anti-ICOS, anti-IL10R, anti-PD-L1, anti-IL-27) and recombinant proteins (rIFNγ, rIL-27) administered at 100 ng/mL.

2.11 MC38 Model

MC38 colorectal cell line was passaged in 10 % FBS (v/v) RPMI containing 1 % penicillin/streptomycin (Life Technologies). On day of experiment, MC38 cells were harvested and resuspended in PBS (Sigma) at a concentration of 2.5 million/mL and 0.25 million MC38 cells injected subcutaneously under the right flank of mice in a final volume of 100 µL PBS. Tumour size was measured using digital callipers.

Mice survival was based on a tumour exceeding 12 mm in length or ulceration of tumour site. For *in vivo* blockade experiments, 0.5 mg *in vivo* grade anti-PD-L1 (clone MIH5[330], rat IgG2a, obtained under MTA from Prof Miyuki Azuma), and/or *in vivo* grade anti-IFNγ (clone XMG1.2, kind gift from Prof Anne Cooke, University of Cambridge, rat IgG1) (1 mg in experiments that had no combination with anti-PD-L1, 0.5 mg in combination experiments) were administered through intraperitoneal injection on days indicated in figure legends. For anti-IFNγ experiments, an isotype control group was used consisting of rat IgG1 (clone MAC221, kind gift from Prof Anne Cooke, University of Cambridge), for anti-PD-L1 experiments, an isotype control group was used consisting of rat IgG2a (clone MAC 219, kind gift from Prof Anne Cooke, University of Cambridge). In combinatorial experiments an isotype pool of rat IgG1 and rat IgG2a was used as a control with addition of the appropriate isotype to single treatment controls.

Whole tumours from mice were excised, weighed, and then dissociated using scissors in 1.2 mL of digestion media containing 1 mg/mL collagenase D (Merck Life Sciences)

and 0.1 mg/mL DNase I (Merck Life Sciences) in 1 % FBS (v/v) RPMI. Samples were then incubated for 20-25 min at 37 °C in a thermo-shaker. Digestion mixture was then passed through a 70 µm filter (BD Biosciences) and washed with 30 mL ice cold media (10 % FBS RPMI). Suspension was then centrifuged at 1500 rpm for 5 min at 4 °C. Pellets were then re-suspended in staining media (2 % FBS PBS) for labelling with fluorescently conjugated antibodies.

2.12 RNA-seq Analysis

Data from GEO: GSE165817 (Elliot et al. [325]) were re-analysed using DESeq2 [331] in R version 4.0**.** Normalized read counts were transformed using the regularised log (rlog) transformation. This function log2 transforms count data and minimizes differences between samples for rows with small counts and normalizes to library size. Heatmap analysis was performed on the rlog transformed data using the R package gplots. The code used can be found in the Appendix.

2.13 Statistical Analysis

Statistical analysis was performed on Prism 9 (GraphPad) software. For comparison of more than two means over time, a two-way ANOVA with Tukey's or Sidak's multiple comparison's test was used. For a comparison of more than two means, a one-way ANOVA with Tukey's multiple comparisons test was used. For comparison of non-parametric data, a Mann Whitney U test was performed or a Kruskal Wallis test with Dunn's multiple comparisons test. Variance is reported as mean ± SEM or bars reflect the median for non-parametric data (unless otherwise stated); data points typically represent individual mice. Linear correlation analysis was performed using Pearson's correlation. *p = < 0.05, **p = < 0.01, ***p = < 0.001, ****p = < 0.0001.

2.14 Reagents and Resources

Antibodies	Source	Cat #	RRID
Rat Anti-Mouse CD19 PerCP-Cy5.5 (clone 6D5)	BioLegend	115533	AB_2259869
Rat Anti-Mouse CD25 PerCP-Cy5.5 (clone PC61)	BioLegend	102030	AB_893288
Rat Anti-Mouse CD40 PerCP-Cy5.5 (clone 3/23)	BioLegend	124624	AB_2561474
Rat Anti-Mouse GITR PerCP-Cy5.5 (clone DTA-1)	BioLegend	126315	AB_2563383
Rat Anti-Mouse OX40 PerCP-Cy5.5 (clone OX-86)	BioLegend	119414	AB_2561724
Rat Anti-Mouse PD-1 PerCP-Cy5.5 (clone 29F.1A12)	BioLegend	135207	AB_10550092
Rat Anti-Mouse CD11b APC (clone M1/70)	BioLegend	101211	AB_312794
Armenian Hamster Anti-Mouse CD11c APC (clone N418)	BioLegend	117309	AB_313778
Rat Anti-Mouse CD25 APC (clone PC61)	BioLegend	102012	AB_312861
Armenian Hamster Anti-Mouse CD69 APC (clone H1.2F3)	BioLegend	104514	AB_492843
Rat Anti-Mouse FoxP3 APC (clone FJK-16s)	Thermo Fisher	17-5773-82	AB_469457
Rat Anti-Mouse LAG3 APC (clone C9B7W)	BioLegend	125209	AB_10639935
Rat Anti-Mouse OX40 APC (clone OX-86)	BioLegend	119413	AB_2561723
Rat Anti-Mouse PD-1 APC (clone 29F.1A12)	BioLegend	135210	AB_2159183
Rat Anti-Mouse PDL1 APC (clone 10F.9G2)	BioLegend	124311	AB_10612935
Rat Anti-Mouse/Human CD11b PE-Cy7 (Clone M1/70)	BioLegend	101215	AB_312798
Armenian Hamster Anti-Mouse CD11c PE-Cy7 (Clone N418)	BioLegend	117317	AB_493569
Rat Anti-Mouse CD19 PE-Cy7 (clone 6D5)	BioLegend	115519	AB_313654
Rat Anti-Mouse CD25 PE-Cy7 (clone PC61)	BioLegend	102015	AB_312864
Rat Anti-Mouse CD86 PE-Cy7 (clone GL-1)	BioLegend	105013	AB_439782
Rat Anti-Mouse GITR PE-Cy7 (clone DTA-1)	BioLegend	126317	AB_2563385
Rat Anti-Mouse ICOS PE-Cy7 (clone 7E.17G9)	BioLegend	117421	AB_2860636
Rat Anti-Mouse LAG3 PE-Cy7 (clone C9B7W)	BioLegend	125225	AB_2715763

Rat Anti-Mouse MHCII I-A/I-E PE-Cy7 (clone M5/114.17.2)	BioLegend	107629	AB_2290801
Mouse Anti-Mouse NK1.1 PE-Cy7 (clone S17016D)	BioLegend	156514	AB_2888852
Rat Anti-Mouse OX40 PE-Cy7 (clone OX-86)	BioLegend	119415	AB_2566154
Rat Anti-Mouse PD-1 PE-Cy7 (clone 29F.1A12)	BioLegend	135215	AB_10696422
Rat Anti-Mouse PDL1 PE-Cy7 (clone 10F.9G2)	BioLegend	124314	AB_10643573
Mouse Anti-Mouse TIGIT PE-Cy7 (clone 1G9)	BioLegend	142107	AB_2565648
Armenian Hamster Anti-Mouse CD11c AF700 (clone N418)	BioLegend	117319	AB_528735
Rat Anti-Mouse CD4 AF700 (clone RM4-4)	BioLegend	116022	AB_2715958
Armenian Hamster Anti-Mouse CD69 AF700 (clone H1.2F3)	BioLegend	104539	AB_2566304
Armenian Hamster Anti-Mouse ICOS AF700 (clone C398.4A)	BioLegend	313528	AB_2566126
Rat Anti-Mouse MHCII I-A/I-E AF700 (clone M5/114.17.2)	BioLegend	107621	AB_493726
Armenian Hamster Anti-Mouse TCRbeta AF700 (clone H57-597)	BioLegend	109224	AB_1027648
Armenian Hamster Anti-Mouse CD11c BUV395 (clone HL3)	BD Biosciences	564060	AB_2738580
Rat Anti-Mouse CD39 (clone Y23-1185)	BD Biosciences	567264	AB_2916524
Rat Anti-Mouse CD4 BUV395 (clone GK1.5)	BD Biosciences	563790	AB_2738426
Rat Anti-Mouse F4/80 BUV395 (clone T45-2342)	BD Biosciences	565614	AB_2739304
Mouse Anti-Mouse TCRVbeta8.1/8.2 BUV395 (clone MR5-2)	BD Biosciences	744335	AB_2742163
Rat Anti-Mouse CD11b BUV737 (clone M1/70)	BD Biosciences	612800	AB_2870127
Rat Anti-Mouse CD19 BUV737 (clone 1D3)	BD Biosciences	612782	AB_2870111
Rat Anti-Mouse CD4 BUV737 (clone GK1.5)	BD Biosciences	612761	AB_2870092

Table 2-2: Flow and Spectral Cytometry Antibodies

Antibodies	Source	Cat #	
Rat IgG1 isotype (clone MAC 221)	Prof. Anne Cooke (University of Cambridge)	Gift from Prof. Anne Cooke (University of Cambridge)	
Rat Anti-Mouse IFNγ (clone XMG1.2)	Prof. Anne Cooke (University of Cambridge)	Gift from Prof. Anne Cooke (University of Cambridge)	
Rat IgG2a isotype (clone MAC 219)	Prof. Anne Cooke (University of Cambridge)	Gift from Prof. Anne Cooke (University of Cambridge)	
Rat anti-mouse PD-L1 (clone MIH5)	Tsushima et al., [330]	PMID: 14515261	
Mouse Anti-Mouse IL-27 p28 (clone MM27.7B1)	BioXCell	BE0326	AB_2819053
Mouse Anti-Mouse IgG2a (clone C1.18.4)	BioXCell	BE0085	AB_1107771
Anti-Mouse NK1.1 (clone PK136)	BioXCell	BE0036	AB_1107737
Anti-Mouse ICOS (clone 7E.17G9) (blocking)	BioXCell	BE0059	AB_1107622
Anti-Mouse/Human/Rat/ Monkey ICOS (clone C398.4A) (stimulating)	BioXCell	BE0353	AB_2894772
Anti-Mouse IL10R (clone 1B1.3A)	BioXCell	BE0050	AB_1107611
Anti-Mouse CD3ε (clone 145-2C11	BioLegend	100301	AB_312666

Table 2-3: Functional Antibodies

Chemicals, Peptides, Cell Lines and Recombinant Proteins	Source	Identifier
MBP Ac1-9[4Y] peptide AcASQYRPSQR	GL Biochem Shanghai	Custom product
Cancer cell line: MC38	Prof. David Withers (University of Birmingham)	CVCL_B288
RPMI 1640 with L-Glutamine	Thermo Fisher	Cat# 21875-034
DNase I, Grade II	Roche	Cat# 10104159001
Collagenase D	Roche	Cat# 11088858001
Foetal Bovine Serum, qualified, heat inactivated, Brazil	Thermo Fisher	Cat# 10500064
Recombinant Mouse IFNγ (Animal-Free)	BioLegend	Cat# 714006
Recombinant Mouse IL-27 (Carrier-Free)	BioLegend	Cat# 577402
β-Mercaptoethanol	Merck	Cat# 444203

Table 2-4: Chemicals, Peptides, Cell Lines and Recombinant Proteins

Critical Commercial Assays	Source	Identifier
eFluor780 fixable viability dye	eBioscience	Cat# 65-0865-14
UltraComp eBeads™ Compensation Beads	Invitrogen	Cat# 01-2222-41
eBioscience™ FoxP3/Transcription Factor Staining Buffer Set	Thermo Fisher	Cat# 00-5523-00
eBioscience™ 1X RBC Lysis Buffer	Thermo Fisher	Cat# 00-4333-57
Mouse IL-10 DuoSet ELISA	R&D Systems	Cat# DY417

Table 2-5: Critical Commercial Assays

Software and Algorithms	Source	Identifier
GraphPad Prism 9	GraphPad Inc	https://www.graphpad.com/scientificsoftware/prism/
FlowJo v10	BD Biosciences	https://www.flowjo.com/solutions/flowjo
Sony ID7000 Software	Sony Biotechnology	https://www.sonybiotechnology.com/us/instruments/id7000-spectral-cell-analyzer/software/
R version 4.0	R Core Team	https://www.r-project.org/
DESeq2	Love et al., [331]	PMID: 25516281

Table 2-6: Software and Algorithms

Analysers		Source	Identifier
BD LSR Fortessa		**BD Biosciences**	**Custom Product**
Ultra-violet	355 nm		
Violet	405 nm		
Blue	488 nm		
Yellow-Green	561 nm		
Red	640 nm		
BD FACS ARIA FUSION		**BD Biosciences**	**Custom Product**
Ultra-violet	355 nm		
Violet	405 nm		
Blue	488 nm		
Yellow-Green	561 nm		
Red	640 nm		
ID7000 Spectral Cell Analyzer		**Sony Biotechnology**	**Custom Product**
Ultra-violet	355 nm		
Violet	405 nm		
Blue	488 nm		
Yellow-Green	561 nm		
Red	637 nm		

Table 2-7: Flow and Spectral Analysers

Chapter 3 : Tr1-like Development in a Murine Model of Rapid Tolerance Induction

3.1 Introduction

3.1.1 Tg4 Model

Tg4 mice express a rearranged transgenic T cell receptor with Vα 4/Vβ 8.2 chains, generated from T cell hybridoma cDNA that was raised against MBP. T cells from these mice, which are from an H-2^U background, express Tg4-TCRs which are MHCII restricted and recognise the immunodominant epitope of MBP – specifically the acetylated N-terminal nonamer Ac1-9. The native Ac1-9 peptide has a low affinity for MHCII I-A^U restriction element, allowing autoreactive T cells to possibly escape self-tolerance [268].

However, this low affinity native Ac1-9 permitting escape of autoreactive T cells is because of unstable complex formation with I-A^U. Within the Ac1-9 nonamer, Glutamine (Q) and Proline (P) in the 3^{rd} and 6^{th} position respectively (3Q and 6P) interact with the TCR, while Lysine (K) and Arginine (R) in the 4^{th} and 5^{th} (4K and 5R) interact with the I-A^U restriction element within MHCII [332]. Replacing the 4K with a tyrosine (Y) significantly increases the affinity for the peptide binding site. Amino acid substitutions within TCR interacting residues can induce different qualitative activation of the same T cell clone. Whilst the native Ac1-9 MBP has low affinity with class II (I-A^U) and lies below the threshold of tolerance, this can be altered through modification of the principal anchor residue; lysine at the 4^{th} (4K) position. Being non-hydrophobic and of smaller size, it fits poorly into the major hydrophobic pocket of I-A^U, a restriction element of MHCII [273]. Mutated peptide analogues that swap 4K for alanine or valine increase affinity, but tyrosine (4Y) demonstrated much stronger affinity than others tested [268]. The higher affinity peptide allows the autoreactive Tg4-TCR to recognise the MBP peptide and mount a stronger tolerogenic response against it, judged by

CD69 upregulation, clonal deletion of DP thymocytes, and TCR modulation by $CD4^+$ thymocytes.

When Tg4 mice are administered spinal cord homogenate in combination with CFA containing heat-killed *Mycobacterium tuberculosis* and pertussis toxin, they break tolerance and develop EAE. Using the Tg4 model in a ten day intranasal administration of 100 µg peptide, lower affinity encephalitogenic [4A] or [4K]-MBP conferred partial protection against EAE, induced three days after the final dose [270]. However higher affinity peptide [4Y]-MBP provided complete protection. Gabryšová et al demonstrate that repeated intranasal doses of higher affinity peptides are protective against EAE, and that this increase is associated with anergy and IL-10 secretion and thus, induction of tolerance in reactive cells. IL-10^+ Tregs express IFNγ under 4 hr restimulation, measured by intracellular cytokine staining. Repeated administration of high affinity peptide leads to a shift in cytokine secretion away from IL-2 and IFNγ to IL-10, but not TGFβ, also reducing $CD4^+$ T cell proliferation capacity [267, 274]. These IL-10^+ $CD4^+$ T cells suppressed proliferating responder cells and were found to be FoxP3 negative and originated from Th1 cells [135, 269, 275].

Burton et al., 2014 use a model of antigen-specific immunotherapy, which aims to establish immunological tolerance without compromising function of the immune system [276]. Starting with very low doses of [4Y]-MBP, they escalate from 0.08 µg to 0.8 µg, then to 8 µg and in certain experiments up to 80 µg, with 3-4 days between treatments. Through escalating dose immunotherapy, not only were Tg4 mice protected from EAE by day 30, but transcriptional and cytometric analysis of IL-10^+ T cells demonstrated positively correlating expression of LAG3, cMaf, TIGIT, PD-1, CD49 and TIM-3 – markers associated with Tr1 cells.

Bevington et al., 2020 show that tolerization of T cells reprogrammes their potential inducible gene expression and that these modifications occur epigenetically. This chromatin remodelling occurs via different DNase I hypersensitive sites in tolerant versus naive T cells, wherein TCR signalling complexes are disrupted in tolerant T cells, including of TCR : CD28 signalling [333].

3.1.2 *Il10* Expression in Rapidly Induced Tr1 cells

Elliot et al., 2021 demonstrate that increasing high-affinity antigen dose in crossed Tg4 *Nr4a3*-Tocky transgenic mice drives digital, yet graded responses from $CD4^+$ T cells both at population and phenotypic levels. They also show that the activation threshold of *Nr4a3* in $CD4^+$ T cells is calibrated by antigen dose dependent negative feedback though *Il10* expression, and that co-inhibitory receptors such as PD-1 and LAG3 (often the target of immune checkpoint blockade) exert control over T cell reactivation after a second stimulation with [4Y]-MBP. This study established a $CD4^+$ T cell metric indicative of strong TCR signalling (called TCR.Strong metric – *Ox40, Icos, Irf8*), which was identified through comparative transcriptional analyses of murine T cells undergoing strong TCR signalling or anti-PD-1 treatment and comparing that to human melanoma samples on anti-PD-1 immunotherapy. In anti-PD-L1 treated tumours, $CD4^+$ TILs show enhanced expression of strong TCR signalling markers compared to isotype treated. Antigen dose also correlates to increasing *Il10*-GFP expression and is associated with stronger TCR signalling, including expression of TIGIT, CTLA-4, LAG3 and PD-1 [325], which includes markers of Tr1-like cells.

Given that Bevington et al shows Tr1 generation by day 30 in an EDI model following high dose of high affinity antigen, but Elliot et al show Tr1 markers by 24 hr in a high dose primary immunisation model, the aim of this chapter was to establish a model for

the rapid induction of Tr1-like cells and understand their cellular phenotype and ontogeny.

3.2 Results

3.2.1 CD4$^+$ splenocyte *Il10* transcription and TCR signalling reporters respond to increasing primary *in vivo* immunising dose.

NFAT, AP-1 and NF-κB initiate transcription of immediate early genes and are activated by TCR signalling, including the NR4A family of orphan nuclear receptors [334]. *Nr4a1*-GFP mice have been used to analyse TCR signal strength, but the half-life prevented analysis of downstream TCR signalling dynamics [23, 335]. The *Nr4a1* relative *Nr4a3* is an NFAT- and calcineurin-dependent transcriptional activator that in T cells is only produced via TCR binding and downstream signalling [336]. Thus, it can be used as a proxy marker for TCR specific T cell activation. The attached Timer protein is a mutated, fluorescent mCherry protein with a half-life of ~4 hr that is detectable in the BV421 channel on a conventional flow cytometer in its initial "blue" form (Timer Blue). After this, it spontaneously converts to a "red" form (Timer Red), detectable in the mCherry or PE-Texas Red channel [337]. By measuring both on a Tocky plot (Timer Blue on Y-axis against Timer Red on X-axis), we can determine whether a population has been recently activated (Timer Blue$^+$, Timer Red$^-$), persistently activated (Timer Blue$^+$, Timer Red$^+$) or if activation has ceased (Timer Blue, Timer Red$^+$).

In Elliot et al., 2021, a single dose of [4Y]-MBP peptide was sufficient to induce a population of CD4$^+$ *Nr4a3*-Timer$^+$ T cells to express *Il10*-GFP, and that the frequency of *Il10*-GFP responders was positively correlated with peptide dose. We first wanted to replicate this finding in the *Nr4a3*-Timer$^+$ and investigate if the same effect is found in the *Nr4a3*-Timer$^-$ cells. Nr4a3-Tocky Tg4 reporter mice were immunised with 0.8, 8 or 80 µg of [4Y]-MBP and splenic CD4$^+$ T cells analysed 24 hr later for *Nr4a3*-Timer (fig.

3-1A) and *Il10*-GFP (fig. 3-1B) expression. We used these doses to demonstrate that *Il10*-GFP expression is graded by the strength of the TCR stimulus.

Figure 3-1A clearly shows population shifts from the *Nr4a3*-Timer$^-$ to *Nr4a3*-Timer$^+$ from 0.8 µg to 8 µg, and further to 80 µg. Administration of the [4Y]-MBP induces *Nr4a3*-Timer expression, and a higher frequency of CD4$^+$ T cells respond to increasing primary immunising dose. Figure 3-1B also shows increasing *Il10*-GFP$^+$ T cells with increasing dose. Increases in *Nr4a3*-Timer$^+$ population frequencies are significant (fig. 3-1C). Likewise, in the *Nr4a3*-Timer$^+$ population, *Il10*-GFP$^+$ frequency significantly increases with increasing peptide dose (fig. 3-1D), and whilst the same is true for *Il10*-GFP$^+$ splenocytes from the *N4a3*-Timer$^-$ population, they contain much fewer *Il10*-GFP$^+$ T cells (note the same scale on figs 3-1D and 3-1E).

These data show that increasing dose increases the frequency of responders (*Nr4a3*-Timer$^+$) and CD4$^+$ T cell *Il10*-GFP expressors. This *Il10*-GFP expression appears to be dose-dependent i.e. graded. Graded expression of *Il10*-GFP expression is seen in both *Nr4a3*-Timer$^+$ and *Nr4a3*-Timer$^-$ cells, but to a lesser extent in the latter. We then investigated whether this increase was related to an increase in markers of strong TCR signalling, as defined by Elliot et al., 2021.

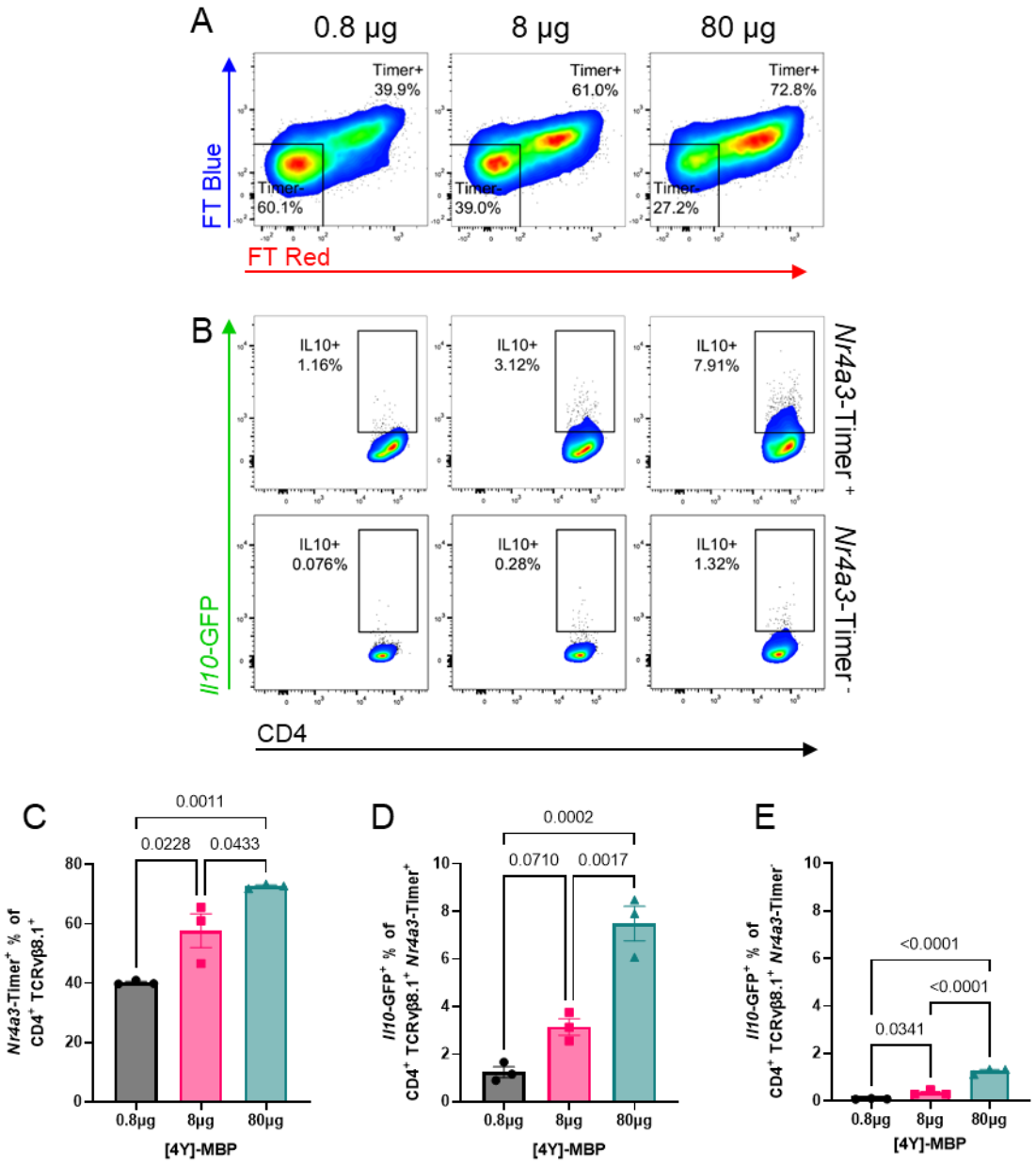

Figure 3-1: CD4$^+$ splenocyte *Il10* transcription and TCR signalling reporters respond to increasing primary *in vivo* immunising dose.
Nr4a3-Tocky Tg4 *Ifng*-YFP *Il10*-GFP mice were immunised with 0.8 µg, 8 µg and 80 µg [4Y]-MBP in 100 µL PBS s.c. **(A)** Splenic CD4$^+$ TCRvβ8.1$^+$ cells were analysed 24 hr post-injection for *Nr4a3*-Timer (FT Blue vs FT Red) expression. **(B)** CD4$^+$ TCRvβ8.1$^+$ *Nr4a3*-Timer$^+$ cells were analysed for *Il10*-GFP expression. Summary of *Nr4a3*-Timer$^+$ frequency **(C)** from **(A)**. Summary of *Il10*-GFP$^+$ in *Nr4a3*-Timer$^+$ **(D)** and *Nr4a3*-Timer$^-$ **(E)** frequency from **(B)**. **(C-E)** from n=3 mice per [4Y]-MBP dose, bars represent mean ±SEM, statistical analysis by one-way ANOVA with Tukey's multiple comparison test. One representative of two experiments.

3.2.2 CD4$^+$ T cell regulation associated markers positively respond to increasing primary *in vivo* immunising dose.

Measuring LAG3 and TIGIT allows us to gauge what tolerogenic activity [4Y]-MBP may be inducing and deeper phenotype *Il10*-GFP CD4$^+$ T cells. Nr4a3-Tocky Tg4 reporter mice were immunised with 0.8, 8 or 80 µg of [4Y]-MBP and their CD4$^+$ T cells analysed 24 hr later for expression.

In the heatmap plots of fig. 3-2A, at all doses but especially prominent at 80 µg, the *Nr4a3*-Timer$^-$ population has a darker colouration, denoting less expression than the lighter found on *Nr4a3*-Timer$^+$. Figures 3-2C and 3-2D show that with increasing dose, there is significantly increasing intensity of TIGIT and LAG3 expression respectively on *Nr4a3*-Timer$^+$ cells. For LAG3, this is only between 8 and 80 µg. TIGIT and LAG3 expression is more significantly intense on *Il10*-GFP$^+$ than *Il10*-GFP$^-$ (fig. 3-2E and 3-2F respectively) across all doses, and TIGIT and LAG3 expression on both *Il10*-GFP$^+$ and *Il10*-GFP$^-$ correlate with peptide dose.

The increased intensity of TIGIT and LAG3 expression, as well as *Il10*-GFP frequency within 24 hr of Tg4-specific peptide [4Y]-MBP administration suggests that a Tr1-like cell differentiation is achievable with a single dose of high affinity self-peptide, with a stronger response at higher doses. Interestingly, the increase in *Il10*-GFP$^+$ frequency (fig. 3-1B) of *Nr4a3*-Timer$^+$ does not equate to a statistically significant increase in MFI (fig. 3-2B), although there is a small positive trend at 80 µg. We decided to next investigate when the Tr1-like phenotype arises after peptide immunisation.

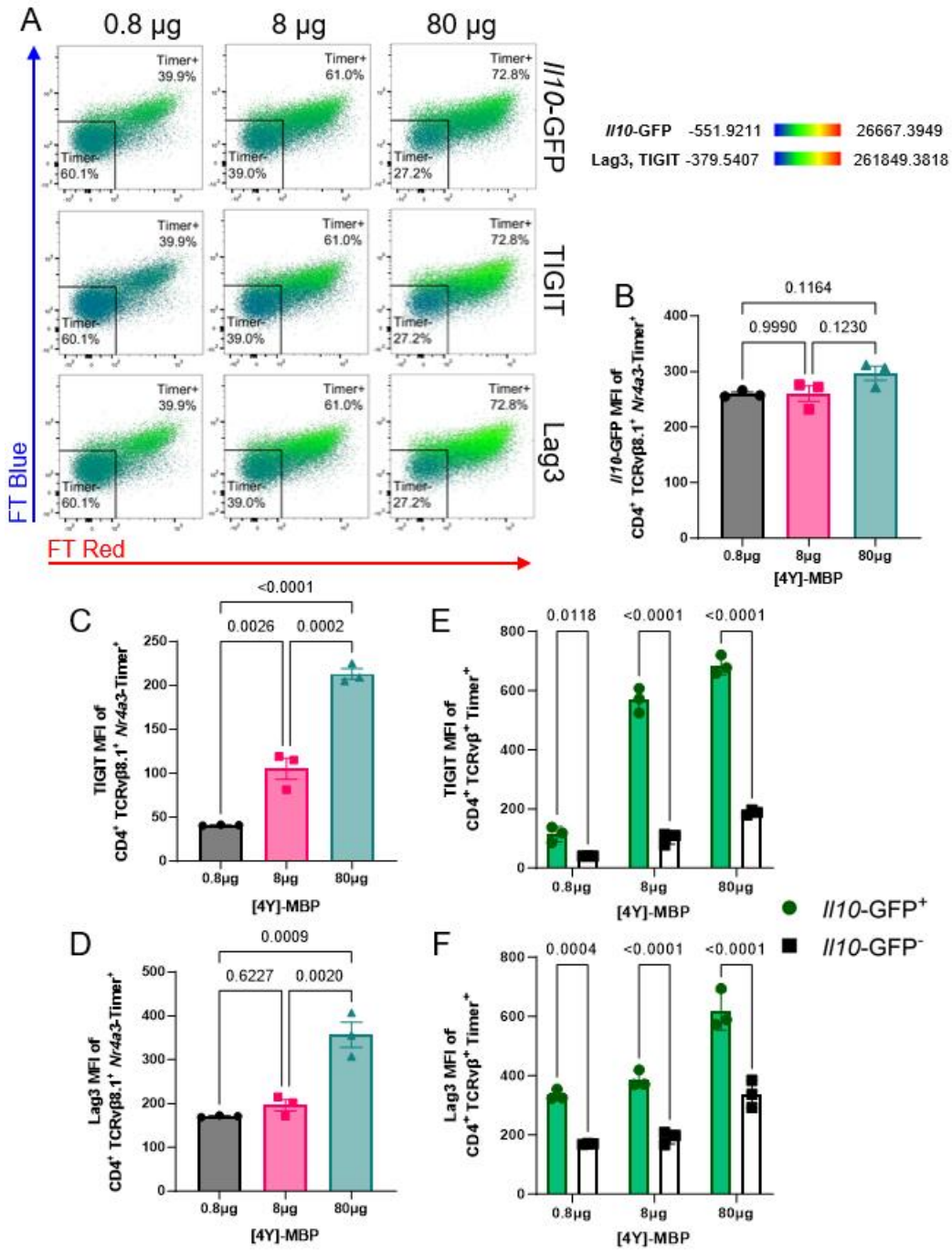

Figure 3-2: CD4$^+$ T cell regulation associated markers positively respond to increasing primary *in vivo* immunising dose.
Nr4a3-Tocky Tg4 *Ifng*-YFP *Il10*-GFP mice were immunised with 0.8 µg, 8 µg and 80 µg [4Y]-MBP in 100 µL PBS s.c. **(A)** Splenic CD4$^+$ TCRvβ8.1$^+$ cells were analysed for *Il10*-GFP, TIGIT and LAG3 MFI at 24 in *Nr4a3*-Timer$^+$ cells. Summary of **(B)** *Il10*-GFP, **(C)** TIGIT and **(D)** LAG3 MFIs from **(A)**. Summary of TIGIT **(E)** and LAG3 **(F)** MFI in *Il10*-GFP$^+$ and *Il10*-GFP$^-$ populations from *Nr4a3*-Timer$^+$. **(B-D)** from n=3 mice per [4Y]-MBP dose, bars represent mean ±SEM, statistical analysis by one-way ANOVA with Tukey's multiple comparisons test **(B-D)** and two-way ANOVA (**E, F**). One representative of two experiments.

3.2.3 High dose primary immunisation induces temporally dynamic TCR signalling reporter

By 24 hr post-injection of high affinity peptide, we saw changes in marker expression that suggest a Tr1-like cell induction. By giving higher doses, we saw higher expression of co-inhibitory receptors. To understand the kinetics of the Tr1-like cell emergence we performed kinetic analysis at high antigen dose. Given that past data has suggested that *Il10*-GFP production can arise from *Ifng* producers in these experiments we incorporated an *Ifng*-YFP reporter for a comparison of induction kinetics and to what extent *Il10*-GFP$^+$ T cells co-produced *Ifng* [270].

After administering 80 µg peptide we measured *Nr4a3*-Timer expression in CD4$^+$ splenocytes at 8, 12 and 16 hr. Figure 3-3B shows that there is no significant increase in the frequency of total *Nr4a3*-Timer$^+$ cells post peptide, regardless of Blue/Red state. Figure 3-3A shows the shift from being mostly Timer Blue at 8 hr, to an intermediate blue-red state by 12 hr, with minor change between 12 and 16 hrs. This change is reflected by figures 3-3C and 3-3D; by 16 hr there is no further change in Timer Blue intensity, but the population has increasing Timer Red intensity. Measuring these changes as a ratio in fig. 3-3E, a more direct relationship is shown; as Timer Red become more intense and dominates the population as it approaches the “arrested” phase, Timer Blue diminishes. In these populations, T cells undergo activation and then shut down signalling around 12-16hrs according to *Nr4a3*-Timer expression. We next determined the expression patterns of *Il10* and *Ifng*.

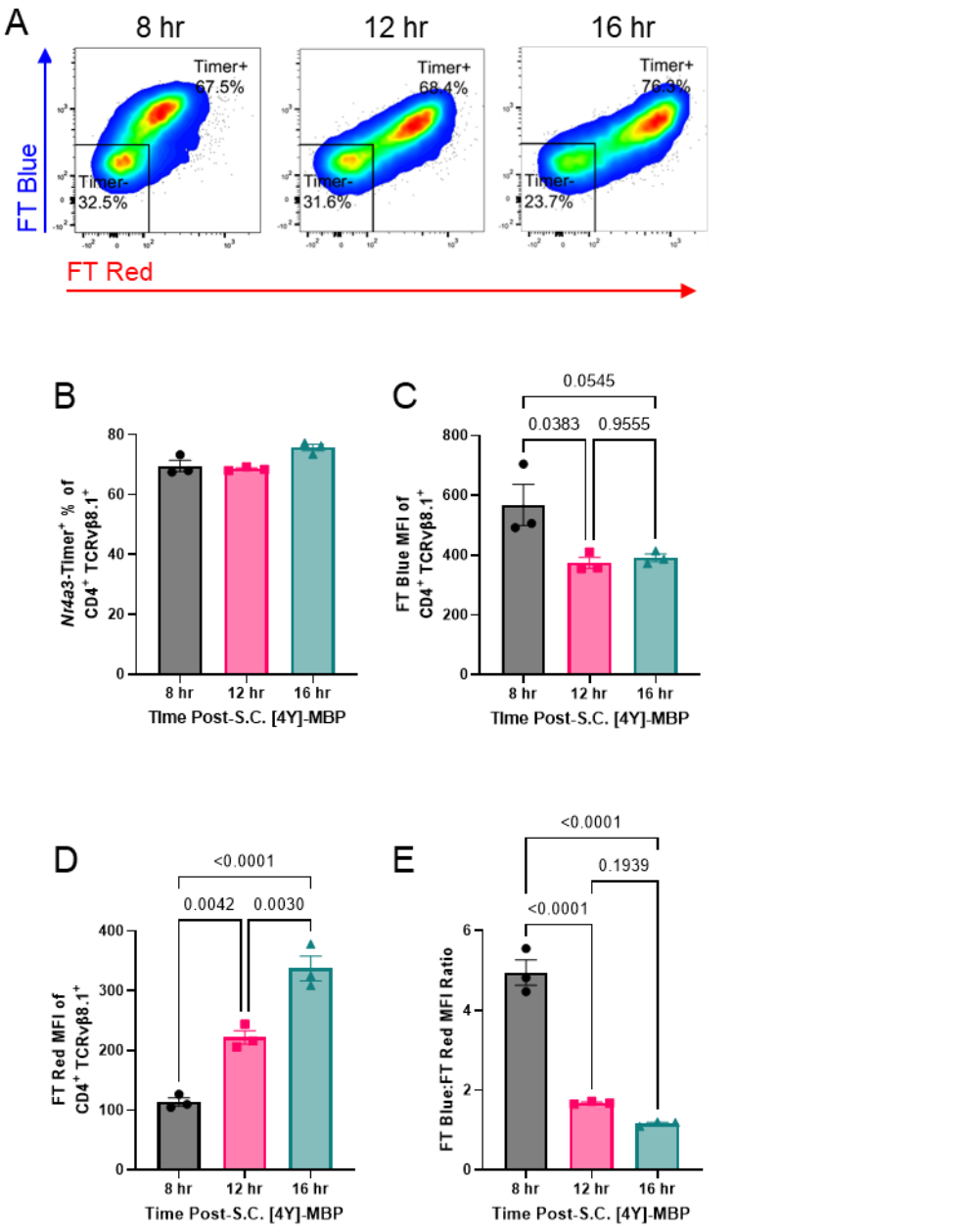

Figure 3-3: High dose primary immunisation induces temporally dynamic TCR signalling reporter

Nr4a3-Tocky Tg4 *Ifng*-YFP *Il10*-GFP mice were immunised with a single dose of 80 µg [4Y]-MBP in 100 µl PBS s.c. and analysed at 8 hr, 12 hr and 16 hr post-injection. **(A)** Splenic CD4$^+$ TCRvβ8.1$^+$ cells were analysed for *Nr4a3*-Timer (FT Blue vs FT Red) expression at the time points indicated. **(B)** Summary of *Nr4a3*-Timer$^+$ frequency **(A)**. MFI changes in CD4$^+$ TCRvβ8.1$^+$ for FT Blue **(C)** and FT Red **(D)**. **(E)** Ratio of FT Blue: FT Red MFI in CD4$^+$ TCRvβ8.1$^+$ cells. **(B-E)** from n=3 mice per time point, bars represent mean ±SEM, statistical analysis by one-way ANOVA with Tukey's multiple comparisons test. One representative of two experiments.

3.2.4 High dose primary immunisation initiates de novo *Il10* and *Ifng* transcription reporter.

Following early TCR signalling kinetic analysis at high dose, we investigated the early (8, 12, 16 hr) cytokine reporter kinetics at high dose (80 µg). At these early time points, we can see that both *Il10*-GFP and *Ifng*-YFP populations in the *Nr4a3*-Timer$^+$ fraction arise between 8 and 12 hrs, continuing to rise afterwards (figs 3-4A and 3-4B). Before then, the cytokine reporter populations (figs 3-4D and 3-4F) show frequencies like the 8 µg dose at 24 hr (fig. 3-1B). The intensity of this fluorescence increases for *Il10*-GFP (fig. 3-4E), but not for *Ifng*-YFP (fig. 3-4G), in *Nr4a3*-Timer$^+$ cells as time progresses. We also see that there are few *Il10*-GFP and *Ifng*-YFP co-expressors (fig. 3-4C), that largely the CD4$^+$ *Nr4a3*-Timer$^+$ expression one reporter or neither, but seldom both. So exclusive induction of *Il10*-GFP and *Ifng*-YFP is delayed in relation to the initial TCR signal.

3.2.5 Early induction of markers associated with regulation following strong TCR stimulus

Reporter kinetics showed cytokine transcription following TCR signalling, but it is unknown if these early kinetics align with strong TCR signalling markers and a Tr1-like phenotype, so we investigated expression of these markers, alongside *Il10*-GFP as a Tr1 indicator, over the first 16 hours of stimulation with high-dose peptide. In figure 3-5A we can see that the *Nr4a3*-Timer$^-$ population is unchanging in its expression of these markers, whereas the *Nr4a3*-Timer$^+$ population instead becomes increasingly lighter in colour, reflecting increasing intensity of expression for LAG3, PD-1, TIGIT, and CD25 (figs. 3-5B/C/D/E respectively).

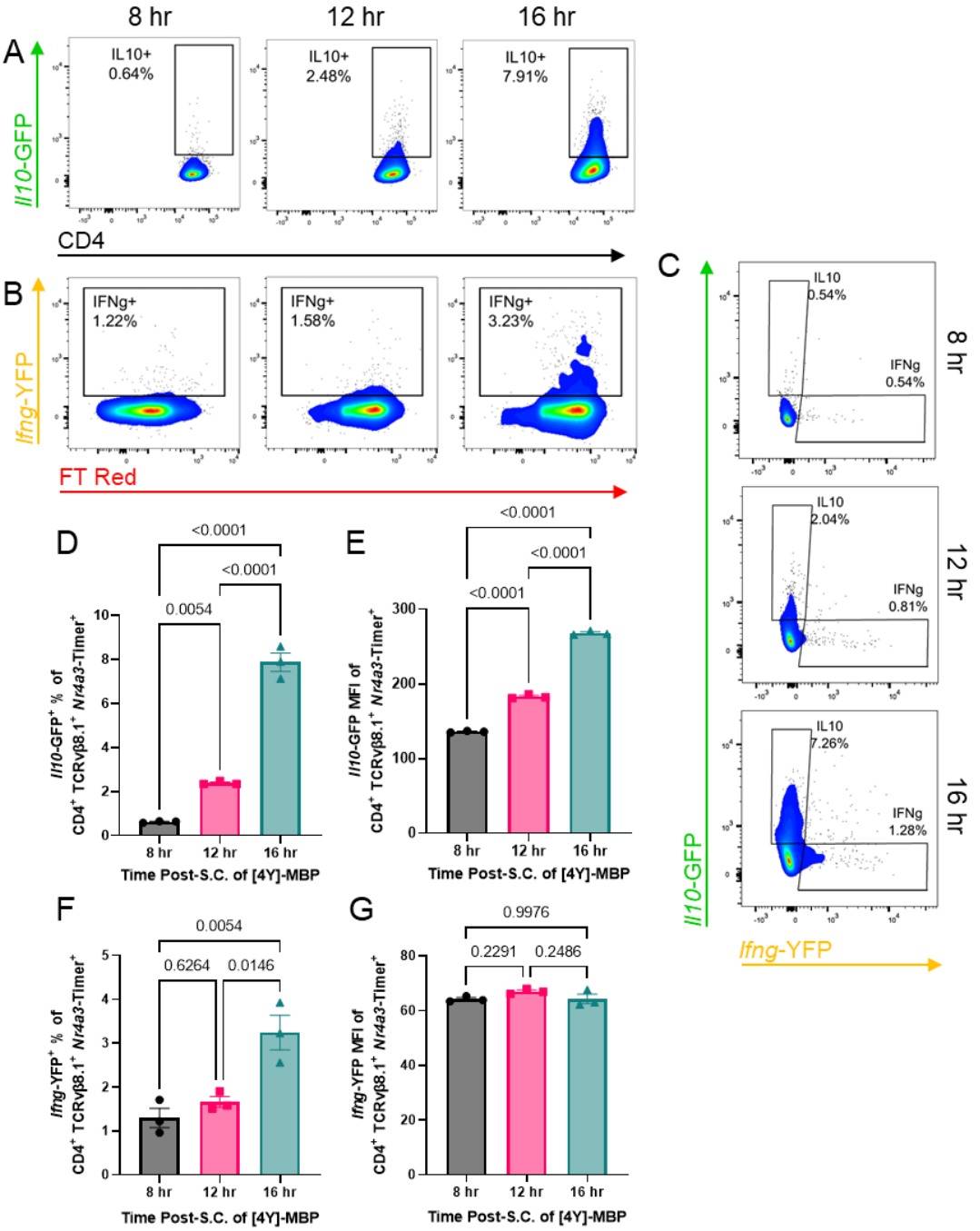

Figure 3-4: High dose primary immunisation initiates *de novo Il10* and *Ifng* transcription reporter.
Nr4a3-Tocky Tg4 *Ifng*-YFP *Il10*-GFP mice were immunised 80 µg [4Y]-MBP in 100 µL PBS s.c. and analysed at 8 hr, 12 hr and 16 hr post-injection. Splenic $CD4^+$ $TCRvβ8.1^+$ *Nr4a3*-$Timer^+$ T cells were analysed for **(A)** *Il10*-GFP and **(B)** *Ifng*-YFP expression. **(C)** *Il10*-GFP vs *Ifng*-YFP from *Nr4a3*-$Timer^+$. Summary of **(A)** as *Il10*-GFP frequency **(D)** and MFI **(E)**. Summary of **(B)** as *Ifng*-YFP frequency **(F)** and MFI **(G)**. **(D-G)** from n=3 mice per time point, bars represent mean ±SEM, statistical analysis by one-way ANOVA with Tukey's multiple comparisons test. One representative of two experiments.

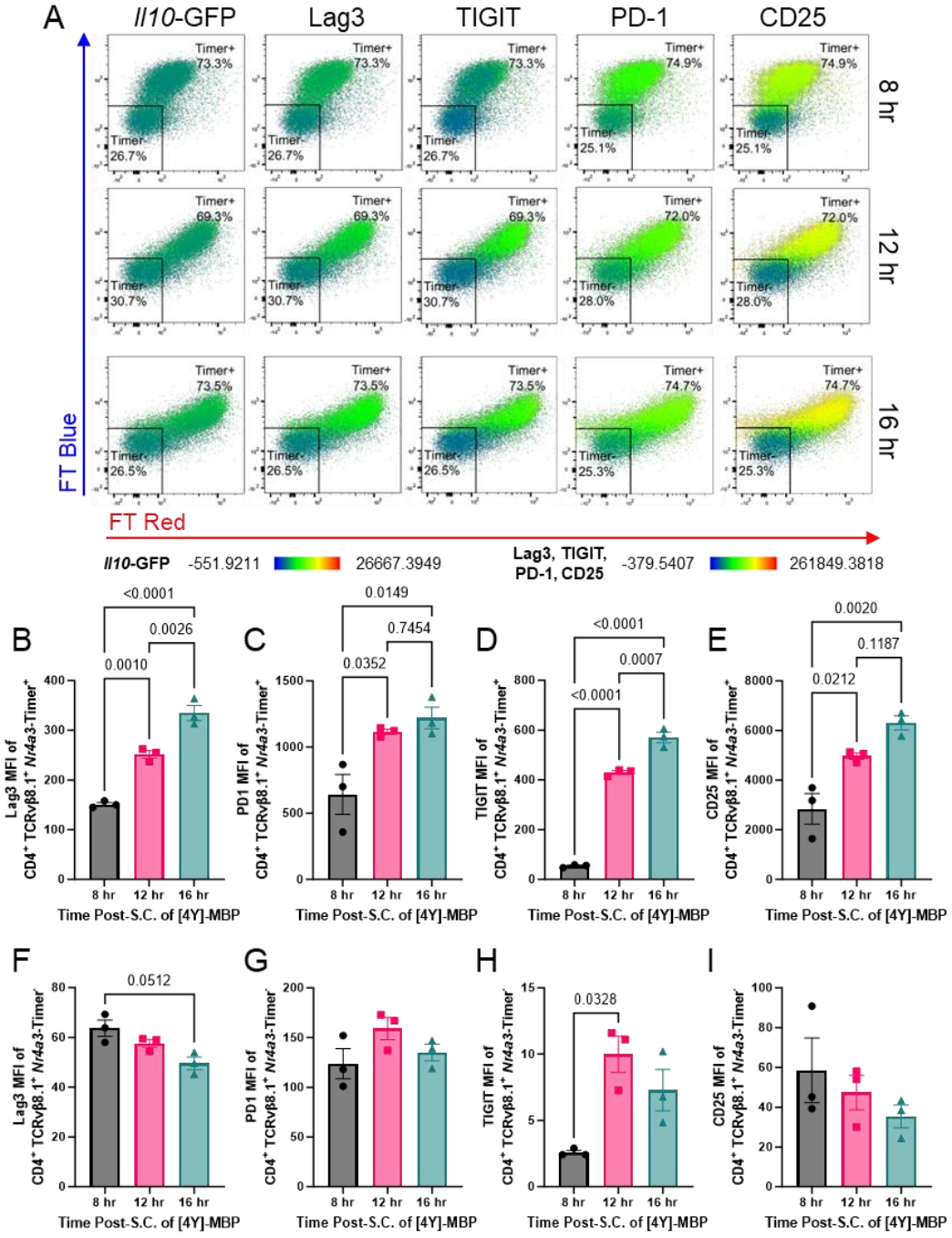

Figure 3-5: Early induction of markers associated with regulation following strong TCR stimulus

Nr4a3-Tocky Tg4 *Ifng*-YFP *Il10*-GFP mice were immunised 80 µg [4Y]-MBP in 100 µL PBS s.c. and analysed at 8 hr, 12 hr and 16 hr post-injection. **(A)** Splenic CD4$^+$ TCRvβ8.1$^+$ were analysed for *Il10*-GFP, LAG3, TIGIT, PD-1 and CD25 according to *Nr4a3*-Timer (FT Blue vs FT Red) expression. Summary of LAG3 **(B),** PD-1 **(C),** TIGIT **(D)** and CD25 **(E)** MFI from *Nr4a3*-Timer$^+$ in **(A)**. Summary of LAG3 **(F),** PD-1 **(G),** TIGIT **(H)** and CD25 **(I)** MFI from *Nr4a3*-Timer$^-$ in **(A)**. **(B-I)** from n=3 mice per time point, bars represent mean ±SEM, statistical analysis by one-way ANOVA with Tukey's multiple comparisons test. One representative of two experiments.

The range of MFIs of LAG3, PD-1, TIGIT and CD25 in *Nr4a3*-Timer$^-$ T cells are much lower than their *Nr4a3*-Timer$^+$ equivalents (fig. 3-5F-I, respectively), nor do they follow the same trend as those in the *Nr4a3*-Timer$^+$ cells. TIGIT, LAG3 and CD25 arise with similar kinetics to *Il10*-GFP, implying induction of a similar phenotype following TCR signalling, but there are other more classical markers of T cell activation that we have not yet observed.

3.2.6 Early changes in markers associated with activation following strong TCR stimulus

T cell regulation markers delineated according to downstream TCR signalling reporter and showed similar kinetics to cytokine induction, but what effect this may have on T cell activation markers, such as CD69 and CD44 is unknown. These are more typical surface markers of T cell activation than *Nr4a3* signalling, but unlike *Nr4a3*-Timer, are not exclusively expressed because of TCR mediated activation, but can represent bystander activation, for example. So, we investigated expression of these markers together with cytokine reporters following 8, 12 and 16 hr stimulation with high dose (80 µg). We can see in figure 3-6A that CD69 and CD44 appear to be slightly more intense in the *Nr4a3*-Timer$^+$ throughout. CD69 in *Nr4a3*-Timer$^+$ has a slight decreasing trend (fig. 3-6B) while CD44 shows significant increases up to 12 hr, and then continuing the positive trend (fig. 3-6C). This implies that CD69 was rapidly expressed (< 8 hr) because of TCR signalling and does not follow the trend of our cytokine reporters or regulation markers. CD44, however, does follow the previously seen trend in Nr4a3-Timer$^+$ and is a late marker of T cell activation. In the *Nr4a3*-Timer$^-$ population, CD69 MFI is decreasing faster than *Nr4a3*-Timer$^+$, and with overall lower intensity than *Nr4a3*-Timer$^+$ (fig. 3-6D). CD44 MFI does not follow the same trend in the *Nr4a3*-

Timer^{+} as it peaks at 12 hr, before dipping at 16 hr (fig. 3-6E). Classical marker CD69 do not follow the same pattern as our reporters or regulatory markers in *Nr4a3*-Timer^{+} populations of figure 3-5. CD44 progressively rises reflecting recent activation, but CD69 remains high despite termination of TCR signals. CD69 becomes decoupled from reflecting 'real-time' T cell activation *in vivo*. Given the suggested regulatory phenotype induction by [4Y]-MBP in our *Il10*-GFP^{+}, we more closely examined the regulatory phenotype of these TCR activated cells.

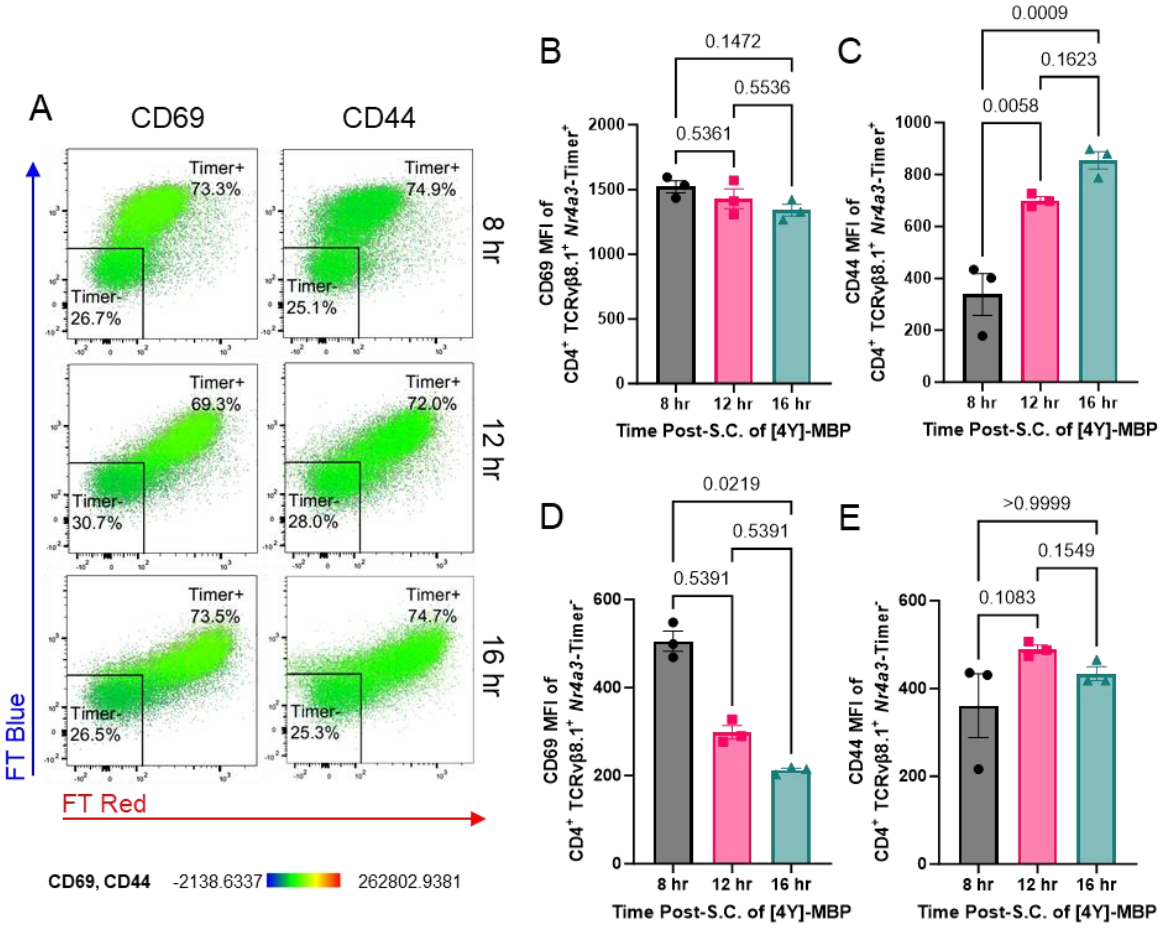

Figure 3-6: Early changes in markers associated with activation following strong TCR stimulus

Nr4a3-Tocky Tg4 *Ifng*-YFP *Il10*-GFP mice were immunised 80 µg [4Y]-MBP in 100 µL PBS s.c. and analysed at 8 hr, 12 hr and 16 hr post-injection. **(A)** Splenic CD4$^+$ TCRvβ8.1$^+$ were analysed for CD69 and CD44 according to *Nr4a3*-Timer (FT Blue vs FT Red) expression. Summary of CD69 **(B)** and CD44 **(C)** from *Nr4a3*-Timer$^+$ in **(A)**. Summary of CD69 **(D)** and CD44 **(E)** from *Nr4a3*-Timer$^-$ in **(A)**. **(B-E)** from n=3 mice per time point, bars represent mean ±SEM, statistical analysis by one-way ANOVA with Tukey's multiple comparisons test. One representative of two experiments.

3.2.7 Low FoxP3 expression in *Il10*-GFP^{+} Tg4 splenocytes

IL-10 is expressed by regulatory CD4^{+} T cells, and we see *Il10*-GFP expression in *Nr4a3*-Timer^{+} T cells with regulatory markers. Also, these Tg4 mice, which are not on a RAG^{KO} background can undergo spontaneous TCRα recombination endogenously in the thymus, producing a different TCR that may be directed into a natural Treg phenotype. FoxP3 is often the dominant Treg subset, but others include Treg 17 and Tr1 cells. We sought to find which subsets were active in the model.

Tg4 *Nr4a3*-Tocky mice were immunised with 4 mg/kg [4Y]-MBP instead of 80 µg as a high peptide dose. This was to refine the protocol and reduce the number of mice required for statistical power. Also, this normalised for weight discrepancies, particularly weight-based sex bias. From this point on, all experiments involving primary immunisation of Tg4 transgenic mice with [4Y]-MBP were conducted with this weight-normalised high dose unless noted. This resulted in a robust response in *Nr4a3*-Timer expression and *Il10*-GFP expression (fig. 3-7A). *Il10*-GFP positive and negative cells from [4Y]-MBP treated CD4^{+} TCRvβ8.1^{+} *Nr4a3*-Timer^{+} populations were sorted by FACS (fig. 3-7A).

The sort was largely successful, with minimal contamination from other populations (fig. 3-7A). Afterwards, the cells were stained intracellularly for FOXP3 (fig. 3-7B), and data acquired by flow cytometry. Due to the fixation/permeabilisation process needed to stain for intracellular markers, fluorescent reporters such as GFP, YFP and Timer are lost during this process. However, given that the populations were sorted according to their reporter status, it is assumed that these populations still phenotypically present as they would have without fix/perm.

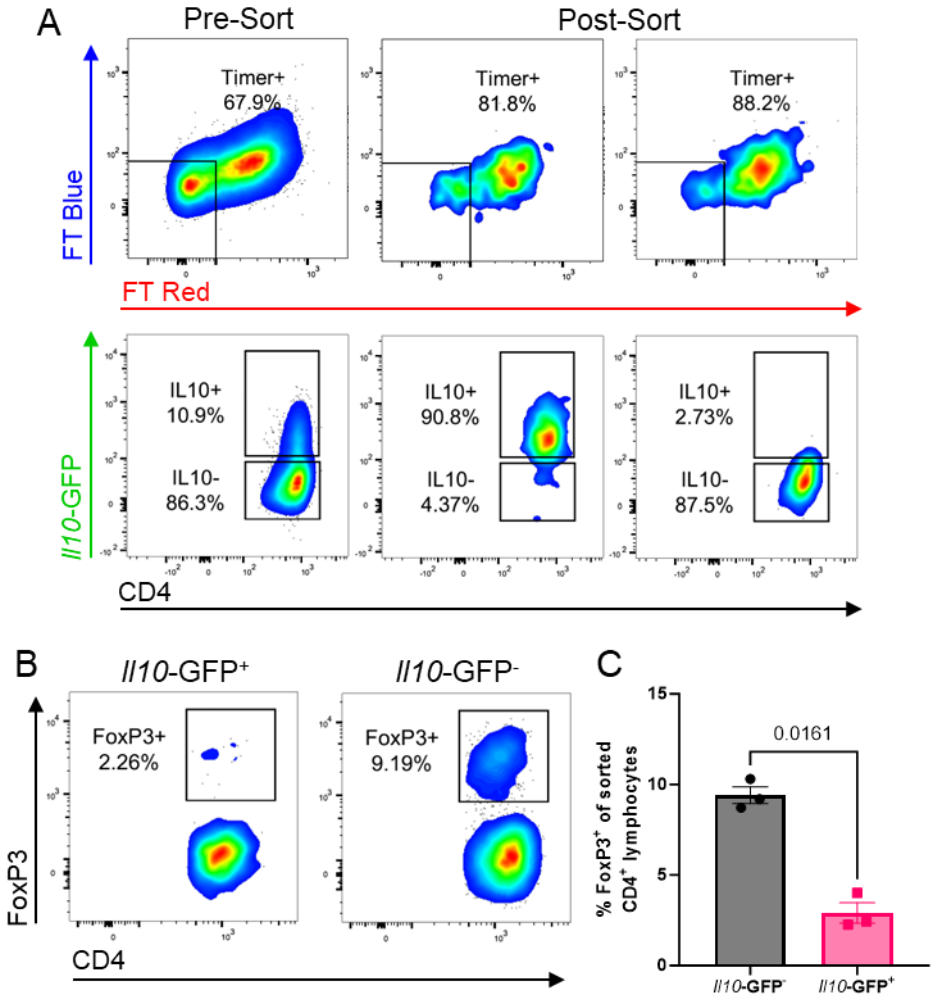

Figure 3-7: Low FOXP3 expression in *Il10*-GFP^{+} Tg4 splenocytes
Nr4a3-Tocky Tg4 *Il10*-GFP mice were immunised with 4 mg/kg [4Y]-MBP in 100 µL PBS s.c. and sorted 24 hr post-injection. **(A)** CD4^{+} TCRvβ8.1^{+} *Nr4a3*-Timer^{+} splenocytes were flow sorted according to *Il10*-GFP expression. **(B)** Sorted *Il10*-GFP cells were analysed for intracellular FoxP3 expression. Summary of FoxP3 frequency **(C)** from **(B)**. **(C)** from n=3 mice, bars represent mean ±SEM, statistical analysis by paired two-tailed t test.

Assuming *Nr4a3*-Timer post-sort positivity, the *Il10*-GFP$^+$ TCR-activated CD4$^+$ T cells in this model are significantly FOXP3$^-$ (fig. 3-7C). Approximately 2 % are FoxP3$^+$, so 98 % are FOXP3$^-$, and probably part of a Treg subset (or subsets) that is not FOXP3 expressing. This shows that *Il10*-GFP$^+$ T cells in the rapid induction model are more likely to reflect Tr1 cells.

3.2.8 Transcriptional profiling of *Il10*-GFP$^+$ vs *Il10*-GFP$^-$ reveals hallmark Tr1 phenotype

To further clarify the phenotype of *Il10*-GFP$^+$ T cells arising in this model, we decided to explore bulk RNA sequencing to transcriptionally profile and assess key CD4$^+$ T cell markers of rapid tolerance induction. We hypothesised that a single high dose of peptide *in vivo* could give rise to transcripts reflective of rapid Tr1 cell development.

Three *Nr4a3*-Tocky Tg4 *Il10*-GFP mice received weight-normalised high dose [4Y]-MBP and the *Nr4a3*-Timer$^+$ splenocytes were flow sorted according to *Il10*-GFP positivity or negativity (fig. 3-8A). Two of these mice (represented by a single plot) appear to be sorted without contamination, however due to time constraints only *Il10*-GFP$^+$ purity checks were taken, and not *Il10*-GFP$^-$. These checks show that the mouse 3 *Il10*-GFP$^+$ sample was over 10% contaminated by *Il10*-GFP$^-$ cells, but more notably had significant contamination from non-CD4s (30-40%; most likely contaminating B cells).

Principal Component Analysis (PCA) summarises information in multivariate datasets by smaller sets of variables to observe trends, clusters, and outliers. Initial PCA (fig. 3-8B) revealed that a single *Il10*-GFP$^+$ and another *Il10*-GFP$^-$ sample sit away from

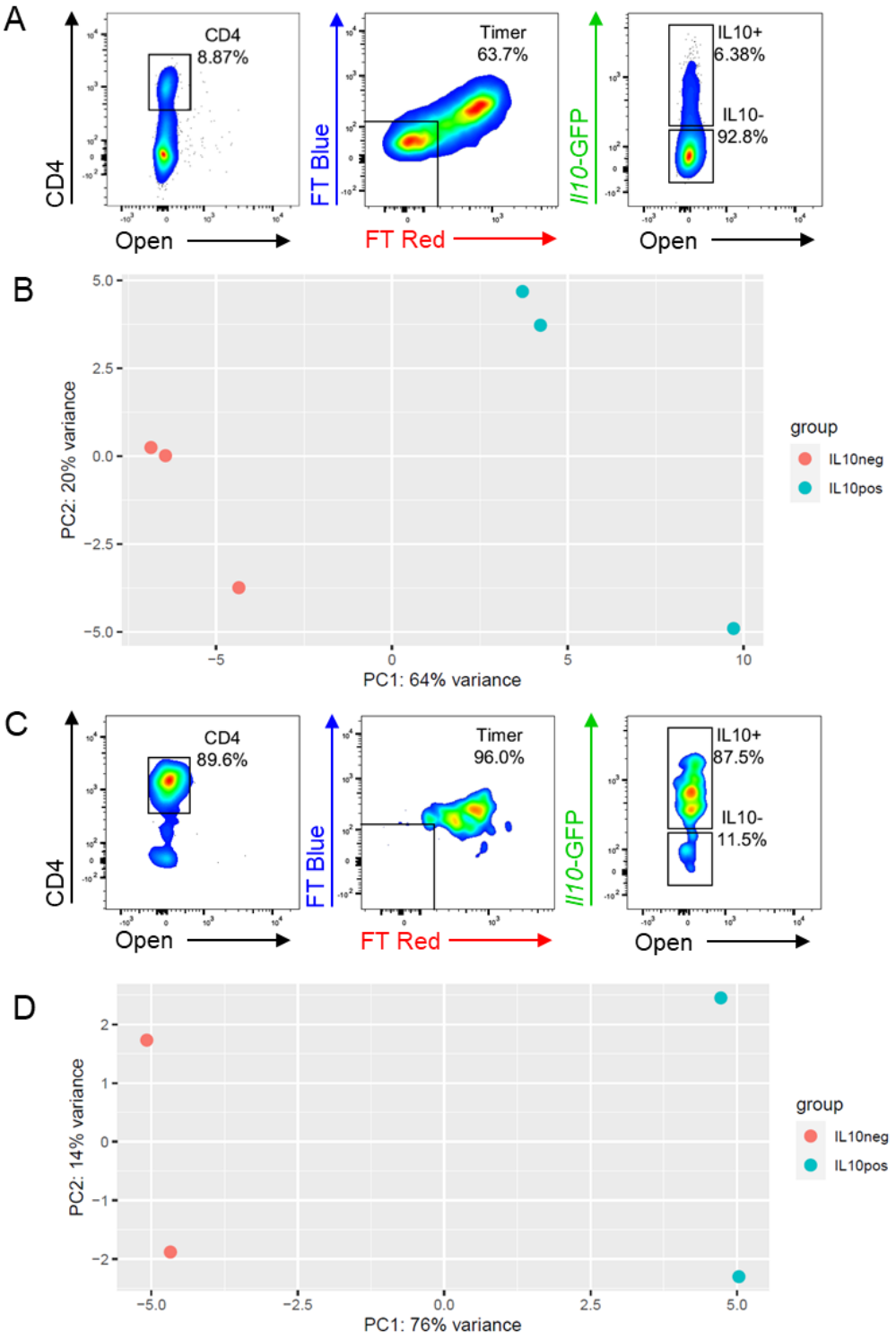

Figure 3-8: Principal component analysis of sorted *Il10*-GFP^{+} T cells
Nr4a3-Tocky Tg4 *Il10*-GFP mice were immunised with 4 mg/kg [4Y]-MBP in 100 µL PBS s.c. and flow sorted 24 hr post-injection. **(A)** CD4^{+} *Nr4a3*-Timer^{+} were flow sorted according to Il10-GFP expression for bulk RNA-seq. **(B)** PCA of sorted *Il10*-GFP+ and *Il10*-GFP^{-} bulk mRNA reads. **(C)** Purity check of outlier samples from PCA **(D)** PCA of **(B)** with outlier samples removed. From n=3 mice, then n=2.

the other clustered samples. These were both mouse 3 samples (already flagged for an issue with the cell sorting), as the mice were coded for RNA-seq, and they were removed from the analysis based on the separation from other clusters in PCA, the presence of non-T cell genes and the purity check (fig. 3-8C). So, we are left with n = 2 per group, and ran another PCA (fig 3-8D), revealing that samples separated largely based on *Il10* transcriptional status.

We defined DEGs based on DESeq2 modelling with a p-adjusted value of <0.05. In an unbiased heatmap of DEGs (fig. 3-9) we see that *Il10*-GFP positive and negative populations have different expression profiles. DEGs with an adjusted P value < 0.05 have been listed in table 3-1 and table 3-2, listing the upregulated and downregulated DEGs respectively. Pathway analysis was not carried out. Many of the increased DEGs are associated with intracellular organisation and mitosis – transcripts whose proteins are involved with formation of the nucleosome, mitotic spindle and cytoskeleton, and mRNA stabilisation. However, there are others that stand out here; *Ctla4*, *Id2*, *Hmgb2* (RAG complex cofactor in VD(J) recombination [338] and also involved in DNA bending), *Gzmb*, *Mki67*, *Ccr7*, *Rora*, *Il7r*, *Maf* and *Icos.*

Decreased DEGs are associated with nucleolus formation, and inflammatory immune response initiation (*Igfbp4, Bach2, Slc10a1*). There are also genes induced by interferon (*Gbp7, Igfbp4, Ifi203*) associated with immune suppression that are spread across increased or decreased DEGs. DEGs related to Tr1 cell phenotype were curated into their own heatmap (fig. 3-10). These were selected from the significantly expressed DEGs as markers known to be associated with Tr1 cells. They were not selected in an unbiased manner.

Genes such as *Prdm1* and *Maf* are essential for *Il10* transcription, and all three are found to be more highly expressed in the *Il10*-GFP positive population than the negative. However, there are also markers of strong TCR signalling, activation and cytotoxicity (*Icos, Gzmb, Ifngr1, Il12rb2*) in the *Il10*-GFP^{+} fraction, which normally wouldn't be associated with the regulatory, anti-inflammatory function of IL-10 [325]. Interestingly, there is also a transcript associated with chromatin bending (*Hmgb2* [339]). Factors that we have uncovered here are similar to findings from Burton et al., 2014, particularly *Il10*, *Icos, Maf, Ctla4* and *Il7r*. This RNA-seq experiment highlighted interesting DEGs between our *Il10*-GFP^{+} and *Il10*-GFP^{-} populations, particularly in negative immune regulation. Importantly, the transcriptome suggests expression of a Tr1-like phenotype.

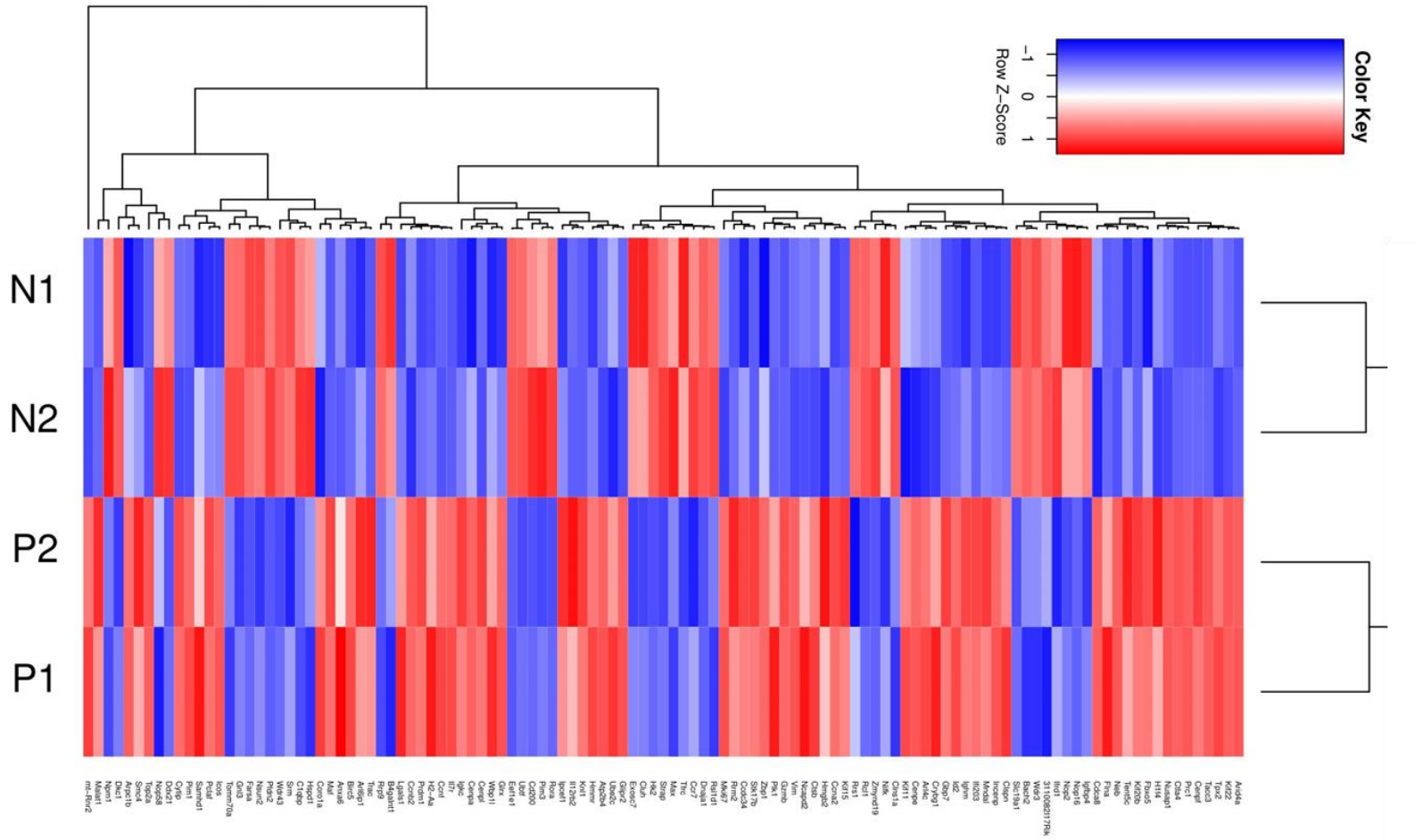

Figure 3-9: Unbiased heatmap of differentially expressed genes in Il10-GFP$^{+/-}$ T cells
Nr4a3-Tocky Tg4 *Il10*-GFP mice were immunised with 4 mg/kg [4Y]-MBP in PBS s.c. and sorted 24 hr post-injection for Timer^{+} CD4^{+} T cells. Following principal component analysis, the transcriptome was used to generate a heatmap from the most differentially expressed genes in an unbiased manner. “N” refers to *Il10*-GFP negative and “P” to *Il10*-GFP positive cells. From n=2 mice.

Gene	log2Fold Change	pvalue	padj
Top2a	0.831305	2.88E-15	1.16E-11
Mki67	1.427824	6.91E-13	1.39E-09
Maf	0.922491	1.04E-11	1.39E-08
Vim	1.437693	4.27E-11	3.43E-08
Igkc	2.761886	5.16E-11	3.45E-08
Gbp7	1.456957	4.22E-10	2.23E-07
Gzmb	1.351334	4.45E-10	2.23E-07
Birc5	0.899186	8.86E-10	3.96E-07
Pclaf	0.916288	4.85E-09	1.95E-06
Id2	1.205888	5.41E-08	1.81E-05
Nusap1	1.295716	6.56E-08	1.88E-05
Plk1	1.169251	6.50E-08	1.88E-05
Prc1	1.089719	1.53E-06	0.000323
Cenpf	1.126342	1.75E-06	0.000339
Icos	0.700132	1.77E-06	0.000339
Ighm	0.990976	3.67E-06	0.00067
Cenpe	1.025189	5.39E-06	0.000902
Hmmr	1.176521	6.75E-06	0.001086
Prdm1	1.227123	9.20E-06	0.001423
Neb	1.027204	1.06E-05	0.001518
Ccdc34	0.756333	1.32E-05	0.001836
Ncapd2	0.828848	1.41E-05	0.001887
Ifi203	0.879362	1.72E-05	0.002162
Cenpl	1.080614	2.34E-05	0.002846
Atp2b4	1.006352	2.87E-05	0.003389
Ctla4	0.834895	5.19E-05	0.005959
Ccna2	0.707692	6.32E-05	0.006686
Anxa6	0.58049	9.83E-05	0.009875
Tpx2	0.787506	0.000115	0.010767
Malat1	0.335522	0.00012	0.010923
Rrm2	0.611976	0.000148	0.012919
Hmgb2	0.670965	0.000165	0.014099
Incenp	0.67548	0.000193	0.015192
Arl6ip1	0.470764	0.000202	0.015596
Trac	0.449647	0.000223	0.016952
Kif11	0.707153	0.000234	0.017414
Tacc3	0.7054	0.000239	0.01749
Glrx	0.737756	0.000255	0.018244
H1f4	0.692248	0.000266	0.01842
Kif22	0.682382	0.00028	0.019105
Pim1	0.489205	0.000317	0.020887
Flna	0.684891	0.000335	0.021715
Arpc1b	0.390489	0.000385	0.024204
Glipr2	0.665916	0.000415	0.024916
Arl4c	0.609799	0.000436	0.025402
Ube2c	0.660236	0.000443	0.025422
Ccnb2	0.632687	0.000455	0.025422
Ccnf	0.606355	0.000539	0.029238
Mndal	0.57255	0.000556	0.029238
Cdca8	0.615292	0.000591	0.029487
Arid4a	0.597156	0.000586	0.029487
Crybg1	0.58353	0.000588	0.029487
Samhd1	0.480343	0.000617	0.030246
Kif20b	0.594118	0.00067	0.031663
H2-Aa	0.574182	0.000668	0.031663
Ctsb	0.498575	0.000673	0.031663
Fbxo5	0.593204	0.000699	0.031687
Knl1	0.590023	0.00071	0.031687
Kif15	0.508309	0.000709	0.031687
Stk17b	0.465905	0.000708	0.031687
Smc4	0.348532	0.000736	0.031798
Il12rb2	0.584654	0.000761	0.031887
Wbp1l	0.573354	0.000758	0.031887
Zbp1	0.528798	0.000799	0.033126
Cytip	0.427692	0.000963	0.038313
Coro1a	0.36935	0.000945	0.038313
Ipcef1	0.550785	0.000988	0.038765
Tent5c	0.542645	0.001019	0.038765
Cenpa	0.51526	0.001051	0.038765
mt-Rnr2	0.22691	0.001092	0.039919
Lgals1	0.480579	0.001207	0.043324
Clspn	0.479977	0.001336	0.047527
Il7r	0.481282	0.001353	0.047561

Table 3-1: Upregulated Differentially Expressed Genes
Sorted by adjusted P value from smallest (most significant) to largest. Showing only those with an adjusted P value < 0.05

Gene	log2Fold Change	pvalue	padj
Wdr43	-0.89943	1.89E-11	1.90E-08
Cd200	-1.86425	8.13E-09	2.97E-06
Srm	-0.79179	1.38E-07	3.70E-05
Dkc1	-0.61392	1.75E-07	4.40E-05
C1qbp	-0.68333	5.91E-07	0.000132
Slc19a1	-1.16846	5.74E-07	0.000132
Ddx21	-0.45897	4.56E-06	0.000796
Nsun2	-0.64207	9.92E-06	0.001477
Gnl3	-0.6575	1.59E-05	0.00206
Pfdn2	-0.54245	6.12E-05	0.006647
Hk2	-0.68058	6.00E-05	0.006647
Npm1	-0.35691	8.68E-05	0.008949
Igfbp4	-0.80626	0.000107	0.010512
Exosc7	-0.63952	0.000111	0.010655
Ccr7	-0.60593	0.000144	0.012895
Zmynd19	-0.69109	0.000182	0.014705
Bach2	-0.71603	0.000183	0.014705
Rora	-0.77499	0.00018	0.014705
Rsl1d1	-0.54272	0.000259	0.018244
Wdr3	-0.65946	0.000308	0.020666
Cluh	-0.56074	0.000385	0.024204
Nop2	-0.6523	0.000395	0.024411
Nop16	-0.65263	0.000414	0.024916
Clns1a	-0.59093	0.000429	0.025368
Tfrc	-0.5179	0.000454	0.025422
Nop58	-0.3543	0.00056	0.029238
Ubtf	-0.622	0.000553	0.029238
Pim3	-0.63259	0.00054	0.029238
Rcl1	-0.54228	0.000594	0.029487
Tomm 70a	-0.45631	0.000677	0.031663
Hspd1	-0.38706	0.000725	0.031687
B4galnt1	-0.55977	0.000718	0.031687
Farsa	-0.41111	0.000756	0.031887
Rrs1	-0.52387	0.000862	0.035369
Rrp9	-0.51291	0.000954	0.038313
Dnaja1	-0.4424	0.001022	0.038765
Strap	-0.45374	0.001012	0.038765
Max	-0.45935	0.001017	0.038765
Ifrd1	-0.53855	0.001048	0.038765
Eef1e1	-0.5408	0.001044	0.038765
Nifk	-0.49942	0.001193	0.04319
3110082 I17Rik	-0.50219	0.001361	0.047561

Table 3-2: Downregulated Differentially Expressed Genes
Sorted by adjusted P value from smallest (most significant) to largest. Showing only those with an adjusted P value < 0.05

3.2.9 Tr1-like transcriptional signatures follow *Ifng* expression

We have identified that a single high dose of peptide was sufficient to induce a Tr1-like transcriptional phenotype in this model within 24 hr and so we re-analysed non-IL-10-sorted bulk data previously generated by Bending group to understand temporal relationships of key modules at different doses. In this dataset, splenocytes from an unimmunised, control mouse and from 0.8 and 80 μg immunised mice were sorted by $CD4^+$ *Nr4a3*-$Timer^+$ at 4, 12 and 24 hr post-injection in the original experiment [325]. These samples were not sorted by *Il10*-GFP positivity or negativity as in figure 3-8 – 3-10 but are separated by low and high dose of [4Y]-MBP. At 24 hr (fig. 3-11A) we see DEGs associated with immune regulation more highly expressed on the higher dose (*Prdm1, Il10, Maf, Ctla4, Lag3*), several of which are, encouragingly also found in our prior RNA-seq. This also suggests that with a higher dose of self-peptide comes a stronger tolerogenic response and Tr1-like phenotype. Given that in our RNA-seq experiment we saw interferon regulated genes in the *Il10*-GFP^+ compartment, we examined the timepoints in the previously generated bulk RNA-sequencing data (fig. 3-11) finding that *Ifng* preceded *Il10* (fig. 3-11B) and *LAG3* (fig. 3-11C) transcripts by around 4 hours, suggesting that *Ifng* may precede *Il10* and *Lag3* expression. This is intriguing given that IFNγ can directly modulate the antigen presenting capacity of APCs, which could indirectly lead to alterations in TCR signal strength.

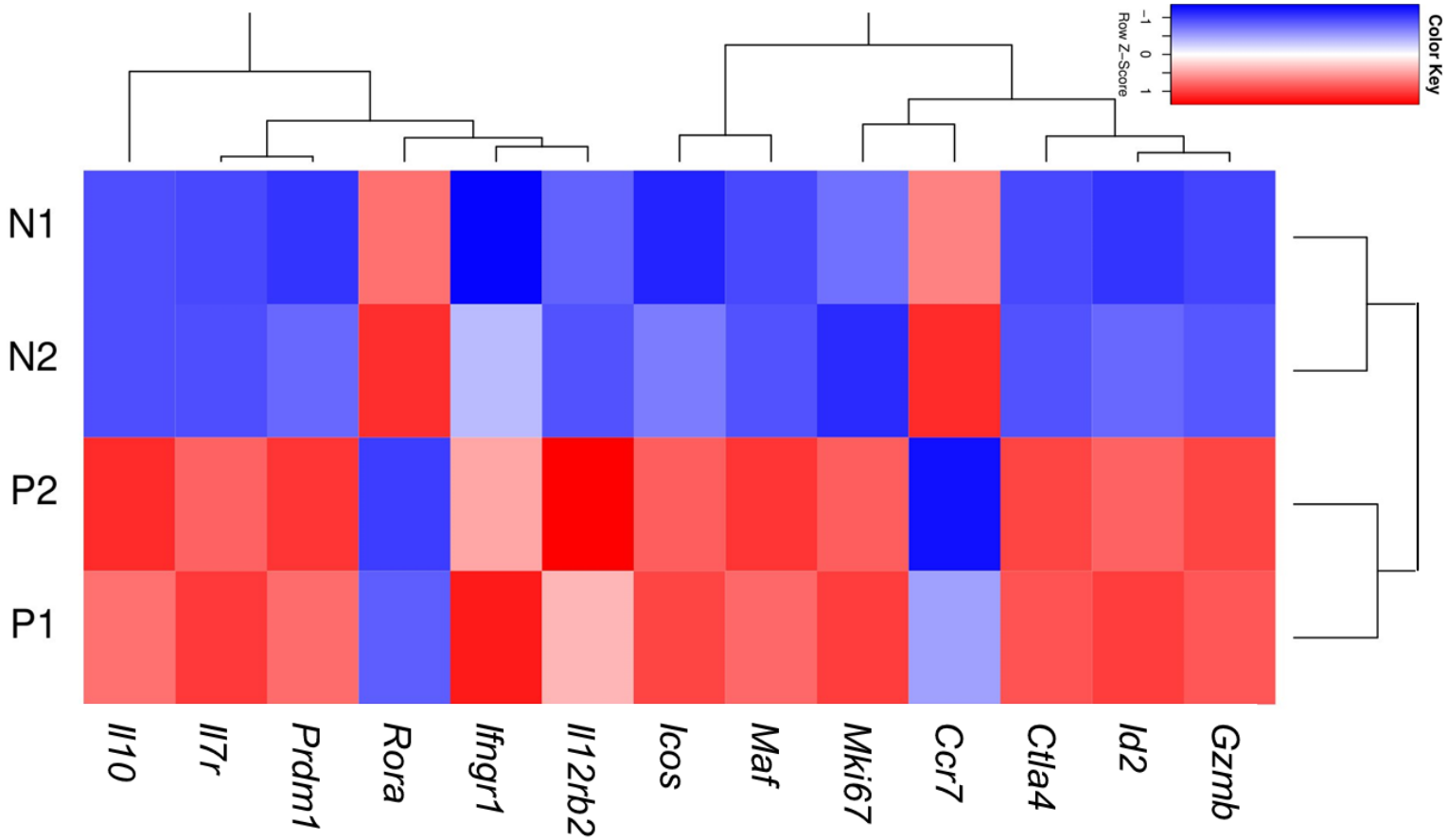

Figure 3-10: Curated heatmap of DEGs in *Il10*-GFP$^{+/-}$ T cells
Nr4a3-Tocky Tg4 *Il10*-GFP mice were immunised with 4 mg/kg [4Y]-MBP in PBS s.c. and sorted 24 hr post-injection. Following principal component analysis, the transcriptome was used to generate a heatmap from the genes associated with Type 1 regulatory T cells. “N” refers to *Il10*-GFP negative and “P” to Il10-GFP positive cells. From n=2 mice.

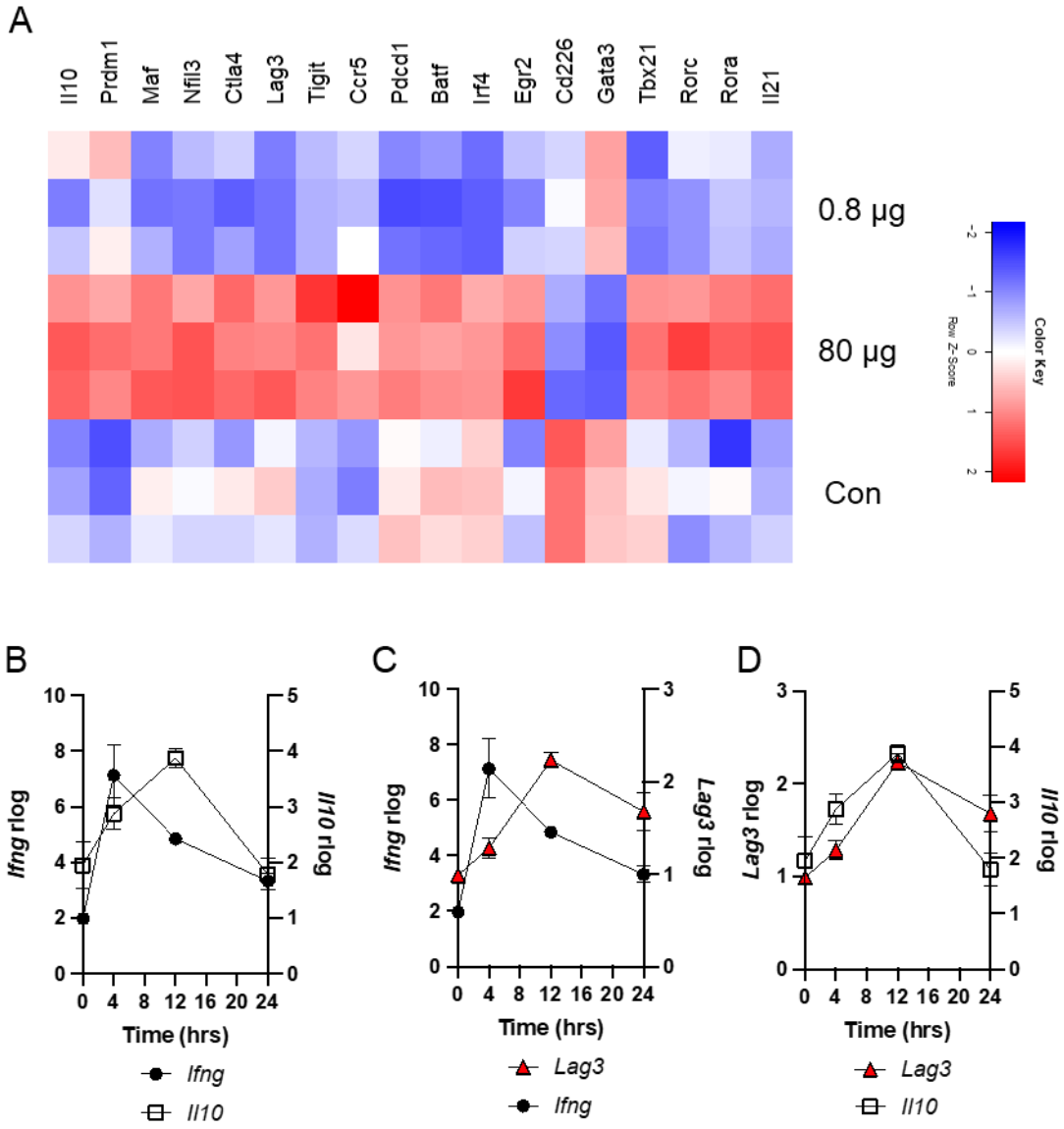

Figure 3-11: Tr1-like transcriptional signatures follow *Ifng* expression
Nr4a3-Tocky Tg4 mice were unimmunised (control) or immunised with 0.8 or 80 µg [4Y]-MBP in 100 µL PBS s.c. and harvested at 4, 12 and 24 hr for harvest of *Nr4a3*-Timer^{+} for bulk RNA-seq. **(A)** Heatmap of DEGs between conditions at 24 hr. Compared temporal expression rlog transcripts for of 80 µg treated mice for **(B)** *Ifng* and *Il10*, **(C)** *Ifng* and *Lag3* and **(D)** *Lag3* and *Il10*. N=3 per condition.

In summary, this chapter established a rapid model for Tr1-like cell induction and suggests that the Tr1 phenotype maybe preceded by a wave of IFNγ transcriptional activity.

3.3 Discussion

The work in this chapter supports earlier findings from Elliot et al., 2021 that the *Nr4a3*-Timer is a dependable proxy readout for TCR activation, and that this activation is graded by the dose of stimulating peptide. It also encourages the idea that high dose of a high MHCII affinity peptide begets a tolerogenic response, as suggested by increasing *Il10*-GFP and LAG3 expression. The *Il10*-GFP and surface markers of regulation are also graded by dose.

By 8 hr, only low amounts of GFP are seen, yet its maturation time is approximately 1 hr. One explanation for this 7 hour discrepancy is that this is due to the circulation time required for the peptide to access the spleen, and then again for T cells to bind enough peptide to generate a response. Another is that there is a cellular, rather than biochemical factor in play, extending the time it takes for a T cell to respond to [4Y]-MBP. However, the *Nr4a3*-Timer which spontaneously matures from blue to red at around 4 hr, is shifting from Timer Blue to Timer Red on a flow plot at around 4 hr also. If there was a delay to TCR activation, this shift would be later post-injection, than post-Timer protein maturation. Also, the RNA-seq shows a clear lag behind *Ifng*. *Il10* transcription appears later compared to other cytokines and transcripts of strong TCR signalling. This raises the question as to whether *Il10*-GFP is in part regulated by a negative feedback loop generated in response to strong tolerogenic TCR stimulation, as has been previously suggested, possibly involving other cell subsets [270].

In $CD4^+$ T cells, IL-10 is predominantly produced by regulatory type cells. A lack of FoxP3 expression at both protein and transcript in *Il10*-GFP and TCR activated populations respectively, but strong expression of LAG3 and TIGIT transcript and

protein in *Il10*-GFP^{+} cells suggests that the main Treg subset in this model is Tr1-like, and not FoxP3^{+} Tregs. Timer Red, Tr1 markers, strong TCR signalling markers and *Il10* correlate with time post high dose of antigen. However, this is not the case for conventional markers of T cell activation such as CD69 and CD44 - the lack of delineation between *Nr4a3*-Timer expression states implies that these markers are not reliable to denote T cell activation specifically via antigen presentation to the TCR.

The real power of the *Nr4a3*-Tocky mouse is the ability to track antigen signalled cells. Using this tool, we can see that *Il10* is not arising in non-TCR signalled, and that TCR signalling is a requirement for *Il10* transcription. Through *Nr4a3*-Tocky mice, we can follow Tr1 cell development *in vivo* by tracing the TCR signalled population. It effectively allows us to investigate temporal relationships that would otherwise be difficult without the Timer system.

In Burton et al., 2014, and Bevington et al., 2020 a Tr1 phenotype was detected after 21 days or more of EDI, whereas in this chapter we demonstrate that there is a rapid induction of Tr1 markers as early as 12 hr post high dose of self-antigen. This suggests that peripheral tolerogenic mechanisms are induced much earlier in T cell activation than the EDI model suggests, wherein there is a chronic presence of antigen for reactive T cells. Th1 cells, which secrete IFNγ, are thought to convert to Tr1 cells [340, 341], however such quick turnaround to a Tr1 phenotype in our rapid induction model suggest *de novo* differentiation to Tr1 cells directly from T cells in the periphery.

Although the Tg4 repertoire is heavy biased, it is important to understand that the Tg4 *Nr4a3*-Tocky Tiger mouse is an F1 cross of two different mouse backgrounds. Namely, the *Nr4a3*-Tocky mice are on the C57/BL6 background, whilst Tg4 mice are B10.PL.

The Tg4 TCR is restricted to I-A^U, but the F1 crossed mice also express I-A^B from the C57/BL6. Therefore, it is possible that some T cells may undergo tonic signalling and/or receive weak signals that may upregulate markers of effector memory T cells in response to antigens presented to the T cell. *Il10* induction could come from a potential effector memory population which has formed during the life of the mouse due to either recognition of MBP itself or from weak peptide : MHC interactions.

In previous RNA-seq data [325], we observed two important findings. Firstly, we see that the *Il10* transcripts in Tr1 cells are transient, peaking at 12 hr and returning to baseline at 24 hr. Secondly, we see the peak of *Ifng* transcription precede *Il10* and *LAG3* by ~8 hr, suggesting that the Tr1 wave is delayed when compared to classic T cell functional transcripts. Given this temporal relationship we were interested to understand whether this relationship was more than correlative, and whether IFNγ itself could directly impact, *Il10*-GFP transcription in Tr1 cells in this model.

Chapter 4 : IFNγ and IL-27 Positively Modulate Tr1-like cell Development

4.1 Introduction

The rapid induction of *Il10* transcription in Chapter 3 demonstrated that $CD4^+$ TCR-activated *Il10*-GFP expressors are Tr1-like in phenotype, and that the Tr1-like module is preceded by *Ifng* expression, a transcript for an inflammatory cytokine. Given that these cytokines have diametrically opposed functions, we sought to determine what effect environmental IFNγ may have on the induction of tolerance, and how the mechanism of this affects Tr1 phenotype outcome.

4.1.1 The Potential Role of IFNγ in Immune Regulation

Initially described as an anti-viral cytokine, IFNγ is one of the most prominent proinflammatory cytokines produced by NK cells, Th1 cells, cytotoxic CD8 T cells, DCs, macrophages, natural killer T (NKT) cells, B cells and type 1 innate lymphoid cells [342-344]. Among its myriad functions, IFNγ activates macrophages and upregulates MHCII expression [345-347]. Notably, the crucial role of IFNγ in anti-tumour responses is widely established both directly on tumour cells and by positive modulation of cancer directed immune effects such DCs, T cells and NK cells [348]. However, IFNγ has been observed in driving tolerogenic outcomes also.

DCs stimulated by IFNγ in the presence of danger or pathogen signals can acquire a tolerogenic phenotype including increased IDO expression following production of IL-12 [349]. IDO removes tryptophan from the environment which stress-response pathways GCN2 and mTOR are sensitive to [350, 351]. Maintenance of the post-inflammatory tolerogenic phenotype is maintained by IFNγ-induced Aryl Hydrocarbon Receptor (AHR) and IDO production of AHR ligand kynurenine [352, 353]. DCs activated by higher concentrations of IFNγ in the absence of other stimuli show

induction of inhibitory molecules like IL-4 and HLA-G but did not produce IL-12p70 and display inhibited proliferation and granzyme B expression [354]. In a mouse model of EAE, DCs pre-treated with IFNγ *in vitro* and injected back into mice had lower expression of CD80/86 and MHCII than untreated DCs upon immunisation [355].

In regulatory T cells, Tregs recruited to environments with a Th1 cytokine profile begin to express Tbet and IFNγ, but do not lose regulatory function [86]. Alloantigen specific Tregs undergoing rechallenge showed a five-fold increase in *Ifng* transcripts and protection of donor skin grafts by Tregs was abolished with IFNγ neutralisation [356]. Similarly, $FoxP3^+$ $IFN\gamma^+$ Tregs were associated with better long-term outcomes in human allogeneic kidney patients [357].

In EAE, which is accepted to be largely Th1 and Th17 cell driven, recombinant IFNγ given before disease onset results in exacerbation, but administration after the first clinical symptom led to significant disease suppression [358, 359]. Furthermore, IFNγ administration diminishes severity and incidence [360, 361], and anti-IFNγ has led to decreased IL-17 secretion by Th17 cells [362]. IFNγ has induced IL-27 production in EAE, experimental arthritis and uveitis [363-365]. This suggests that IFNγ can have context and time dependent roles in both promoting and inhibiting autoinflammatory responses.

4.1.2 Interleukin-27 as a Driver of IL-10 Expression and the Tr1 Phenotype

IL-27 is a well-documented inducer of the Tr1 phenotype. pTreg modification of DCs leads to IL-27 secretion which in turn directly induces naïve T cells via IL-27R to become Tr1 cells and produce IL-10 [160]. IL-27 appears to drive IL-10 in a pSTAT1 and pSTAT3 dependent manner, and is enhanced by TGFβ [223, 366] in Th1 and Th2

cells, but IL-27 inhibits Th17 differentiation [367, 368]. cMaf, IL-21 and ICOS have been demonstrated as essential to IL-27 induced Tr1 differentiation [161]. AHR is found in high concentrations in Tr1 cells, and when it is activated by IL-27, it induces *Il10* and *Il21* transcription [141]. In EAE models, DC production of IL-27 is significantly induced by IFNγ, which inhibit Th17 responses while contributing to IL-10^{+} Treg development [364, 369]. IFNγ$^{-/-}$ produced much less IL-27 than their wild-type counterparts in these experiments.

Given past reports that IFNγ can ameliorate autoimmune EAE and Chapter 3's findings that Tr1 cell development was preceded by a wave of *Ifng* transcription, we aimed to establish whether IFNγ itself played an active role in the generation of Tr1 cells *in vivo*.

4.2 Results

4.2.1 *In vivo* anti-IFNγ decreases expression of *Il10*-GFP in TCR activated CD4$^+$ T cells

Given that the *Ifng* transcriptional module preceded *Il10*, and that IFNγ has a role in modulating APCs, we investigated whether IFNγ could play a role in the development of IL-10$^+$ T cells. As in the previous chapter, we used the *Nr4a3*-Tocky Tg4 *Il10*-GFP *Ifng*-YFP reporter mice, administering a weight-normalised high dose of self-peptide, [4Y]-MBP at 4 mg/kg. We administered 1 mg anti-IFNγ (XMG1.2) as it was assumed to be saturating dose and is sufficient to rapidly sequester much of the active IFNγ in the system [370]. An isotype, IgG1 (MAC221) was given as a control, and the CD4$^+$ TCRvβ8.1$^+$ splenocytes measured for *Nr4a3*-Timer frequency and from this, *Il10*-GFP and *Ifng*-YFP frequency and fluorescence intensity (fig. 4-1A).

Anti-IFNγ mAb did not affect the frequency of *Nr4a3*-Timer$^+$ (fig. 4-1B), but did reduce *Il10*-GFP expression in the *Nr4a3*-Timer$^+$ fraction significantly (fig. 4-1C), by about a quarter from isotype. *Il10*-GFP MFI is significantly lower for the anti-IFNγ treated, however that actual difference is very slight (fig. 4-1D). The frequency of *Ifng*-YFP$^+$ T cells is unchanged (fig. 4-1E), but interestingly the MFI intensity is significantly increased upon IFNγ neutralisation (fig. 4-1F). These data demonstrate that IFNγ has a positive role in regulating the development and IL10 transcriptional levels of rapidly induced *Il10*-GFP$^+$ T cells.

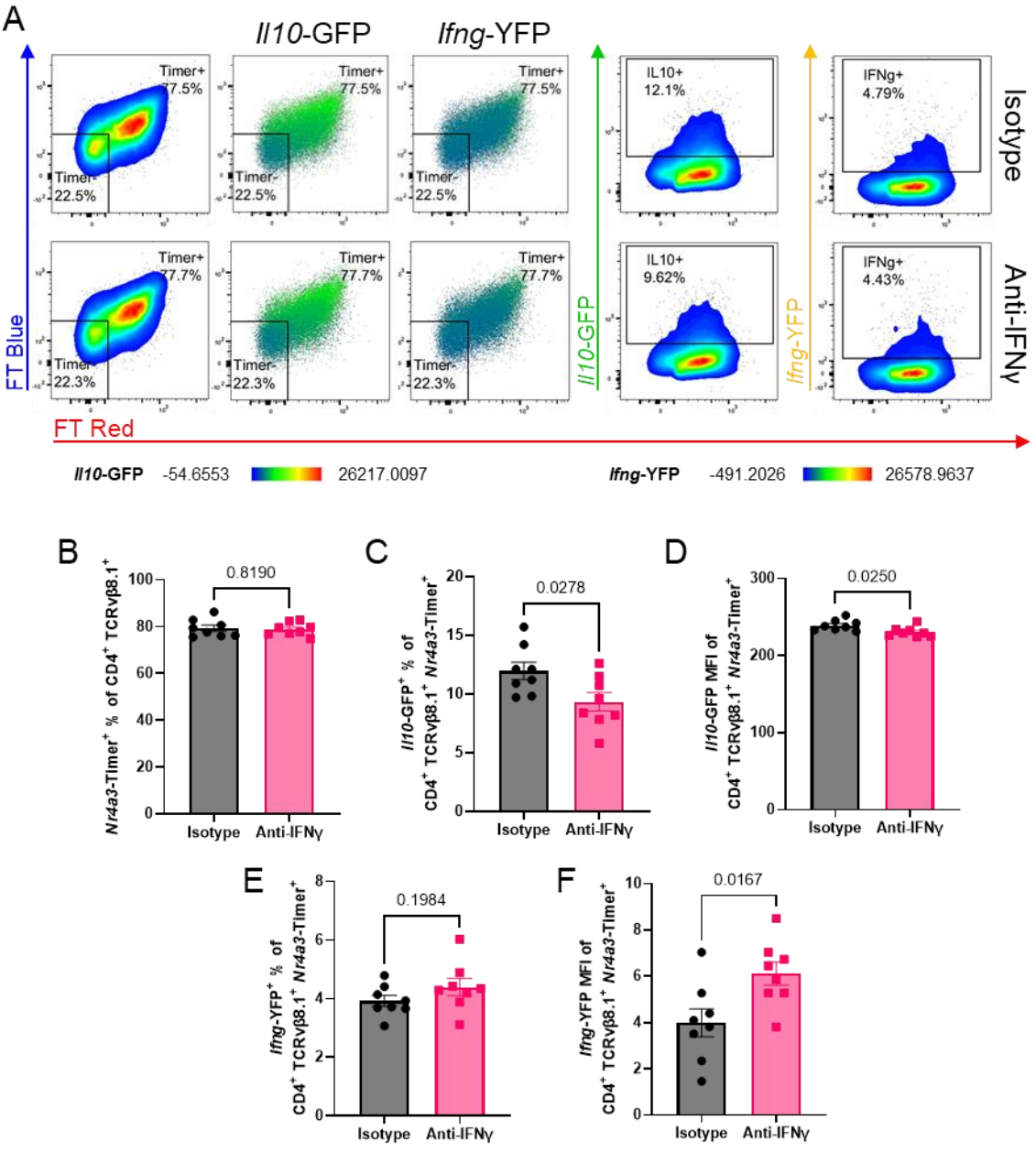

Figure 4-1: *In vivo* anti-IFNγ decreases expression of *Il10*-GFP in TCR activated CD4$^+$ T cells

Nr4a3-Tocky Tg4 *Il10*-GFP *Ifng*-YFP mice were immunised with 4 mg/kg [4Y]-MBP in 100 µL PBS s.c. and 1 mg isotype or anti-IFNγ antibody in 200 µL PBS i.p. **(A)** At 24 hr, splenic CD4$^+$ TCRvβ8.1$^+$ cells for *Nr4a3*-Timer (FT Blue vs FT Red) expression, and subsequently *Il10*-GFP and *Ifng*-YFP in *Nr4a3*-Timer$^+$ population. Summary of *Nr4a3*-Timer$^+$ frequency **(B)**, *Il10*-GFP$^+$ frequency **(C)** and MFI **(D)**, *Ifng*-YFP$^+$ population **(E)** and MFI **(F)** from **(A)**. **(B-F)** from n=8 mice per treatment, bars represent mean ±SEM, statistical analysis by unpaired two-tailed t test. One representative of two experiments

4.2.2 *In vivo* anti-IFNγ alters regulation and activation markers in activated T cells

Il10-GFP$^+$ T cells develop in response to strong TCR stimulation, so we wanted to evaluate whether anti-IFNγ could alter the perceived TCR signal strength on CD4$^+$ T cells *in vivo*. *Nr4a3*-Timer expression is a measure of overall TCR engagement and downstream TCR signalling in a population, but markers such as ICOS and OX40 are a measure of how strong a TCR signalling is, as well as being activation markers. With a weight-normalised high dose of [4Y]-MBP there is strong expression of activation and regulation markers (Chapter 3), but it is unknown in this rapid induction of tolerance model how much IFNγ controls their expression. Fig 4-2A shows that the CD4$^+$ T cells expressing the most *Nr4a3*-Timer$^+$ have the strongest expression of the markers shown. Regulatory marker LAG3, associated with Tr1 cells and IL-10 production though MHCII sequestration, has a downward trend in expression fig 4-2B). TIGIT also has a decreasing trend (fig.4-2C), whilst PD-1 (fig. 4-2D) has a significant increase in expression in response to anti-IFNγ. ICOS (fig. 4-2E), a marker of activation as it is an Induced co-stimulator of T cells, and GITR (fig. 4-2F) associated with CD25$^+$ Tregs and expressed upon T cell activation, are both significantly reduced by treatment. CD69 (fig. 4-2G), is unaffected by anti-IFNγ mAb, likely reflecting the previous chapter's findings that CD69 becomes rapidly dissociated from active TCR signalling *in vivo*. These data demonstrate that CD4$^+$ T cells activated in the presence of neutralising antibodies to IFNγ show on the whole reduced expression of strong TCR signalling markers.

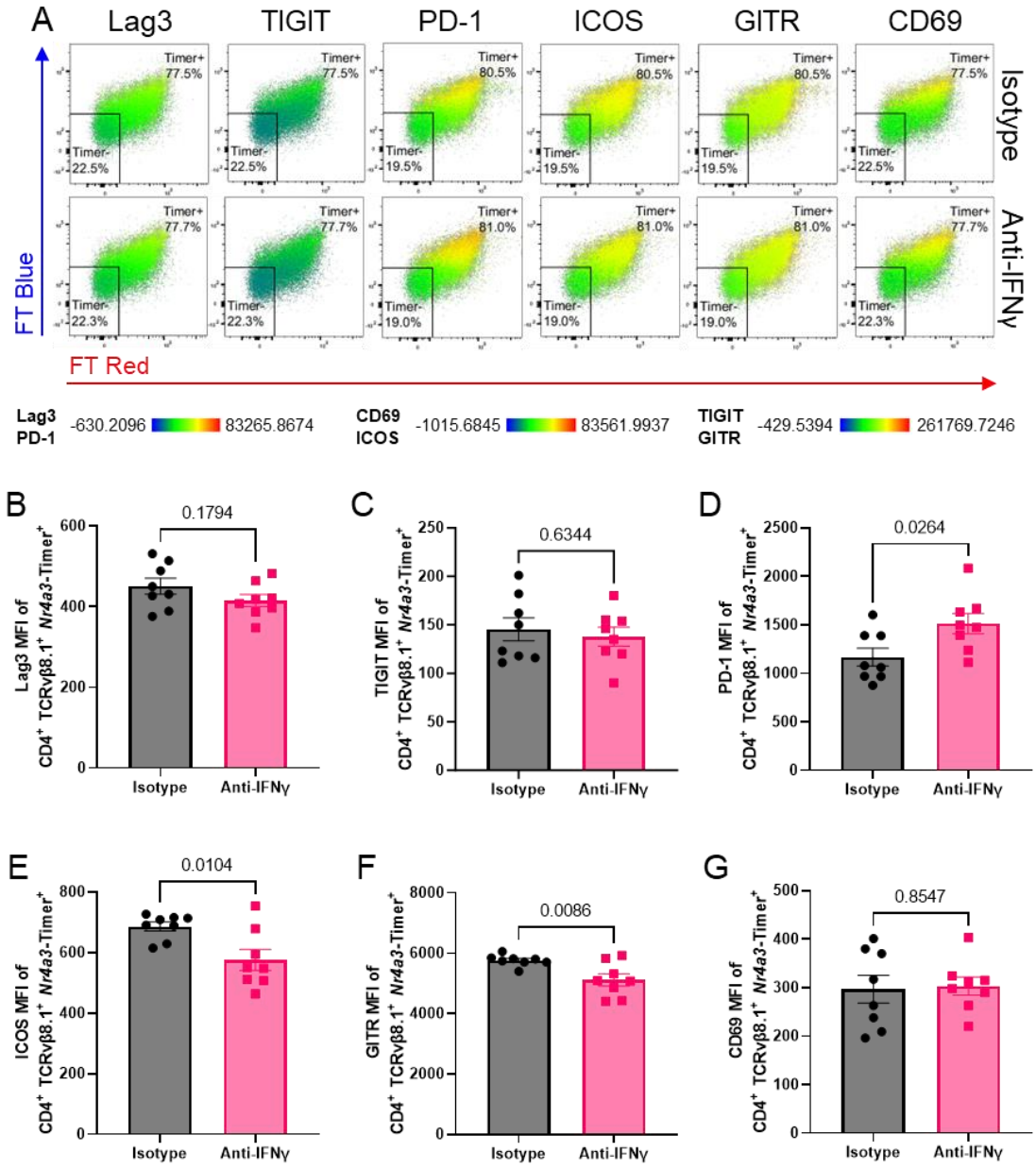

Figure 4-2: *In vivo* anti-IFNγ alters regulation and activation markers in activated T cells

Nr4a3-Tocky Tg4 *Il10*-GFP *Ifng*-YFP mice were immunised with 4 mg/kg [4Y]-MBP in 100 µL PBS s.c. and 1 mg isotype or anti-IFNγ antibody in 200 µL PBS i.p. **(A)** At 24 hr, splenic CD4$^+$ TCRvβ8.1$^+$ cells analysed for *Nr4a3*-Timer (FT Blue vs FT Red) expression. Summary of MFIs for LAG3 **(B)**, TIGIT **(C)**, PD-1 **(D)**, ICOS **(E)**, GITR **(F)** and CD69 **(G)** in *Nr4a3*-Timer$^+$ population from **(A)**. **(B-G)** from n=8 mice per treatment, bars represent mean ±SEM, statistical analysis by unpaired two-tailed t test. One representative of four experiments

4.2.3 *In vivo* anti-IL-10 and anti-IFNγ antibody may have opposing effects on CD4$^+$ splenic lymphocyte *Il10*-GFP expression.

The previous data highlighted that IFNγ positively influences *Il10*-GFP$^+$ T cell development and this was correlated with TCR signal strength. Given that IL-10 has an opposing role on IFNγ, we wondered whether neutralisation of IL-10 may further enhance *Il10*-GFP$^+$ T cells *in vivo*. (fig. 4-3A). We did not see any significant changes in *Nr4a3*-Timer$^+$ expression when isotype is compared to anti-IL-10 and anti-IFNγ, however, there is a downward trend for anti-IFNγ treatment (fig. 4-3B).

For the *Il10*-GFP reporter, anti-IFNγ mAb brings *Il10*-GFP frequency down, approaching statistical significance (fig. 4-3C). Anti-IL-10 mAb shows an increasing trend in *Il10*-GFP frequency, but neither of these are reflected in MFI (fig. 4-3D). These data demonstrate that IL-10 itself does not play a major positive role in driving Tr1-like cell development in this model.

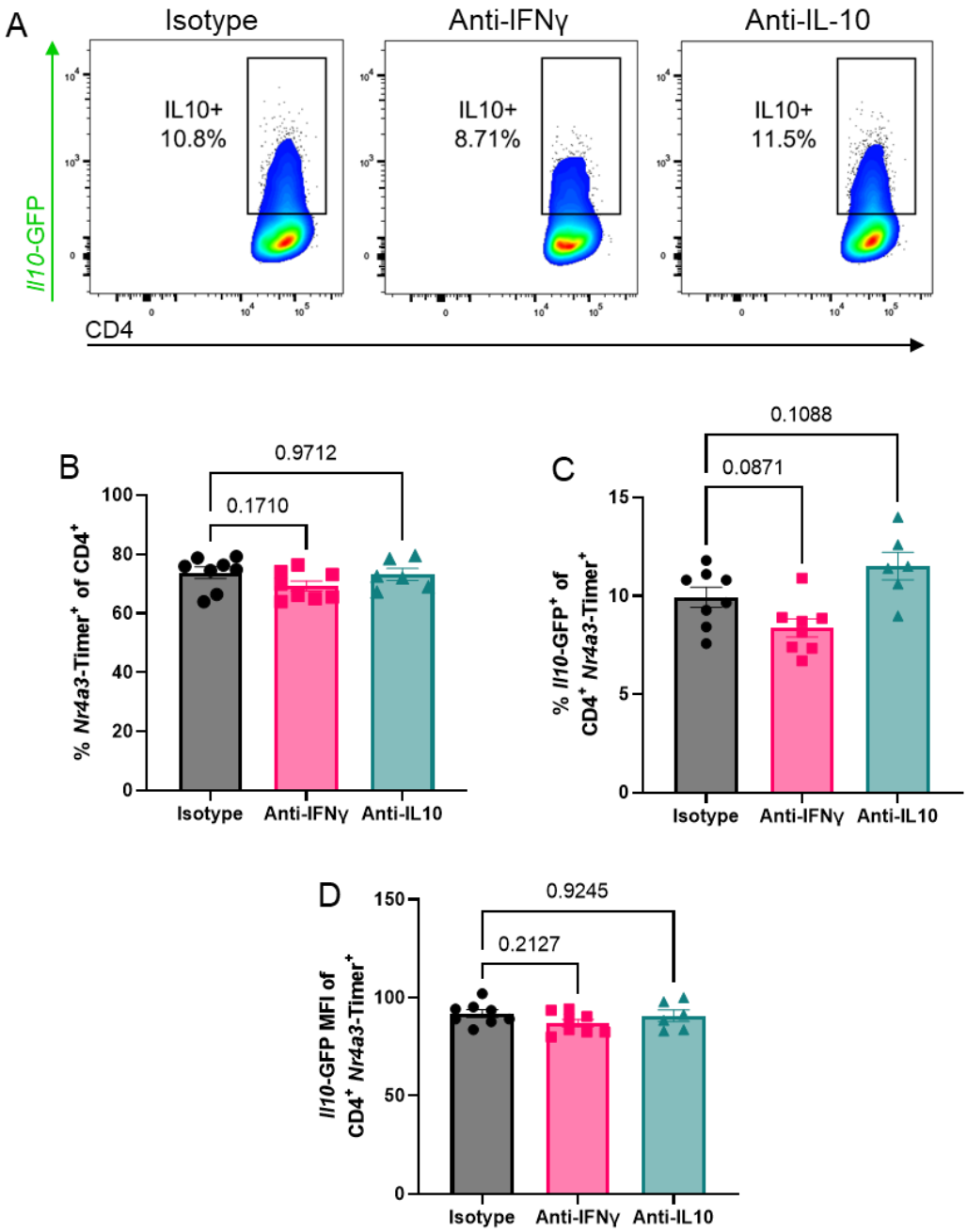

Figure 4-3: *In vivo* anti-IL-10 and anti-IFNγ antibody may have opposing effects on CD4⁺ splenic lymphocyte *Il10*-GFP expression.
Nr4a3-Tocky Tg4 *Il10*-GFP mice were injected with 4 mg/kg [4Y]-MBP s.c. in 100 µL PBS and either 1 mg anti-IFNγ, 0.5 mg anti-IL10 or 1 mg isotype i.p. in 200 µL PBS. **(A)** At 24 hr splenocytes were analysed for *Il10*-GFP$^+$ % of CD4$^+$ *Nr4a3*-Timer$^+$ splenocytes. Summary of *Nr4a3*-Timer$^+$ from CD4$^+$ splenocytes **(B)**. Summary of *Il10*-GFP$^+$ frequency **(C)** and MFI **(D)**. **(B-D)** from n=8 mice per treatment, bars represent mean ±SEM, statistical analysis by one-way ANOVA with Dunnett's test. Two were excluded from the Anti-IL-10 group, one due to sample processing error and another to sample acquisition error.

4.2.4 NK1.1 expressing cells are major sources or IFNγ *in vivo* and augment expression under anti-IFNγ treatment.

Given that IFNγ can positively regulate Tr1-like cell development, we wished to further characterise sources of IFNγ *in vivo*. In this model, splenic CD4$^+$ TCRvβ8.1$^+$ *Nr4a3*-Timer$^+$ cells produce very little *Ifng*-YFP, yet there is a sufficient, potent quantity of IFNγ in the system to modulate *Il10*-GFP expression. We know this because when IFNγ is sequestered by mAb, *Il10*-GFP in CD4$^+$ TCRvβ8.1$^+$ *Nr4a3*-Timer$^+$ is significantly affected, but it is not the source of IFNγ.

Of the lymphoid compartment, NK cells are IFNγ producers, as are cytotoxic CD8$^+$ T cells and a few subtypes of CD4$^+$ T cells, namely Th1 and Th17. Initially, we gated for total *Ifng*-YFP$^+$ cells, before separating them according to TCRvβ8.1 vs NK1.1 expression (fig. 4-4A). Gating out TCRvβ8.1$^+$ cells (which would include CD4 and CD8 T cells), we're left with a double negative population and an NK1.1$^+$ population, which is ~73% of the *Ifng*-YFP cells. Although there is a trend of increased *Ifng*-YFP in response to anti-IFNγ, it is not significant (fig. 4-4C). The *Ifng*-YFP$^+$ / NK1.1$^+$ TCRvβ8.1$^-$ population (not shown) also showed no significant difference between isotype and anti-IFNγ.

However, when we examine this data a slightly different way, we're given a different perspective. In figure 4-4B, we first gated for NK1.1$^+$ TCRvβ8.1$^-$ cells – comprising ~6% of the total cells. When we then examine *Ifng*-YFP frequency of this population, it is significantly increased by anti-IFNγ treatment compared to isotype (fig. 4-4D). By correlating *Il10*-GFP frequency from CD4$^+$ TCRvβ8.1$^+$ *Nr4a3*-Timer$^+$ against *Ifng*-YFP from NK1.1$^+$ TCRvβ8.1$^-$, we see a positive correlation for isotype treated, that appears to be decoupled by anti-IFNγ treatment, reflecting the fact that the effects of IFNγ are

now lost in these mice (fig. 4-4E). NK1.1^{+} *Ifng*-YFP producers are sensitive to mAb treatment, but not all *Ifng*-YFP producers are, and not all NK1.1^{+} cells report *Ifng*-YFP. In administering anti-IFNγ mAb, there is a reduced frequency of NK1.1^{+} cells in the spleen, but the population present has a higher frequency of *Ifng*-YFP production.

These data show that in addition to T cells, NK cells are the major producers of IFNγ, and their expression can be modulated by anti-IFNγ treatment and that in untreated mice, the frequency of NK cell *Ifng*-YFP expression positively correlates with il10-GFP expression.

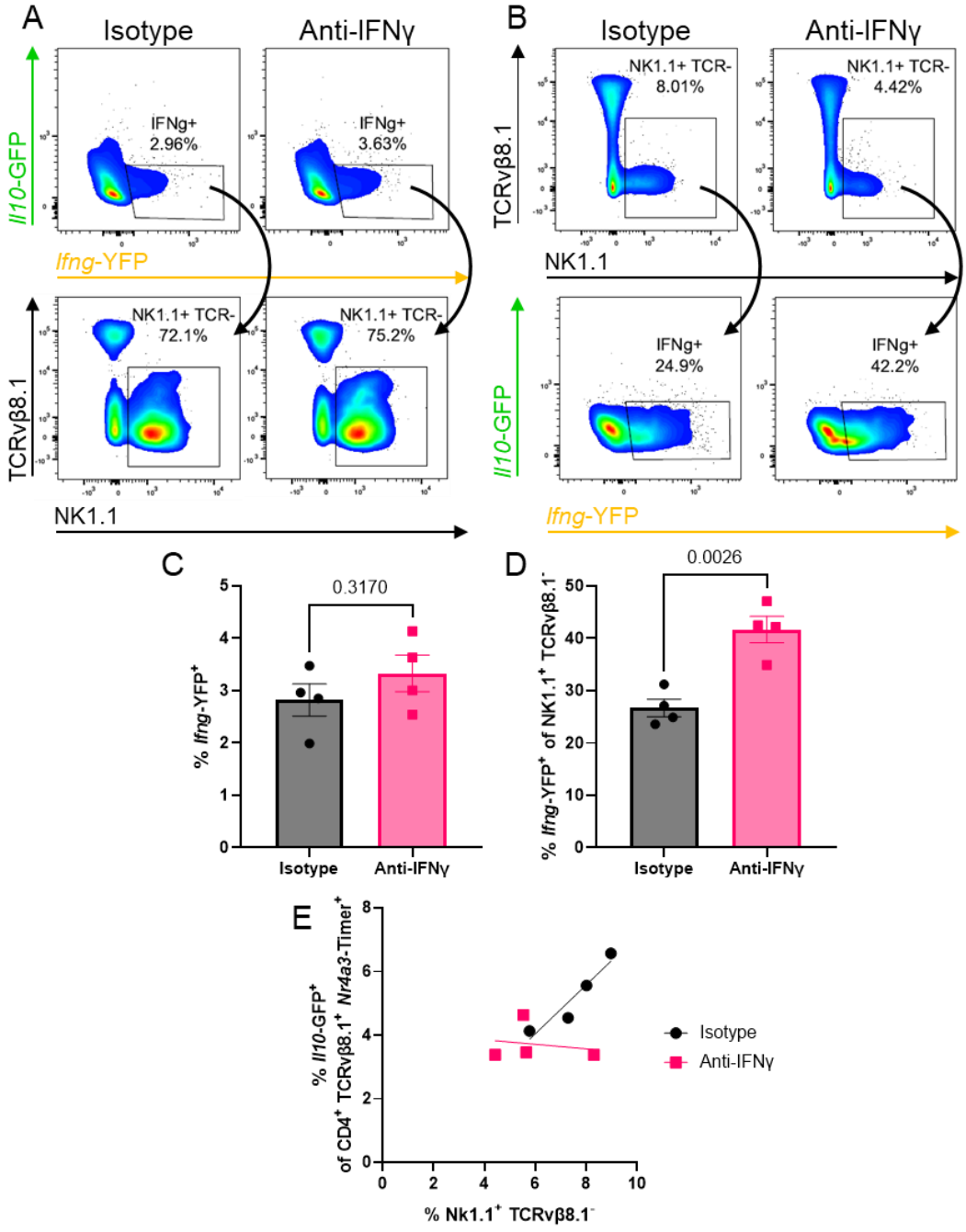

Figure 4-4: NK1.1 expressing cells are major sources or IFNγ *in vivo* and augment expression under anti-IFNγ treatment.
Nr4a3-Tocky Tg4 *Il10*-GFP *Ifng*-YFP mice were injected with 4 mg/kg [4Y]-MBP s.c. and either 1 mg anti-IFNγ or isotype i.p. in PBS and analysed at 24 hr for **(A)** global splenocyte *Ifng*-YFP expression and NK1.1 vs TCRvβ8.1 from *Ifng*-YFP^{+} and **(B)** *Ifng*-YFP expression from NK1.1^{+} TCRvβ8.1^{-} splenocytes. **(C)** Summary of **(A,** top**)**. **(D)** Summary of **(B,** bottom**)**. **(E)** Correlated NK1.1^{+} TCRvβ8.1^{-} cells with CD4^{+} TCRvβ8.1^{+} *Nr4a3*-Timer^{+} cells *Il10*-GFP^{+}. **(C, D)** from n=4 mice per treatment, bars represent mean ±SEM, statistical analysis by unpaired two-tailed t test. One representative of two experiments

4.2.5 *In vivo* anti-NK1.1 treatment has no effect on CD4$^+$ splenocytes *Il10*-GFP reporter expression

As we had seen that NK1.1$^+$ cells were the major *Ifng*-YFP expressors in this model, we depleted them using an anti-NK1.1 antibody. We hypothesised that by depleting the major *Ifng*-YFP expressors, we would greatly reduce *Il10*-GFP expression in CD4$^+$ T cells, given anti-IFNγ treatment reduced *Il10*-GFP expression (fig. 4-5A).

Anti-NK1.1 depleting antibody was given 48 hr before peptide, and spleens were harvested 24 post-peptide. The antibody treatment successfully and significantly reduced the frequency of NK1.1$^+$ cells *in vivo* (fig. 4-5A and B), however there is no discernible effect on the *Il10*-GFP expression of CD4$^+$ TCRvβ8.1/2$^+$ *Nr4a3*-Timer$^+$ cells (fig. 4-5C). Not only is there no significant change in frequency (fig. 4-5D), but there is also no change in intensity of ICOS (fig. 4-5E) or OX40 (fig. 4-5F), markers of strong TCR signalling which were decreased by anti-IFNγ treatment. These findings reveal that NK cell derived IFNγ is redundant for Tr1 cell induction, and therefore implicating other cell types as the relevant source of IFNγ in the model.

4.2.6 *In vitro* IFNγ treatment has no direct effect on CD4$^+$ splenocytes *Il10*-GFP reporter expression.

We have shown that an anti-IFNγ mAb effectively decreased *Il10*-GFP expression, but anti-IL-10 mAb had no effect. As such we sought to then increase *Il10*-GFP by adding more IFNγ to the system. Inferring the positive effect of IFNγ on *Il10*-GFP expression, we wished to define how IFNγ exerted its effect. To rule out a potential direct effect, we cultured CD4$^+$ T cells in the presence of rmIFNγ. To achieve this, we cultured CD4$^+$ splenocytes with anti-CD3 and anti-CD28 *in vitro* at different concentrations of rmIFNγ (fig. 4-6A).

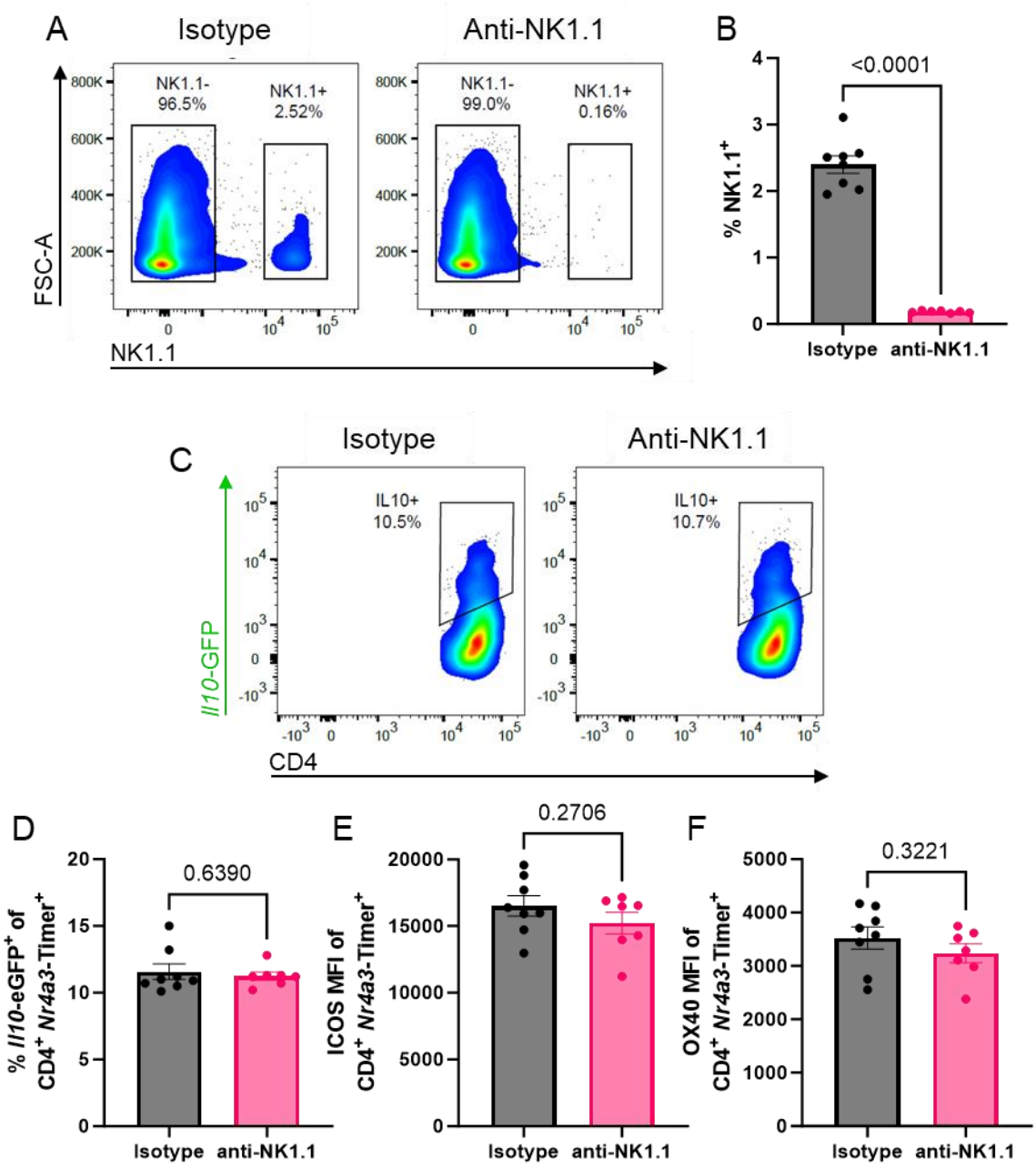

Figure 4-5: *In vivo* anti-NK1.1 treatment has no effect on CD4+ splenocytes *Il10*-GFP reporter expression.

Nr4a3-Tocky Tg4 *Il10*-GFP mice were administered 1 mg anti-NK1.1 or anti-IgG2a isotype in 200 µL PBS i.p. and 4 mg/kg [4Y]-MBP s.c. 48 hr later. Spleens were harvested 24 hr after peptide.. Representative flow plots at 24 hr showing NK1.1 against FSC-A **(A)**. Summary of NK1.1$^+$ **(B)** of **(A)**. Representative flow plots at 24 hr showing *Il10*-GFP against CD4 **(C)**. Summary of *Il10*-GFP$^+$ frequency **(D)** and ICOS **(E)** and OX40 **(F)** MFI of CD4$^+$ *Nr4a3*-Timer$^+$. **(B, D-F)** bars represent median with interquartile range. Statistical analysis by Mann-Whitney test. N = 8 per treatment.

In giving 10-fold increases in rmIFNγ, we see no change in *Il10*-GFP frequency (fig. 4-6B) or fluorescence intensity (fig. 4-6C), at either 24 or 48 hr. We do, however, see an increase in *Il10*-GFP reporter between 24 and 48 hr for all conditions, although the mean expression is approximately the same and may reflect increased autofluorescence from T cell blasting. Similarly, we see no change in any of the surface markers' fluorescence intensity (fig. 4-6D – F), at either 24 or 48 hr. We do, however, see an increase in intensity between 24 and 48 hr for all conditions, although the mean expression is approximately the same. These data show that *in vitro* activation of T cells in the presence of high concentrations of IFNγ is not sufficient for *Il10* transcriptional enhancement.

4.2.7 *In vivo* rmIFNγ treatment has no effect on CD4$^+$ T cells

To assess *in vivo* potency of IFNγ for a potential direct effect, we treated mice *in vivo* with rmIFNγ. With no success in generating a response from *in vitro* treatment of anti-CD3 and anti-CD28 treated splenocytes, we returned to the Tg4 model, and opted to carry out the experiment *in vivo*, giving 25 ng rmIFNγ and measuring the effect on *Nr4a3*-Timer and *Il10*-GFP expression (fig. 4-7A). As with the *in vitro* experiments, we detected no change in reporter (fig. 4-7B – D) or surface marker (fig. 4-7E – H) expression. These data showed that addition of rmIFNγ at this concentration did not alter Tr1-like cell development. Collectively, both *in vitro* and *in vivo* addition had no effect on *Il10*-GFP expression, suggesting that IFNγ is not exerting a direct effect on CD4$^+$ T cells, or that the site of IFNγ production is critical to its effect on Tr1 cells i.e. at the immune synapse.

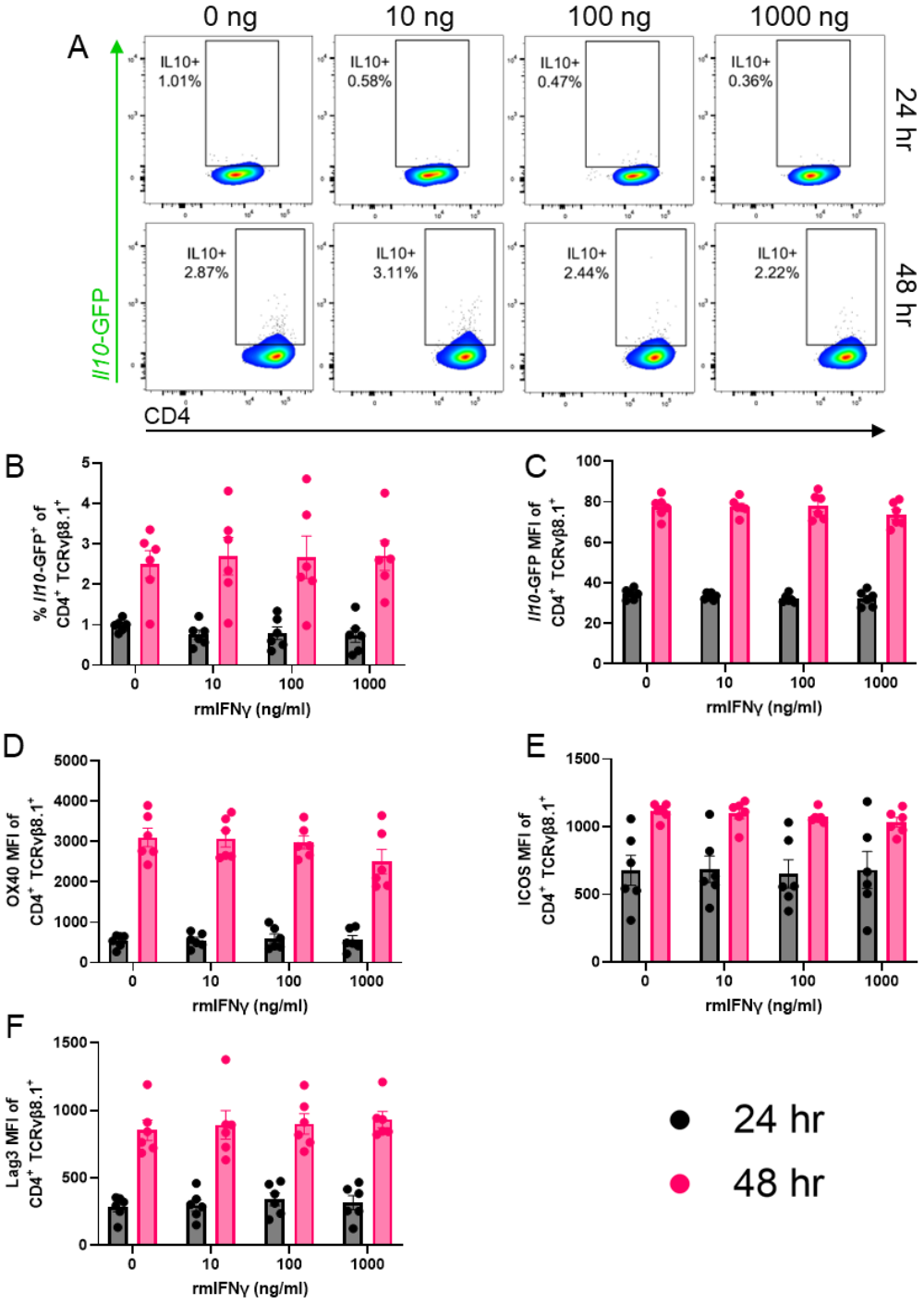

Figure 4-6: *In vitro* IFNγ treatment has no effect of CD4$^+$ splenocytes *Il10*-GFP reporter expression.

CD4$^+$ splenocytes from *Il10*-GFP mice were cultured with anti-CD3, anti-CD28 and recombinant murine IFNγ at 0, 10, 100 and 1000 ng/ml for 24 and 48 hr **(A)**. **(B)** *Il10*-GFP$^+$ frequency for CD4$^+$ TCRvβ8.1$^+$ population. Summary of **(C)** *Il10*-GFP, **(D)** OX40, **(E)** ICOS, and **(F)** LAG3 MFI from CD4$^+$ TCRvβ8.1$^+$ population. **(B-F)** from n=6 mice per treatment, bars represent mean ±SEM.

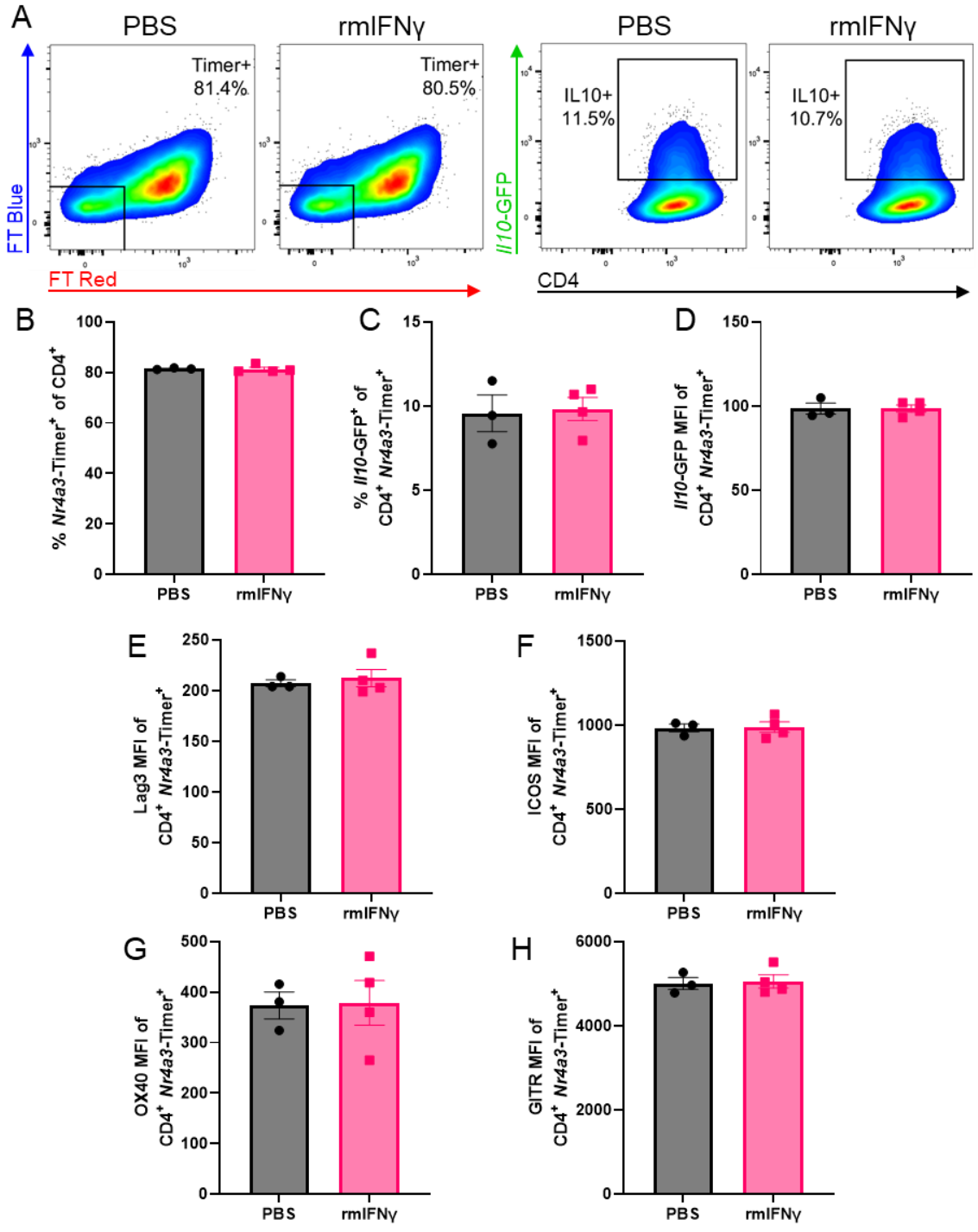

Figure 4-7: *In vivo* IFNγ treatment has no effect on CD4$^+$ splenocytes. *Nr4a3*-Tocky Tg4 *Il10*-GFP mice were given 25 ng of recombinant murine IFNγ in PBS or PBS alone i.p., followed by 4 mg/kg [4Y]-MBP in PBS s.c. and analysed 24 hr later for *Nr4a3*-Timer and *Il10*-GFP **(A)**. Summary of **(B)** Nr4a3-Timer frequency of CD4$^+$ splenocyte population, **(C)** *Il10*-GFP frequency, **(D)** *Il10*-GFP, **(E)** LAG3, **(F)** ICOS, **(G)** OX40 and **(H)** GITR MFI from CD4$^+$ Nr4a3-Timer$^+$ population. **(B-H)** from n=3 mice per PBS and n=4 for rmIFNγ treatment, bars represent mean ±SEM.

4.2.8 *In vivo* anti-IFNγ antibody treatment reduces MHCII and PD-L1 expression at 24 hr.

We next explored the hypothesis that anti-IFNγ may cause a reduction in APC potency and thereby mediated an indirect effect on $CD4^+$ T cell activation and TCR signal strength. In this rapid induction of tolerance model, NK1.1 cells are making almost ¾ of the IFNγ. Some of the remaining 25 % are $CD4^+$ or $CD8^+$, but there are others non-lymphoid subsets. Considering that *Ifng* transcripts in Chapter 3 preceded *Il10* by at least 4 hours, this suggests an indirect cellular mechanism, rather than a direct biochemical mechanism, is responsible for the anti-IFNγ effect on *Il10*-GFP.

We started by looking at changes to populations and generic markers intensity for professional APCs. To separate the lymphoid and myeloid, we first gated for $MHCII^+$ and $CD19^{+/-}$ (fig. 4-8A). $CD19^+$ $MHCII^+$, i.e., B cells, showed no change to frequency in response to anti-IFNγ treatment (fig. 4-8B), but the $CD19^-$ compartment did (fig. 4-8C) – this includes macrophages and DCs. Within these populations, both showed that PD-L1 was sensitive to anti-IFNγ mAb (fig. 4-8D and E for $CD19^-$ and $CD19^+$ respectively).

Within the $MHCII^+$ $CD19^-$ gate, we then stratified populations based on CD11c positivity (fig. 4-8F). CD11c mostly identifies DCs, and some monocytes and macrophages. In figures 4-8G and 4-8H respectively we see that anti-IFNγ does not affect either the frequency of the CD11c positive (DC) or negative populations. However, on both fractions, PD-L1 fluorescence intensity is significantly reduced by anti-IFNγ (fig. 4-8I and 4-8J). This would suggest that of the $MHCII^+$ $CD19^-$ fraction, it is not the $CD11c^+$ frequency that is affected by anti-IFNγ treatment. At 24 hrs post immunisation we saw a reduction in MHCII and PD-L1 intensity in anti-IFNγ treated mice in DC and B cell subsets, but no change to population frequency.

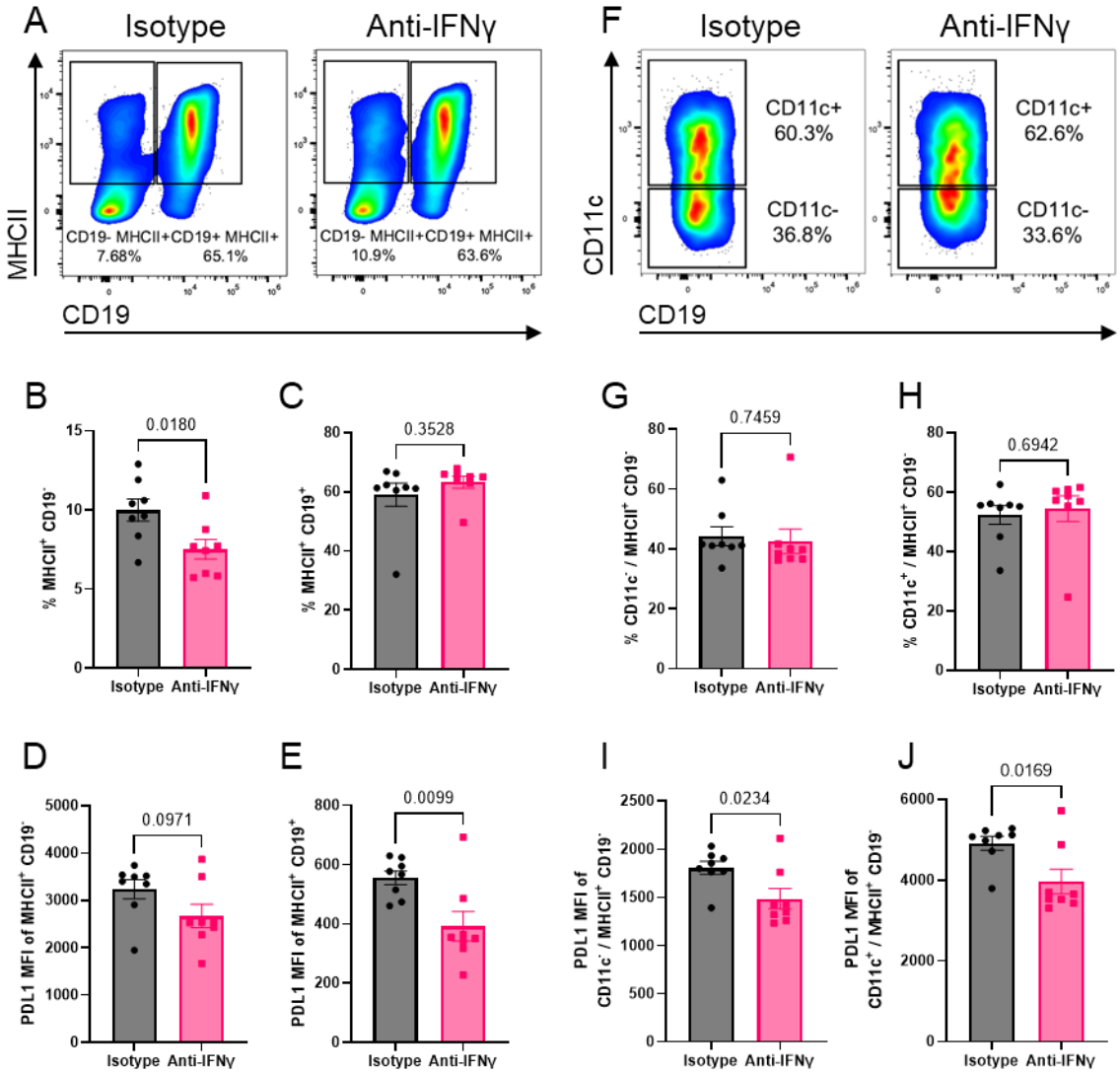

Figure 4-8: *In vivo* anti-IFNγ antibody treatment reduces MHCII and PD-L1 expression at 24 hr.
Nr4a3-Tocky Tg4 *Il10*-GFP mice were injected with 4 mg/kg [4Y]-MBP s.c. and either 1 mg anti-IFNγ or isotype i.p. in PBS and analysed at 24 hr for **(A)** MHCII+ vs CD19-/+ expression from live. Summary of MHCII+ CD19-/+ frequency **(B/C)** and PDL1 MFI respectively **(D/E)** from **(A)**. Also analysed **(F)** CD11c+/- in MHCII+ CD19+ expression. Summary of CD11c-/+ frequency **(G/H)** and PDL1 MFI respectively **(I/J)** from **(F)**. **(B-E, G-J)** from n=8 mice per treatment, bars represent mean ±SEM, statistical analysis by unpaired two-tailed t test. One representative of two experiments

4.2.9 *In vivo* anti-IFNγ antibody treatment reduces macrophage activation expression at 12 hr.

The previous data had an analysis time point of 24 hr. However, as per Chapter 3, the IL-10 transcriptional burst appears at 12 hr, so we therefore wanted to evaluate APC phenotypes in detail at the 12 hr time point in the presence and absence of IFNγ. Here we included analysis of macrophage and DC, which are the two major APCs aside from B cells. Reasoning that by 24 hr any effect on APCs by anti-IFNγ that impacts $CD4^+$ T cell *Il10*-GFP expression would have already occurred, we decided to look at 12 hr. Also, we began profiling other subtypes in the immunised Tg4 spleen. As the $CD11c^+$ populations profiled in the above experiment showed no change in frequency but some change to PD-L1 intensity in response to anti-IFNγ, we decided to look at $CD11b^+$ population, which also express PD-L1 (fig. 4-9A). It is a non-exclusive marker of macrophages, but with F4/80, an activation marker in mice, these reasonably distinguish an inflammatory myeloid compartment. At 12 hr, anti-IFNγ treatment strongly reduces the $CD11b^+$ $F4/80^+$ $MHCII^+$ population (fig. 4-9B), and significantly reduces activation markers CD40 (fig. 4-9D) and CD86 (fig. 4-9F). As seen in the previous experiment, MHCII and PD-L1 are both reduced by anti-IFNγ (figs. 4-9C and 4-9E respectively). Analysis at 12 hr revealed that most changes were seen in macrophages and not so much DCs.

Furthermore, intensity of inflammatory myeloid activation markers PD-L1, MHCII, CD86 and CD40 (figs. 4-10 A – D, respectively) correlated positively with the frequency of *Il10*-GFP^+ in $CD4^+$ *Nr4a3*-$Timer^+$ T cells regardless of treatment. When delineated by treatment, anti-IFNγ treated mice, show positive correlations between activation marker intensity and $CD4^+$ *Nr4a3*-$Timer^+$ *Il10*-GFP frequency, but the isotype treated

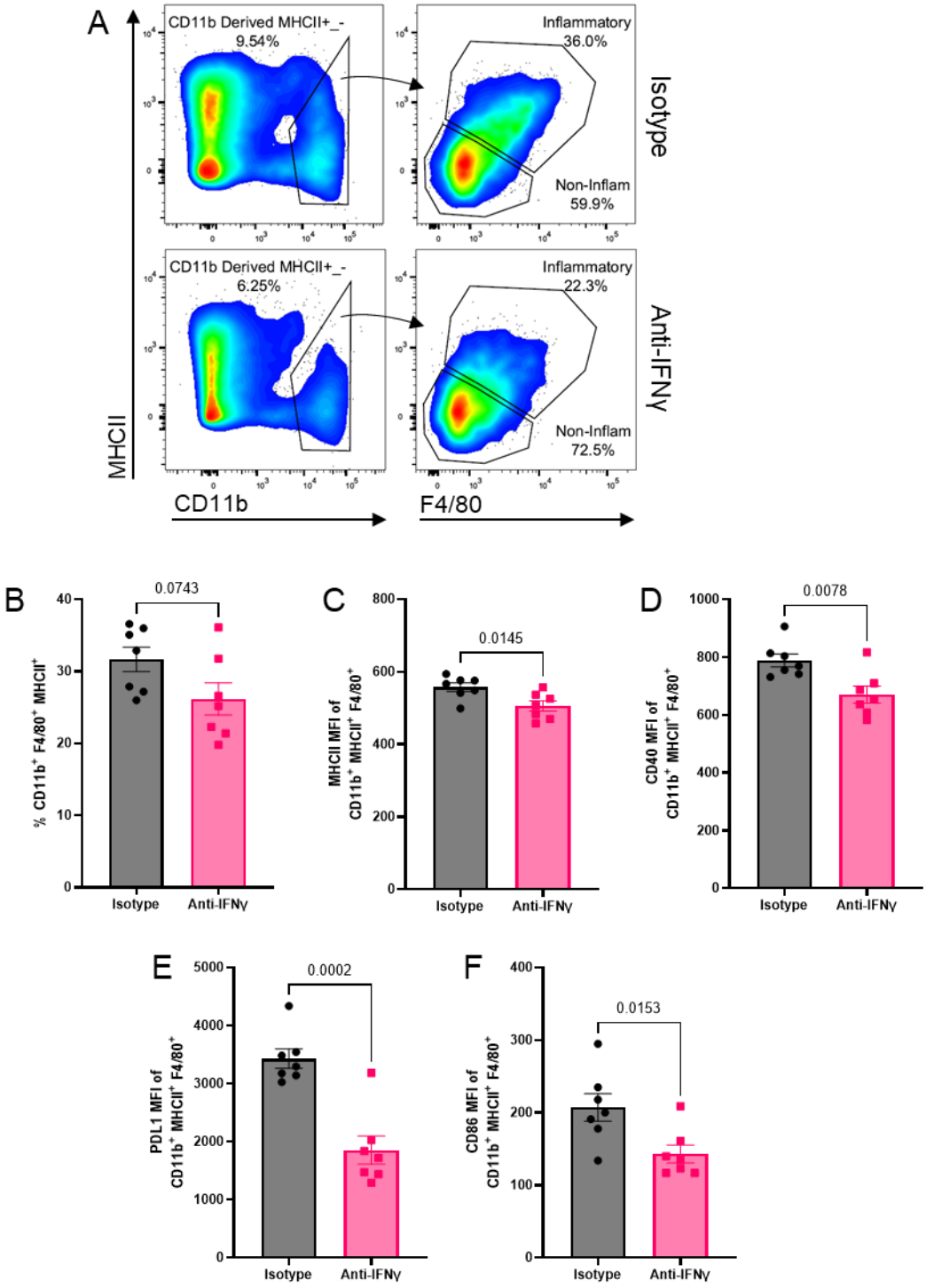

Figure 4-9: *In vivo* anti-IFNγ antibody treatment reduces MHCII expression at 12 hr.

Nr4a3-Tocky Tg4 *Il10*-GFP mice were injected with 4 mg/kg [4Y]-MBP s.c. and either 1 mg anti-IFNγ or isotype i.p. in PBS and analysed at 12 hr for **(A)** MHCII vs CD11b and MHCII vs F4/80 from CD11b derived MHCII$^{+/-}$. **(B)** Summary of "Inflammatory" Myeloid cells (CD11b^{+} F4/80^{+} MHCII^{+}) from **(A)**. **(C)** MHCII MFI, **(D)** CD40 MFI, **(E)** PDL1 MFI, **(F)** CD86 MFI from "Inflammatory" Myeloid cells from **(A)**. **(B-F)** from n=7 mice per treatment, bars represent mean ±SEM, statistical analysis by unpaired two-tailed t test. One representative of three experiments.

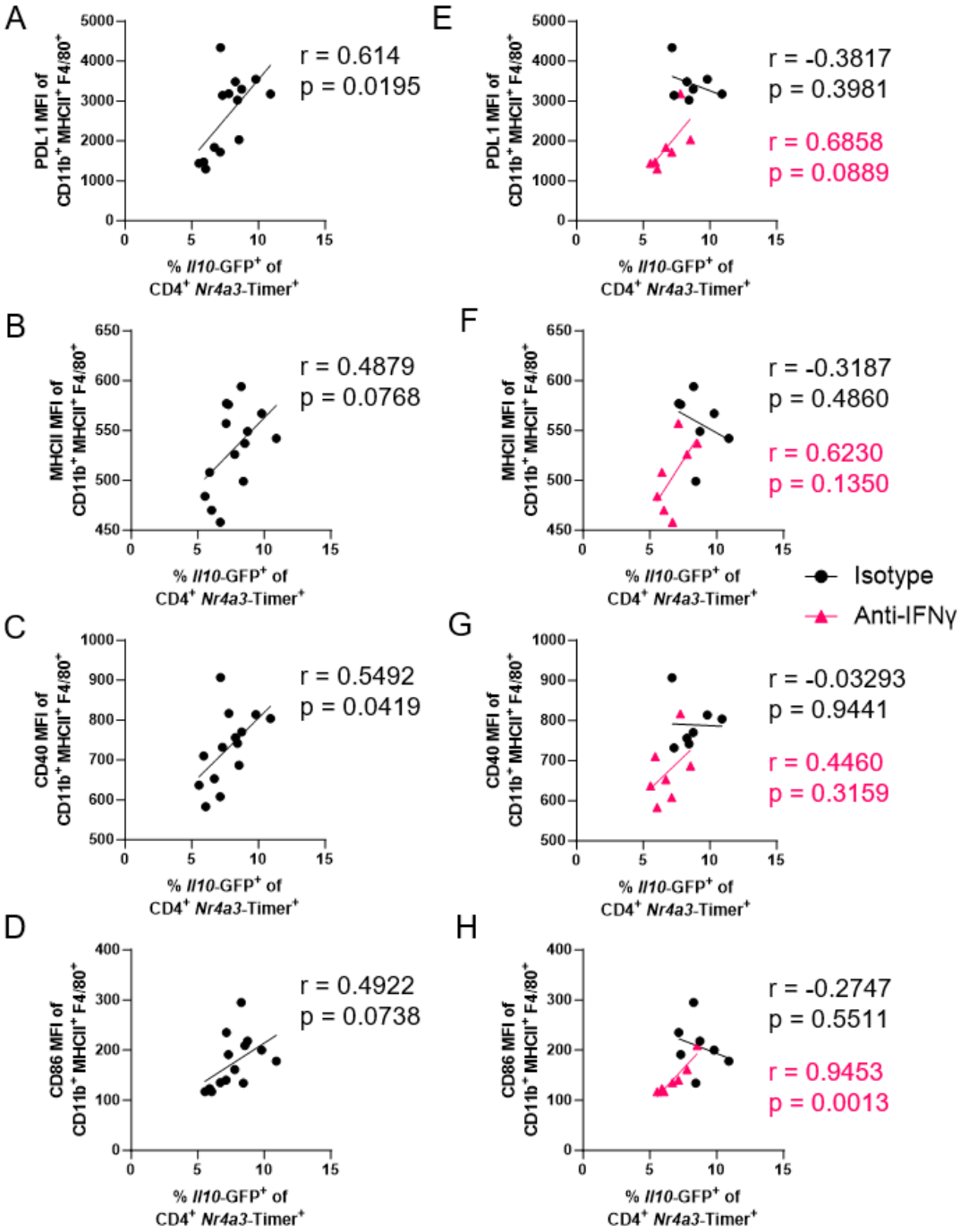

Figure 4-10: *In vivo* anti-IFNγ antibody enhances inflammatory myeloid activation correlation with CD4$^+$ *Il10*-GFP expression at 12 hr.
Nr4a3-Tocky Tg4 *Il10*-GFP mice were injected with 4 mg/kg [4Y]-MBP s.c. and either 1 mg anti-IFNγ or isotype i.p. in PBS and analysed at 12 hr. Correlations of PD-L1 **(A)**, MHCII **(B)**, CD40 **(C)**, and CD86 **(D)** MFI in CD11b$^+$ MHCII$^+$ F4/80$^+$ against % *Il10*-GFP$^+$ CD4$^+$ *Nr4a3*-Timer$^+$ in all samples. Correlations delineated by treatment for PD-L1 **(E)**, MHCII **(F)**, CD40 **(G)**, and CD86 **(H)** MFI from the same mice as **(A-D)**. **(A-H)** from n=7 mice per treatment, statistical analysis by Pearson correlation coefficient and two-tailed test. One representative of three experiments.

show no correlation for CD40 (fig 4-10G), and negative correlations for PD-L1, MHCII and CD86 (figs. 4-10E, F and H, respectively).

4.2.10 Effect of anti-IFNγ treated macrophages on CD4$^+$ T cell priming and *Il10* expression

To test whether macrophages generated *in vivo* in the presence or absence of IFNγ could differ in functional potency and alter IL-10 induction we decided to co-culture peptide bearing macrophages with antigen experience or inexperienced T cells. To determine how important APCs are for the anti-IFNγ effect on Tg4 CD4$^+$ *Nr4a3*-Timer$^+$ *Il10*-GFP expressors, we flow sorted CD11b$^+$ F4/80$^+$ APCs from high dose immunised mice and co-cultured them for 18 hr at 3:1 with CD4$^+$ T cells from an unimmunised mouse in 0 or 0.4 μM [4Y]-MBP with isotype or anti-IFNγ. As the CD4$^+$ T cells are unimmunised, this is not a restimulation/recall response experiment, they are receiving their first dose *in vitro*, from the peptide-loaded APCs or the *in situ* peptide (fig 4-11A).

At 0 μM *in situ* peptide, there is still ~5 % of *Nr4a3*-Timer$^+$ expression, mostly in the “arrested” region. The 0.4 μM treated, however, have a lot more *Nr4a3*-Timer$^+$ expression, particularly in the “persistent” region, suggesting that while peptide-loaded macrophages can activate CD4$^+$ T cells via their TCR, *in situ* peptide is more effective at activation in this experiment. There is no significant difference between isotype and anti-IFNγ treated, but a downward trend (fig. 4-11B). The fluorescence intensity of Timer Blue is significantly increased compared to 0 μM (fig. 4-11C), but Timer red has a downward trend (fig 4-11D)

Anti-IFNγ has no impact on *Il10*-GFP expression in the CD4$^+$ *Nr4a3*-Timer$^+$ compartment and is decreased between 0 and 0.4 μM (fig 4-11E). In figure 4-11F, we

see that ICOS frequency is increased significantly increased by 0.4 μM peptide, but not anti-IFNγ, whilst figure 4-11G shows that OX40 is unaffected by mAb treatment and peptide. Finally, figure 4-11H shows that GITR, a marker associated with Tregs and TCR signal strength [325], is decreased by anti-IFNγ only with peptide administration.

Whilst we saw some evidence of reduced TCR signal strength from anti-IFNγ treated macrophages, we were unable to see any effect on *Il10* expression. These data suggest that other factors are required aside from MHCII, macrophages, and IFNγ to drive *Il10*-GFP *in vivo.*

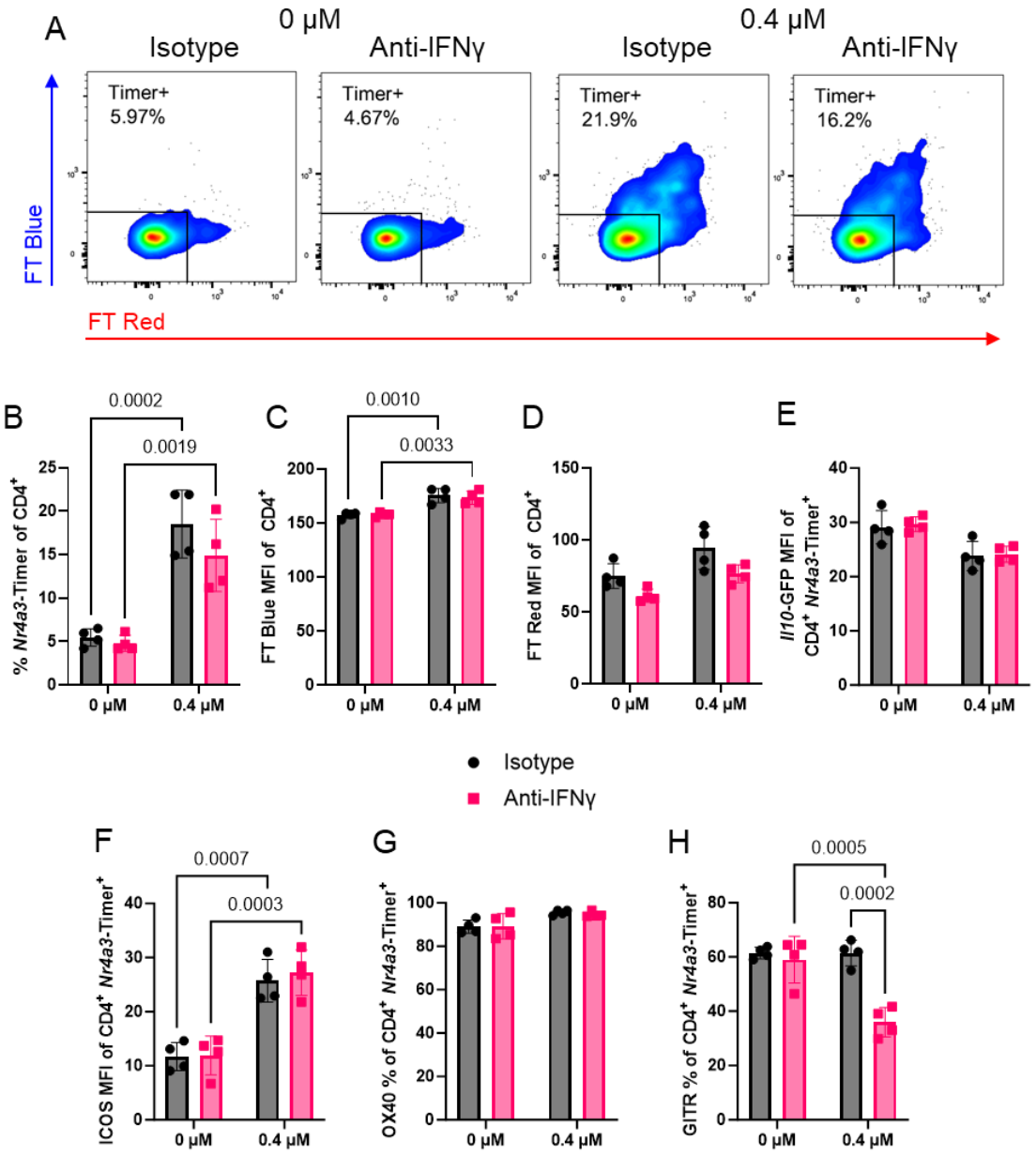

Figure 4-11: Naïve CD4$^+$ T cells co-cultured with peptide bearing, anti-IFNγ-treated macrophages.

Nr4a3-Tocky Tg4 *Il10*-GFP mice were injected with 4 mg/kg [4Y]-MBP s.c. and either 1 mg anti-IFNγ antibody or isotype i.p. in PBS and CD11b$^+$ F4/80$^+$ cells flow sorted 24 hr later. These were co-cultured in either 0 μM or 0.4 μM [4Y]-MBP at a 3:1 (CD4$^+$:CD11b$^+$ F4/80$^+$) ratio with flow sorted splenic *Nr4a3*-Tocky Tg4 *Il10*-GFP T cells from an unimmunised, untreated mouse for 18 hr before analysis of CD4$^+$ *Nr4a3*-Timer$^+$ **(A)**. **(B)** Summary of *Nr4a3*-Timer$^+$ population changes from **(A)**. **(C)** Summary of FT Blue MFI in CD4$^+$. **(D)** Summary of FT Red MFI in CD4$^+$. **(E)** Summary of *Il10*-GFP MFI in *Nr4a3*-Timer$^+$ from **(A)**. Summary of **(F)** ICOS, **(G)** OX40 and **(H)** GITR frequency in CD4$^+$ Nr4a3-Timer$^+$ from **(A)**. **(B-H)** from n=4 samples per [4Y]-MBP concentration and antibody treatment. Analysis by Ordinary two-way ANOVA with Tukey's multiple comparisons test. Bars represent mean ±SEM

4.2.11 *Il10* transcription sensitivity to restimulation dose and antibody/cytokine treatment

Multiple other signalling pathways have been reported to be involved in Tr1 cell development. To screen for potential other regulators of IL-10 induction we developed a restimulation assay *in vitro* where we could culture *in vivo* stimulated T cells and restimulate with peptide and assess the ability of different pathways to control IL-10 secretion. Having conducted some work *in vivo* and *in vitro* regarding the primary response to immunisation under anti-IFNγ and rmIFNγ, we chose to investigate the recall response and how it was affected by different conditions. In this 'hybrid model', Tg4 mice were first given 4 mg/kg [4Y]-MBP and 24 hr later, the splenocytes were co-cultured for a further 24 hr with an increasing dose of peptide (from 0 to 100 nM) and a variety of antibodies or cytokines, and how they might impact recall was assessed. Anti-IFNγ was chosen as it was the focus of our primary immunisation experiments, and we hypothesised that in a secondary immunisation would sustain decreased *Il10*-GFP expression. We also hypothesised that direct application of recombinant IFNγ to already activated T cells would alter *Il10*-GFP expression although it had no effect *in vivo*. We also explored the role of known IL-10 inducing cytokine IL-27 through supplementation and blockade. Previous work by the group had established that anti-PD-L1 treatment boosted *Il10*-GFP in primary immunisation, and anti-IL-10 was included to interrupt T cell secreted IL-10 feedback and test whether the ELISA was capturing IL-10 protein. Downstream signalling of ICOS, a marker of strong TCR signalling, reportedly leads to *Il10* transcription, so we used antagonising and agonising antibody to modulate *Il10*-GFP [371].

In figure 4-12A we see that with increasing secondary peptide dose comes an increasingly persistent $CD4^+$ T cell population, and similarly in figure 4-12B, an increasingly *Il10*-GFP positive population. In 4-12C, *Il10*-GFP positivity clearly correlates with increasing restimulation concentration across all treatment conditions. IL-10 secretion by [4Y]-MBP restimulation correlates positive with dose (fig. 4-12D). At the highest restimulation concentration, 100 nM, we see that only anti-IL-10 and anti-IL-27 have a significant reduction in *Il10*-GFP expression (fig. 4-12E). Conditions that elicited a significant effect *in vivo* (anti-IFNγ) did not have a significant effect in the hybrid model, but there is still a decreasing trend. Many of the treatments lead to a non-significant decrease in *Il10*-GFP, even when logically they should have the opposite effect i.e., recombinant IL-27 and IFNγ against anti-IL-27 and anti-IFNγ. There is not, however, a discernible reduction in IL-10 protein (fig. 4-12.F) for anti-IL-27 despite a reduction in *Il10*-GFP. The reduction from anti-IL-10 treatment is logical in an ELISA, as the treatment antibody captures IL-10 protein from the supernatant, and therefore there is less available for the ELISA capture antibody. Our data suggested that IL-27, which has been identified previously as a Tr1 cell inducer, may also have positive roles in driving *Il10*-GFP transcription in our model.

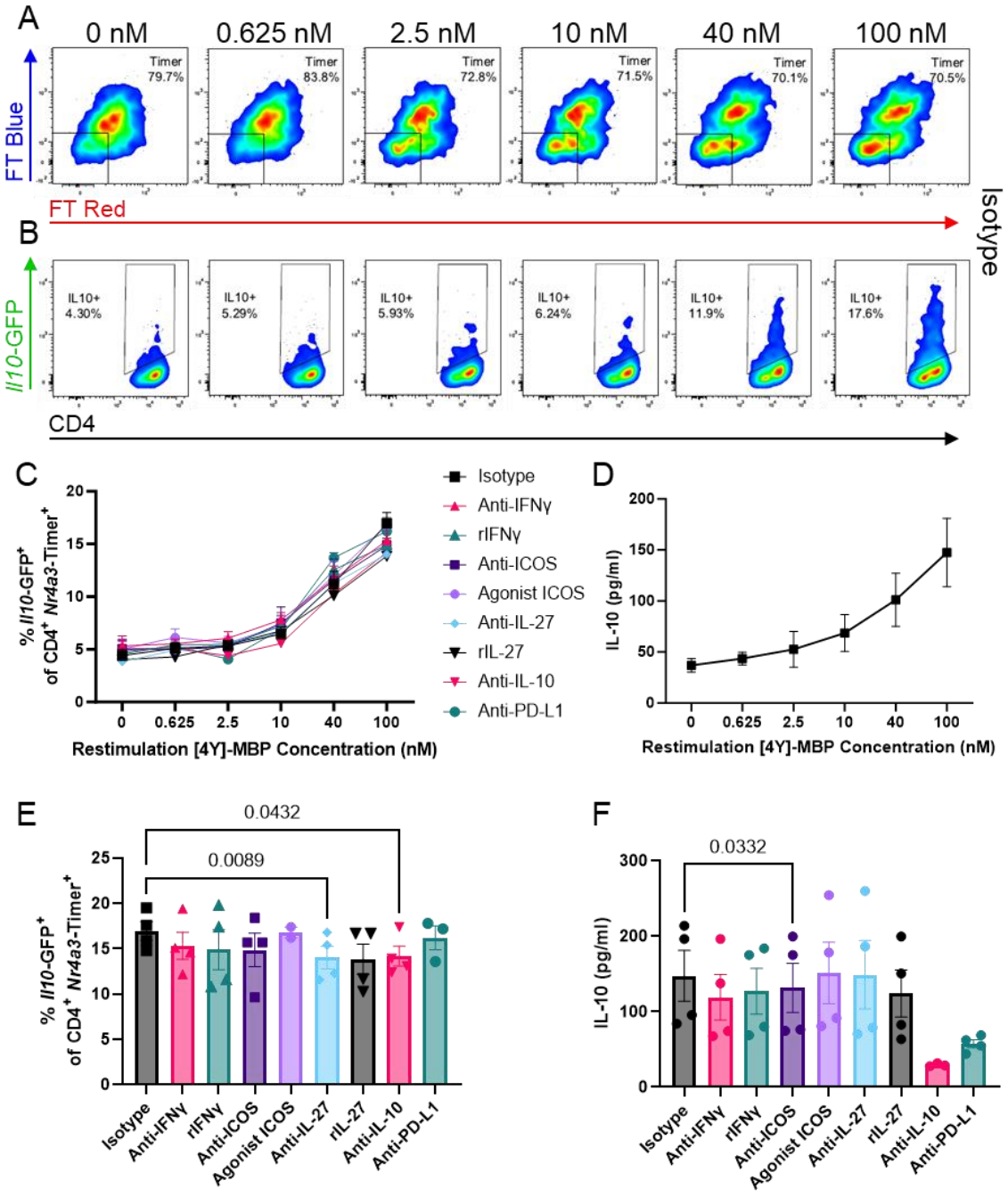

Figure 4-12: *Il10* transcription sensitivity to restimulation dose and antibody/cytokine treatment.

Nr4a3-Tocky Tg4 *Il10*-GFP mice were injected with 4 mg/kg [4Y]-MBP s.c. in PBS and 24 hr later their splenocytes harvested for culture in 0, 0.625, 2.5, 10, 40 or 100 nM [4Y]-MBP and Isotype, anti-IFNγ, recombinant (r)IFNγ, anti-ICOS, agonist ICOS, anti-IL-27, recombinant (r)IL-27, anti-IL-10 or anti-PD-L1 for a further 24 hr at 37 °C 5 % CO_2 before analysis of *Nr4a3*-Timer$^+$ population **(A)** and *Il10*-GFP$^+$ **(B)**. **(C)** Summary of all conditions and [4Y]-MBP concentrations. **(D)** Quantification of IL-10 in isotype treated supernatants. **(E)** Summary of **(B)** at 100 nM only. **(F)** Quantification of IL-10 in supernatants at 100 nM only. From n=4 mice, **(E, F)** analysis by mixed effect analysis. Bars represent mean ±SEM. One representative of four experiments.

4.2.12 Anti-IL-27 effect on CD4$^+$ Timer$^+$ *Il10*-GFP$^+$ splenocytes.

IL-27 is considered a pioneer factor in *Il10*-GFP$^+$ Tr1 cell development. Here we investigated the effect of anti-IL-27 antibody on *Il10*-GFP expression under a primary *in vivo* immunisation, having seen anti-IL-27 reduce *Il10*-GFP during a secondary immunisation in the hybrid model. Anti-IL-27 reduced *Il10*-GFP in the hybrid recall, and in this primary immunisation experiment we see that there is no effect on *Nr4a3*-Timer expression (fig. 4-13A, C), but that *Il10*-GFP is strongly and significantly reduced (fig. 4-13B, D). *Il10*-GFP fluorescence intensity appears to be unaffected (fig. 4-13E). Although there is a significant reduction (similar to the anti-IFNγ effect) on *Il10*-GFP, this is not reflected in the surface markers OX40 (fig. 4-13F) and ICOS (fig.4-13G), which are unaffected. This difference prompted us to investigate any potential crossover between their mechanisms of action. These data suggest that IL-27 neutralisations significantly effected *Il10*-GFP expression but not markers associated with TCR strong signalling.

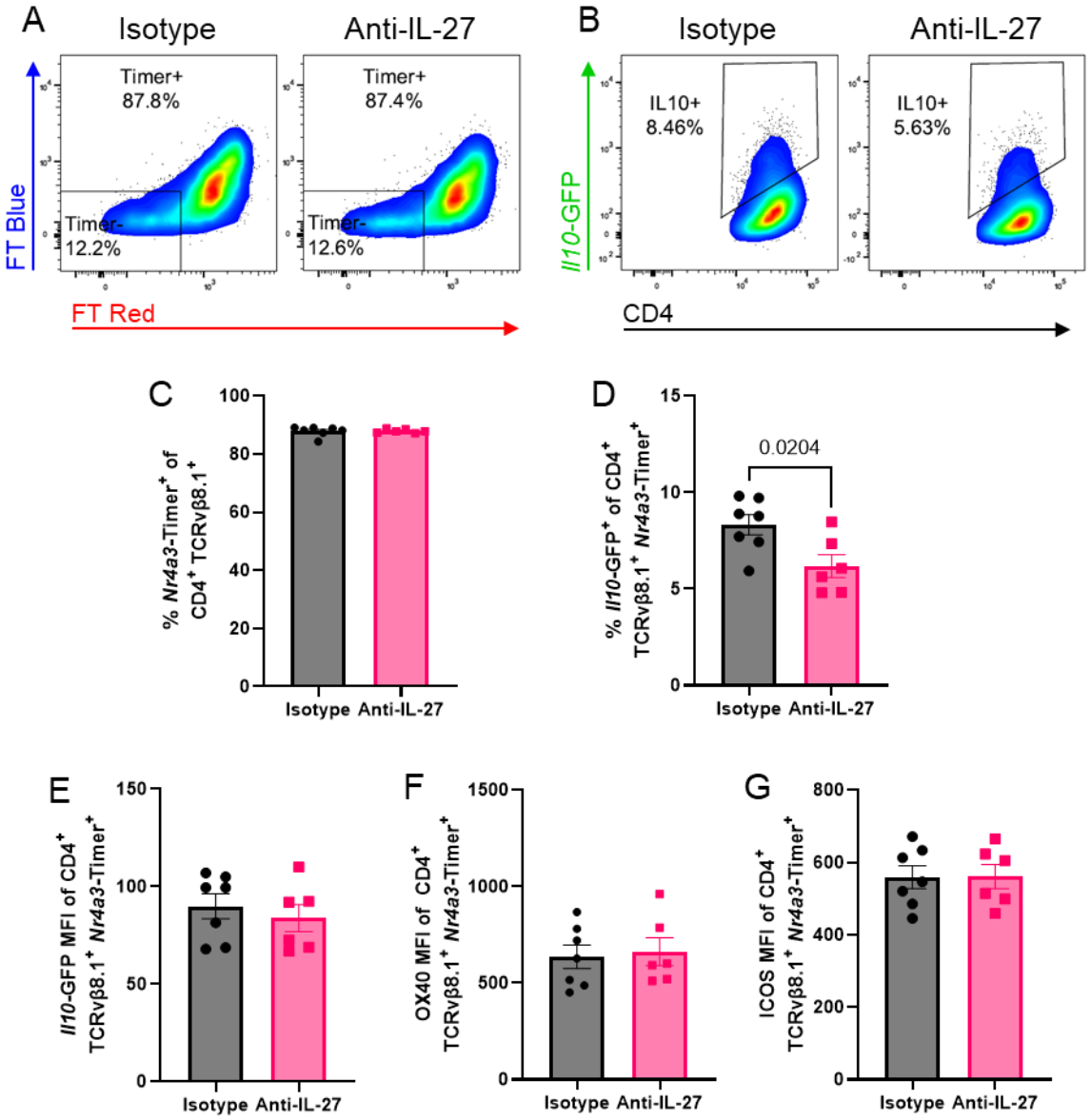

Figure 4-13: Anti-IL-27 effect on CD4$^+$ Timer$^+$ *Il10*-GFP$^+$ splenocytes.
Nr4a3-Tocky Tg4 *Il10*-GFP mice were injected with 4 mg/kg [4Y]-MBP s.c. and 200 µg anti-IL-27 or isotype i.p. in PBS before analysis for *Nr4a3*-Timer **(A)** and *Il10*-GFP **(B)** expression. **(C)** Summary of **(A)**. **(D, E)** Summary of **(B)**. **(F, G)** Summary of OX40 and ICOS MFI respectively. From n=7 mice for isotype and 6 for anti-IL-27, **(C-G)** analysis by unpaired t test. Bars represent mean ±SEM. One representative of two experiments.

4.2.13 Anti-IFNγ and anti-IL-27 effect on CD4$^+$ *Nr4a3*-Timer$^+$ *Il10*-GFP$^+$ splenocytes

Given that both IFNγ and IL-27 can modulate IL-10 development, we wanted to understand whether these worked in an additive or redundant fashion. Having profiled the effects of anti-IFNγ and anti-IL-27 on *Il10*-GFP expression in the hybrid system and separately through primary immunisations, we observed the effect of these antibodies in combination, administering either 200 µg anti-IL-27 or 500 µg anti-IFNγ, or both in combination intraperitoneally 30 min before administering 4 mg/kg [4Y]-MBP subcutaneously and analysing splenocytes 24 hr later (fig. 4-14A). Not only did anti-IFNγ and anti-IL-27 reduce *Il10*-GFP individually, in combination they show a larger reduction in frequency (fig. 4-14B) and intensity (fig. 4-14C). This suggests that anti-IFNγ and anti-IL-27 modulate *Il10-GFP* by different mechanisms.

4.2.14 Anti-IFNγ and anti-IL-27 effect on surface markers of CD4$^+$ Nr4a3-Timer$^+$ splenocytes

The use of spectral cytometry for this experiment allowed us to observe more markers than flow at the same time (fig. 4-15A). In the CD4$^+$ TCRvβ8.1$^+$ *Nr4a3*-Timer$^+$ population, we see that OX40 (fig. 4-15B), LAG3 (fig. 4-15E), ICOS (fig. 4-15F) and GITR (fig. 4-15G) intensity is modestly reduced by anti-IFNγ but brought up by anti-IL-27. Combination treatment shows little compared to isotype. In fig. 4-15C, all treatments suggest increased CD25 compared to isotype. PD-1 intensity is driven slightly up by anti-IFNγ, and to a lesser extent by anti-IL-27, with the combination effect being closer to anti-IFNγ (fig. 4-15D).

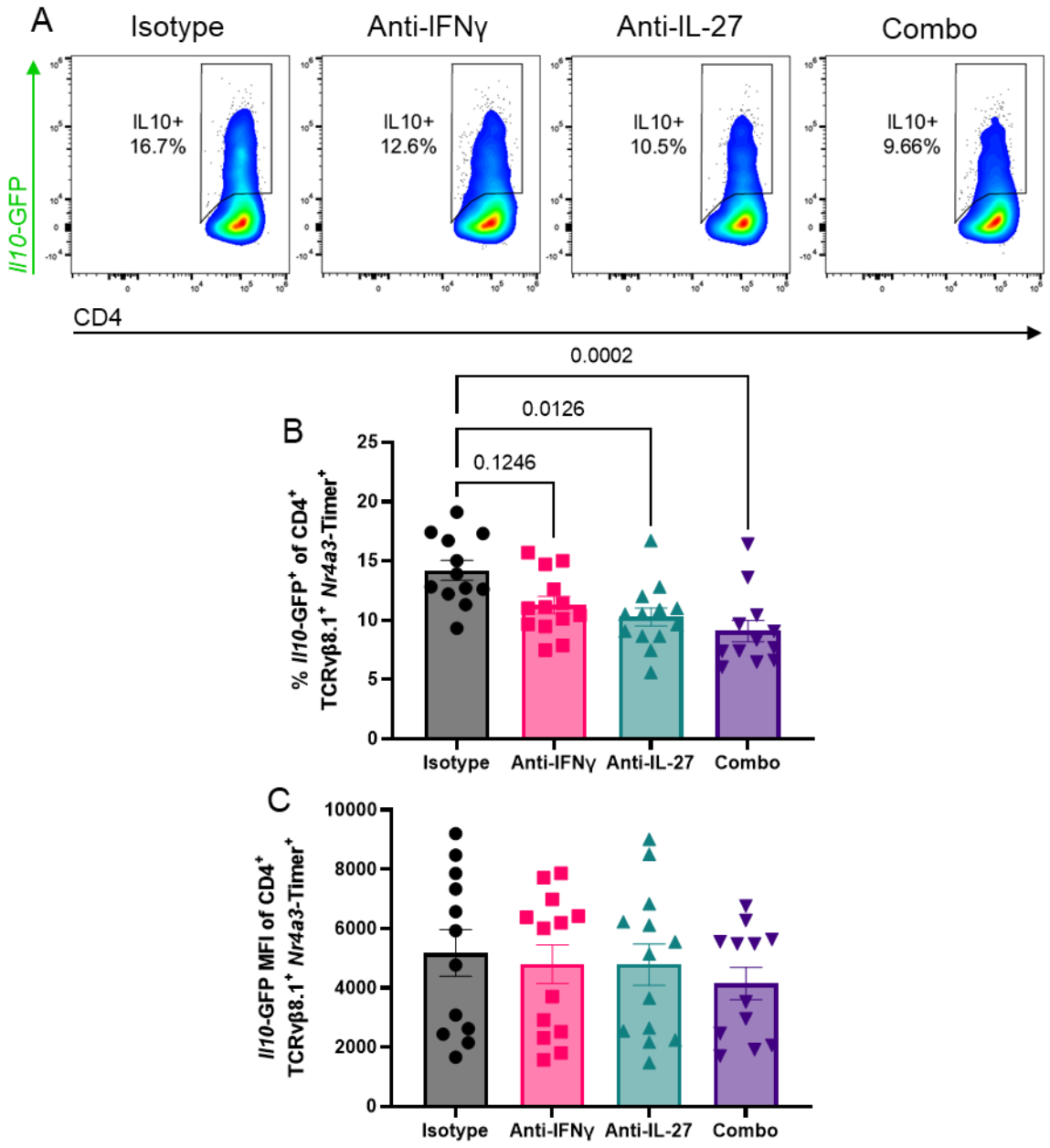

Figure 4-14: Anti-IFNγ and anti-IL-27 effect on CD4$^+$ *Nr4a3*-Timer$^+$ *Il10*-GFP$^+$ splenocytes.
Nr4a3-Tocky Tg4 *Il10*-GFP mice were injected with 4 mg/kg [4Y]-MBP s.c. and 500 µg anti-IFNγ, 200 µg anti-IL-27, both (combo) or isotype pool i.p. in PBS before analysis for CD4$^+$ *Nr4a3*-Timer$^+$ *Il10*-GFP$^+$ expression **(A)**. **(B)** Summary of *Il10*-GFP$^+$ frequency from **(A)**. **(C)** Summary of Il10-GFP MFI. From n=12 mice for isotype and combo, and n=13 mice for anti-IFNγ and anti-IL-27. Analysis by Kruskal-Wallis test. Bars represent mean ±SEM. Pooled from two experiments, representative of three.

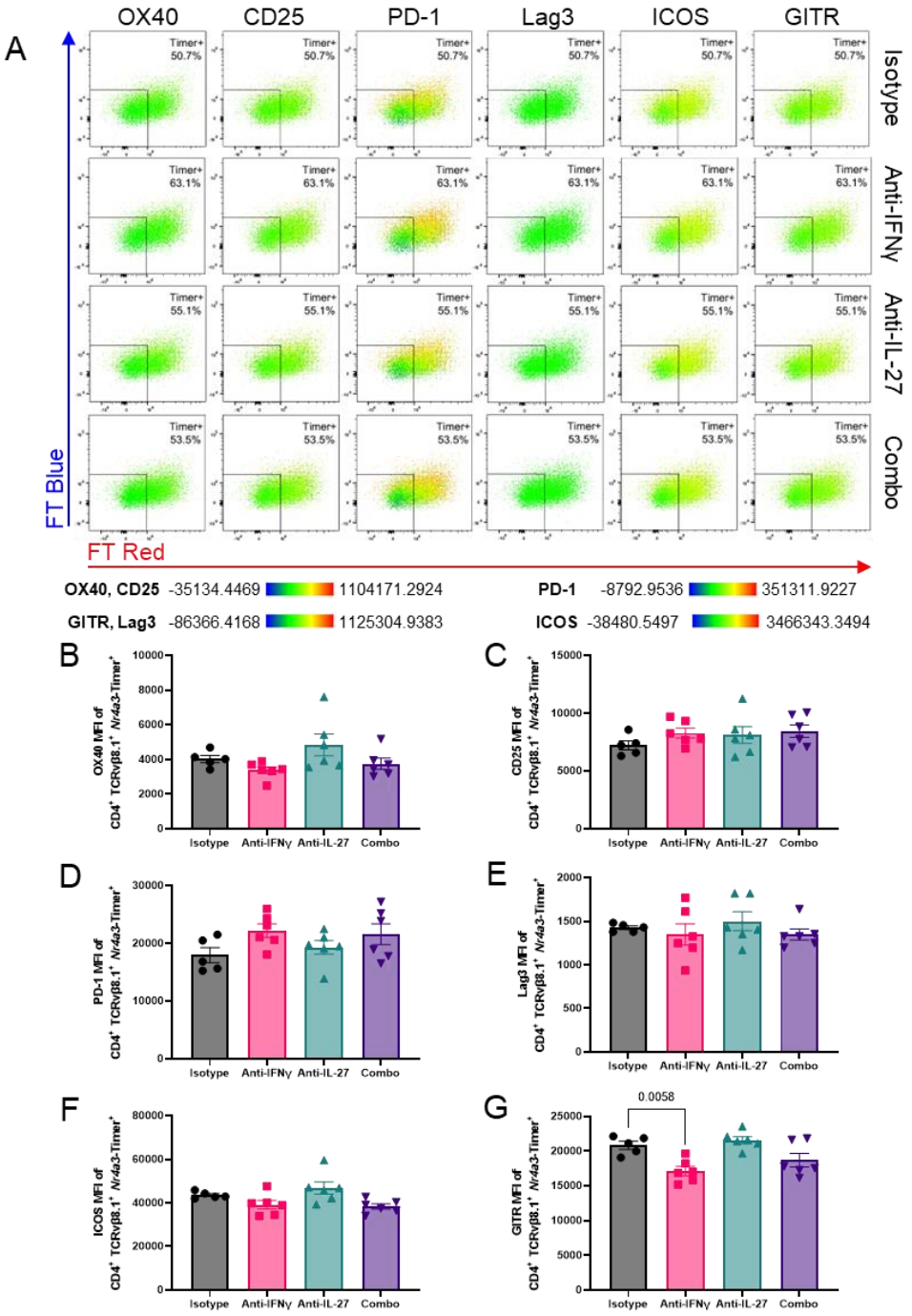

Figure 4-15: Anti-IFNγ and anti-IL-27 effect on surface markers of CD4$^+$ *Nr4a3*-Timer$^+$ splenocytes.

Nr4a3-Tocky Tg4 *Il10*-GFP mice were injected with 4 mg/kg [4Y]-MBP s.c. and 500 µg anti-IFNγ, 200 µg anti-IL-27, both (combo) or isotype pool i.p. in PBS before analysis for markers by CD4$^+$ TCRvβ8.1$^+$ *Nr4a3*-Timer$^+$ expression **(A)**. Summary of treatment effect on **(B)** OX40, **(C)** CD25, **(D)** PD-1, **(E)** LAG3, **(F)** ICOS and **(G)** GITR MFI. From n=5 mice for isotype and n=6 mice for anti-IFNγ, anti-IL-27 and combo. Analysis by one-way ANOVA with Dunnett's correction. Bars represent mean ±SEM. One representative of three experiments.

4.2.15 Anti-IFNγ and anti-IL-27 effect on antigen presenting populations

Anti-IFNγ treatment not only modulated $CD4^+$ *Nr4a3*-Tocky$^+$ *Il10*-GFP expression but also antigen presentation in our earlier experiments *in vivo* anti-IFNγ only treated mice. So, we looked at antigen presentation in the combination treated mice following primary immunisation (fig. 4-16A), first gating for B cells, then inflammatory and non-inflammatory myeloid from the non-B cells. The presenting B cells ($MHCII^+$ $B220^+$ of fig. 4-16C) show little impact from anti-IFNγ, but a small downward trend from anti-IL-27. The myeloid antigen presenters ($MHCII^+$ $B220^-$ of fig 4-16B), the further subset of $CD11b^+$ $MHCII^{+/-}$ (fig. 4-16D) and its "inflammatory" compartment of $MHCII^+$ $F4/80^+$ (fig. 4-16E) all show a significant reduction by anti-IFNγ and no change by anti-IL-27.

4.2.16 Anti-IFNγ and anti-IL-27 effect on surface markers of antigen presentation markers from $CD11b^+$ $MHCII^+$ $F4/80^+$ population

Within the "inflammatory" myeloid compartment (fig. 4-17A) we see much the same result with MHCII (fig. 4-17B)– a reduction in signal with anti-IFNγ but no change with anti-IL-27 and combination an average of the two. Other surface markers only partially follow this trend. PD-L1, F4/80 and CD86 (fig. 4-17C, D and E) are all reduced by anti-IFNγ and combination treatments but show a partial increase with anti-IL-27 treatment.

In summary, this chapter demonstrates roles for IFNγ and IL-27 in driving Tr1-like cell induction in a rapid model of tolerance in an indirect manner, and that the sources of these cytokines is crucial to understanding the mechanisms at play.

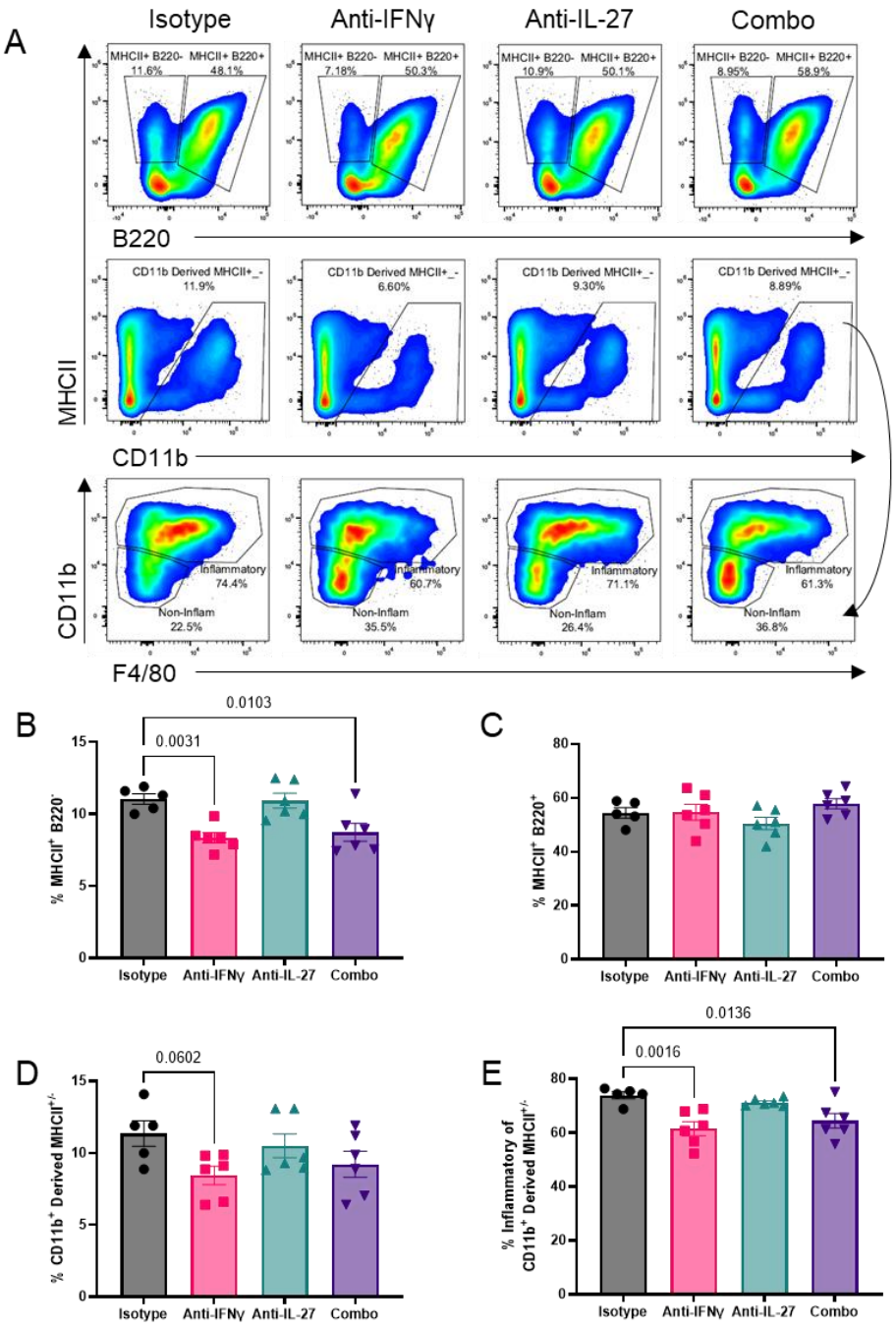

Figure 4-16: Anti-IFNγ and anti-IL-27 effect on surface markers of antigen presentation.

Nr4a3-Tocky Tg4 *Il10*-GFP mice were injected with 4 mg/kg [4Y]-MBP s.c. and 500 µg anti-IFNγ, 200 µg anti-IL-27, both (combo) or isotype pool i.p. in PBS before analysis for antigen presentation populations **(A)**, including $B220^{+/-}$, $CD11b^{+}$ $MHCII^{+/-}$ and $F4/80^{+/-}$ from $CD11b^{+}$ $MHCII^{+/-}$ Summary of **(B)** $MHCII^{+}$ $B220^{-}$, **(C)** $MHCII^{+}$ $B220^{+}$, **(D)** $CD11b^{+}$ $MHCII^{+/-}$ and **(E)** Inflammatory ($F4/80^{+}$) from **(D). (B-E)** from n=5 mice for isotype and n=6 mice for anti-IFNγ, anti-IL-27 and combo. Analysis by one-way ANOVA with Dunnett's correction. Bars represent mean ±SEM. One representative of three experiments.

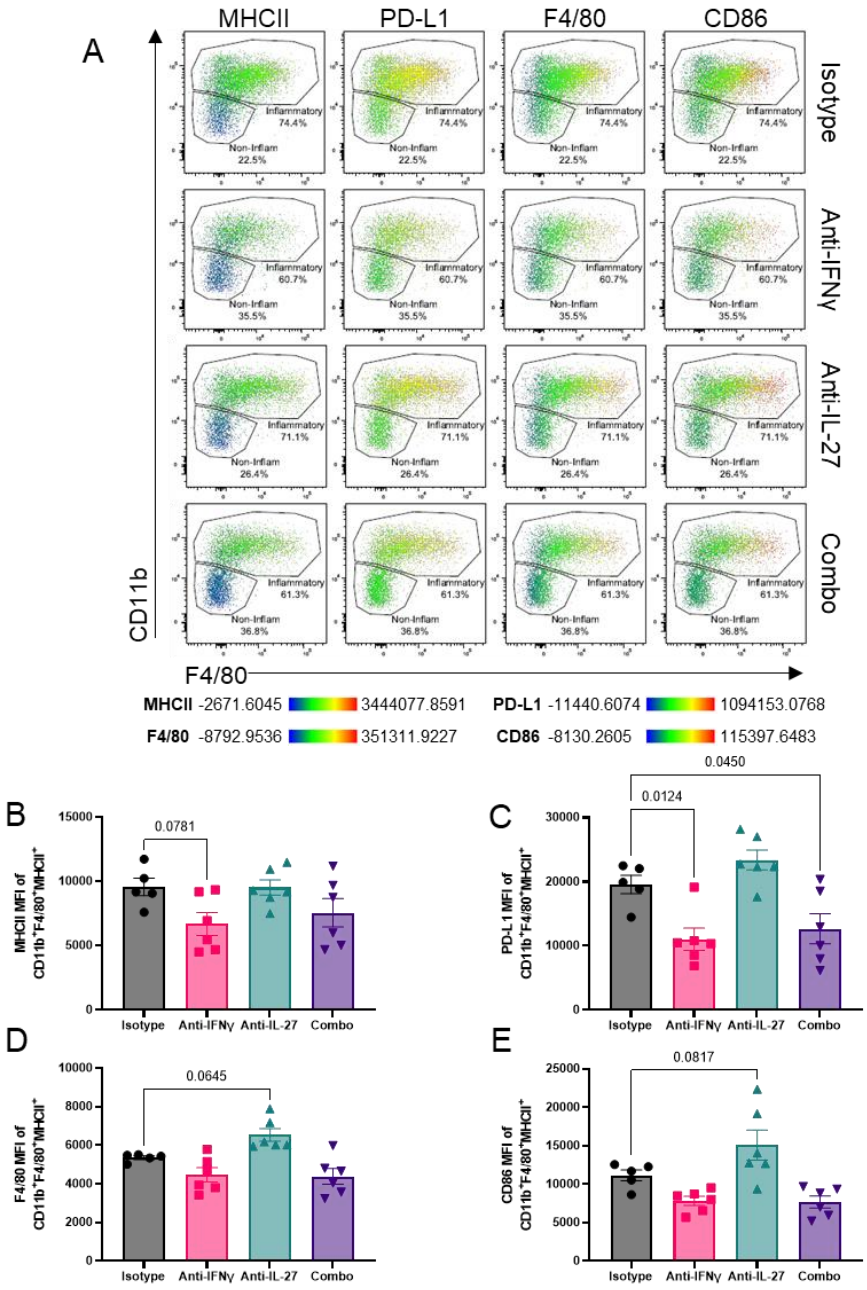

Figure 4-17: Anti-IFNγ and anti-IL-27 effect on surface markers of antigen presentation markers from CD11b+ MHCII$^+$ F4/80$^+$ population.
Nr4a3-Tocky Tg4 *Il10*-GFP mice were injected with 4 mg/kg [4Y]-MBP s.c. and 500 µg anti-IFNγ, 200 µg anti-IL-27, both (combo) or isotype pool i.p. in PBS before analysis for antigen presentation in CD11b$^+$ MHCII$^+$ F4/80$^+$ compartment **(A)**, including **(B)** MHCII MFI, **(C)** PD-L1 MFI **(D)** F4/80 MFI and **(E)** CD86 MFI. **(B-E)** from n=5 mice for isotype and n=6 mice for anti-IFNγ, anti-IL-27 and combo. Analysis by one-way ANOVA with Dunnett's correction. Bars represent mean ±SEM. One representative of three experiments.

4.3 Discussion

The frequency of *Nr4a3*-Timer$^+$ is unchanged by anti-IFNγ. This lack of effect on *Nr4a3*-Timer reflects that *Nr4a3* signalling is digital, and when switched on cannot be switched on again. A reduction in MHCII and therefore reduction in antigen presentation should result in a lower number of TCRs being engaged, and therefore reduced TCR signalling and population of *Nr4a3*-Timer$^+$, but this is not the case. There is a reduction in markers that are associated with TCR and CD28 signalling i.e., *Il10*-GFP, LAG3, ICOS etc., but no change in *Nr4a3*-Timer itself. This is reflective of the quality of TCR signal received by the CD4$^+$ T cell population, not the quantity of that signal.

Any increase in *Il10*-GFP expression between 24 and 48 hr in fig. 4-6 is likely due to the blast effect of activated T cells, getting larger to accommodate increased metabolic demand, and not a result of any exposure to rmIFNγ. No APCs were present, and it likely that this is why there was no effect. Validating the potency of rmIFNγ would rule out that it was a defective reagent, lending credence to APCs as the agent of change in the anti-IFNγ mechanism.

Ifng-YFP$^+$ cells make up around 3 % of splenocytes, and of those ~75 % are NK1.1$^+$. The remaining ~25 % are likely to be CD8$^+$ T cells and APCs, as well as others. Total *Ifng*-YFP$^+$ cells are increased by anti-IFNγ mAb, likely by negative feedback, but overall frequency of NK1.1$^+$ cells from the *Ifng*-YFP$^+$ fraction doesn't change. The *Ifng*-YFP$^+$ cells from the total NK1.1$^+$ fraction does increase *Ifng*-YFP in response to anti-IFNγ, however the population of NK1.1$^+$ decreases.

The unresponsiveness to rmIFNγ could be attributed to too low a dose, but the dose we gave would be about 1 ng/ml of blood – quite high for a mouse. Perhaps the rmIFNγ could not permeate the tissues or enter the immune synapse in sufficient quantities at the cell surface level to reach the IFNγR.

Anti-IFNγ decreasing *Il10*-GFP, LAG3, ICOS, OX40 and GITR whilst anti-IL-10 does not and only increase *Il10*-GFP frequency, suggesting that both antibodies modulate T cell expression through different signalling pathways, rather than both solely though TCR-MHCII reduction, and that a secondary signal or threshold may be required for the effect.

Anti-IFNγ decreasing the frequency of $CD19^{-}$ $MHCII^{+}$ but not $CD19^{+}$ encourages the idea that it is acting through a myeloid, rather than lymphoid, professional APC. However, seeing that they are unaffected by treatment according to CD11c frequency and that PD-L1 intensity is decreased on all subsets suggests that it may be a phenotypic change rather than population. In the subsequent experiment, we see that there is an inflammatory, activated antigen-presenting myeloid population that is decreased by anti-IFNγ ($CD11b^{+}$ $MHCII^{+}$ $F4/80^{+}$). Short of identifying them as macrophages, this population also showed phenotypic change with reduced inflammatory markers. Overall, these investigations of APC phenotype under mAb treatment suggest that by reducing environmental IFNγ then there are fewer activated APCs. This reduction in activation is associated with decreased expression of MHCII and therefore reduced TCR signalling, having the downstream effect of reduced *Il10*-GFP and other markers of regulation (LAG3, TIGIT) and activation (GITR, ICOS).

The *ex vivo* co-culture of peptide bearing macrophages and antigen experienced or inexperienced T cells has several flaws. We didn't have an unimmunised APC control, or a sample that was only T cells. Not all the APCs sorted could be specific to [4Y]-MBP, even with a high dose. There is no 3D architecture (ECM) for APCs to move around in and contact multiple T cells to activate, which could explain the weak response we see in this experiment. Additionally, we did not phenotype the co-cultured macrophages, so we do not know whether the anti-IFNγ influenced them here, even if we assume that it did. Changes in ICOS and GITR are very different to those seen in the *in vivo* model, and *Nr4a3*-Timer expression was strongly affected by the *in vitro* dose, which would be a secondary effect for the macrophages, but primary one for the T cells.

In examining how the recall response would be affected by antibody treatments, we began using a hybrid *in vivo* : *in vitro* model, with antibody or cytokine treatments at the 2nd (*in vitro*) immunisation. Secondary immunisations are routinely carried out *in vivo*, but for the purposes of screening like we have done in 4-12, this was far more time and cost efficient. Although in a limited manner, it did show that anti-IFNγ reduces *Il10*-GFP and IL-10 expression on secondary immunisation and revealed that anti-ICOS and anti-IL-27 significantly reduced IL-10 and *Il10*-GFP respectively. We had hypothesised that anti-IL-27 would have this effect, given that its cMaf is a result of downstream IL-27 signalling in Tregs. Anti-IL-10 significantly reducing *Il10*-GFP suggests a feedback mechanism, that be reducing exogenous IL-10, this influences *Il10* expression, be it direct or indirect.

Primary anti-IL-27 treatment did not affect expression of OX40 or ICOS, which anti-IFNγ does. By reducing the number of interactions between IL-27 and IL-27R and

subsequent signalling, it is a separate mechanism of action that we hypothesise from the anti-IFNγ, reducing MHCII on APCs and therefore pMHCII : TCR interactions.

Through a combination of both antibodies, we see that the effect on *Il10*-GFP expression is greater than the sum of its parts. The effect is additive, not redundant and there is significant reduction in expression, implying that they are working through different pathways. This assumption is reinforced by anti-IFNγ altered markers not being changed by anti-IL27 on T cells, particularly LAG3, PD-1 and GITR. If there is an effect, such as OX40 or ICOS, it's slightly an opposite effect of anti-IFNγ and the combination evens out to no response compared to isotype. Only CD25 is increased by both. Anti-IL-27 has no effect on the APCs populations compared to anti-IFNγ, and the combination again evens out as a mixture of the two, there is no additive effect. This further strengthens the idea that they are operating through two independent mechanisms, however, inflammatory markers on the inflammatory myeloid population appear to be driven up by anti-IL-27, whilst anti-IFNγ drives them down. When a combination is given, it more closely resembles anti-IFNγ than anti-IL-27. By removing IL-27 from the environment, and then IL-10 as a result, it's possible that there is more IFNγ in the environment leading to increased inflammation and reduced tolerance.

It was a surprise to find that the anti-IL-10R antibody was not very effective at elucidating any strong response. For what effect we can see, removing IL-10 from the environment may have removed a negative feedback loop causing T cells to synthesise more *Il10*-GFP when it detects a low concentration, leading to a cumulative GFP in the cells.

In this chapter we have demonstrated that rapid induction of *Il10*$^{+}$ Tr1-like cells *in vivo* requires IFNγ-induced strong TCR and IL-27 signalling via independent, additive modulation involving negative feedback through cellular mechanisms of antigen presentation.

Chapter 5 : Effect of Interferon-γ Signalling on $CD4^+$ T cell *Il10* Transcription in a Murine Model of Cancer

5.1 Introduction

[4Y]-MBP can also be viewed as “modified self”, which in many ways parallels properties of cancer neoantigens are which are the result of mutations of DNA. We therefore wanted to investigate whether a similar IFNγ : IL10 axis existed in cancer settings. In this chapter, we used our *Nr4a3*-Tocky *Il10*-GFP *Ifng*-YFP mice to evaluate the relationship of *Ifng* and *Il10* transcription in $CD4^+$ TILs.

5.1.1 Role of IL-10 in Tumours

The role of IFNγ in the tumour is more established – high baseline expression indicates that there is already cytotoxic activity against the tumour, hence its inclusion in the Co-ordinate Immune Response Cluster (CIRC) score in stratifying colorectal cancer outcomes [372]. IL-10 has a more controversial role. Mostly produced by tumour-associated macrophages (TAMs), DCs, Tregs, and tumour cells, it promotes tumour immune escape through reduction in antigen presentation to lymphocytes, mediated by a reduction in MHCII expression [297, 373]. High serum IL-10 is associated with poor prognosis across different cancers, including melanoma [374-376]. IL-10 reduces MHCI expression on tumour cells, restraining the anti-tumour response from $CD8^+$ TILs [377].

5.1.2 Effect of Immune Checkpoint Blockade on T cells and IL-10

ICB is an immunotherapy that uses antibodies to block key signalling pathways in the suppression of lymphocyte function. Whilst initially achieving remarkable clinical success, most patients fail to respond [378-381]. It is believed that the low response rate is partially due to exhausted TILs, that become unable to control tumour progression [382-384]. ICB causes a temporary reinvigoration of exhausted T cells

[385, 386]. Induction of IFNγ and associated genes is thought to be an important mechanisms and *Ifng* related mRNA profiles predict outcomes to immunotherapy [387].

Within $CD8^+$ TILs, two exhaustion subsets have been identified, progenitor exhausted ($TCF\text{-}1^+$ $TIM\text{-}3^-$ $PD\text{-}1^{Int}$) and terminally exhausted ($TCF\text{-}1^-$ $TIM\text{-}3^{+\,-}$ $PD\text{-}1^{Hi}$) [388-390]. Progenitor exhausted $CD8^+$ TILs show a higher proliferative capacity than terminally exhausted TILs. Anti-PD-1 immunotherapy relies on the progenitor exhausted subset and induces proliferation and differentiation, leading to an expansion of terminally exhausted $CD8^+$ TILs that exert cytotoxic function against cancer cells [391, 392]. Although the terminally exhausted subset is short-lived and incapable of self-renewal, they possess superior cytotoxic function to progenitor exhausted TILs, but do not respond to immunotherapies [392-394]. In addition to increasing proliferative capacity exhausted TIL subsets, anti-PD-1 therapy upregulates IL-10R on $CD8^+$ T cells [395], which promotes maintenance of progenitor exhausted TILs that sustain anti-tumour immunity [396]. This highlights the multifaceted and interrelated function that effective ICB relies on for effective outcomes and the potential for IFNγ and IL-10 to modulate the immune response to tumours.

Advanced melanoma patients are more likely to respond to anti-PD-1 therapy if they have a higher IFNγ : IL-10 ratio in their PBMC-derived $CD4^+$ T cells [397]. The use of anti-IL-10R partially relieved anti-PD-L1 driven reductions in $CD80^+$ $CD86^+$ cDC2 subsets in murine splenocytes [317]. Cytotoxic T Lymphocyte Associated protein (CTLA-4) inhibits T cell activation and proliferation by preventing T cell access to costimulatory signals on antigen-presenting cells [398].

IL-10 has a mixed role in tumours and although IFNγ is beneficial for tumour outcome, the influence of IFNγ on IL-10 in this context is unclear, with examples of interference leading to both improved and worsened outcomes. To assess whether modulation of pro-inflammatory IFNγ affects *Il10* expression within $CD4^+$ TILs, we used an *in vivo* immunogenic MC38 tumour model that uses a colorectal cancer cell line injected subcutaneously and cytokine sequestering antibodies.

5.2 Results

5.2.1 Baseline cytokine transcription reporter expression in TCR activated tumour infiltrating T cells.

In the previous chapter we demonstrated that IFNγ was key for the development of *Il10*-GFP$^+$ Tr1-like cells through antibody mediated cytokine sequestration that hindered antigen presentation. Now we sought to determine how our the immunogenic MC38 tumour model (derived from murine colorectal cancer cells) and our reporters behaved at baseline before exploring whether IFNγ could also regulate IL10 transcription in CD4$^+$ TILs.

We administered 250,000 MC38s subcutaneously in 100 µL PBS and harvested the resulting solid tumours from the flank on days 10 and 14 for analysis by flow cytometry. The MC38 tumours are palpable by day 7 and by day 14 are visible to the naked eye. We can demonstrate that our tumours implant, and that they grow in volume (fig. 5-1A) and weight (fig. 5-1B). When we analyse the digested tumours as a single cell suspension, we can measure *Nr4a3*-Timer$^+$ cells in both the CD4$^+$ and CD8$^+$ fraction of T cells (fig. 5-1C). Moreover, CD4$^+$ and CD8$^+$ T cells have slightly different *Nr4a3*-Timer expression, with CD8$^+$ T cells expressing more Timer Red. Day 14 CD4$^+$ and CD8$^+$ TILs have less *Nr4a3*-Timer expression compared to Day 10 (figs. 5-1DE). Immune checkpoint expression was also analysed according to *Nr4a3*-Timer expression (fig. 5-1F). PD-1 intensity is decreased by day 14 in CD4$^+$ (fig. 5-1G) and CD8$^+$ TILs, with the effect more pronounced in CD8$^+$ (fig. 5-1I). LAG3 shows an opposite pattern, increased between days 10 and 14 and more pronounced in CD4$^+$ TILs (fig. 5-1H) than CD8$^+$ (fig. 5-1J).

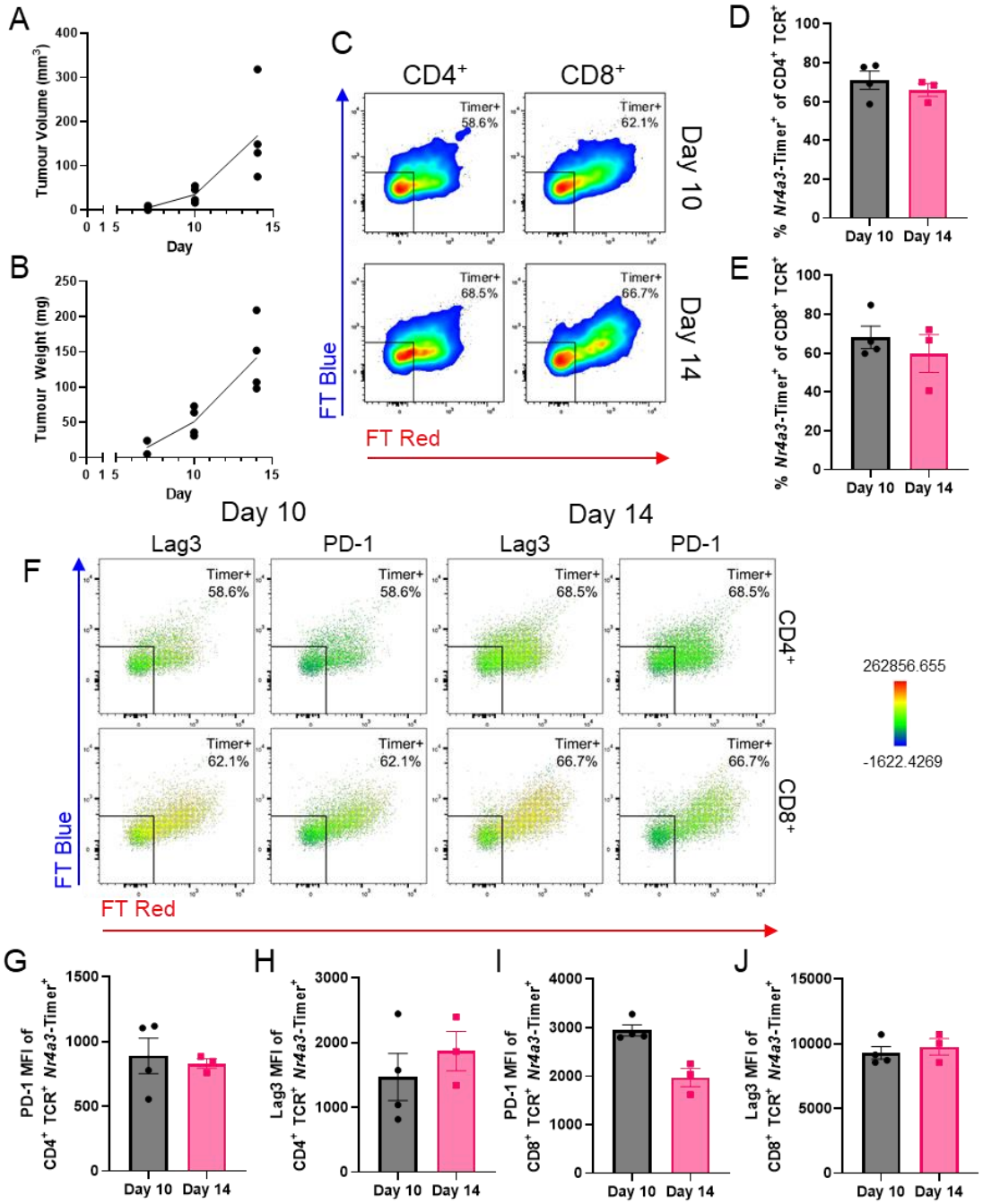

Figure 5-1: Baseline cytokine transcription reporter expression in TCR activated tumour infiltrating T cells.
Nr4a3-Tocky *Il10*-GFP Ifng-YFP mice were inoculated with 0.25 million MC38 colorectal cancer cells in 100 µL PBS s.c. and analysed on days 10 and 14 for **(C)** $CD4^+$ and $CD8^+$ TCR^+ *Nr4a3*-$Timer^+$ populations. Tumour volumes **(A)** and **(B)** weights. Summary of Nr4a3-$Timer^+$ in $CD4^+$ **(D)** and $CD8^+$ **(E)** TCR^+ cells. In $CD4^+$ TCR^+ *Nr4a3*-$Timer^+$, summary of **(G)** PD-1 and **(H)** LAG3 MFI and $CD8^+$ TCR^+ Nr4a3-$Timer^+$, of **(I)** PD-1 and **(J)** LAG3 MFI from **(F). (A, B, D, E, G-J)** from n=4 mice in day 10 group and 3 in day 14 group, bars represent mean ±SEM.

In this MC38 tumour model when used with the *Il10*-GFP *Ifng*-YFP reporter we observed that $CD4^+$ express mostly *Il10*-GFP and very little to none *Ifng*-YFP, whilst $CD8^+$ TILs have the opposite phenotype – making almost exclusively *Ifng*-YFP and very little *Il10*-GFP (fig. 5-2A). Frequency and intensity of both $CD4^+$ TIL *Il10*-GFP (fig. 5-2B, D) and $CD8^+$ TIL *Ifng*-YFP (fig. 5-2C, E) are higher at day 10 than 14.

This model in combination with our fluorescent transcription reporters demonstrates dynamic expression between days, highlighting that it is not a static environment, but that there is peak expression on day 10. Higher expression on day 10 suggests that any effect on these markers will be more pronounced on that day, and at this timepoint the tumours are less likely to exceed their size limit. Knowing our reporters and the tumour model work, we sought to determine what regulatory subsets were present.

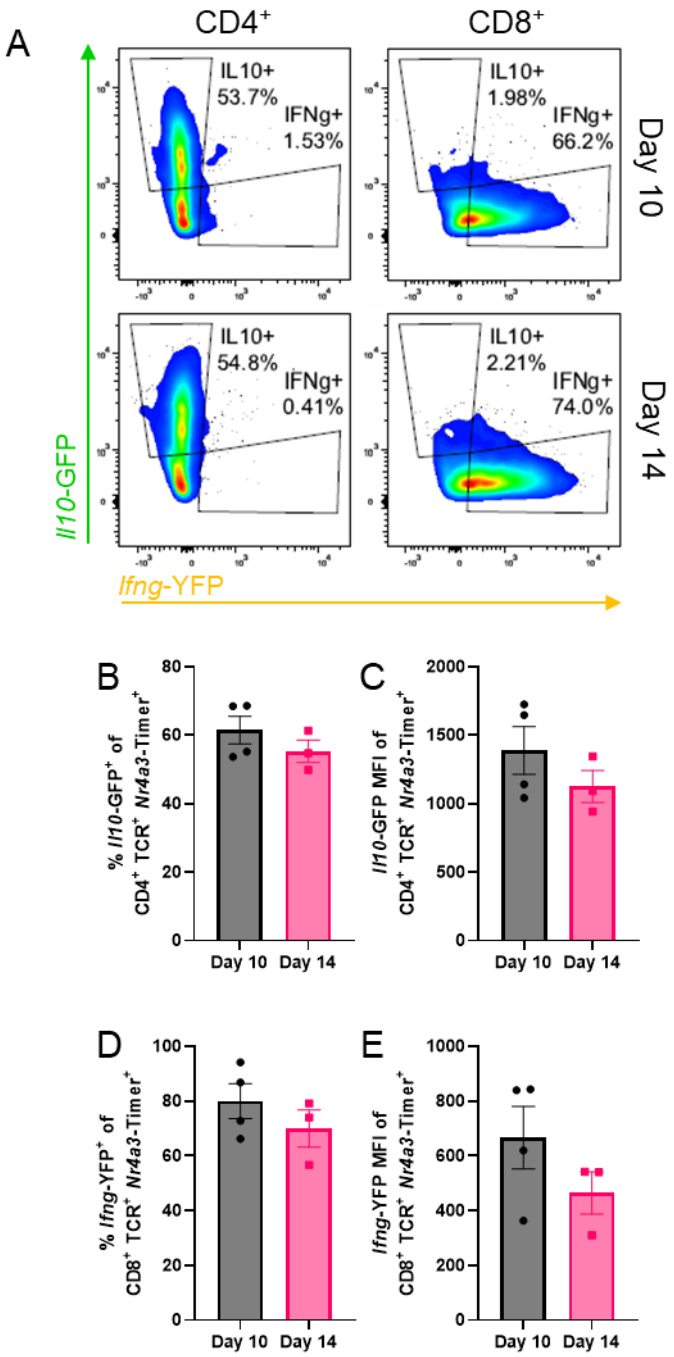

Figure 5-2: Baseline cytokine transcription reporter expression in TCR activated tumour infiltrating T cells.
Nr4a3-Tocky *Il10*-GFP *Ifng*-YFP mice were inoculated with 0.25 million MC38 colorectal cancer cells in 100 µL PBS s.c. and analysed on days 10 and 14 for **(A)** *Il10*-GFP$^+$ and *Ifng*-YFP$^+$ expression in CD4$^+$ and CD8$^+$ TCR$^+$ *Nr4a3*-Timer$^+$ populations. **(B)** Summary of *Il10*-GFP$^+$ frequency **(C)** and MFI in *Nr4a3*-Timer$^+$ CD4$^+$ TCR$^+$. **(D)** Summary of *Ifng*-YFP$^+$ frequency **(E)** and MFI in *Nr4a3*-Timer$^+$ CD8$^+$ TCR. **(B-E)** from n=4 mice in day 10 group and 3 in day 14 group, bars represent mean ±SEM.

5.2.2 CD4$^+$ TILs expressing *Il10*-GFP are *FoxP3*$^+$ Tregs

To establish what Treg subsets were producing *Il10*-GFP in our MC38 model, we used a *FoxP3* and *Il10* reporter – *FoxP3*-Tocky *Il10*-GFP – to profile the CD4$^+$ TILs. Although this sacrifices our ability observe specifically TCR activated CD4$^+$ Tregs, it is a reliable method of determining recent *FoxP3* transcription without losing other cytokine reporters to fixation.

FoxP3-Tocky *Il10*-GFP mice were inoculated with 250,000 MC38s subcutaneously in 100 µL PBS and harvested from the flank on day 9 for analysis by flow cytometry. We separated our CD4$^+$ TCR$^+$ TILs by *Il10*-GFP positivity or negativity (fig. 5-3A) and then gated for *FoxP3*-Timer positivity (fig. 5-3B) and surface markers therein.

Il10-GFP$^+$ CD4$^+$ TILs make up the majority of CD4$^+$ TILs in this model (>65 %), and of those *Il10*-GFP$^+$, more than 85 % are *FoxP3*-Timer$^+$ (fig. 5-3C). This is significantly higher than the *Il10*-GFP$^-$, where ~50 % are *FoxP3*-Timer$^+$. Of the *Il10*-GFP$^+$ CD4$^+$ TILs, ~15 % are *FoxP3*-Timer$^-$, potentially representing other, non-FoxP3$^+$ Tregs such as Tr1 cells.

For surface markers associated with regulation, we can see in figure 5-3B that CD39, CD25 and CD49b expression is more intense at those cells that also express more Timer. LAG3 does not appear to show the same pattern. Of total CD4$^+$ TCR$^+$ TILs, CD39 (fig. 5-3D), CD25 (fig. 5-3E), CD49b (fig. 5-3F), and LAG3 (fig. 5-3G) are all expressed significantly higher on the *Il10*-GFP$^+$ population than *Il10*-GFP$^-$. CD4$^-$ cells (including CD8 TILs) from these tumours do not express *FoxP3*-Timer (fig. 5-3H), and *FoxP3*-Timer is therefore associated with CD4$^+$ cells only.

FoxP3^{+} Tregs are the main expressors of *Il10*-GFP in this model, and there is a *FoxP3*$^{+}$ Treg population that expresses no *Il10*-GFP at all. The *Il10*-GFP^{+} also express significantly more Treg markers, including Tr1-like markers, and seem to be heterogeneous and prolific in nature, taking up most of the CD4^{+} *Il10*-GFP^{+} and half of the *Il10*-GFP^{-}.

In the previous chapter, we saw that IFNγ sequestration significantly reduced the Tr1-like phenotype and capacity to express *Il10*-GFP in a tolerogenic setting. Given the abundance of CD8^{+} *Ifng*-YFP^{+} T cells, we wanted to understand whether IFNγ also played a direct role in regulating *FoxP3*$^{+}$ Treg *Il10* expression.

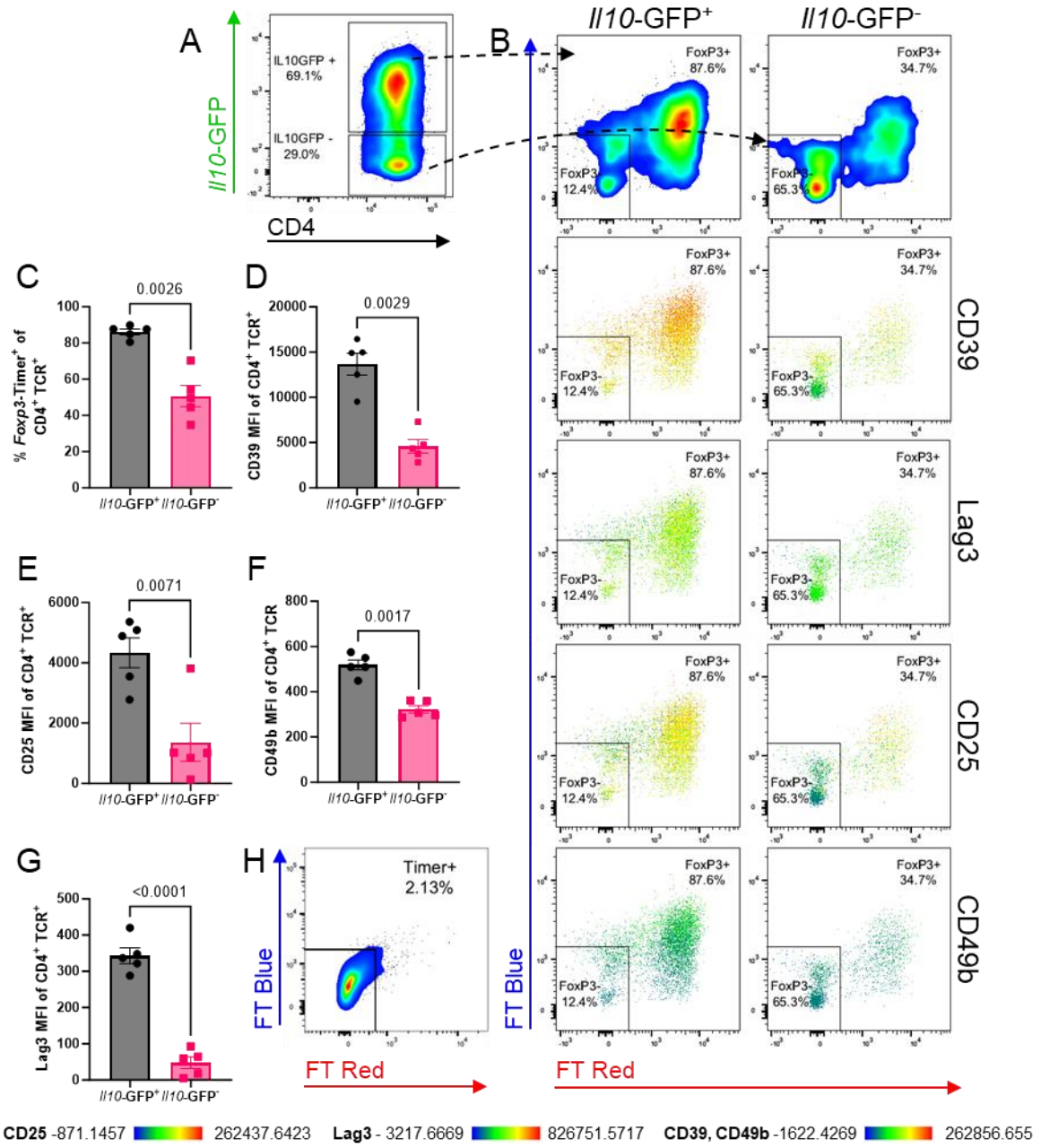

Figure 5-3: *Foxp3*-Timer expression according to *Il10*-GFP expression in tumour infiltrating CD4$^+$ T cells.

Foxp3-Tocky *Il10*-GFP mice were inoculated with 0.25 million MC38 colorectal cancer cells in 100 µL PBS s.c. After 9 days, the tumours were harvested and analysed for **(A)** *Il10*-GFP$^+$ and *Il10*-GFP$^-$ CD4$^+$ TCR$^+$ populations, and within those **(B)** *Foxp3*-Timer and regulatory marker expression. **(C)** Summary of *Foxp3*-Timer population differences between CD4$^+$ TCR$^+$ *Il10*-GFP$^{+/-}$. Summary of CD39 **(D)**, CD25 **(E)**, CD49b **(F)** and LAG3 **(G)** MFI from **(B)**. **(H)** *Foxp3*-Timer from CD4$^-$ TCR$^-$ cells. From n=5 mice, bars represent mean ±SEM. Analysis by paired two-tailed t test.

5.2.3 $CD4^{Cre}$ $IFNgR^{fl/fl}$ tumour bearing mice have higher tumour burden.

We decided it was important to establish what effect loss of IFNγ sensitivity on TILs would have on the MC38 tumour, so we gave $CD4^{Cre}$ $IFNgR^{fl/fl}$ 250,000 MC38s subcutaneously in 100 µL PBS and harvested from the flank on day 9 for analysis. These mice have no IFNγR on their CD4 or CD8 T cells, and so IFNγ cannot have a direct effect on these cell types. In figure 5-4A, $CD4^{Cre}$ $IFNgR^{fl/fl}$ mice have increased tumour volume compared to CD4 $IFNgR^{fl/fl}$ (no Cre) as early as day 7, which becomes increasing significant as time progresses (days 9, 12 and 14). On day 14 (fig. 5-4B), the $CD4^{Cre}$ tumours are larger on average than the non-Cre.

Given that this experiment demonstrated T cell desensitivity to IFNγ being significantly worse for tumour burden, we decided that to pursue our antibody-based model of cytokine depletion. This allowed us to retain lymphocyte sensitivity to IFNγ whilst reducing it *in vivo* was the most appropriate as it could be more directly compared to other antibody-based treatments such as anti-PD-L1 and is more compatible with our current mouse strain colonies.

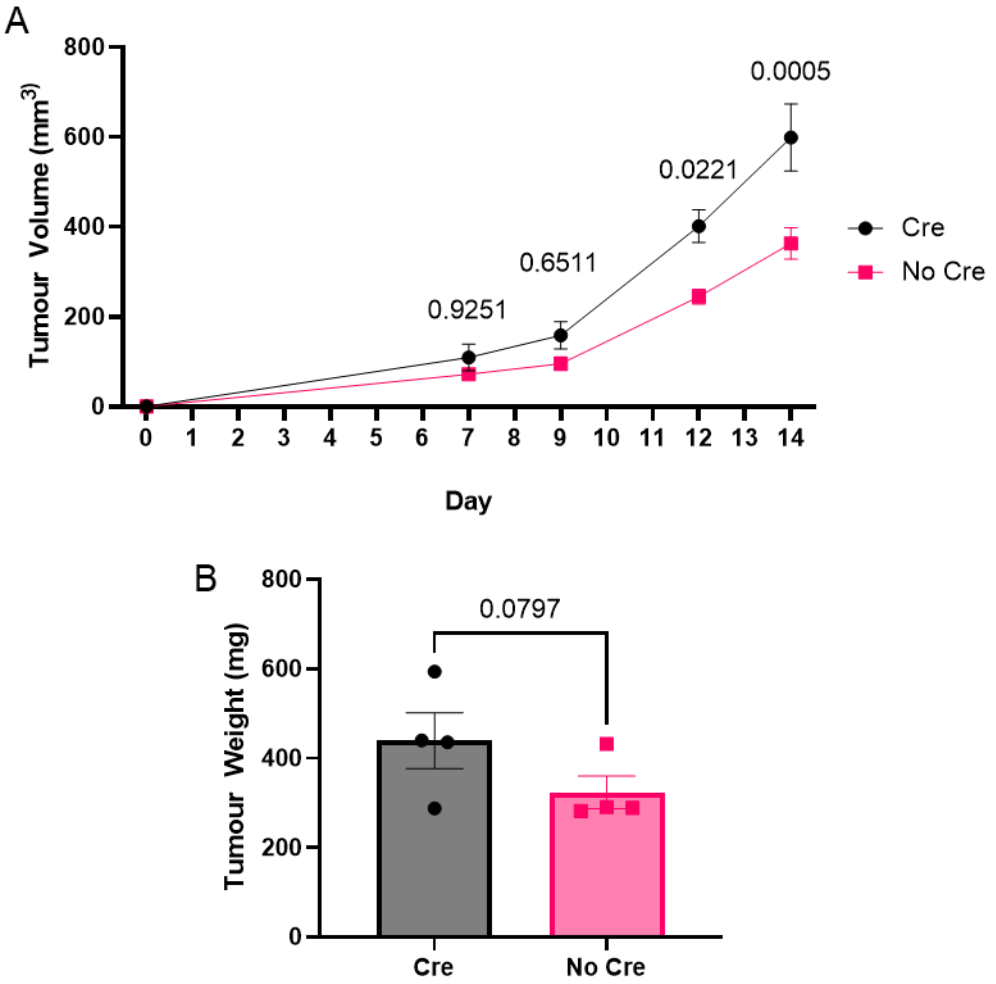

Figure 5-4: CD4^{Cre} IFNgR$^{fl/fl}$ tumour bearing mice have higher tumour burden. CD4^{Cre} IFNgR$^{fl/fl}$ and IFNgR$^{fl/fl}$ only mice were inoculated with 0.25 million MC38 colorectal cancer cells in 100 µL PBS s.c. Tumours were measured for volume on days 7, 10 and 14 **(A)** and on day 14 were weighed **(B)**. From n=4 mice per group, bars represent mean ±SEM. Analysis by unpaired t test.

5.2.4 Phenotypes in TCR activated infiltrating T cells from a single dose anti-IFNγ treated tumour.

T lymphocyte sensitivity to IFNγ was clearly important to tumour outcome, so we began to influence the presence of IFNγ via antibody treatments. We started by administering 1 mg anti-IFNγ on day 10 following inoculation with 250,000 MC38 cells. This was when we saw the highest expression of *Nr4a3*-Timer, *Il10*-GFP and *Ifng*-YFP in figs. 5-1 and 5-2 and used this timepoint to measure the changes in reporter expression (fig. 5-5A) 24 hr later, on day 11.

With a single anti-IFNγ treatment we see a reduction in both *Il10*-GFP frequency (fig. 5-5B) and intensity (fig. 5-5D), and the same for *Ifng*-YFP fluorescence (fig. 5-5C) and intensity (fig. 5-5E). This reduction is not significant following a single dose of anti-IFNγ. *Nr4a3*-Timer frequency in both subsets was unaffected (not shown). In both $CD4^+$ and $CD8^+$ TCR^+ *Nr4a3*-$Timer^+$ TILs (fig. 5-6A), LAG3 intensity was decreased by anti-IFNγ treatment (fig 5-6BC), whilst PD-1 increased (fig. 5-6D, E).

Although this demonstrates the ability of anti-IFNγ to impact expression, a single dose was unlikely to lead to a significant change in tumour outcomes, so we started to give repeated doses of IFNγ. This pilot experiment revealed trends from a single dose that we followed with continual dosing to investigate a more effective change in the tumour.

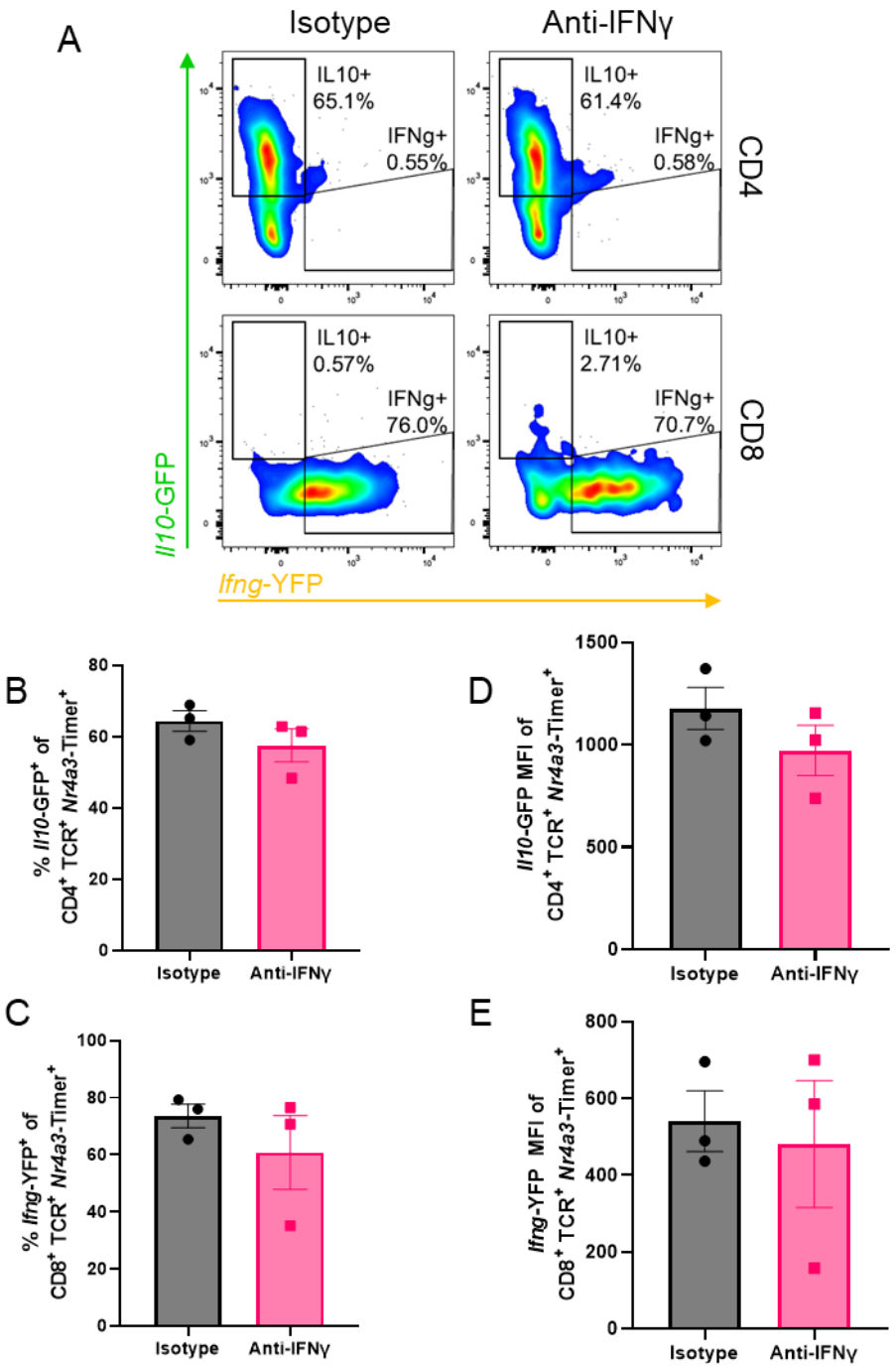

Figure 5-5: Cytokine transcription reporter expression in TCR activated infiltrating T cells from a single dose anti-IFNγ treated tumour.
Nr4a3-Tocky *Il10*-GFP *Ifng*-YFP mice were inoculated with 0.25 million MC38 colorectal cancer cells in 100 µL PBS s.c. On day 10, 1 mg anti-IFNγ or isotype was administered in 200 µL PBS and tumours harvested on day 11 and analysed for **(A)** *Il10*-GFP$^+$ and *Ifng*-YFP$^+$ expression in CD4$^+$ and CD8$^+$ TCR$^+$ *Nr4a3*-Timer$^+$ populations. **(B)** Summary of *Il10*-GFP frequency in CD4$^+$ TCR$^+$ cells and **(C)** of *Ifng*-YFP frequency in CD8$^+$ TCR$^+$ cells. **(D)** Summary of *Il10*-GFP MFI in CD4$^+$ TCR$^+$ *Nr4a3*-Timer$^+$ and **(E)** *Ifng*-YFP MFI in CD8$^+$ TCR$^+$ *Nr4a3*-Timer$^+$. From n=3 mice per group, bars represent mean ±SEM.

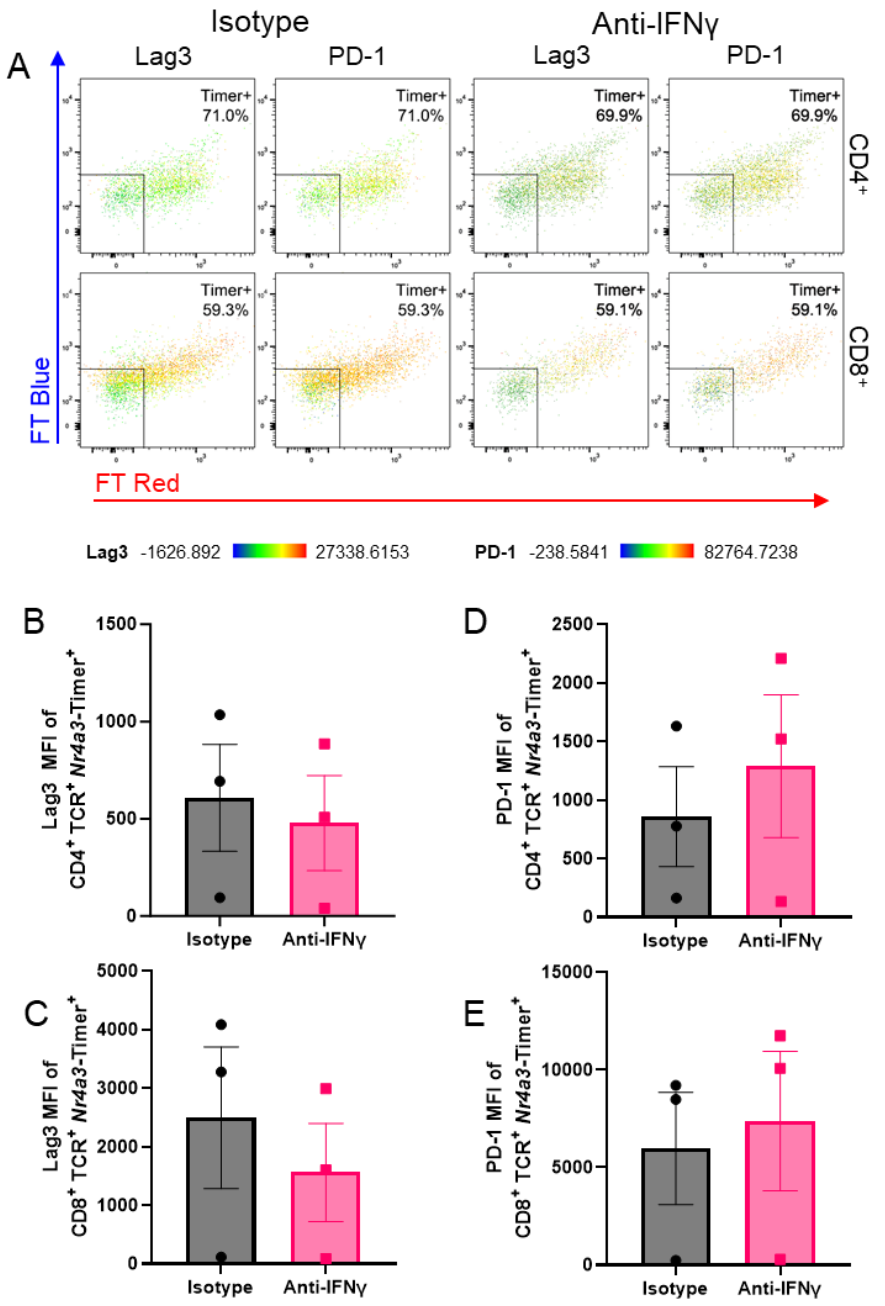

Figure 5-6: Surface marker expression in TCR activated infiltrating T cells from a single dose anti-IFNγ treated tumour.
Nr4a3-Tocky *Il10*-GFP *Ifng*-YFP mice were inoculated with 0.25 million MC38 colorectal cancer cells in 100 µL PBS s.c. On day 10, 1 mg anti-IFNγ or isotype was administered in 200 µL PBS and tumours harvested on day 11 and analysed for **(A)** *Il10*-GFP$^+$ and *Ifng*-YFP$^+$ expression in CD4$^+$ and CD8$^+$ TCR$^+$ *Nr4a3*-Timer$^+$ populations. Summary of LAG3 MFI in CD4$^+$ **(B)** and CD8$^+$ **(C)** TCR$^+$ *Nr4a3*-Timer$^+$ populations. Summary of PD-1 MFI in CD4$^+$ **(D)** and CD8$^+$ **(E)** TCR$^+$ *Nr4a3*-Timer$^+$ populations. From n=3 mice per group, bars represent mean ±SEM.

5.2.5 Phenotypes in TCR activated infiltrating T cells from a multi-dose anti-IFNγ treated tumour.

Although interesting that anti-IFNγ mAb able to affect TIL phenotypes within 24 hr, we wanted to know what impact this would have on a tumour long-term, in terms of phenotype and burden. Instead of harvesting at day 14 in the baseline experiments, we decided to end the experiments around day 10 because our baseline showed that expression of surface markers and reporters was higher on day 10 than 14, and any change seen would be of greater magnitude.

We dosed MC38 tumour bearing mice with 1 mg anti-IFNγ on days 2, 5 and 7 post inoculation before harvesting on day 9 and measuring expression of reporters and surface markers from $CD4^+$ and $CD8^+$ *Nr4a3*-$Timer^+$ subsets (fig. 5-7A).

With a multiple dosing regimen, we see that anti-IFNγ treated tumours have much larger weights (fig. 5-7B) and bigger volumes (fig. 5-7C). *Nr4a3*-Timer expression was unaffected by anti-IFNγ treatment in both $CD4^+$ (fig. 5-7D) and $CD8^+$ (fig. 5-7E) TCR^+ cells as in the single dose treatment. We see within the *Nr4a3*-$Timer^+$ populations that LAG3 and OX40 are decreased by anti-IFNγ in both *Nr4a3*-$Timer^+$ $CD4^+$ and $CD8^+$ (figs. 5-7F – I), suggesting a reduction in strong TCR signalling through OX40, a component of the TCR.Strong metric.

We then examined cytokine reporter expression within the *Nr4a3*-$Timer^+$ populations (fig. 5-8A) finding that in $CD4^+$ *Nr4a3*-$Timer^+$ TILs, *Il10*-GFP frequency is significantly and strongly reduced (fig. 5-8B), whilst *Ifng*-YFP frequency in $CD8^+$ *Nr4a3*-$Timer^+$ is unchanged. Similarly, the fluorescence of *Il10*-GFP is significantly reduced (fig. 5-8D) while *Ifng*-YFP is not significantly affected (fig. 5-8E).

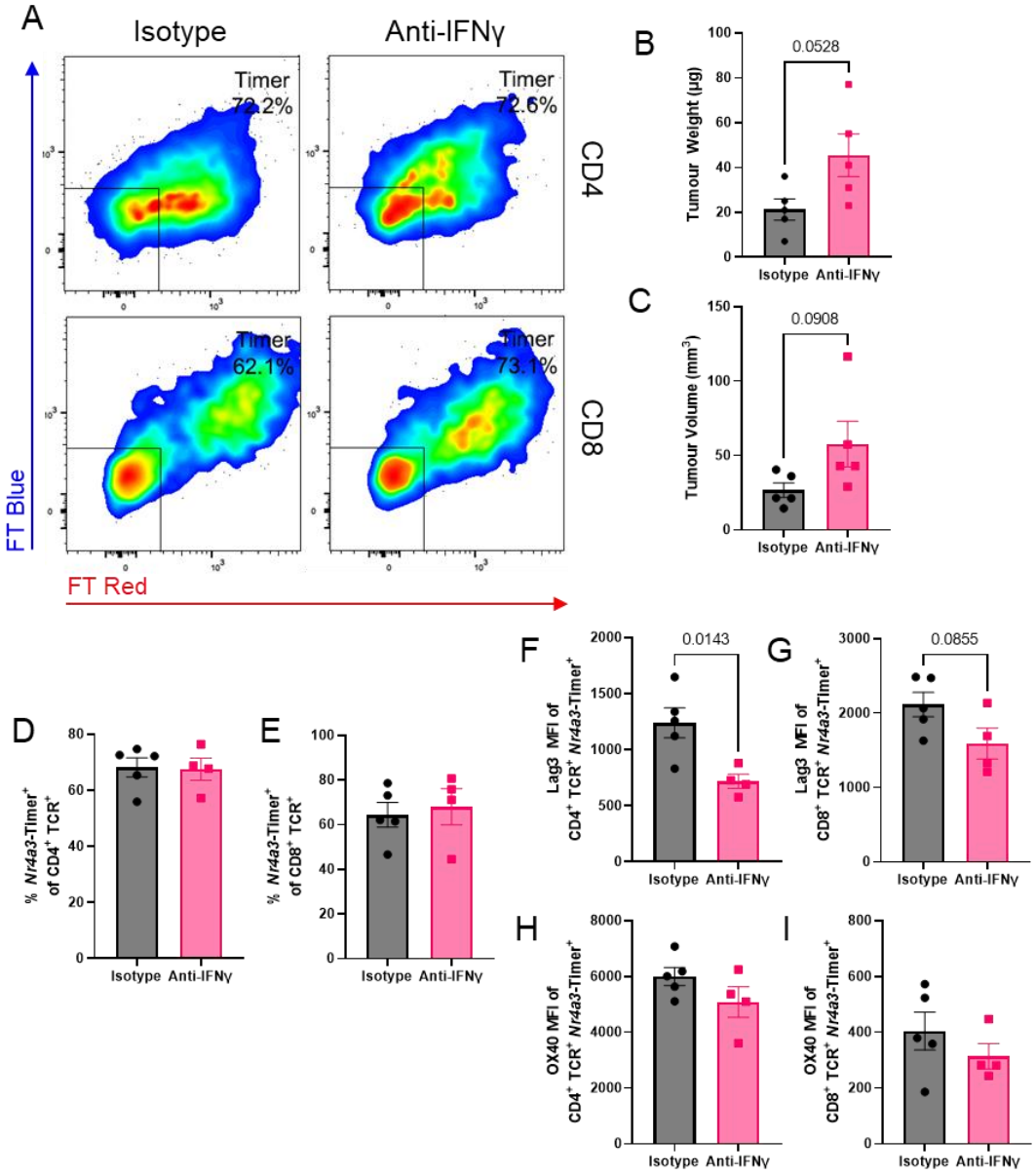

Figure 5-7: Timer and surface marker expression in TCR activated infiltrating T cells from a multi-dose anti-IFNγ treated tumour.
Nr4a3-Tocky *Il10*-GFP *Ifng*-YFP mice were inoculated with 0.25 million MC38 colorectal cancer cells in 100 µL PBS s.c. On day 2, 5 and 7, 1 mg anti-IFNγ or isotype was administered in 200 µL PBS and tumours harvested on day 9 and analysed for **(A)** *Nr4a3*-Timer$^+$ expression in CD4$^+$ and CD8$^+$ TCR$^+$ populations. **(B)** Day 9 tumour weights and **(C)** tumour volumes. **(D)** Summary of *Nr4a3*-Timer$^+$ in CD4$^+$ **(E)** and CD8$^+$ TCR$^+$ cells. Summary of LAG3 MFI in CD4$^+$ **(F)** and **(G)** CD8$^+$ TCR$^+$ *Nr4a3*-Timer$^+$. Summary of OX40 MFI in CD4$^+$ **(H)** and **(I)** CD8$^+$ TCR$^+$ *Nr4a3*-Timer$^+$. **(B-I)** from n=5 mice in isotype group and 4 in anti-IFNγ group, bars represent mean ±SEM. Analysis by unpaired t test.

Anti-IFNγ demonstrably reduces Tr1-like phenotype and markers of strong TCR signalling in Tg4 tolerance model. Interestingly, it does not appear to affect *Ifng*-YFP expression as much as *Il10*-GFP suggesting that lymphocyte IFNγ expression is not as dependent on positive feedback loops. Bearing in mind that in Chapter 4 we saw that anti-IFNγ was influencing *Il10*-GFP through antigen presentation, we sought to establish if this was true in the tumour model.

5.2.6 Anti-IFNγ treatment effect of tumour associated APCs

Anti-IFNγ was having a strong effect on $CD4^+$ TIL *Il10*-GFP expression but given that they had very little *Ifng*-YFP expression of their own, we sought to determine if there was an indirect cellular mechanism at work here, much as in Chapter 4. Likewise, anti-IFNγ treatment was only having a modest effect on $CD8^+$ TIL capacity to express *Ifng*-YFP so it may be acting through another mediator. We administered 1 mg anti-IFNγ antibody to MC38 tumour bearing mice on days 2, 5 and 7 post-inoculation, harvesting on day 9 for analysis.

A profile of these subsets shows that the $CD11c^+$ population is mostly $MHCII^-$, and therefore less likely to have been activated and presenting antigen to TILs (fig. 5-9A). The total fluorescence of MHCII (fig. 5-9B) and frequency of $MHCII^+$ $CD11c^-$ cells (fig. 5-9C) are significantly reduced by anti-IFNγ mAb. Within the $MHCII^+$ $CD11c^-$, F4/80 (fig. 5-9D) and CD11b (fig. 5-9F) fluorescence intensities are also significantly reduced. PD-L1 is also reduced but not significantly (fig. 5-9E). The reduction of F4/80, CD11b and MHCII suggest that macrophages, and not DCs, are the important APC subset being reduced by anti-IFNγ in this model. IFNγ is clearly important for limiting tumour burden and is closely tied to *Il10*-GFP expression. We wanted to see if improving tumour outcomes likewise was related to *Il10*-GFP^+ cells.

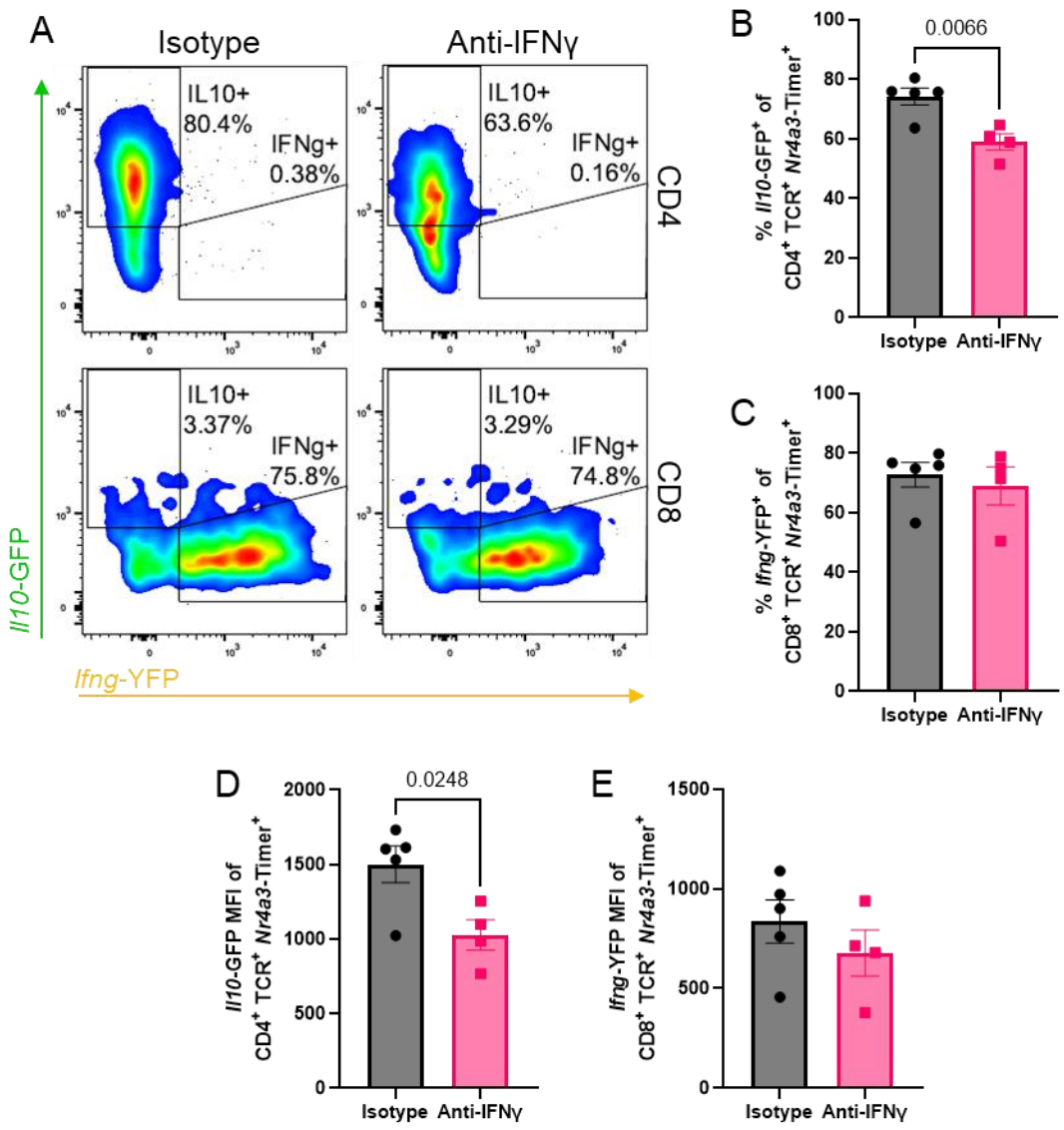

Figure 5-8: Cytokine transcription reporter expression in TCR activated infiltrating T cells from a repeatedly anti-IFNγ treated tumour.
Nr4a3-Tocky *Il10*-GFP *Ifng*-YFP mice were inoculated with 0.25 million MC38 colorectal cancer cells in 100 µL PBS s.c. On day 2, 5 and 7, 1 mg anti-IFNγ or isotype was administered in 200 µL PBS and tumours harvested on day 9 and analysed for **(A)** *Il10*-GFP$^+$ and *Ifng*-YFP$^+$ expression in CD4$^+$ and CD8$^+$ TCR$^+$ *Nr4a3*-Timer$^+$ populations Summary of *Il10*-GFP$^+$ frequency **(B)** and MFI **(D)** in *Nr4a3*-Timer$^+$ CD4$^+$ TCR$^+$. Summary of *Ifng*-YFP$^+$ frequency **(C)** and MFI **(E)** in *Nr4a3*-Timer$^+$ CD8$^+$ TCR$^+$. **(B-E)** from n=5 mice in isotype group and 4 in anti-IFNγ group, bars represent mean ±SEM. Analysis by unpaired t test.

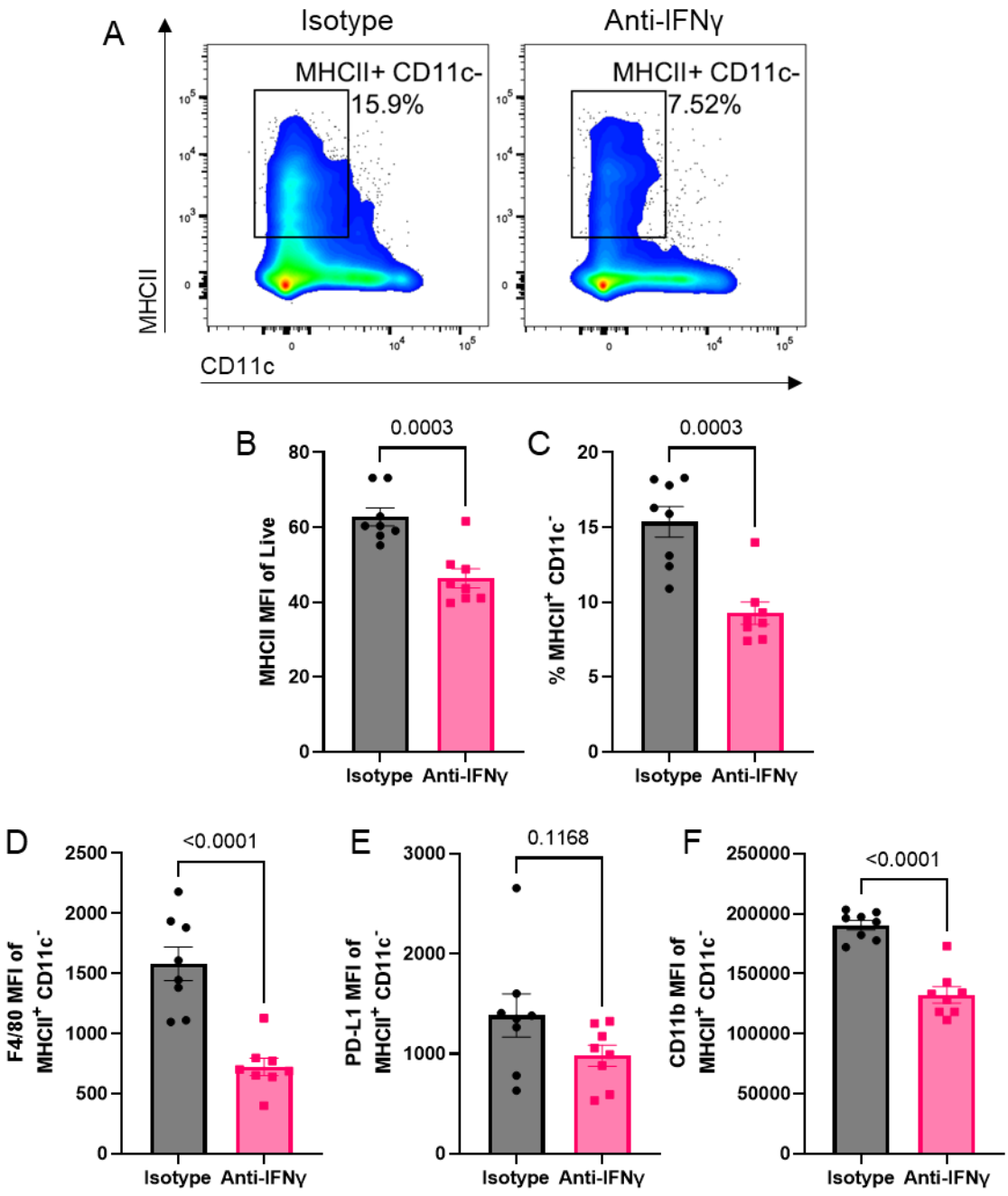

Figure 5-9: APC populations and markers from a repeatedly anti-IFNγ treated tumour.

Nr4a3-Tocky *Il10*-GFP *Ifng*-YFP mice were inoculated with 0.25 million MC38 colorectal cancer cells in 100 µL PBS s.c. On day 2, 5 and 7, 1 mg anti-IFNγ or isotype was administered in 200 µL PBS and tumours harvested on day 9 and analysed for **(A)** *Il10*-GFP^{+} and *Ifng*-YFP^{+} expression in CD4^{+} and CD8^{+} TCR^{+} *Nr4a3*-Timer^{+} populations. **(B)** Summary of MHCII MFI on total live cells and **(C)** MHCII frequency on CD11c^{-} cells. Summary of **(D)** F4/80, **(E)** PD-L1, **(F)** CD11b MFI on MHCII^{+} CD11b^{-} population**. (B-F)** from n=8 mice per group, bars represent mean ±SEM. Analysis by unpaired t test.

5.2.7 Anti-PD-L1 drives tumour regression and enhances regulatory phenotypes

The dynamics of *Nr4a3* activation are not affected by TCR signalling strength, as in Elliot et al., 2021, *Nr4a3*-Timer$^+$ responders have highly similar Timer trajectories (an average position of *Nr4a3*-Timer in T cell Blue-Red space). However, it is the proportion of responding cells that are dependent on TCR signalling strength [325]. PD-1 is an established gatekeeper of TCR signal strength and blocking it allows us to investigate if signalling strength is altered in this model. Again, in Elliot et al., 2021, in immunisation rechallenge experiments, anti-PD-1 blockade induced increased T cell responders, and higher amounts of *Nr4a3*-Blue in said responders than isotype or anti-LAG3 treatment. *Nr4a3*-Blue CD4$^+$ T cells expressed higher intensities of OX40, GITR and IRF8 when under anti-PD-1 treatment. In MC38 tumour experiments from the same paper, anti-PD-L1 treated mice expressed higher amounts of transcripts associated with strong TCR signalling (*Irf8, Icos, Tnfrsf4*).

Anti-PD-L1 is well documented at reducing tumour weight and volume in MC38 tumours, often leading to elimination of the tumour. Another antibody based treatment, we investigated whether its tumour-regressing ability was associated with increasing *Il10*-GFP expression in CD4$^+$ TILs, as an increase in tumour burden from anti-IFNγ is associated with decreasing *Il10*-GFP. We administered 0.5 mg anti-PD-L1 on days 5, 7 and 9 to MC38 tumour bearing mice and analysed the tumours by flow on day 12.

Here we can see the effect of anti-PD-L1 on TIL expression of our reporters, including *Nr4a3*-Timer (fig. 5-10A). Anti-PD-L1 dosing on days 2, 5, and 7 led to a reduction in tumour weight (fig. 5-10B) and volume (fig. 5-10C). Anti-PD-L1 drives expression of *Nr4a3*-Timer in both CD4$^+$ (fig. 5-10D) and CD8$^+$ TILs (fig. 5-10E). Within the *Nr4a3*-Timer$^+$ cells (fig. 5-10F), anti-PD-L1 also increased expression of OX40 and ICOS,

markers of strong TCR and CD28 signalling, in both $CD4^+$ (fig. 5-10G, H) and $CD8^+$ (fig. 5-10I, J) TILs.

Anti-PD-L1 appears to drive both inflammatory and tolerogenic responses in the MC38 tumour model (fig. 5-11A). $CD4^+$ and $CD8^+$ TILs express *Il10*-GFP and *Ifng*-YFP exclusively in this model and anti-PD-L1 treatment does not change this. Instead, anti-PD-L1 increases *Il10*-GFP frequency and intensity (fig. 5-11B, C) on $CD4^+$ TILs, and *Ifng*-YFP frequency and intensity (fig. 5-11D, E) on $CD8^+$ TILs.

The effect we see with anti-PD-L1 is quite the opposite compared to anti-IFNγ, with tumours demonstrating less growth and significant increases in cytokine reporting. Interestingly, it also increased the proportion of activated T cells via *Nr4a3*-Timer expression, particularly $CD8^+$ T cells, which anti-IFNγ does not affect. We wondered, therefore, whether IFNγ also plays a role in the mechanism of action/s of anti-PD-L1 on increasing Treg IL-10 expression in tumours.

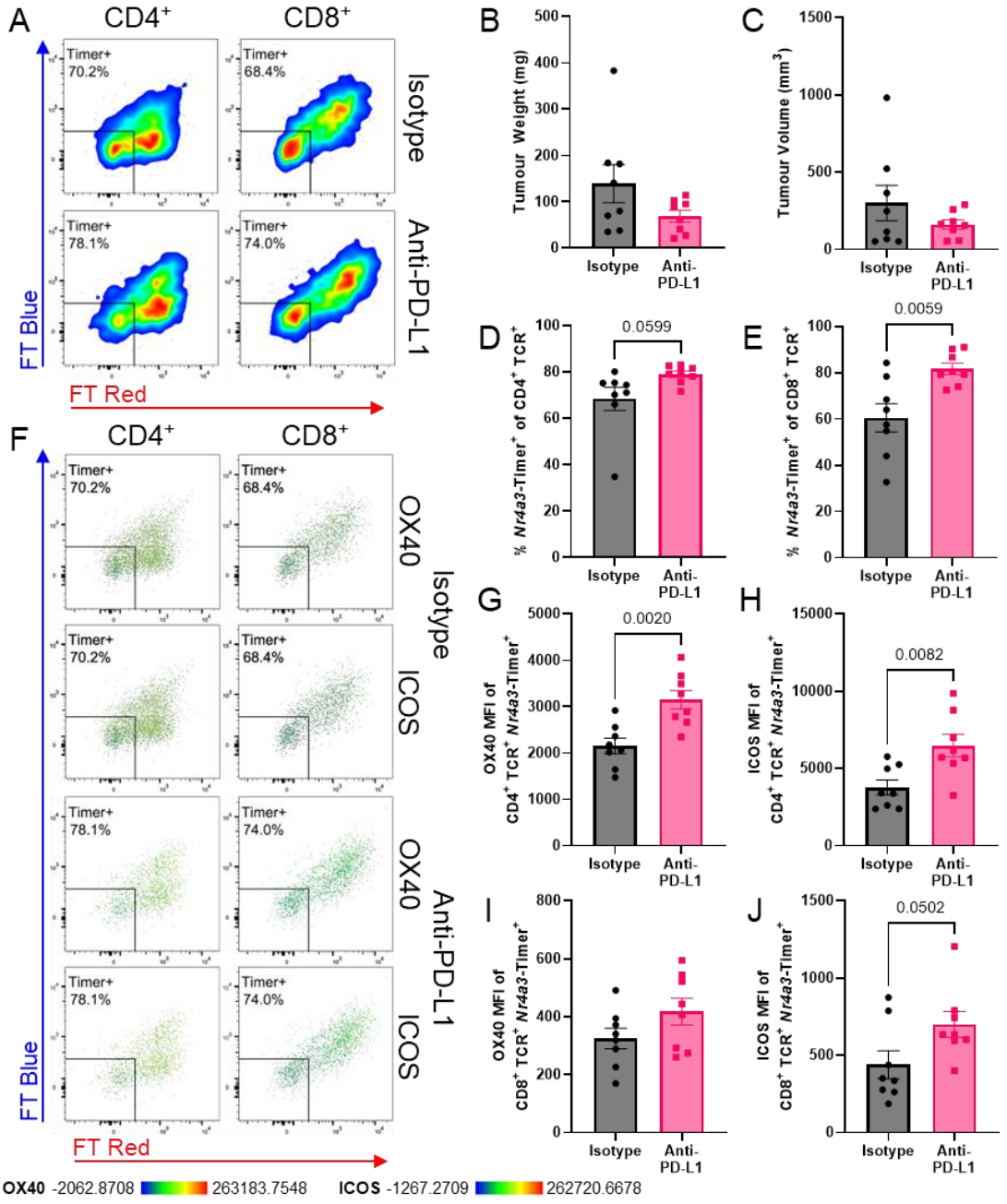

Figure 5-10: Repeated anti-PD-L1 treatment enhances surface marker expression in TCR activated infiltrating T cells.

Nr4a3-Tocky *Il10*-GFP *Ifng*-YFP mice were inoculated with 0.25 million MC38 colorectal cancer cells in 100 µL PBS s.c. On day 5, 7 and 9, 0.5 mg anti-PD-L1 or isotype was administered in 200 µL PBS and tumours harvested on day 12 and analysed for **(A)** *Il10*-GFP$^+$ and *Ifng*-YFP$^+$ expression in CD4$^+$ and CD8$^+$ TCR$^+$ *Nr4a3*-Timer$^+$ populations. Day 12 tumour weights **(B)** and tumour volumes **(C)**. Summary of *Nr4a3*-Timer$^+$ in CD4$^+$ **(D)** and CD8$^+$ **(E)** TCR$^+$ cells. In CD4$^+$ TCR$^+$ *Nr4a3*-Timer$^+$, summary of OX40 **(G)** and ICOS **(H)** MFI from **(F)**. In CD8$^+$ TCR$^+$ *Nr4a3*-Timer$^+$, summary of OX40 **(I)** and ICOS MFI **(J)** from **(F)**. **(B-E, G-J)** from n=8 mice per group, bars represent mean ±SEM. Analysis by unpaired t test.

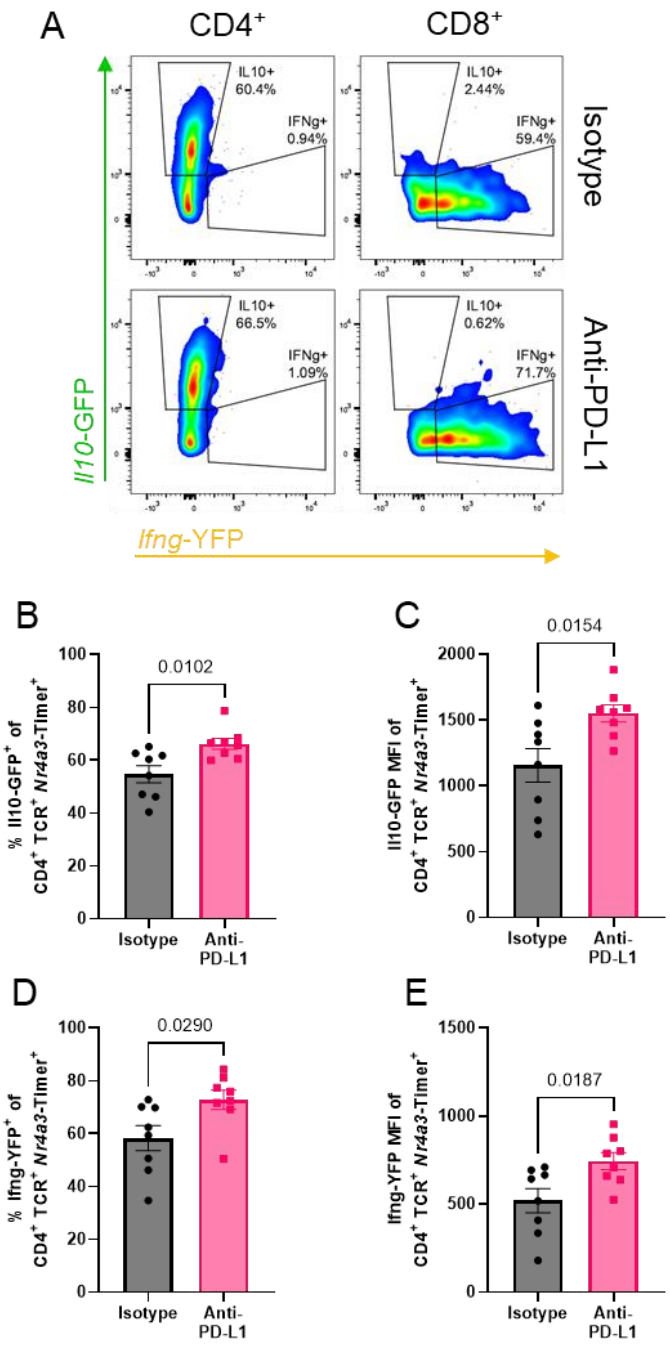

Figure 5-11: Cytokine transcription reporter expression in TCR activated infiltrating T cells from a repeatedly anti-PD-L1 treated tumour.
Nr4a3-Tocky *Il10*-GFP *Ifng*-YFP mice were inoculated with 0.25 million MC38 colorectal cancer cells in 100 µL PBS s.c. On day 5, 7 and 9, 0.5 mg anti-PD-L1 or isotype was administered in 200 µL PBS and tumours harvested on day 12 and analysed for **(A)** Il10-GFP$^+$ and Ifng-YFP$^+$ expression in CD4$^+$ and CD8$^+$ TCR$^+$ Nr4a3-Timer$^+$ populations. Summary of *Il10*-GFP$^+$ frequency **(B)** and MFI **(C)** in Nr4a3-Timer$^+$ CD4$^+$ TCR$^+$. Summary of *Ifng*-YFP$^+$ frequency **(D)** and MFI **(E)** in Nr4a3-Timer$^+$ CD8$^+$ TCR$^+$. **(B-E)** from n=8 mice per group, bars represent mean ±SEM. Analysis by unpaired t test.

5.2.8 Anti-IFNγ treatment abrogates anti-PD-L1 effects in MC38 tumours.

We had observed that anti-PD-L1 and anti-IFNγ had the opposite effect on tumours burden and cytokine reporters. Anti-IFNγ decreased *Il10*-GFP and increased tumour weight and volume, whilst anti-PD-L1 increased *Il10*-GFP and decreased tumour weight and volume. To understand whether anti-PD-L1 worked though increasing IFNγ which in turn upregulated IL-10, we conducted a survival experiment, pitting the antibodies against each other, and in combination, against isotype (fig. 5-12A) to investigate this circuit. MC38 tumour bearing C57BL/6 mice received antibody treatments on days 5, 7 and 10, and outcomes were measured daily before a day 21 cut-off.

Here we see how quickly anti-IFNγ contributes to a lethal outcome, with all treated mice dead by day 14, then isotype by day 20, and by the day 21 cut-off, only one combination treated mouse remained. The anti-PD-L1 treated, however, had a 75 % survival rate by day 21. On average, the isotype and combination tumours had similar volumes (fig. 5-12B), with the anti-IFNγ larger than the other groups, and the anti-PD-L1 smaller. Looking at individual tumour volumes as time progressed in fig. 5-12C, we can see that three of the anti-PD-L1 tumour regressed completely and were eliminated.

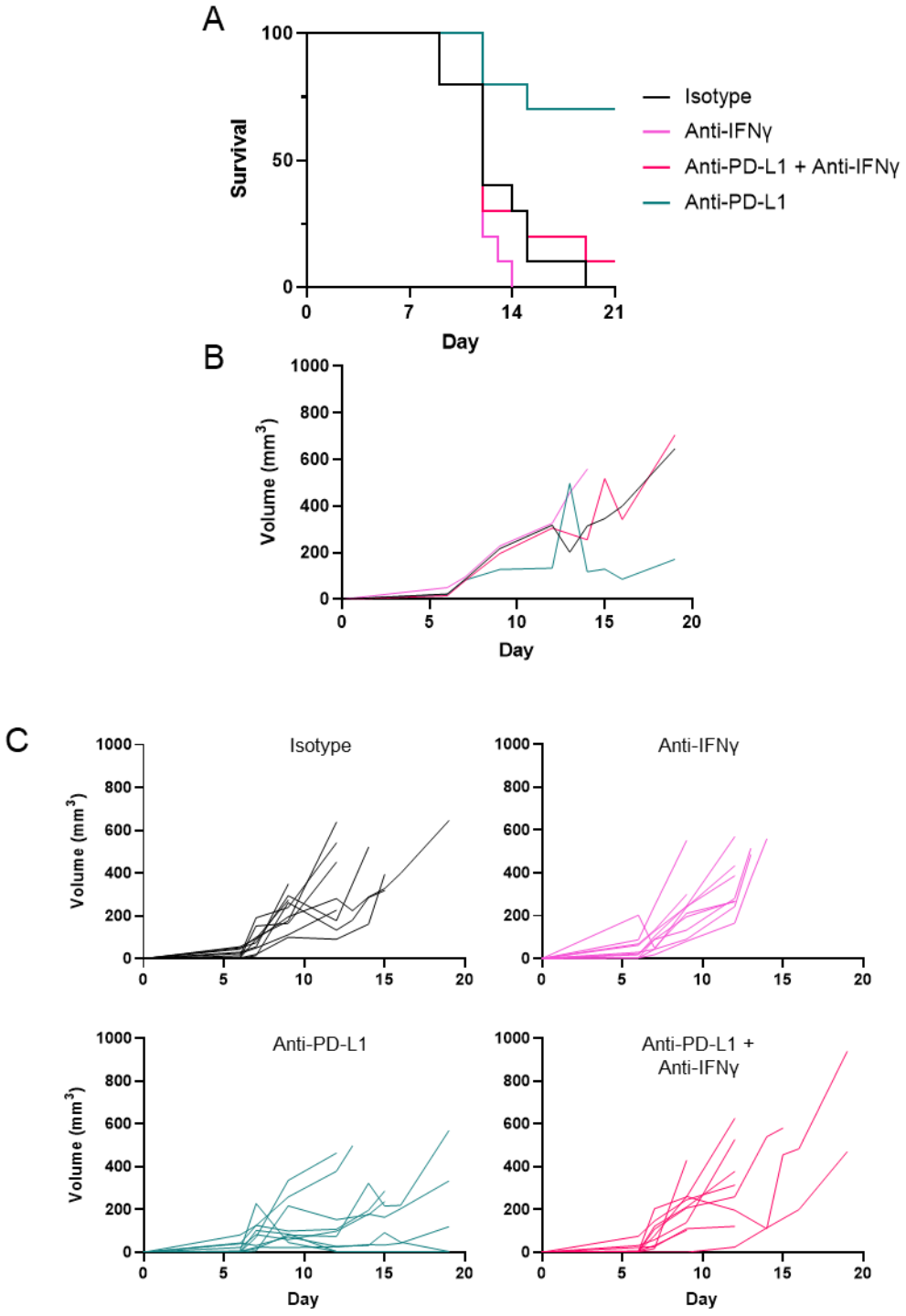

Figure 5-12: Survival of anti-IFNγ and anti-PD-L1 treated tumour bearing mice. C57BL/6 mice were inoculated with 0.25 million MC38 colorectal cancer cells in 100 µL PBS s.c. on day 0 and 0.5 mg isotype, anti-IFNγ, anti-PD-L1 or a combination of both in 200 µL PBS i.p. on days 5, 7 and 10. **(A)** Survival of mice by treatment group. **(B)** Mean volumes of MC38 tumours by treatment group. **(C)** Individual volumes of MC38 tumours by treatment group. N = 10 mice per group

Interested in observing intratumoural effects, we repeated the experiment, harvesting on day 11. We see in fig. 5-13A that isotype and combination treated mice have similar patterns of tumour volume, and tumour weight (fig. 5-13B), whilst anti-PD-L1 treated have smaller volumes and weights. Combination treatment again appears to be redundant. Comparing anti-PD-L1 to the combination for *Nr4a3*-Timer (fig. 5-14A), we see that combination has a *Nr4a3*-Timer frequency between isotype and anti-PD-L1 alone, on $CD4^+$ TILs (fig. 5-14B). Combination has an intermediate expression of ICOS (fig. 5-14C), but this drives OX40 intensity (fig. 5-14D). These $CD4^+$ TILs again, make almost exclusively *Il10*-GFP and little *Ifng*-YFP (fig. 5-14E). Frequency of both cytokine reporters is intermediate (figs. 5-14F, G) compared to isotype or anti-PD-L1 alone.

Overall, it appears that combination leads to a mixture of anti-PD-L1 and anti-IFNγ treatments, but the effect is overall redundant, and the outcome is as if no treatment has been given, highlighting that the anti-PD-L1 effect is dependent on IFNγ in the TME.

In summary, this chapter established that both IFNγ and manipulation of TCR signal strength via anti-PD-L1 can modulate $CD4^+$ T cell *Il10* transcription, but in the context of MC38 tumours this is almost entirely due to modulation of $FoxP3^+$ Treg activity.

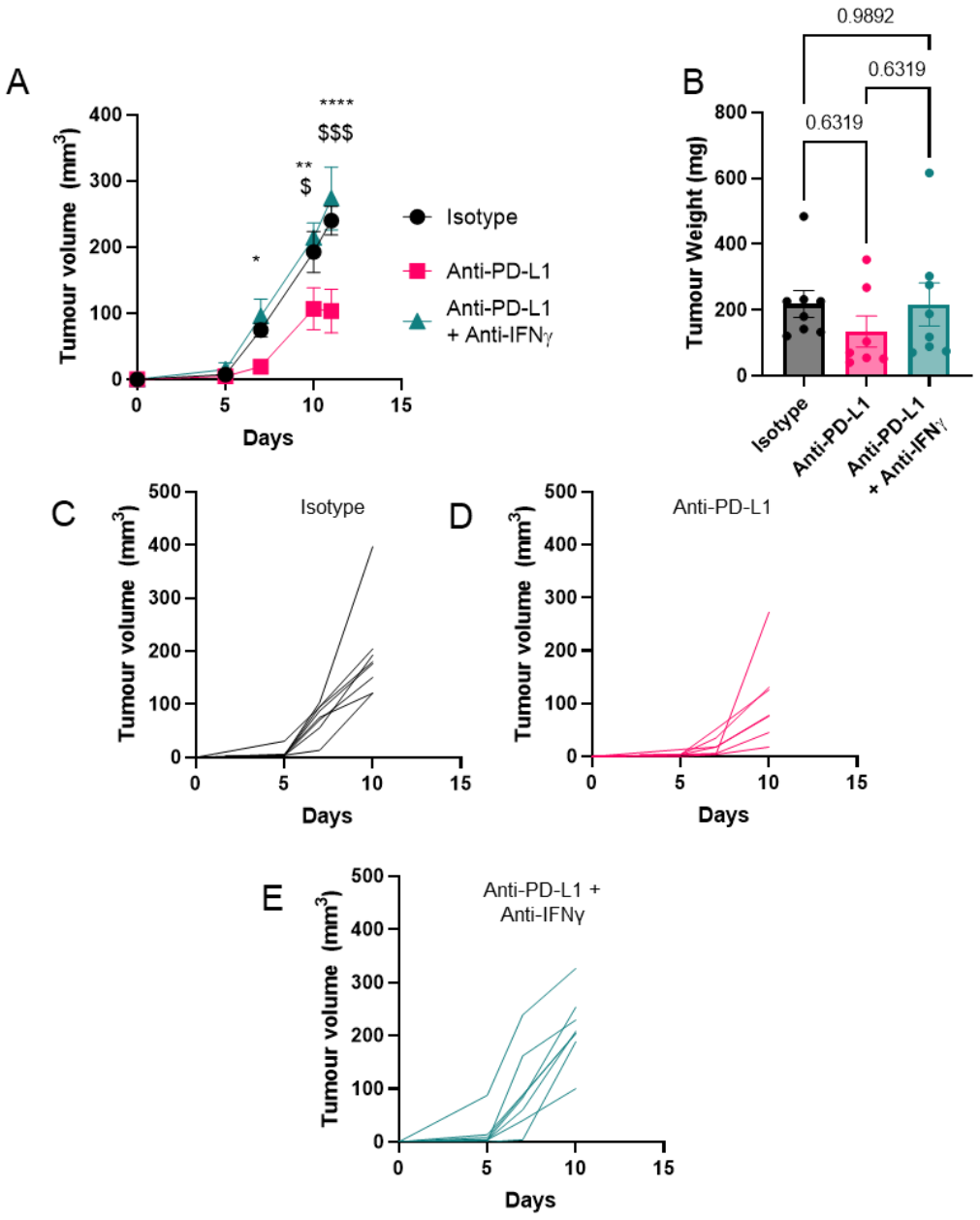

Figure 5-13: Tumours repeatedly treated with combined anti-PD-L1 and anti-IFNγ abrogates anti-PD-L1 benefits to tumour volume and weight.
Nr4a3-Tocky *Il10*-GFP *Ifng*-YFP mice were inoculated with 0.25 million MC38 colorectal cancer cells in 100 µL PBS s.c. On day 5, 7 and 10, 0.5 mg anti-PD-L1, 1 mg anti-IFNγ and 0.5 mg anti-PD-L1 or isotype was administered in 200 µL PBS and tumours harvested on day 11 and analysed for *Il10*-GFP^{+} and *Ifng*-YFP^{+} expression in CD4^{+} and CD8^{+} TCR^{+} *Nr4a3*-Timer^{+} populations. **(A)** Tumour volumes over the treatment course and **(B)** Day 11 tumour weights. Individual mouse tumour volume according to treatment type for **(C)** isotype, **(D)** anti-PD-L1, and **(E)** anti-PD-L1 and anti-IFNγ. **(A,B)** from n=8 mice per group, bars represent mean ± SEM. Analysis by Kruskal-Wallis test. *P = <0.05, **P = <0.01, ***P = <0.001. $^{\$}$P = <0.05, $^{\$\$}$P = <0.01, $^{\$\$\$}$P = <0.001.

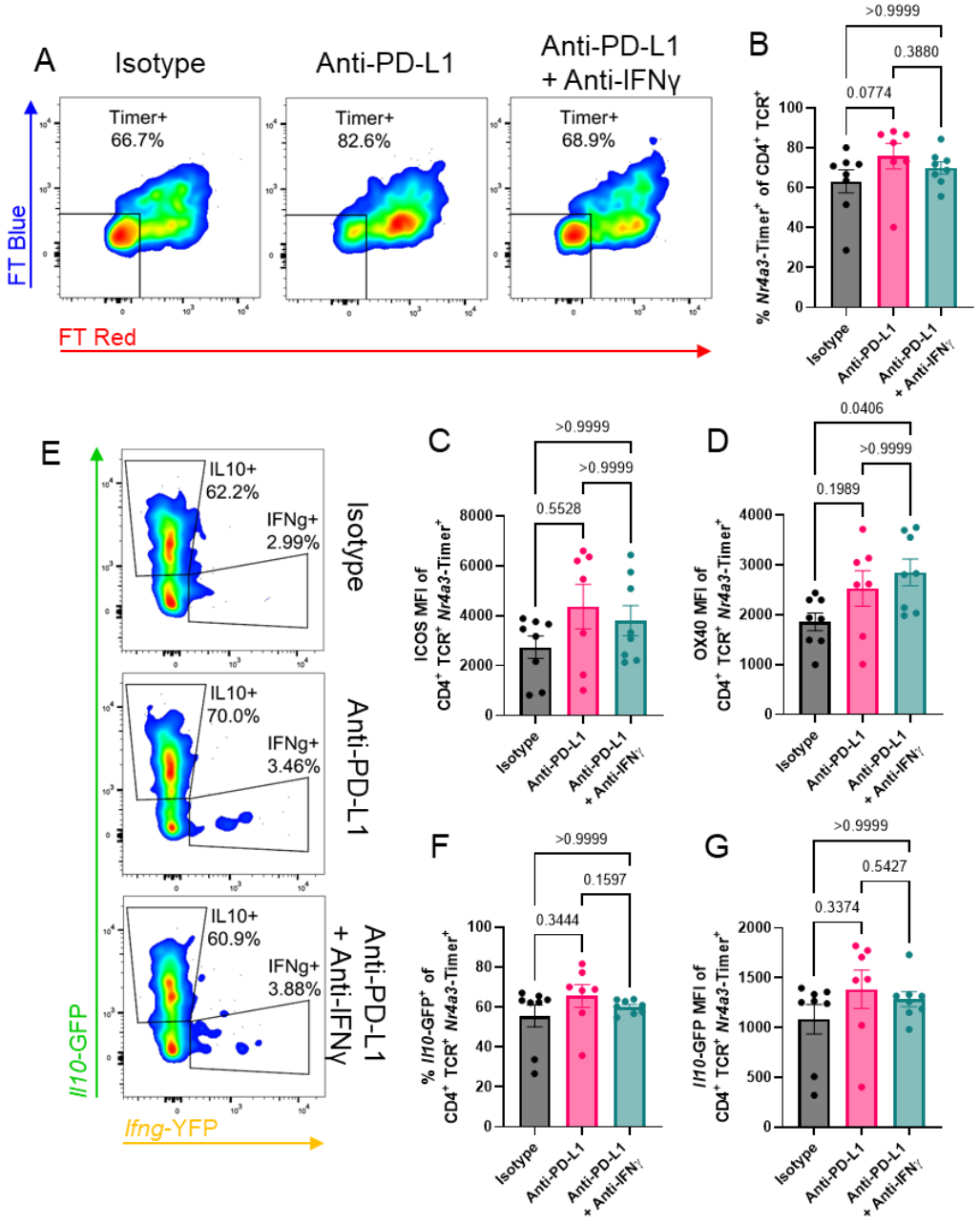

Figure 5-14: Cytokine transcription reporter expression in TCR activated infiltrating T cells from a repeatedly combination treated tumour.
Nr4a3-Tocky *Il10*-GFP *Ifng*-YFP mice were inoculated with 0.25 million MC38 colorectal cancer cells in 100 µL PBS s.c. On day 5, 7 and 10, 0.5 mg anti-PD-L1, 1 mg anti-IFNγ and 0.5 mg anti-PD-L1 or isotype was administered in 200 µL PBS and tumours harvested on day 11 and analysed for *Il10*-GFP$^+$ and *Ifng*-YFP$^+$ expression in CD4$^+$ and CD8$^+$ TCR$^+$ *Nr4a3*-Timer$^+$ populations. Summary of *Nr4a3*-Timer$^+$ in CD4$^+$ TCR$^+$ cells **(B)**. In CD4$^+$ TCR$^+$ *Nr4a3*-Timer$^+$, summary of **(B)** ICOS and **(C)** OX40 MFI. Summary of *Il10*-GFP$^+$ frequency **(F)** and MFI **(G)** in *Nr4a3*-Timer$^+$ CD4$^+$ TCR$^+$ **(E)**. **(B-D, F, G)** from n=8 mice per group, bars represent mean ±SEM. Analysis by Kruskal-Wallis test.

5.3 Discussion

The MC38 tumour in an immunogenic and dynamic environment. Not only do we see infiltrating T cells, but they are activated with no other stimulus than the tumour neoantigens. The frequency of activation and the marker expression likewise changes between the timepoints that we have observed, and we did not examine more detailed timepoints to establish the kinetics of these changes. The uniform increases of weight and volume make for a practical measurement when investigating tumour responses to treatment, however before day 7 the tumours are very small, and do not yield enough TILs for analysis. Unfortunately, this prevented any attempt at observing the early anti-MC38 immune response *in vivo*. Additionally, the tumour could not exceed 12 mm in any dimension, so we had a limited window to analyse the TILs. Whilst we were not concerned about the impact that a more chronic tumour may have, it still a limitation of the model.

Although a Day 7 time point is not shown due to insufficient replicates for reliable statistical analyses, they indicated that Day 10 had peak frequency of *Nr4a3*-Timer and *Il10*-GFP and *Ifng*-YFP cytokine reporters in $CD4^+$ and $CD8^+$ TILs respectively, with the added benefit that they were less likely to exceed 12 mm in any dimension by day 10, compared to later. It was a surprise to find that $CD4^+$ and $CD8^+$ T cells express *Il10*-GFP and *Ifng*-YFP respectively and at such high frequencies. There are very few double expressors in this model, and this was consistent throughout treatments and timepoints. This would suggest that there are few Th1 cells present, as they are IFNγ secreting and furthermore that Tregs would not adopt their Tbet transcription factor and cytokine profile [399].

Profiling the Tregs revealed a different phenotype than the tolerance model, with over 80 % of *Il10*-GFP^{+} T cells being *FoxP3*-Timer^{+}, although ~50 % of *Il10*-GFP^{-} CD4^{+} T cells were also *FoxP3*-Timer^{+}. This implies that only ~35 % of total CD4^{+} in the MC38 tumour are non-Treg (helper, effector, etc.), however the *Il10*-GFP^{-} CD4^{+} T cells have much lower intensity of other Treg markers, including CD25 and CD39. It seems likely, given that most of the CD4^{+} T cells in the tumour microenvironment are canonical *Il10*-GFP^{+} Tregs and assumedly effector Tregs, that they are contributing to an increased tumour burden. However, although reducing *Il10*-GFP expression via IFNγ sequestration correlates with significantly increased tumour burden, the role of IFNγ is not just to promote *Il10* transcription. These experiments to not highlight the complex roles that IFNγ plays in tumour homeostasis.

Our first foray into modulating IFNγ expression was the use of a Cd4^{Cre} IFNgR$^{fl/fl}$ model, removing all IFNγ signalling from CD4^{+} and CD8^{+} T cells, which led to noticeably larger tumours compared to non-Cre mice. Clearly, IFNγ sensitivity by lymphocytes is key to MC38 tumour control. We decided not to continue using this model for two reasons. Firstly, it would have been costly to cross it with the reporters, when we had an abundance of anti-IFNγ antibody available, and more analogous to antibody based treatments that we later compared. Secondly, the COVID-19 pandemic substantially reduced our initial plans with the animal unit, and we were solely dependent on Dr David Bending to conduct most of the in-house mouse experiments in the first 12 months, after which other models were prioritised.

A single dose of anti-IFNγ can reduce expression of *Il10*-GFP and *Ifng*-YFP in CD4^{+} and CD8^{+} TILs respectively, but not enough to change the outcome of a tumour long term. There's no effect on size with a single dose, but its evidence that the mAb can

modulate TILs in this system. With repeated doses, we can see that restricting TME IFNγ worsens tumour burden, much like the Cre model shows us with lymphocyte IFNγ insensitivity, and a strong decrease in markers associated with strong TCR signalling (ICOS, OX40). With less environmental IFNγ, there are fewer MHCII molecules expressed on tumour APCs and fewer pMHCII : TCR interactions, therefore a reduced chance of strong interaction and signalling. This reduces activation of $CD4^+$ T cells, and with less Th1 cells who have inhibited IFNγ signalling to prime other immune cells ultimately reduces cytotoxic $CD8^+$ T cell proliferation and function. With reduced activation of the $CD4^+$ T cell population, there are fewer strong TCR interactions occurring to activate Tregs, and reduced *Il10*-GFP as a result. A key future question is whether in this model IL-10 is crucial to the tumour outcome or not, which could entail IL-10 or IL-10R knockouts in lymphocytes crossed with *Ifng*-YFP reporters to detail any impact on their transcription. Cautiously, we can suggest that IL-10 may not have affect tumour outcomes in our experiments.

Anti-PD-L1 one notably increased *Il10* and *Ifng* expression and lead to improved tumour outcomes. Again, is IL-10 expression important to tumour outcome? Or is it an artefact? ICB of IL-10(R) knockouts mice could be used to demonstrate how anti-PD-L1 changes to IL-10 are functionally important to tumour outcomes. IFNγ is clearly important to this outcome, due to the abrogation of anti-PD-L1 benefit and the enhanced *Ifng*-YFP expression following treatment. In addition, IL-10 upregulation from $CD4^+$ TILs may boost their immunosuppressive function, which could represent a potential dampening mechanism for PD-1 checkpoint immunotherapy.

To delve into what populations are specifically being affected by anti-IFNγ treatment, RNA-seq could be used to highlight key signalling and developmental pathways of

niche populations that we are unable to identify using a flow cytometry approach. This could involve Tr1 and Th1 population changes that affect tumour outcome. A single cell RNA-seq dataset was generated from anti-IFNγ treated MC38 tumours in collaboration with Dr James Thaventhiran's group at the University of Cambridge but analysis of this dataset was not possible before submission of this thesis.

The data here suggest that a majority of *Il10*$^{+}$ T cells are in fact FoxP3^{+} Tregs, and the upregulation of markers such as OX40, ICOS, and *Il10* are indicative of effector Tregs, which display enhanced immunosuppressive activity . However, we have not been able to establish whether the changes in *Il10*$^{+}$ T cells during IFNγ neutralisation of PD-L1 treatment arise in the FoxP3^{+} fraction or whether Tr1 cells are also differentiated within the MC38 model. Future experiments would benefit from a dual *Il10* and *FoxP3* reporter where changes within the *FoxP3*$^{+}$ and *FoxP3*$^{-}$ compartments could be generated. Given that tumours may express neoantigens, it is entirely possible that chronic CD4^{+} T cell stimulation could lead to generation of Tr1-like cells in such settings. However, a high frequency Tr1 cells in a tumour is associated with tumour progression in multiple cancers, including colorectal cancer, metastatic melanoma and head and neck squamous cell carcinoma [373, 400-402]

In summary, the major findings from this chapter are that an IFNγ : IL-10 axis exists within the MC38 tumour environment, with IFNγ positively driving *Il10* transcriptional increases within CD4^{+} T cells. In addition, we discovered that IFNγ is crucial for controlling MC38 tumour burden, and that anti-PD-L1 treatment is dependent on IFNγ for positive outcomes.

Chapter 6 : Final Discussion

Tolerance is exceedingly hard to break, as attempts by lymphocytes to respond to self are immediately counteracted by negative feedback loops, such as IL-10. In the EAE model of multiple sclerosis, not only is MBP or SCH given to mice with transgenic, responsive TCRs, but it must be given with complete Freud's adjuvant usually with *M. tuberculosis* and pertussis toxin to be successfully induced. This hefty cocktail of highly immunogenic reagents stimulates cellular immunity via Th cells and mice that are induced with EAE consequently become very ill. As IFNγ boosts IL-10 production in the Tg4 model, we would hypothesise that anti-IFNγ in the EAE Tg4 model could significantly increase disease progression as it may disrupt the feedback control generation of Tr1-like cells. This has been demonstrated as IFNγ is protective in EAE, acting via microglia in the central nervous system [403, 404].

It is known that expression of a Tr1-like phenotype can be transient, although in models of repeated stimulation inducing tolerance the Tr1 phenotype is stabilised [276, 405]. We did not assess whether Tr1-like cells from mice that received a primary high strength immunisation retained their phenotype after 24 hr, which could reveal that the Tr1-like cells in the Tg4 model are not true Tr1 cells. Repeated dosing with self-peptide could lead to a more stable Tr1 phenotype but may also induce exhaustion in reactive T cells, thereby limiting any tolerogenic effect they produce. Perhaps Tr1 cells become constitutive and permanent only when there are DAMPs present, such as in the pertussis toxin administered to induce EAE. Potentially, Tr1 cells or the Tr1 phenotype seen in this study is a T cell in an acute state of negative feedback following exposure to abundant self-antigen and tolerising signals. The Cockerill Group have shown that a single activation cycle of TCR/CD28 signalling pathways is sufficient to reprogram chromatin domains of immune response genes in naïve T cells, leading to stable

maintenance of altered chromatin states regulating gene accessibility and expression [406, 407]. It seems likely that this is required for long term stability, but that chronic exposure to antigens is required for permanent epigenetic changes leading to a more permanent phenotype. In a phase II EDI clinical trial of multiples sclerosis, a cocktail of immunodominant epitopes for major autoantigens including MBP, proteolipid protein (PLP) and myelin oligodendrocyte glycoprotein (MOG) called ATX-MS-1467. Subcutaneous injection of ATX-MS-1467 induced a significant decrease in new or persisting gadolinium-enhancing (GdE) lesions from baseline to week 16 of treatment. However, the GdE lesions returned to baseline by week 48 [408] and therefore any benefit was transient. When used in mice, ATX-MS-1467 induced stable IL-10^{+} Tr1 cells [409]. This raises the question of how long T cells must be exposed to an antigen before they tolerate it via Tr1 generation.

Production of IL-10 may also depend on TCR engagement. In our rapid Tr1 model, *Il10* transcription followed a burst of TCR signalling. Elliot et al., 2021, reported that by 12 – 24 hr the TCR signal had ceased in this model. However, our data in our hybrid culture model suggest that the memory for IL-10 transcription is not lost and that re-culture of splenocytes from tolerised mice with increased [4Y]-MBP can induce both *Il10* transcription and IL-10 protein secretion. Therefore, like FoxP3 Treg, Tr1 phenotype may switch from a dormant to “effector”-like states upon TCR ligation.

In the MC38 model, we did not fully confirm if Tr1 cells were present, but a small percentage of CD4^{+} IL-10^{+} T cells are FoxP3^{-}, which is consistent with the Tr1 phenotype. Although important in determining tumour outcomes, we do not know how crucial they are compared Tregs in an MC38 tumour. Given that more than 80 % of CD4^{+} *Il10*-GFP^{+} are FoxP3^{+}, it is unlikely that they have a more substantial effect on

tumour outcome compared to Tregs. scRNA-seq of MC38 TILs under anti-IFNγ treatment may show Tr1-like cell populations has been performed and it will be of interest to assess whether there are differential contractions of Tr1-like cells within this dataset. This experiment will also identify unbiased changes across immune cell populations within tumours where IFNγ has been neutralised.

Anti-IFNγ treatment reduced the $CD4^+$ *Il10*-GFP^+ compartment in both tolerance and cancer models, but it was not investigated whether Tr1 cells or Tregs were affected to the same proportion, or if it was more significantly affecting one population over the other. It is perhaps more accurate to think of chapters 3 and 4's Tg4 model as probing tolerogenic responses, as autoimmune disease was never fully established and mice showed no signs of sickness/distress, and chapter 5's MC38 model as testing the IFNγ regulatory circuits in tumours, as the tolerising environment that arises from tumour survival mechanisms is not strictly one of tolerance to self. Non-self-neoantigens can develop because of tumour growth and development, providing novel (and potentially response-worthy) targets. Additionally, the Tg4 model is a monoclonal response, whereas in the MC38 tumours, the response is polyclonal, so they are not directly comparable.

Anti-IFNγ nullified the anti-PD-L1 effect, but what about other immune checkpoint therapies? Approved treatments such as Anti-CTLA-4 or those under clinical trial like Anti-LAG3 may have very different mechanisms of action that are much less dependent on IFNγ. However, given that IFNγ plays a large role in controlling tumour growth, this is likely not the case when ICB "takes off the handbrake" of the adaptive immune response. One large unanswered question in this thesis is how does anti-IL-27 treatment affect the TIL phenotype and tumour outcome? If we speculate based on

the result of our Tg4 model results, anti-IL-27 would drive *Il10* down and increase tumour burden. Using the *Ifng*-YFP reporter, we may even see what whether it drives IFNγ or not. Given that IFNγ can drive IL-27 expression, identifying sources of IL-27 will be important, and whether this cytokine is also important for FoxP3^{+} Treg IL-10 activity remains to be determined. Indeed, combination therapy of anti-IFNγ and anti-IL-27 would be very interesting to establish the effect not only on Treg *Il10* but also on the outcome of tumour development.

Much like the finding that IFNγ was protective in EAE via microglia [404], this work adds to potential regulatory roles of IFNγ, via increasing IL-10 expression in regulatory T cells. It is worth noting that our attempts to increase IL-10 via recombinant IFNγ and IL-27 *in vitro* had little effect. It is possible that the cytokines did not achieve the sufficient dose to elicit a response such as the concentrations within the immune synapse, that they required an additional signal to fully enact their effect, or a combination of these factors. We have not fully assessed the molecular mechanisms involved in the IL-10 : IFNγ axis, and what impact the treatments administered had on the functionality of the cells involved. Proliferation dyes, for example, could highlight some of the functional response, if any, to anti-IFNγ, anti-IL-27, anti-PD-L1 or combinations therein. Cytokine secretion assays also could be used with the hybrid model experiments, particularly for IL-2 or IFNγ to observe the effects on other T cell subsets. Anti-PD-L1 treated tumours expressed higher amounts of *Il10*-GFP and *Ifng*-YFP – is this an artefact or important to outcomes? *In vitro* treatment of activated T cells or induced Tregs with anti-PD-L1 or IL-10 and IFNγ in combination may shed some light on changes to TCR signalling strength or markers thereof.

In our tumour model, does it matter which cell type the IFNγ is secreted? In the Tg4 mice, it was clear that despite NK cells expressing more than 70 % of the total *Ifng*-YFP in immunised mice, that their IFNγ was inconsequential to changes in Tr1 phenotypes, perhaps relying on a co-signal from inflammatory myeloid cells, which would also be an interesting target of depletion, for effect. However, this may not be the case in the tumour model where IFNγ can act directly on cancer cells and is largely $CD8^+$ derived. Microscopy of intact spleens and tumours could have shown us where NK cells sit in comparison to *Il-10*-GFP^+ cells i.e. close or distant, relative to their importance on *IL10*-GFP signalling, and shown us whether these cells clustered together around inflammatory myeloid cells or where dispersed.

Although cytokine transcription is still a critical readout, rarely did we investigate protein concentrations in our samples. This gap could have been easily filled with the use of Brefeldin A to retain cytokines within the endoplasmic for intracellular staining. Ultimately, despite changes to transcript, we cannot confirm that cytokines in our primary immunisation and tumour models ever became protein or were secreted – although given the effect of anti-IFNγ antibody, it appears likely that it was. In homeostatic conditions, IL-10 and IFNγ have a clear relationship in resolving inflammation with some diametrically opposed functions (fig. 6.1), from Th1 polarisation and Treg phenotype, to MHCII expression and IL-6 secretion (a Treg antagonist). In disease states such as tumour this balance and the role of negative feedback mechanisms becomes more complicated. The many roles that T cells and APCs conduct finetune an inflammatory response, and when the balance between the two is severely disrupted from cytokine sequestration, for example, it did not lead to a beneficial outcome. To investigate how IL-10 and IFNγ modulation may lead to

improved disease outcomes, I speculate that further boosting of both IL-10 and IFNγ may lead to resolution, as seen in anti-PD-L1 treated tumours, but it is a question of how this boost is delivered, and whether boosting leads to more cytokine and strong TCR signalling markers in a population, or whether a population expresses more of them. We see that when IFNγ is sequestered, *Il10* expression is reduced, which would suggest that there will be greater anti-tumour effects. However, the overall effect is pro-tumour, as they quickly grow and exceed set limits. This is supported by anti-PD-L1, which boosts $CD4^+$ *Il10* transcription, $CD8^+$ *Ifng* transcription and reduces tumour growth, but this is mitigated by anti-IFNγ, reducing any benefit so that the overall outcome is like the isotype treated tumour bearing mice. This suggests that IFNγ is key to anti-PD-L1 treatment outcome – even though it also boosts *Il10* expression. Whilst the data in this thesis demonstrates the relationship in one direction, I speculate that IL-10 and IFNγ appear to be inextricably linked, and that by increasing one, you can increase the other and that better patient outcomes may require an increase in both, as opposed to disrupting their balance and retaining high expression of only one.

With growing interest in using immune checkpoint blockade for autoimmune diseases, combination immune checkpoint blockade therapies gaining traction for cancer treatment, and agonising antibodies under development, it will be interesting to continue engaging with the treatment optimisation field for decades to come. For highly complex diseases like cancers, it appears that an even more multi-faceted approach may be more beneficial, not only to prevent immune exhaustion, but also to stimulate and supplement output, and carefully regulate all at once. Are this generation's treatments fully optimised to their absolute limit? Are we making only marginal gains? We will see. It will be a team effort.

Appendix R Code for RNA-seq Analysis (Adapted from Scripts from Dr David Bending)

```
#Blue bee software used to align files and generate raw HTseq count (HTseq-
count v0.6.0) files mapped to the ensembl gene id from GRCm38 (mm10)
#set working directory to tell R to locate files "raw.txt" and "coldata.csv"
cts=as.matrix(read.table("raw.txt"))
coldata=read.csv("coldata.csv", row.names=1)
library(DESeq2)
dds=DESeqDataSetFromMatrix(countData=cts,colData=coldata,design=~condition
)
keep=rowSums(counts(dds))>=10
dds=dds[keep,]
dds=DESeq(dds)

#rlog function normalisation of library and plotting of PCA
rld=rlog(dds,blind=F)
write.csv(assay(rld),file="norm.csv")
pdf("PCAall.pdf")
plotPCA(rld, intgroup="condition", ntop=1000)
dev.off()
pcaData=plotPCA(rld, intgroup="condition", ntop=500, returnData=TRUE)
write.csv(pcaData,file="all.csv")


#lfc shrink data and identify DEGs
deg=lfcShrink(dds,contrast=c("condition","IL10pos","IL10neg"), type="ashr")
deg=deg[order(deg$padj),]
deg=subset(deg,padj<0.05)
write.csv(deg, file="padjdeg.csv")


#Read in file of gene names to convert ensemble gene ids
x=read.csv("degnamed.csv")
pan = padj degnamed
pan=read.csv("padjdeg.csv", header=T)
colnames(pan)[1]="ensembl_gene_id"
m=merge(pan,x,by="ensembl_gene_id")
#reordered m
rm=m[,c(1,7,2:6)]
write.csv(rm,file="degfinal.csv")

#norm2 doesn't have gene names which we will now assign
norm2all=read.csv("norm2.csv",header=T)
#egn = external gene names
egn=read.csv("names.csv",header=T)
colnames(norm2all)[1]="ensembl_gene_id"
#nan = norm all names
nan=merge(norm2all,egn,by="ensembl_gene_id")
```

```
rownames(nan)=nan[,6]
#remove duplicate gene names
nan2=nan[!duplicated(nan[,6]),]
rownames(nan2)=nan2[,6]
#remove column 1 and 6 from nan2 and make new file (nan3) to remove the
outliers
nan3=nan2[,c(-1,-6)]
write.csv(nan3,file="normrlognamed.csv")

#degv = deg vector
degv=rm[,2]
head(nan3)
nan4=nan3[degv,]
library(gplots)
nan4=as.matrix(nan4)

 #Heatmap merge of DEG from IL10pos vs IL10neg versus normalised read counts
  library(gplots)
  pdf("alldeg.pdf", height=12, width=6)
  heatmap.2(nan4,   scale="row",   col=bluered(100),   density.info="none",
trace="none", cexRow=0.4)
  dev.off()

 #Curated gene expression list
cur=c("Il10","Maf","Prdm1","Il12rb2","Icos","Ctla4","Il7r","Ccr7","Rora","
Id2","Mki67","Ifngr1","Gzmb")
nan5=nan3[cur,]
str(nan5)
nan5=as.matrix(nan5)
pdf("curdeg2.pdf", height=12, width=6)
heatmap.2(nan5,    scale="row",    col=bluered(100),    density.info="none",
trace="none", cexRow=0.4)
dev.off()
```

References

1. Miller, J.F., *Immunological function of the thymus.* Lancet, 1961. **2**(7205): p. 748-9.
2. Donskoy, E. and I. Goldschneider, *Thymocytopoiesis is maintained by blood-borne precursors throughout postnatal life: A study in parabiotic mice.* Journal of Immunology, 1992. **148**(6): p. 1604-1612.
3. Ceredig, R., *Differentiation potential of 14-day fetal mouse thymocytes in organ culture. Analysis of CD4/CD8-defined single-positive and double-negative cells.* J Immunol, 1988. **141**(2): p. 355-62.
4. Germain, R.N., *MHC-dependent antigen processing and peptide presentation: Providing ligands for T lymphocyte activation.* Cell, 1994. **76**(2): p. 287-299.
5. Godfrey, D.I., et al., *A Developmental Pathway Involving Four Phenotypically and Functionally Distinct Subsets of CD3-CD4-CD8- Triple-Negative Adult Mouse Thymocytes Defined by CD44 and CD25 Expression.* Journal of Immunology, 1993. **150**(10): p. 4244-4252.
6. Hoffman, E.S., et al., *Productive T-cell receptor β-chain gene rearrangement: Coincident regulation of cell cycle and clonality during development in vivo.* Genes and Development, 1996. **10**(8): p. 948-962.
7. Aifantis, I., et al., *Early T cell receptor β gene expression is regulated by the pre-T cell receptor-CD3 complex.* Journal of Experimental Medicine, 1999. **190**(1): p. 141-144.
8. Blom, B., et al., *TCR gene rearrangements and expression of the pre-T cell receptor complex during human T-cell differentiation.* Blood, 1999. **93**(9): p. 3033-3043.
9. Alberola-Ila, J., et al., *Positive and negative selection invoke distinct signaling pathways.* Journal of Experimental Medicine, 1996. **184**(1): p. 9-18.
10. Lind, E.F., et al., *Mapping precursor movement through the postnatal thymus reveals specific microenvironments supporting defined stages of early lymphoid development.* Journal of Experimental Medicine, 2001. **194**(2): p. 127-134.
11. Kisielow, P. and A. Miazek, *Positive selection of T cells: Rescue from programmed cell death and differentiation require continual engagement of the T cell receptor.* Journal of Experimental Medicine, 1995. **181**(6): p. 1975-1984.
12. Luckheeram, R.V., et al., *CD4(+)T cells: differentiation and functions.* Clin Dev Immunol, 2012. **2012**: p. 925135.
13. Legoux, F.P., et al., *CD4+ T Cell Tolerance to Tissue-Restricted Self Antigens Is Mediated by Antigen-Specific Regulatory T Cells Rather Than Deletion.* Immunity, 2015. **43**(5): p. 896-908.
14. Malhotra, D., et al., *Tolerance is established in polyclonal CD4 + T cells by distinct mechanisms, according to self-peptide expression patterns.* Nature Immunology, 2016. **17**(2): p. 187-195.
15. Thapa, P. and D.L. Farber, *The Role of the Thymus in the Immune Response.* Thoracic surgery clinics, 2019. **29**(2): p. 123-131.
16. Lio, C.W.J. and C.S. Hsieh, *A Two-Step Process for Thymic Regulatory T Cell Development.* Immunity, 2008. **28**(1): p. 100-111.
17. Burchill, M.A., et al., *Linked T Cell Receptor and Cytokine Signaling Govern the Development of the Regulatory T Cell Repertoire.* Immunity, 2008. **28**(1): p. 112-121.

18. Aschenbrenner, K., et al., *Selection of Foxp3+ regulatory T cells specific for self antigen expressed and presented by Aire+ medullary thymic epithelial cells.* Nature Immunology, 2007. **8**(4): p. 351-358.
19. Cowan, J.E., et al., *The thymic medulla is required for Foxp3+ regulatory but not conventional CD4+ thymocyte development.* Journal of Experimental Medicine, 2013. **210**(4): p. 675-681.
20. Cosway, E.J., et al., *The thymus medulla and its control of αβT cell development.* Seminars in Immunopathology, 2021. **43**(1): p. 15-27.
21. Yang, S., et al., *Regulatory T cells generated early in life play a distinct role in maintaining self-tolerance.* Science, 2015. **348**(6234): p. 589-594.
22. Jordan, M.S., et al., *Thymic selection of CD4+CD25+ regulatory T cells induced by an agonist self-peptide.* Nature Immunology, 2001. **2**(4): p. 301-306.
23. Moran, A.E., et al., *T cell receptor signal strength in Treg and iNKT cell development demonstrated by a novel fluorescent reporter mouse.* Journal of Experimental Medicine, 2011. **208**(6): p. 1279-1289.
24. Morikawa, H. and S. Sakaguchi, *Genetic and epigenetic basis of Treg cell development and function: From a FoxP3-centered view to an epigenome-defined view of natural Treg cells.* Immunological Reviews, 2014. **259**(1): p. 192-205.
25. Malchow, S., et al., *Aire Enforces Immune Tolerance by Directing Autoreactive T Cells into the Regulatory T Cell Lineage.* Immunity, 2016. **44**(5): p. 1102-1113.
26. Lin, J., et al., *Increased generation of Foxp3+ regulatory T cells by manipulating antigen presentation in the thymus.* Nature Communications, 2016. **7**.
27. Benvenuti, F., et al., *Dendritic cell maturation controls adhesion, synapse formation, and the duration of the interactions with naive T lymphocytes.* J Immunol, 2004. **172**(1): p. 292-301.
28. Wilson, N.S., D. El-Sukkari, and J.A. Villadangos, *Dendritic cells constitutively present self antigens in their immature state in vivo and regulate antigen presentation by controlling the rates of MHC class II synthesis and endocytosis.* Blood, 2004. **103**(6): p. 2187-95.
29. Curtsinger, J.M., et al., *Inflammatory cytokines provide a third signal for activation of naive CD4+ and CD8+ T cells.* J Immunol, 1999. **162**(6): p. 3256-62.
30. Hutloff, A., et al., *ICOS is an inducible T-cell co-stimulator structurally and functionally related to CD28.* Nature, 1999. **397**(6716): p. 263-266.
31. Mahajan, S., et al., *The role of ICOS in the development of CD4 T cell help and the reactivation of memory T cells.* Eur J Immunol, 2007. **37**(7): p. 1796-808.
32. Appleman, L.J. and V.A. Boussiotis, *T cell anergy and costimulation.* Immunol Rev, 2003. **192**: p. 161-80.
33. Paliard, X., et al., *Simultaneous production of IL-2, IL-4, and IFN-γ by activated human CD4+ and CD8+ T cell clones.* Journal of Immunology, 1988. **141**(3): p. 849-855.
34. Bacchetta, R., et al., *Host-reactive CD4+ and CD8+ T cell clones isolated from a human chimera produce IL-5, IL-2, IFN-γ and granulocyte/macrophage-colony-stimulating factor but not IL-4.* Journal of Immunology, 1990. **144**(3): p. 902-908.

35. Brehm, M.A., K.A. Daniels, and R.M. Welsh, *Rapid production of TNF-alpha following TCR engagement of naive CD8 T cells.* J Immunol, 2005. **175**(8): p. 5043-9.
36. Schoenborn, J.R. and C.B. Wilson, *Regulation of interferon-gamma during innate and adaptive immune responses.* Adv Immunol, 2007. **96**: p. 41-101.
37. Hay, Z.L.Z. and J.E. Slansky, *Granzymes: The Molecular Executors of Immune-Mediated Cytotoxicity.* Int J Mol Sci, 2022. **23**(3).
38. Juo, P., et al., *Essential requirement for caspase-8/FLICE in the initiation of the Fas-induced apoptotic cascade.* Curr Biol, 1998. **8**(18): p. 1001-8.
39. Bending, D., et al., *Highly purified Th17 cells from BDC2.5NOD mice convert into Th1-like cells in NOD/SCID recipient mice.* J Clin Invest, 2009. **119**(3): p. 565-72.
40. Kleinewietfeld, M. and D.A. Hafler, *The plasticity of human Treg and Th17 cells and its role in autoimmunity.* Semin Immunol, 2013. **25**(4): p. 305-12.
41. McBlane, J.F., et al., *Cleavage at a V(D)J recombination signal requires only RAG1 and RAG2 proteins and occurs in two steps.* Cell, 1995. **83**(3): p. 387-395.
42. Zemmour, D., et al., *Single-cell gene expression reveals a landscape of regulatory T cell phenotypes shaped by the TCR.* Nature Immunology, 2018. **19**(3): p. 291-301.
43. Gaud, G., R. Lesourne, and P.E. Love, *Regulatory mechanisms in T cell receptor signalling.* Nat Rev Immunol, 2018. **18**(8): p. 485-497.
44. Bhattacharyya, N.D. and C.G. Feng, *Regulation of T Helper Cell Fate by TCR Signal Strength.* Front Immunol, 2020. **11**: p. 624.
45. Sakaguchi, S., et al., *Regulatory T Cells and Immune Tolerance.* Cell, 2008. **133**(5): p. 775-787.
46. Zhang, X., et al., *Activation of CD25+CD4+ regulatory T cells by oral antigen administration.* Journal of Immunology, 2001. **167**(8): p. 4245-4253.
47. Dembic, Z., *Beginning of the end of (understanding) the immune response.* Scandinavian Journal of Immunology, 2008. **68**(4): p. 381-382.
48. Aluvihare, V.R., M. Kallikourdis, and A.G. Betz, *Regulatory T cells mediate maternal tolerance to the fetus.* Nature Immunology, 2004. **5**(3): p. 266-271.
49. Eming, S.A., T.A. Wynn, and P. Martin, *Inflammation and metabolism in tissue repair and regeneration.* Science, 2017. **356**(6342): p. 1026-1030.
50. Castiglioni, A., et al., *FOXP3+ T cells recruited to sites of sterile skeletal muscle injury regulate the fate of satellite cells and guide effective tissue regeneration.* PLoS ONE, 2015. **10**(6).
51. Ali, N., et al., *Regulatory T Cells in Skin Facilitate Epithelial Stem Cell Differentiation.* Cell, 2017. **169**(6): p. 1119-1129.e11.
52. Weirather, J., et al., *Foxp3+ CD4+ T cells improve healing after myocardial infarction by modulating monocyte/macrophage differentiation.* Circulation Research, 2014. **115**(1): p. 55-67.
53. Brunkow, M.E., et al., *Disruption of a new forkhead/winged-helix protein, scurfin, results in the fatal lymphoproliferative disorder of the scurfy mouse.* Nature Genetics, 2001. **27**(1): p. 68-73.
54. Bennett, C.L., et al., *The immune dysregulation, polyendocrinopathy, enteropathy, X-linked syndrome (IPEX) is caused by mutations of FOXP3.* Nature Genetics, 2001. **27**(1): p. 20-21.

55. Hori, S., T. Nomura, and S. Sakaguchi, *Control of regulatory T cell development by the transcription factor Foxp3.* Science, 2003. **299**(5609): p. 1057-1061.
56. Kisielow, P., et al., *Tolerance in T-cell-receptor transgenic mice involves deletion of nonmature CD4+8+ thymocytes.* Nature, 1988. **333**(6175): p. 742-746.
57. O'Garra, A. and K. Murphy, *Role of cytokines in determining T-lymphocyte function.* Current Opinion in Immunology, 1994. **6**(3): p. 458-466.
58. Chen, Y., et al., *Regulatory T cell clones induced by oral tolerance: Suppression of autoimmune encephalomyelitis.* Science, 1994. **265**(5176): p. 1237-1240.
59. Almeida, A.R.M., et al., *Homeostasis of peripheral CD4+ T cells: IL-2Rα and IL-2 shape a population of regulatory cells that controls CD4+ T cell numbers.* Journal of Immunology, 2002. **169**(9): p. 4850-4860.
60. Malek, T.R., et al., *CD4 regulatory T cells prevent lethal autoimmunity in IL-2Rβ-deficient mice: Implications for the nonredundant function of IL-2.* Immunity, 2002. **17**(2): p. 167-178.
61. Furtado, G.C., et al., *Interleukin 2 signaling is required for CD4+ regulatory T cell function.* Journal of Experimental Medicine, 2002. **196**(6): p. 851-857.
62. Song, G.Z., et al., *IL-2 is essential for TGF-β to convert naive CD4+CD25 - cells to CD25+Foxp3+ regulatory T cells and for expansion of these cells.* Journal of Immunology, 2007. **178**(4): p. 2018-2027.
63. Wyss, L., et al., *Affinity for self antigen selects Treg cells with distinct functional properties.* Nature Immunology, 2016. **17**(9): p. 1093-1101.
64. Sprouse, M.L., et al., *Cutting edge: Low-Affinity TCRs support regulatory t cell function in autoimmunity.* Journal of Immunology, 2018. **200**(3): p. 909-914.
65. Wei, X., et al., *Reciprocal Expression of IL-35 and IL-10 Defines Two Distinct Effector Treg Subsets that Are Required for Maintenance of Immune Tolerance.* Cell Reports, 2017. **21**(7): p. 1853-1869.
66. Okeke, E.B. and J.E. Uzonna, *The pivotal role of regulatory T cells in the regulation of innate immune cells.* Frontiers in Immunology, 2019. **10**(APR).
67. Onishi, Y., et al., *Foxp3+ natural regulatory T cells preferentially form aggregates on dendritic cells in vitro and actively inhibit their maturation.* Proceedings of the National Academy of Sciences of the United States of America, 2008. **105**(29): p. 10113-10118.
68. Fallarino, F., et al., *Modulation of tryptophan catabolism by regulatory T cells.* Nature Immunology, 2003. **4**(12): p. 1206-1212.
69. Ernst, P.B., J.C. Garrison, and L.F. Thompson, *Much ado about adenosine: Adenosine synthesis and function in regulatory T cell biology.* Journal of Immunology, 2010. **185**(4): p. 1993-1998.
70. Zhu, Z., et al., *IL-35 promoted STAT3 phosphorylation and IL-10 production in B cells, but its production was reduced in patients with coronary artery diseases.* Human Immunology, 2018. **79**(12): p. 869-875.
71. Tsuchida, Y., et al., *TGF-β3 inhibits antibody production by human B cells.* PLoS ONE, 2017. **12**(1).
72. Dooley, A., et al., *The B cell IL-10 receptor suppresses antibody production.* J Immunol, 2018. **200**.
73. Schmidt, A., N. Oberle, and P.H. Krammer, *Molecular mechanisms oftreg-mediatedt cell suppression.* Frontiers in Immunology, 2012. **3**(MAR).

74. Boks, M.A., et al., *IL-10-generated tolerogenic dendritic cells are optimal for functional regulatory T cell induction - A comparative study of human clinical-applicable DC.* Clinical Immunology, 2012. **142**(3): p. 332-342.
75. Strobl, H. and W. Knapp, *TGF-β1 regulation of dendritic cells.* Microbes and Infection, 1999. **1**(15): p. 1283-1290.
76. Wallet, M.A., P. Sen, and R. Tisch, *Immunoregulation of dendritic cells.* Clinical medicine & research, 2005. **3**(3): p. 166-175.
77. Speck, S., et al., *TGF-β signaling initiated in dendritic cells instructs suppressive effects on Th17 differentiation at the site of neuroinflammation.* PLoS ONE, 2014. **9**(7).
78. Thepmalee, C., et al., *Inhibition of IL-10 and TGF-β receptors on dendritic cells enhances activation of effector T-cells to kill cholangiocarcinoma cells.* Human Vaccines and Immunotherapeutics, 2018. **14**(6): p. 1423-1431.
79. Schwarz, A., et al., *Fine-tuning of regulatory T cell function: The role of calcium signals and naive regulatory T cells for regulatory T cell deficiency in multiple sclerosis.* Journal of Immunology, 2013. **190**(10): p. 4965-4970.
80. Grossman, W.J., et al., *Human T regulatory cells can use the perforin pathway to cause autologous target cell death.* Immunity, 2004. **21**(4): p. 589-601.
81. Chinen, T., et al., *An essential role for the IL-2 receptor in T reg cell function.* Nature Immunology, 2016. **17**(11): p. 1322-1333.
82. Bodmer, J.L., et al., *TRAIL receptor-2 signals apoptosis through FADD and caspase-8.* Nature Cell Biology, 2000. **2**(4): p. 241-243.
83. Ren, X., et al., *Involvement of cellular death in TRAIL/DR5-dependent suppression induced by CD4+CD25+ regulatory T cells.* Cell Death and Differentiation, 2007. **14**(12): p. 2076-2084.
84. Yu, X., et al., *The surface protein TIGIT suppresses T cell activation by promoting the generation of mature immunoregulatory dendritic cells.* Nature Immunology, 2009. **10**(1): p. 48-57.
85. Kučan Brlić, P., et al., *Targeting PVR (CD155) and its receptors in anti-tumor therapy.* Cellular and Molecular Immunology, 2019. **16**(1): p. 51-63.
86. Koch, M.A., et al., *The transcription factor T-bet controls regulatory T cell homeostasis and function during type 1 inflammation.* Nature Immunology, 2009. **10**(6): p. 595-602.
87. Levine, A.G., et al., *Stability and function of regulatory T cells expressing the transcription factor T-bet.* Nature, 2017. **546**(7658): p. 421-425.
88. Joller, N., et al., *Treg cells expressing the coinhibitory molecule TIGIT selectively inhibit proinflammatory Th1 and Th17 cell responses.* Immunity, 2014. **40**(4): p. 569-581.
89. Shevyrev, D. and V. Tereshchenko, *Treg Heterogeneity, Function, and Homeostasis.* Front Immunol, 2019. **10**: p. 3100.
90. Chaudhry, A., et al., *CD4+ regulatory T cells control TH17 responses in a stat3-dependent manner.* Science, 2009. **326**(5955): p. 986-991.
91. Silva, S.L., et al., *Human naïve regulatory T-cells feature high steady-state turnover and are maintained by IL-7.* Oncotarget, 2016. **7**(11): p. 12163-12175.
92. Schadenberg, A.W.L., et al., *Differential homeostatic dynamics of human regulatory T-cell subsets following neonatal thymectomy.* Journal of Allergy and Clinical Immunology, 2014. **133**(1): p. 277-280.e6.

93. Rosenblum, M.D., et al., *Response to self antigen imprints regulatory memory in tissues.* Nature, 2011. **480**(7378): p. 538-542.
94. Gratz, I.K., et al., *Cutting edge: Memory regulatory T cells require IL-7 and not IL-2 for their maintenance in peripheral tissues.* Journal of Immunology, 2013. **190**(9): p. 4483-4487.
95. Smigiel, K.S., et al., *CCR7 provides localized access to IL-2 and defines homeostatically distinct regulatory T cell subsets.* Journal of Experimental Medicine, 2014. **211**(1): p. 121-136.
96. Levine, A.G., et al., *Continuous requirement for the TCR in regulatory T cell function.* Nature Immunology, 2014. **15**(11): p. 1070-1078.
97. Li, J., et al., *Regulatory T-cells: Potential regulator of tissue repair and regeneration.* Frontiers in Immunology, 2018. **9**(MAR).
98. Vahl, J., et al., *Continuous T Cell Receptor Signals Maintain a Functional Regulatory T Cell Pool.* Immunity, 2014. **41**(5): p. 722-736.
99. Schmidt, A.M., et al., *Regulatory T cells require TCR signaling for their suppressive function.* Journal of Immunology, 2015. **194**(9): p. 4362-4370.
100. Golovina, T.N., et al., *CD28 costimulation is essential for human T regulatory expansion and function.* Journal of Immunology, 2008. **181**(4): p. 2855-2868.
101. He, X., et al., *Single CD28 stimulation induces stable and polyclonal expansion of human regulatory T cells.* Scientific Reports, 2017. **7**.
102. Fan, M.Y., et al., *Differential Roles of IL-2 Signaling in Developing versus Mature Tregs.* Cell Reports, 2018. **25**(5): p. 1204-1213.e4.
103. Jeon, P.H. and K.I. Oh, *IL2 is required for functional maturation of regulatory T cells.* Animal Cells and Systems, 2017. **21**(1): p. 1-9.
104. Siegmund, K., et al., *Migration matters: Regulatory T-cell compartmentalization determines suppressive activity in vivo.* Blood, 2005. **106**(9): p. 3097-3104.
105. Dudda, J.C., et al., *Foxp3+ regulatory T cells maintain immune homeostasis in the skin.* Journal of Experimental Medicine, 2008. **205**(7): p. 1559-1585.
106. Zhang, N., et al., *Regulatory T Cells Sequentially Migrate from Inflamed Tissues to Draining Lymph Nodes to Suppress the Alloimmune Response.* Immunity, 2009. **30**(3): p. 458-469.
107. Scheinecker, C., et al., *Constitutive presentation of a natural tissue autoantigen exclusively by dendritic cells in the draining lymph node.* Journal of Experimental Medicine, 2002. **196**(8): p. 1079-1090.
108. Liu, Z., et al., *Immune homeostasis enforced by co-localized effector and regulatory T cells.* Nature, 2015. **528**(7581): p. 225-230.
109. Suffner, J., et al., *Dendritic cells support homeostatic expansion of Foxp3+ regulatory T cells in Foxp3.LuciDTR mice.* Journal of Immunology, 2010. **184**(4): p. 1810-1820.
110. Darrasse-Jèze, G., et al., *Feedback control of regulatory T cell homeostasis by dendritic cells in vivo.* Journal of Experimental Medicine, 2009. **206**(9): p. 1853-1862.
111. Bar-On, L., et al., *Dendritic cell-restricted CD80/86 deficiency results in peripheral regulatory T-cell reduction but is not associated with lymphocyte hyperactivation.* European Journal of Immunology, 2011. **41**(2): p. 291-298.
112. Tang, Q., et al., *Cutting edge: CD28 controls peripheral homeostasis of CD4 +CD25+ regulatory T cells.* Journal of Immunology, 2003. **171**(7): p. 3348-3352.

113. Zheng, Y., et al., *CD86 and CD80 Differentially Modulate the Suppressive Function of Human Regulatory T Cells.* Journal of Immunology, 2004. **172**(5): p. 2778-2784.
114. Roncarolo, M.G., et al., *Antigen recognition by mhc-incompatible cells of a human mismatched chimera.* Journal of Experimental Medicine, 1988. **168**(6): p. 2139-2152.
115. Bacchetta, R., et al., *High levels of interleukin 10 production in vivo are associated with tolerance in SCID patients transplanted with HLA mismatched hematopoietic stem cells.* Journal of Experimental Medicine, 1994. **179**(2): p. 493-502.
116. Gagliani, N., et al., *Coexpression of CD49b and LAG-3 identifies human and mouse T regulatory type 1 cells.* Nature Medicine, 2013. **19**(6): p. 739-746.
117. Alfen, J.S., et al., *Intestinal IFN-γ–producing type 1 regulatory T cells coexpress CCR5 and programmed cell death protein 1 and downregulate IL-10 in the inflamed guts of patients with inflammatory bowel disease.* Journal of Allergy and Clinical Immunology, 2018. **142**(5): p. 1537-1547.e8.
118. Brockmann, L., et al., *Molecular and functional heterogeneity of IL-10-producing CD4 + T cells.* Nature Communications, 2018. **9**(1).
119. Sumitomo, S., et al., *Identification of tonsillar CD4+CD25−LAG3+ T cells as naturally occurring IL-10-producing regulatory T cells in human lymphoid tissue.* Journal of Autoimmunity, 2017. **76**: p. 75-84.
120. Amodio, G., et al., *HLA-G expressing DC-10 and CD4+ T cells accumulate in human decidua during pregnancy.* Human Immunology, 2013. **74**(4): p. 406-411.
121. Groux, H., et al., *A CD4+ T-cell subset inhibits antigen-specific T-cell responses and prevents colitis.* Nature, 1997. **389**(6652): p. 737-742.
122. Brockmann, L., et al., *IL-10 receptor signaling is essential for TR1 cell function in vivo.* Journal of Immunology, 2017. **198**(3): p. 1130-1141.
123. Bacchetta, R., et al., *Growth and expansion of human T regulatory type 1 cells are independent from TCR activation but require exogenous cytokines.* European Journal of Immunology, 2002. **32**(8): p. 2237-2245.
124. De Waal Malefyt, R., et al., *Interleukin 10 (IL-10) and viral IL-10 strongly reduce antigen-specific human T cell proliferation by diminishing the antigen-presenting capacity of monocytes via downregulation of class II major histocompatibility complex expression.* Journal of Experimental Medicine, 1991. **174**(4): p. 915-924.
125. Ding, L., et al., *IL-10 inhibits macrophage costimulatory activity by selectively inhibiting the up-regulation of B7 expression.* Journal of Immunology, 1993. **151**(3): p. 1224-1234.
126. Willems, F., et al., *Interleukin-10 inhibits B7 and intercellular adhesion molecule-1 expression on human monocytes.* European Journal of Immunology, 1994. **24**(4): p. 1007-1009.
127. Chang, C.H., M. Furue, and K. Tamaki, *B7-1 expression of Langerhans cells is up-regulated by proinflammatory cytokines, and is down-regulated by interferon-γ or by interleukin-10.* European Journal of Immunology, 1995. **25**(2): p. 394-398.

128. Tree, T.I.M., et al., *Naturally arising human CD4 T-cells that recognize islet autoantigens and secrete interleukin-10 regulate proinflammatory T-cell responses via linked suppression.* Diabetes, 2010. **59**(6): p. 1451-1460.
129. Gruarin, P., et al., *Eomesodermin controls a unique differentiation program in human IL-10 and IFN-γ coproducing regulatory T cells.* European Journal of Immunology, 2019. **49**(1): p. 96-111.
130. Magnani, C.F., et al., *Killing of myeloid APCs via HLA class I, CD2 and CD226 defines a novel mechanism of suppression by human Tr1 cells.* European Journal of Immunology, 2011. **41**(6): p. 1652-1662.
131. Meiler, F., et al., *In vivo switch to IL-10-secreting T regulatory cells in high dose allergen exposure.* Journal of Experimental Medicine, 2008. **205**(12): p. 2887-2898.
132. Chen, P.P., et al., *Alloantigen-specific type 1 regulatory T cells suppress through CTLA-4 and PD-1 pathways and persist long-term in patients.* Science Translational Medicine, 2021. **13**(617).
133. Facciotti, F., et al., *IL-10-producing forkhead box protein 3-negative regulatory T cells inhibit B-cell responses and are involved in systemic lupus erythematosus.* Journal of Allergy and Clinical Immunology, 2016. **137**(1): p. 318-321.e5.
134. Altin, J.A., C.C. Goodnow, and M.C. Cook, *IL-10 +CTLA-4 + Th2 inhibitory cells form in a Foxp3-independent, IL-2-dependent manner from Th2 effectors during chronic inflammation.* Journal of Immunology, 2012. **188**(11): p. 5478-5488.
135. Gabryšová, L., et al., *Negative feedback control of the autoimmune response through antigen-induced differentiation of IL-10-secreting Th1 cells.* Journal of Experimental Medicine, 2009. **206**(8): p. 1755-1767.
136. Uyeda, M.J., et al., *BHLHE40 Regulates IL-10 and IFN-gamma Production in T Cells but Does Not Interfere With Human Type 1 Regulatory T Cell Differentiation.* Front Immunol, 2021. **12**: p. 683680.
137. Huard, B., et al., *CD4/major histocompatibility complex class II interaction analyzed with CD4- and lymphocyte activation gene-3 (LAG-3)-Ig fusion proteins.* Eur J Immunol, 1995. **25**(9): p. 2718-21.
138. Bauché, D., et al., *LAG3 + Regulatory T Cells Restrain Interleukin-23-Producing CX3CR1 + Gut-Resident Macrophages during Group 3 Innate Lymphoid Cell-Driven Colitis.* Immunity, 2018. **49**(2): p. 342-352.e5.
139. Banerjee, H., et al., *Expression of Tim-3 drives phenotypic and functional changes in Treg cells in secondary lymphoid organs and the tumor microenvironment.* Cell Reports, 2021. **36**(11).
140. Ahlers, J., et al., *A Notch/STAT3-driven Blimp-1/c-Maf-dependent molecular switch induces IL-10 expression in human CD4+ T cells and is defective in Crohn´s disease patients.* Mucosal Immunology, 2022. **15**(3): p. 480-490.
141. Apetoh, L., et al., *The aryl hydrocarbon receptor interacts with c-Maf to promote the differentiation of type 1 regulatory T cells induced by IL-27.* Nature Immunology, 2010. **11**(9): p. 854-861.
142. Zhang, H., et al., *An IL-27-Driven Transcriptional Network Identifies Regulators of IL-10 Expression across T Helper Cell Subsets.* Cell Rep, 2020. **33**(8): p. 108433.
143. Freeborn, R.A., S. Strubbe, and M.G. Roncarolo, *Type 1 regulatory T cell-mediated tolerance in health and disease.* Front Immunol, 2022. **13**: p. 1032575.

144. Okamura, T., et al., *CD4+CD25-LAG3+ regulatory T cells controlled by the transcription factor Egr-2.* Proceedings of the National Academy of Sciences of the United States of America, 2009. **106**(33): p. 13974-13979.
145. Häringer, B., et al., *Identification and characterization of IL-10/IFN-γ-producing effector-like T cells with regulatory function in human blood.* Journal of Experimental Medicine, 2009. **206**(5): p. 1009-1017.
146. Veldman, C., et al., *Type I Regulatory T Cells Specific for Desmoglein 3 Are More Frequently Detected in Healthy Individuals than in Patients with Pemphigus Vulgaris.* Journal of Immunology, 2004. **172**(10): p. 6468-6475.
147. Li, D., et al., *Targeting self- and foreign antigens to dendritic cells via DC-ASGPR generates IL-10-producing suppressive CD4+ T cells.* Journal of Experimental Medicine, 2012. **209**(1): p. 109-121.
148. Kim, J.E., et al., *Lactobacillus pentosus modulates immune response by inducing IL-10 producing Tr1 cells.* Immune Network, 2019. **19**(6).
149. Maquet, C., et al., *Ly6Chi monocytes balance regulatory and cytotoxic CD4 T cell responses to control virus-induced immunopathology.* Science Immunology, 2022. **7**(73).
150. Gregori, S., et al., *Differentiation of type 1 T regulatory cells (Tr1) by tolerogenic DC-10 requires the IL-10-dependent ILT4/HLA-G pathway.* Blood, 2010. **116**(6): p. 935-944.
151. Mfarrej, B., et al., *Key role of macrophages in tolerance induction via T regulatory type 1 (Tr1) cells.* Clinical and Experimental Immunology, 2020. **201**(2): p. 222-230.
152. Wakkach, A., F. Cottrez, and H. Groux, *Differentiation of regulatory T cells 1 is induced by CD2 costimulation.* Journal of Immunology, 2001. **167**(6): p. 3107-3113.
153. Sutavani, R.V., et al., *CD55 costimulation induces differentiation of a discrete T regulatory type 1 cell population with a stable phenotype.* Journal of Immunology, 2013. **191**(12): p. 5895-5903.
154. Ito, T., et al., *Plasmacytoid dendritic cells prime IL-10-producing T regulatory cells by inducible costimulator ligand.* Journal of Experimental Medicine, 2007. **204**(1): p. 105-115.
155. Ding, Q., et al., *B7H1-Ig fusion protein activates the CD4+ IFN-γ receptor+ type 1 T regulatory subset through IFN-γ-secreting Th1 cells.* Journal of Immunology, 2006. **177**(6): p. 3606-3614.
156. Kemper, C., et al., *Activation of human CD4+ cells with CD3 and CD46 induces a T-regulatory cell 1 phenotype.* Nature, 2003. **421**(6921): p. 388-392.
157. Le Friec, G., et al., *The CD46-Jagged1 interaction is critical for human T H 1 immunity.* Nature Immunology, 2012. **13**(12): p. 1213-1221.
158. Choileain, S.N., et al., *TCR-stimulated changes in cell surface CD46 expression generate type 1 regulatory T cells.* Science Signaling, 2017. **10**(502).
159. Zhang, P., et al., *Eomesodermin promotes the development of type 1 regulatory T (TR1) cells.* Science Immunology, 2017. **2**(10).
160. Awasthi, A., et al., *A dominant function for interleukin 27 in generating interleukin 10-producing anti-inflammatory T cells.* Nature Immunology, 2007. **8**(12): p. 1380-1389.
161. Pot, C., et al., *Cutting edge: IL-27 induces the transcription factor c-Maf, cytokine IL-21, and the costimulatory receptor ICOS that coordinately act*

together to promote differentiation of IL-10-producing Tr1 cells. Journal of Immunology, 2009. **183**(2): p. 797-801.
162. Sumida, T.S., et al., *Type I interferon transcriptional network regulates expression of coinhibitory receptors in human T cells.* Nature Immunology, 2022. **23**(4): p. 632-642.
163. Bacchetta, R., et al., *Molecular and functional characterization of allogantigen specific anergic T cells suitable for cell therapy.* Haematologica, 2010. **95**(12): p. 2134-2143.
164. Kapur, S., et al., *Reliability of a simple non-invasive method for the evaluation of 5-HT2 receptors using [18F]-setoperone PET imaging.* Nucl Med Commun, 1997. **18**(5): p. 395-9.
165. Wang, P., et al., *IL-10 inhibits transcription of cytokine genes in human peripheral blood mononuclear cells.* J Immunol, 1994. **153**(2): p. 811-6.
166. Cassatella, M.A., et al., *Interleukin 10 (IL-10) inhibits the release of proinflammatory cytokines from human polymorphonuclear leukocytes. evidence for an autocrine role of tumor necrosis factor and IL-1γ in mediating the production of IL-8 triggered by lipopolysaccharide.* Journal of Experimental Medicine, 1993. **178**(6): p. 2207-2211.
167. Kane, M.M. and D.M. Mosser, *The role of IL-10 in promoting disease progression in Leishmaniasis.* Journal of Immunology, 2001. **166**(2): p. 1141-1147.
168. Murray, P.J. and R.A. Young, *Increased antimycobacterial immunity in interleukin-10-deficient mice.* Infection and Immunity, 1999. **67**(6): p. 3087-3095.
169. Deckert, M., et al., *Endogenous interleukin-10 is required for prevention of a hyperinflammatory intracerebral immune response in Listeria monocytogenes meningoencephalitis.* Infection and Immunity, 2001. **69**(7): p. 4561-4571.
170. Li, C., I. Corraliza, and J. Langhorne, *A defect in interleukin-10 leads to enhanced malarial disease in Plasmodium chabaudi chabaudi infection in mice.* Infection and Immunity, 1999. **67**(9): p. 4435-4442.
171. Saxena, A., et al., *Interleukin-10 paradox: A potent immunoregulatory cytokine that has been difficult to harness for immunotherapy.* Cytokine, 2015. **74**(1): p. 27-34.
172. Zdanov, A., *Structural analysis of cytokines comprising the IL-10 family.* Cytokine and Growth Factor Reviews, 2010. **21**(5): p. 325-330.
173. Windsor, W.T., et al., *Disulfide bond assignments and secondary structure analysis of human and murine interleukin 10.* Biochemistry, 1993. **32**(34): p. 8807-15.
174. Liu, Y., et al., *Expression cloning and characterization of a human IL-10 receptor.* J Immunol, 1994. **152**(4): p. 1821-9.
175. Tan, J.C., et al., *Characterization of interleukin-10 receptors on human and mouse cells.* Journal of Biological Chemistry, 1993. **268**(28): p. 21053-21059.
176. Yoon, S.I., et al., *Structure and mechanism of receptor sharing by the IL-10R2 common chain.* Structure, 2010. **18**(5): p. 638-648.
177. Kotenko, S.V., *The family of IL-10-related cytokines and their receptors: Related, but to what extent?* Cytokine and Growth Factor Reviews, 2002. **13**(3): p. 223-240.

178. Reineke, U., et al., *Evidence for conformationally different states of interleukin-10: binding of a neutralizing antibody enhances accessibility of a hidden epitope.* J Mol Recognit, 1999. **12**(4): p. 242-8.
179. Sung, I.Y., et al., *Conformational changes mediate interleukin-10 receptor 2 (IL-10R2) binding to IL-10 and assembly of the signaling complex.* Journal of Biological Chemistry, 2006. **281**(46): p. 35088-35096.
180. Wolk, K., et al., *Is there an interaction between interleukin-10 and interleukin-22?* Genes and Immunity, 2005. **6**(1): p. 8-18.
181. Wolk, K., et al., *IL-22 increases the innate immunity of tissues.* Immunity, 2004. **21**(2): p. 241-254.
182. Tan, J.C., et al., *Characterization of recombinant extracellular domain of human interleukin- 10 receptor.* Journal of Biological Chemistry, 1995. **270**(21): p. 12906-12911.
183. Moore, K.W., et al., *Interleukin-10 and the interleukin-10 receptor*, in *Annual Review of Immunology*. 2001. p. 683-765.
184. Riley, J.K., et al., *Interleukin-10 receptor signaling through the JAK-STAT pathway. Requirement for two distinct receptor-derived signals for anti-inflammatory action.* Journal of Biological Chemistry, 1999. **274**(23): p. 16513-16521.
185. Valle Oseguera, C.A. and J.V. Spencer, *cmvIL-10 stimulates the invasive potential of MDA-MB-231 breast cancer cells.* PLoS ONE, 2014. **9**(2).
186. Weber-Nordtt, R.M., et al., *Stat3 recruitment by two distinct ligand-induced, tyrosine- phosphorylated docking sites in the interleukin-10 receptor intracellular domain.* Journal of Biological Chemistry, 1996. **271**(44): p. 27954-27961.
187. Wehinger, J., et al., *IL-10 induces DNA binding activity of three STAT proteins (Stat1, Stat3, and Stat5) and their distinct combinatorial assembly in the promoters of selected genes.* FEBS Lett, 1996. **394**(3): p. 365-70.
188. Gemelli, C., et al., *MafB is a downstream target of the IL-10/STAT3 signaling pathway, involved in the regulation of macrophage de-activation.* Biochimica et Biophysica Acta - Molecular Cell Research, 2014. **1843**(5): p. 955-964.
189. Kotenko, S.V., et al., *Identification and functional characterization of a second chain of the interleukin-10 receptor complex.* EMBO Journal, 1997. **16**(19): p. 5894-5903.
190. Finbloom, D.S. and K.D. Winestock, *IL-10 induces the tyrosine phosphorylation of tyk2 and Jak1 and the differential assembly of STAT1α and STAT3 complexes in human T cells and monocytes.* Journal of Immunology, 1995. **155**(3): p. 1079-1090.
191. Herrero, C., et al., *Reprogramming of IL-10 Activity and Signaling by IFN-γ1.* Journal of Immunology, 2003. **171**(10): p. 5034-5041.
192. Bowman, T., et al., *STATs in oncogenesis.* Oncogene, 2000. **19**(21): p. 2474-2488.
193. Bromberg, J.F., et al., *Stat3 as an oncogene.* Cell, 1999. **98**(3): p. 295-303.
194. Rubin Grandis, J., et al., *Requirement of Stat3 but not Stat1 activation for epidermal growth factor receptor-mediated cell growth in vitro.* Journal of Clinical Investigation, 1998. **102**(7): p. 1385-1392.

195. Pajkrt, D., et al., *Attenuation of proinflammatory response by recombinant human IL-10 in human endotoxemia: effect of timing of recombinant human IL-10 administration.* J Immunol, 1997. **158**(8): p. 3971-7.
196. Avdiushko, R., et al., *IL-10 receptor dysfunction in macrophages during chronic inflammation.* J Leukoc Biol, 2001. **70**(4): p. 624-32.
197. Chomarat, P., et al., *Interferon γ inhibits interleukin 10 production by monocytes.* Journal of Experimental Medicine, 1993. **177**(2): p. 523-527.
198. Blanco, P., et al., *Dendritic cells and cytokines in human inflammatory and autoimmune diseases.* Cytokine and Growth Factor Reviews, 2008. **19**(1): p. 41-52.
199. Seki, S., et al., *Role of liver NK cells and peritoneal macrophages in gamma interferon and interleukin, 10 production in experimental bacterial peritonitis in mice.* Infection and Immunity, 1998. **66**(11): p. 5286-5294.
200. Gabryšová, L., et al., *The regulation of IL-10 expression*, in *Current Topics in Microbiology and Immunology*. 2014. p. 157-190.
201. Gazzinelli, R.T., et al., *Parasite-induced IL-12 stimulates early IFN-gamma synthesis and resistance during acute infection with Toxoplasma gondii.* J Immunol, 1994. **153**(6): p. 2533-43.
202. Geginat, J., F. Sallusto, and A. Lanzavecchia, *Cytokine-driven proliferation and differentiation of human naive, central memory, and effector memory CD4+ T cells.* Journal of Experimental Medicine, 2001. **194**(12): p. 1711-1719.
203. Lucas, M., et al., *ERK activation following macrophage FcγR ligation leads to chromatin modifications at the IL-10 locus.* Journal of Immunology, 2005. **175**(1): p. 469-477.
204. Powell, M.J., et al., *Posttranscriptional regulation of IL-10 gene expression through sequences in the 3'-untranslated region.* Journal of Immunology, 2000. **165**(1): p. 292-296.
205. Stoecklin, G., et al., *Genome-wide analysis identifies interleukin-10 mRNA as target of tristetraprolin.* Journal of Biological Chemistry, 2008. **283**(17): p. 11689-11699.
206. Curran, M.A., et al., *Systemic 4-1BB activation induces a novel T cell phenotype driven by high expression of eomesodermin.* Journal of Experimental Medicine, 2013. **210**(4): p. 743-755.
207. Dibra, D., J.J. Cutrera, and S. Li, *Coordination between TLR9 signaling in macrophages and CD3 signaling in T cells induces robust expression of IL-30.* Journal of Immunology, 2012. **188**(8): p. 3709-3715.
208. Van Seventer, J.M., T. Nagai, and G.A. Van Seventer, *Interferon-β differentially regulates expression of the IL-12 family members p35, p40, p19 and EBI3 in activated human dendritic cells.* Journal of Neuroimmunology, 2002. **133**(1-2): p. 60-71.
209. Remoli, M.E., et al., *IFN-beta modulates the response to TLR stimulation in human DC: involvement of IFN regulatory factor-1 (IRF-1) in IL-27 gene expression.* Eur J Immunol, 2007. **37**(12): p. 3499-508.
210. Molle, C., et al., *IL-27 synthesis induced by TLR ligation critically depends on IFN regulatory factor 3.* Journal of Immunology, 2007. **178**(12): p. 7607-7615.
211. Liu, J., X. Guan, and X. Ma, *Regulation of IL-27 p28 gene expression in macrophages through MyD88- and interferon-γ-mediated pathways.* Journal of Experimental Medicine, 2007. **204**(1): p. 141-152.

212. Pirhonen, J., et al., *IFN-alpha regulates Toll-like receptor-mediated IL-27 gene expression in human macrophages.* J Leukoc Biol, 2007. **82**(5): p. 1185-92.
213. Hall, A.O., J.S. Silver, and C.A. Hunter, *The Immunobiology of IL-27*, in *Advances in Immunology*. 2012. p. 1-44.
214. Hall, A., et al., *The Cytokines Interleukin 27 and Interferon-γ Promote Distinct Treg Cell Populations Required to Limit Infection-Induced Pathology.* Immunity, 2012. **37**(3): p. 511-523.
215. Artis, D., et al., *The IL-27 receptor (WSX-1) is an inhibitor of innate and adaptive elements of type 2 immunity.* Journal of Immunology, 2004. **173**(9): p. 5626-5634.
216. Villarino, A., et al., *The IL-27R (WSX-1) is required to suppress T cell hyperactivity during infection.* Immunity, 2003. **19**(5): p. 645-655.
217. Chihara, N., et al., *Induction and transcriptional regulation of the co-inhibitory gene module in T cells.* Nature, 2018. **558**(7710): p. 454-459.
218. DeLong, J.H., et al., *IL-27 and TCR stimulation promote T cell expression of multiple inhibitory receptors.* Immunohorizons, 2019. **3**(1): p. 13-25.
219. Batten, M., et al., *Cutting edge: IL-27 is a potent inducer of IL-10 but not FoxP3 in murine T cells.* Journal of Immunology, 2008. **180**(5): p. 2752-2756.
220. Roncarolo, M.G., et al., *Autoreactive T cell clones specific for class I and class II HLA antigens isolated from a human chimera.* J Exp Med, 1988. **167**(5): p. 1523-34.
221. Fitzgerald, D.C., et al., *Suppression of autoimmune inflammation of the central nervous system by interleukin 10 secreted by interleukin 27-stimulated T cells.* Nature Immunology, 2007. **8**(12): p. 1372-1379.
222. Stumhofer, J.S., et al., *Interleukin 27 negatively regulates the development of interleukin 17-producing T helper cells during chronic inflammation of the central nervous system.* Nat Immunol, 2006. **7**(9): p. 937-45.
223. Stumhofer, J.S., et al., *Interleukins 27 and 6 induce STAT3-mediated T cell production of interleukin 10.* Nature Immunology, 2007. **8**(12): p. 1363-1371.
224. Terai, M., et al., *Interleukin 6 mediates production of interleukin 10 in metastatic melanoma.* Cancer Immunology, Immunotherapy, 2012. **61**(2): p. 145-155.
225. Maynard, C.L., et al., *Regulatory T cells expressing interleukin 10 develop from Foxp3+ and Foxp3- precursor cells in the absence of interleukin 10.* Nature Immunology, 2007. **8**(9): p. 931-941.
226. Taylor, A., et al., *Mechanisms of immune suppression by interleukin-10 and transforming growth factor-beta: the role of T regulatory cells.* Immunology, 2006. **117**(4): p. 433-42.
227. McGeachy, M.J., et al., *TGF-β and IL-6 drive the production of IL-17 and IL-10 by T cells and restrain TH-17 cell-mediated pathology.* Nature Immunology, 2007. **8**(12): p. 1390-1397.
228. Neumann, C., et al., *Role of blimp-1 in programing th effector cells into IL-10 producers.* Journal of Experimental Medicine, 2014. **211**(9): p. 1807-1819.
229. Koppelman, B., et al., *Interleukin-10 down-regulates MHC class II αβ peptide complexes at the plasma membrane of monocytes by affecting arrival and recycling.* Immunity, 1997. **7**(6): p. 861-871.
230. D'andrea, A., et al., *Interleukin 10 (IL-10) Inhibits human lymphocyte interferon γ-production by suppressing natural killer cell stimulatory factor/IL-12 synthesis*

in accessory cells. Journal of Experimental Medicine, 1993. **178**(3): p. 1041-1048.
231. Ito, S., et al., *Interleukin-10 inhibits expression of both interferon α- and interferon γ-induced genes by suppressing tyrosine phosphorylation of STAT1.* Blood, 1999. **93**(5): p. 1456-1463.
232. Joss, A., et al., *IL-10 directly acts on T cells by specifically altering the CD28 co-stimulation pathway.* Eur J Immunol, 2000. **30**(6): p. 1683-90.
233. Rutz, S. and W. Ouyang, *Regulation of interleukin-10 expression*, in *Advances in Experimental Medicine and Biology*. 2016. p. 89-116.
234. Yamaoka, K., et al., *Selective DNA-binding activity of interleukin-10-stimulated STAT molecules in human monocytes.* Journal of Interferon and Cytokine Research, 1999. **19**(6): p. 679-685.
235. Dagvadorj, J., et al., *Interleukin-10 inhibits tumor necrosis factor-alpha production in lipopolysaccharide-stimulated RAW 264.7 cells through reduced MyD88 expression.* Innate Immun, 2008. **14**(2): p. 109-15.
236. Chang, J., S.L. Kunkel, and C.H. Chang, *Negative regulation of MyD88-dependent signaling by IL-10 in dendritic cells.* Proceedings of the National Academy of Sciences of the United States of America, 2009. **106**(43): p. 18327-18332.
237. Abrams, J., et al., *Interleukin 10(IL-10) inhibits cytokine synthesis by human monocytes: An autoregulatory role of IL-10 produced by monocytes.* Journal of Experimental Medicine, 1991. **174**(5): p. 1209-1220.
238. Go, N.F., et al., *Interleukin 10, a novel B cell stimulatory factor: Unresponsiveness of X chromosome-linked immunodeficiency B cells.* Journal of Experimental Medicine, 1990. **172**(6): p. 1625-1631.
239. Llorente, L., et al., *Role of interleukin 10 in the B lymphocyte hyperactivity and autoantibody production of human systemic lupus erythematosus.* Journal of Experimental Medicine, 1995. **181**(3): p. 839-844.
240. Ragheb, S., et al., *Multiple sclerosis: BAFF and CXCL13 in cerebrospinal fluid.* Mult Scler, 2011. **17**(7): p. 819-29.
241. Groux, H., et al., *Inhibitory and stimulatory effects of IL-10 on human CD8+ T cells.* J Immunol, 1998. **160**(7): p. 3188-93.
242. Groux, H., et al., *Interleukin-10 induces a long-term antigen-specific anergic state in human CD4+ T cells.* Journal of Experimental Medicine, 1996. **184**(1): p. 19-29.
243. Schottelius, A.J.G., et al., *Interleukin-10 signaling blocks inhibitor of κB kinase activity and nuclear factor κB DNA binding.* Journal of Biological Chemistry, 1999. **274**(45): p. 31868-31874.
244. Livolsi, A., et al., *Tyrosine phosphorylation-dependent activation of NF-kappa B. Requirement for p56 LCK and ZAP-70 protein tyrosine kinases.* Eur J Biochem, 2001. **268**(5): p. 1508-15.
245. Schuetze, N., et al., *IL-12 family members: Differential kinetics of their TLR4-mediated induction by Salmonella Enteritidis and the impact of IL-10 in bone marrow-derived macrophages.* International Immunology, 2005. **17**(5): p. 649-659.
246. D'Andrea, A., et al., *Stimulatory and inhibitory effects of interleukin (il)-4 and id13 on the production of cytokines by human peripheral blood mononuclear*

cells: Priming for id12 and tumor necrosis factor α production. Journal of Experimental Medicine, 1995. **181**(2): p. 537-546.
247. Kamanaka, M., et al., *Memory/effector (CD45RBlo) CD4 T cells are controlled directly by IL-10 and cause IL-22-dependent intestinal pathology.* Journal of Experimental Medicine, 2011. **208**(5): p. 1027-1040.
248. Huber, S., et al., *Th17 Cells Express Interleukin-10 Receptor and Are Controlled by Foxp3- and Foxp3+ Regulatory CD4+ T Cells in an Interleukin-10-Dependent Manner.* Immunity, 2011. **34**(4): p. 554-565.
249. Coomes, S.M., et al., *CD4 + Th2 cells are directly regulated by IL-10 during allergic airway inflammation.* Mucosal Immunology, 2017. **10**(1): p. 150-161.
250. Chaudhry, A., et al., *Interleukin-10 Signaling in Regulatory T Cells Is Required for Suppression of Th17 Cell-Mediated Inflammation.* Immunity, 2011. **34**(4): p. 566-578.
251. Turovskaya, O., et al., *Interleukin 10 acts on regulatory t cells to maintain expression of the transcription factor foxp3 and suppressive function in mice with colitis.* Nature Immunology, 2009. **10**(11): p. 1178-1184.
252. Chen, W.F. and A. Zlotnik, *IL-10: a novel cytotoxic T cell differentiation factor.* J Immunol, 1991. **147**(2): p. 528-34.
253. Kühn, R., et al., *Interleukin-10-deficient mice develop chronic enterocolitis.* Cell, 1993. **75**(2): p. 263-274.
254. Shim, J.O., *Recent Advance in Very Early Onset Inflammatory Bowel Disease.* Pediatr Gastroenterol Hepatol Nutr, 2019. **22**(1): p. 41-49.
255. Spencer, S.D., et al., *The orphan receptor CRF2-4 is an essential subunit of the interleukin 10 receptor.* Journal of Experimental Medicine, 1998. **187**(4): p. 571-578.
256. Denning, T.L., et al., *Lamina propria macrophages and dendritic cells differentially induce regulatory and interleukin 17-producing T cell responses.* Nature Immunology, 2007. **8**(10): p. 1086-1094.
257. Hadis, U., et al., *Intestinal Tolerance Requires Gut Homing and Expansion of FoxP3+ Regulatory T Cells in the Lamina Propria.* Immunity, 2011. **34**(2): p. 237-246.
258. Murai, M., et al., *Interleukin 10 acts on regulatory T cells to maintain expression of the transcription factor Foxp3 and suppressive function in mice with colitis.* Nat Immunol, 2009. **10**(11): p. 1178-84.
259. Hoshi, N., et al., *MyD88 signalling in colonic mononuclear phagocytes drives colitis in IL-10-deficient mice.* Nature Communications, 2012. **3**.
260. Rakoff-Nahoum, S., L. Hao, and R. Medzhitov, *Role of toll-like receptors in spontaneous commensal-dependent colitis.* Immunity, 2006. **25**(2): p. 319-29.
261. Siewe, L., et al., *Interleukin-10 derived from macrophages and/or neutrophils regulates the inflammatory response to LPS but not the response to CpG DNA.* Eur J Immunol, 2006. **36**(12): p. 3248-55.
262. Zigmond, E., et al., *Macrophage-restricted interleukin-10 receptor deficiency, but not IL-10 deficiency, causes severe spontaneous colitis.* Immunity, 2014. **40**(5): p. 720-733.
263. Rubtsov, Y.P., et al., *Regulatory T Cell-Derived Interleukin-10 Limits Inflammation at Environmental Interfaces.* Immunity, 2008. **28**(4): p. 546-558.
264. McBerry, C., et al., *PD-1 modulates steady-state and infection-induced IL-10 production in vivo.* European Journal of Immunology, 2014. **44**(2): p. 469-479.

265. Belkaid, Y., et al., *The role of interleukin (IL)-10 in the persistence of Leishmania major in the skin after healing and the therapeutic potential of anti-IL-10 receptor antibody for sterile cure.* Journal of Experimental Medicine, 2001. **194**(10): p. 1497-1506.
266. Freitas do Rosario, A.P., et al., *IL-27 promotes IL-10 production by effector Th1 CD4+ T cells: a critical mechanism for protection from severe immunopathology during malaria infection.* J Immunol, 2012. **188**(3): p. 1178-90.
267. Burkhart, C., et al., *Peptide-induced T cell regulation of experimental autoimmune encephalomyelitis: A role for IL-10.* International Immunology, 1999. **11**(10): p. 1625-1634.
268. Liu, G.Y., et al., *Low avidity recognition of self-antigen by T cells permits escape from central tolerance.* Immunity, 1995. **3**(4): p. 407-415.
269. Sundstedt, A., et al., *Role for IL-10 in suppression mediated by peptide-induced regulatory T cells in vivo.* Journal of Immunology, 2003. **170**(3): p. 1240-1248.
270. Gabryšová, L. and D.C. Wraith, *Antigenic strength controls the generation of antigen-specific IL-10-secreting T regulatory cells.* European Journal of Immunology, 2010. **40**(5): p. 1386-1395.
271. Nicolson, K.S., et al., *Antigen-induced IL-10+ regulatory T cells are independent of CD25+ regulatory cells for their growth, differentiation, and function.* Journal of Immunology, 2006. **176**(9): p. 5329-5337.
272. Metzler, B. and D.C. Wraith, *Inhibition of experimental autoimmune encephalomyelitis by inhalation but not oral administration of the encephalitogenic peptide: influence of MHC binding affinity.* Int Immunol, 1993. **5**(9): p. 1159-65.
273. Fairchild, P.J., et al., *Modulation of the immune response with T-cell epitopes: the ultimate goal for specific immunotherapy of autoimmune disease.* Immunology, 1994. **81**(4): p. 487-96.
274. Anderson, P.O., et al., *IL-2 overcomes the unresponsiveness but fails to reverse the regulatory function of antigen-induced T regulatory cells.* J Immunol, 2005. **174**(1): p. 310-9.
275. Vieira, P.L., et al., *IL-10-Secreting Regulatory T Cells Do Not Express Foxp3 but Have Comparable Regulatory Function to Naturally Occurring CD4+CD25 + Regulatory T Cells.* Journal of Immunology, 2004. **172**(10): p. 5986-5993.
276. Burton, B.R., et al., *Sequential transcriptional changes dictate safe and effective antigen-specific immunotherapy.* Nat Commun, 2014. **5**: p. 4741.
277. Thrower, S.L., et al., *Proinsulin peptide immunotherapy in type 1 diabetes: Report of a first-in-man Phase I safety study.* Clinical and Experimental Immunology, 2009. **155**(2): p. 156-165.
278. Fousteri, G., et al., *Subcutaneous insulin B:9-23/IFA immunisation induces Tregs that control late-stage prediabetes in NOD mice through IL-10 and IFNγ.* Diabetologia, 2010. **53**(9): p. 1958-1970.
279. Campbell, J.D., et al., *Peptide immunotherapy in allergic asthma generates IL-10-dependent immunological tolerance associated with linked epitope suppression.* Journal of Experimental Medicine, 2009. **206**(7): p. 1535-1547.
280. Tarzi, M., et al., *Induction of interleukin-10 and suppressor of cytokine signalling-3 gene expression following peptide immunotherapy.* Clin Exp Allergy, 2006. **36**(4): p. 465-74.

281. Giovarelli, M., et al., *Local release of IL-10 by transfected mouse mammary adenocarcinoma cells does not suppress but enhances antitumor reaction and elicits a strong cytotoxic lymphocyte and antibody-dependent immune memory.* Journal of Immunology, 1995. **155**(6): p. 3112-3123.
282. Emmerich, J., et al., *IL-10 directly activates and expands tumor-resident CD8+ T cells without De Novo infiltration from secondary lymphoid organs.* Cancer Research, 2012. **72**(14): p. 3570-3581.
283. Naing, A., et al., *PEGylated IL-10 (Pegilodecakin) Induces Systemic Immune Activation, CD8+ T Cell Invigoration and Polyclonal T Cell Expansion in Cancer Patients.* Cancer Cell, 2018. **34**(5): p. 775-791.e3.
284. Kundu, N., et al., *Antimetastatic and antitumor activities of interleukin 10 in a murine model of breast cancer.* J Natl Cancer Inst, 1996. **88**(8): p. 536-41.
285. Huang, S., et al., *Interleukin 10 suppresses tumor growth and metastasis of human melanoma cells: potential inhibition of angiogenesis.* Clin Cancer Res, 1996. **2**(12): p. 1969-79.
286. Richter, G., et al., *Interleukin 10 transfected into Chinese hamster ovary cells prevents tumor growth and macrophage infiltration.* Cancer Res, 1993. **53**(18): p. 4134-7.
287. Naing, A., et al., *Pegilodecakin combined with pembrolizumab or nivolumab for patients with advanced solid tumours (IVY): a multicentre, multicohort, open-label, phase 1b trial.* The Lancet Oncology, 2019. **20**(11): p. 1544-1555.
288. Carlino, M.S., et al., *Outcomes by line of therapy and programmed death ligand 1 expression in patients with advanced melanoma treated with pembrolizumab or ipilimumab in KEYNOTE-006: A randomised clinical trial.* European Journal of Cancer, 2018. **101**: p. 236-243.
289. Motzer, R.J., et al., *Nivolumab versus everolimus in advanced renal-cell carcinoma.* New England Journal of Medicine, 2015. **373**(19): p. 1803-1813.
290. Naing, A., et al., *Safety, antitumor activity, and immune activation of pegylated recombinant human interleukin-10 (AM0010) in patients with advanced solid tumors.* Journal of Clinical Oncology, 2016. **34**(29): p. 3562-3569.
291. Lauw, F.N., et al., *Proinflammatory effects of IL-10 during human endotoxemia.* Journal of Immunology, 2000. **165**(5): p. 2783-2789.
292. Tilg, H., et al., *Treatment of Crohn's disease with recombinant human interleukin 10 induces the proinflammatory cytokine interferon γ.* Gut, 2002. **50**(2): p. 191-195.
293. Asadullah, K., et al., *IL-10 is a key cytokine in psoriasis. Proof of principle by IL-10 therapy: a new therapeutic approach.* J Clin Invest, 1998. **101**(4): p. 783-94.
294. Berg, D.J., et al., *Enterocolitis and colon cancer in interleukin-10-deficient mice are associated with aberrant cytokine production and CD4+ Th1-like responses.* Journal of Clinical Investigation, 1996. **98**(4): p. 1010-1020.
295. Neven, B., et al., *A Mendelian predisposition to B-cell lymphoma caused by IL-10R deficiency.* Blood, 2013. **122**(23): p. 3713-3722.
296. Krüger-Krasagakes, S., et al., *Expression of interleukin 10 in human melanoma.* British Journal of Cancer, 1994. **70**(6): p. 1182-1185.
297. Steinbrink, K., et al., *Interleukin-10-treated human dendritic cells induce a melanoma-antigen- specific anergy in CD8+ T cells resulting in a failure to lyse tumor cells.* Blood, 1999. **93**(5): p. 1634-1642.

298. Chen, Q., et al., *Production of IL-10 by melanoma cells: examination of its role in immunosuppression mediated by melanoma.* Int J Cancer, 1994. **56**(5): p. 755-60.
299. Sato, T., et al., *Interleukin 10 in the tumor microenvironment: A target for anticancer immunotherapy.* Immunologic Research, 2011. **51**(2-3): p. 170-182.
300. Guo, Y., et al., *Metabolic reprogramming of terminally exhausted CD8(+) T cells by IL-10 enhances anti-tumor immunity.* Nat Immunol, 2021. **22**(6): p. 746-756.
301. Mumm, J.B., et al., *IL-10 Elicits IFNγ-Dependent tumor immune surveillance.* Cancer Cell, 2011. **20**(6): p. 781-796.
302. Qiao, J., et al., *Targeting Tumors with IL-10 Prevents Dendritic Cell-Mediated CD8+ T Cell Apoptosis.* Cancer Cell, 2019. **35**(6): p. 901-915.e4.
303. Tannir, N.M., et al., *Pegilodecakin as monotherapy or in combination with anti-PD-1 or tyrosine kinase inhibitor in heavily pretreated patients with advanced renal cell carcinoma: Final results of cohorts A, G, H and I of IVY Phase I study.* Int J Cancer, 2021. **149**(2): p. 403-408.
304. Fujii, S.I., et al., *Interleukin-10 promotes the maintenance of antitumor CD8+ T-cell effector function in situ.* Blood, 2001. **98**(7): p. 2143-2151.
305. Tanikawa, T., et al., *Interleukin-10 ablation promotes tumor development, growth, and metastasis.* Cancer Research, 2012. **72**(2): p. 420-429.
306. Scharping, N.E., et al., *Mitochondrial stress induced by continuous stimulation under hypoxia rapidly drives T cell exhaustion.* Nature Immunology, 2021. **22**(2): p. 205-215.
307. Yu, Y.R., et al., *Disturbed mitochondrial dynamics in CD8+ TILs reinforce T cell exhaustion.* Nature Immunology, 2020. **21**(12): p. 1540-1551.
308. Vardhana, S.A., et al., *Impaired mitochondrial oxidative phosphorylation limits the self-renewal of T cells exposed to persistent antigen.* Nature Immunology, 2020. **21**(9): p. 1022-1033.
309. Peng, W., et al., *PD-1 blockade enhances T-cell migration to tumors by elevating IFN-γ inducible chemokines.* Cancer Research, 2012. **72**(20): p. 5209-5218.
310. Shi, L.Z., et al., *Interdependent IL-7 and IFN-γ signalling in T-cell controls tumour eradication by combined α-CTLA-4+α-PD-1 therapy.* Nature Communications, 2016. **7**.
311. Dong, H., et al., *Tumor-associated B7-H1 promotes T-cell apoptosis: A potential mechanism of immune evasion.* Nature Medicine, 2002. **8**(8): p. 793-800.
312. Rosenberg, S.A. and M.E. Dudley, *Adoptive cell therapy for the treatment of patients with metastatic melanoma.* Current Opinion in Immunology, 2009. **21**(2): p. 233-240.
313. Tumeh, P.C., et al., *PD-1 blockade induces responses by inhibiting adaptive immune resistance.* Nature, 2014. **515**(7528): p. 568-571.
314. Apetoh, L., et al., *Consensus nomenclature for CD8+ T cell phenotypes in cancer.* OncoImmunology, 2015. **4**(4).
315. Spigel, D., et al., *Randomized Phase 2 Studies of Checkpoint Inhibitors Alone or in Combination With Pegilodecakin in Patients With Metastatic NSCLC (CYPRESS 1 and CYPRESS 2).* J Thorac Oncol, 2021. **16**(2): p. 327-333.
316. Liu, Y.W., et al., *Functional cooperation of simian virus 40 promoter factor 1 and CCAAT/enhancer-binding protein β and δ in lipopolysaccharide-induced gene*

activation of IL-10 in mouse macrophages. Journal of Immunology, 2003. **171**(2): p. 821-828.
317. Perry, J.A., et al., *PD-L1-PD-1 interactions limit effector regulatory T cell populations at homeostasis and during infection.* Nat Immunol, 2022.
318. Macian, F., *NFAT proteins: key regulators of T-cell development and function.* Nat Rev Immunol, 2005. **5**(6): p. 472-84.
319. Im, S.H., et al., *Chromatin-level regulation of the IL10 gene in T cells.* Journal of Biological Chemistry, 2004. **279**(45): p. 46818-46825.
320. Saraiva, M., et al., *Interleukin-10 Production by Th1 Cells Requires Interleukin-12-Induced STAT4 Transcription Factor and ERK MAP Kinase Activation by High Antigen Dose.* Immunity, 2009. **31**(2): p. 209-219.
321. Trandem, K., et al., *Highly activated cytotoxic CD8 T cells express protective IL-10 at the peak of coronavirus-induced encephalitis.* J Immunol, 2011. **186**(6): p. 3642-52.
322. Koh, B., et al., *Etv5 regulates il-10 production in th cells.* Journal of Immunology, 2017. **198**(5): p. 2165-2171.
323. Ahyi, A.N.N., et al., *IFN regulatory factor 4 regulates the expression of a subset of Th2 cytokines.* Journal of Immunology, 2009. **183**(3): p. 1598-1606.
324. Lee, C.G., et al., *A distal cis-regulatory element, CNS-9, controls NFAT1 and IRF4-mediated IL-10 gene activation in T helper cells.* Molecular Immunology, 2009. **46**(4): p. 613-621.
325. Elliot, T.A.E., et al., *Antigen and checkpoint receptor engagement recalibrates T cell receptor signal strength.* Immunity, 2021. **54**(11): p. 2481-2496 e6.
326. Bending, D., et al., *A timer for analyzing temporally dynamic changes in transcription during differentiation in vivo.* J Cell Biol, 2018. **217**(8): p. 2931-2950.
327. Price, A.E., et al., *Marking and quantifying IL-17A-producing cells in vivo.* PLoS One, 2012. **7**(6): p. e39750.
328. Kamanaka, M., et al., *Expression of interleukin-10 in intestinal lymphocytes detected by an interleukin-10 reporter knockin tiger mouse.* Immunity, 2006. **25**(6): p. 941-52.
329. Subach, F.V., et al., *Monomeric fluorescent timers that change color from blue to red report on cellular trafficking.* Nature Chemical Biology, 2009. **5**(2): p. 118-126.
330. Tsushima, F., et al., *Preferential contribution of B7-H1 to programmed death-1-mediated regulation of hapten-specific allergic inflammatory responses.* Eur J Immunol, 2003. **33**(10): p. 2773-82.
331. Love, M.I., W. Huber, and S. Anders, *Moderated estimation of fold change and dispersion for RNA-seq data with DESeq2.* Genome Biol, 2014. **15**(12): p. 550.
332. Anderton, S.M., et al., *Fine specificity of the myelin-reactive T cell repertoire: implications for TCR antagonism in autoimmunity.* J Immunol, 1998. **161**(7): p. 3357-64.
333. Bevington, S.L., et al., *Chromatin Priming Renders T Cell Tolerance-Associated Genes Sensitive to Activation below the Signaling Threshold for Immune Response Genes.* Cell Reports, 2020. **31**(10).
334. Oh, H. and S. Ghosh, *NF-κB: Roles and regulation in different CD4+ T-cell subsets.* Immunological Reviews, 2013. **252**(1): p. 41-51.

335. Sacchetti, A., et al., *Efficient GFP mutations profoundly affect mRNA transcription and translation rates.* FEBS Letters, 2001. **492**(1-2): p. 151-155.
336. Jennings, E., et al., *Nr4a1 and Nr4a3 Reporter Mice Are Differentially Sensitive to T Cell Receptor Signal Strength and Duration.* Cell Rep, 2020. **33**(5): p. 108328.
337. Khmelinskii, A., et al., *Tandem fluorescent protein timers for in vivo analysis of protein dynamics.* Nature Biotechnology, 2012. **30**(7): p. 708-714.
338. Aidinis, V., et al., *The RAG1 homeodomain recruits HMG1 and HMG2 to facilitate recombination signal sequence binding and to enhance the intrinsic DNA-bending activity of RAG1-RAG2.* Mol Cell Biol, 1999. **19**(10): p. 6532-42.
339. Chen, K., et al., *HMGB2 orchestrates mitotic clonal expansion by binding to the promoter of C/EBPbeta to facilitate adipogenesis.* Cell Death Dis, 2021. **12**(7): p. 666.
340. Cardone, J., et al., *Complement regulator CD46 temporally regulates cytokine production by conventional and unconventional T cells.* Nature Immunology, 2010. **11**(9): p. 862-871.
341. Lönnberg, T., et al., *Single-cell RNA-seq and computational analysis using temporal mixture modeling resolves TH1/TFH fate bifurcation in malaria.* Science Immunology, 2017. **2**(9).
342. Eberl, G., et al., *Innate lymphoid cells: A new paradigm in immunology.* Science, 2015. **348**(6237).
343. Schroder, K., et al., *Interferon-γ: An overview of signals, mechanisms and functions.* Journal of Leukocyte Biology, 2004. **75**(2): p. 163-189.
344. Frucht, D.M., et al., *IFN-γ production by antigen-presenting cells: Mechanisms emerge.* Trends in Immunology, 2001. **22**(10): p. 556-560.
345. Nathan, C.F., et al., *Identification of interferon-γ, as the lymphokine that activates human macrophage oxidative metabolism and antimicrobial activity.* Journal of Experimental Medicine, 1983. **158**(3): p. 670-689.
346. Murray, H.W., G.L. Spitalny, and C.F. Nathan, *Activation of mouse peritoneal macrophages in vitro and in vivo by interferon-γ.* Journal of Immunology, 1985. **134**(3): p. 1619-1622.
347. Young, H.A. and K.J. Hardy, *Role of interferon-γ in immune cell regulation.* Journal of Leukocyte Biology, 1995. **58**(4): p. 373-381.
348. Dunn, G.P., C.M. Koebel, and R.D. Schreiber, *Interferons, immunity and cancer immunoediting.* Nature Reviews Immunology, 2006. **6**(11): p. 836-848.
349. Jürgens, B., et al., *Interferon-γ-triggered indoleamine 2,3-dioxygenase competence in human monocyte-derived dendritic cells induces regulatory activity in allogeneic T cells.* Blood, 2009. **114**(15): p. 3235-3243.
350. Munn, D.H., et al., *GCN2 kinase in T cells mediates proliferative arrest and anergy induction in response to indoleamine 2,3-dioxygenase.* Immunity, 2005. **22**(5): p. 633-642.
351. Cobbold, S.P., et al., *Infectious tolerance via the consumption of essential amino acids and mTOR signaling.* Proceedings of the National Academy of Sciences of the United States of America, 2009. **106**(29): p. 12055-12060.
352. Li, Q., et al., *Tolerogenic phenotype of IFN-γ-induced IDO+ dendritic cells is maintained via an autocrine IDO-kynurenine/ AhR-IDO loop.* Journal of Immunology, 2016. **197**(3): p. 962-970.

353. Nguyen, N.T., et al., *Aryl hydrocarbon receptor negatively regulates dendritic cell immunogenicity via a kynurenine-dependent mechanism.* Proceedings of the National Academy of Sciences of the United States of America, 2010. **107**(46): p. 19961-19966.
354. Švajger, U., N. Obermajer, and M. Jeras, *IFN-γ-rich environment programs dendritic cells toward silencing of cytotoxic immune responses.* Journal of Leukocyte Biology, 2014. **95**(1): p. 33-46.
355. Xiao, B.G., et al., *Therapeutic potential of IFN-γ-modified dendritic cells in acute and chronic experimental allergic encephalomyelitis.* International Immunology, 2004. **16**(1): p. 13-22.
356. Sawitzki, B., et al., *IFN-γ production by alloantigen-reactive regulatory T cells is important for their regulatory function in vivo.* Journal of Experimental Medicine, 2005. **201**(12): p. 1925-1935.
357. Daniel, V., et al., *Observational support for an immunoregulatory role of CD3 +CD4+CD25+IFN-γ+ blood lymphocytes in kidney transplant recipients with good long-term graft outcome.* Transplant International, 2008. **21**(7): p. 646-660.
358. Naves, R., et al., *The interdependent, overlapping, and differential roles of type i and II IFNs in the pathogenesis of experimental autoimmune encephalomyelitis.* Journal of Immunology, 2013. **191**(6): p. 2967-2977.
359. Furlan, R., et al., *Intrathecal delivery of IFN-γ protects C57BL/6 mice from chronic-progressive experimental autoimmune encephalomyelitis by increasing apoptosis of central nervous system-infiltrating lymphocytes.* Journal of Immunology, 2001. **167**(3): p. 1821-1829.
360. Billiau, A., et al., *Enhancement of experimental allergic encephalomyelitis in mice by antibodies against IFN-γ.* Journal of Immunology, 1988. **140**(5): p. 1506-1510.
361. Heremans, H., et al., *Chronic relapsing experimental autoimmune encephalomyelitis (CREAE) in mice: Enhancement by monoclonal antibodies against interferon-γ.* European Journal of Immunology, 1996. **26**(10): p. 2393-2398.
362. Berghmans, N., et al., *Interferon-γ orchestrates the number and function of Th17 cells in experimental autoimmune encephalomyelitis.* Journal of Interferon and Cytokine Research, 2011. **31**(7): p. 575-587.
363. Rajaiah, R., et al., *Interleukin-27 and interferon-γ are involved in regulation of autoimmune arthritis.* Journal of Biological Chemistry, 2011. **286**(4): p. 2817-2825.
364. Murugaiyan, G., A. Mittal, and H.L. Weiner, *Identification of an IL-27/osteopontin axis in dendritic cells and its modulation by IFN-γ limits IL-17-mediated autoimmune inflammation.* Proceedings of the National Academy of Sciences of the United States of America, 2010. **107**(25): p. 11495-11500.
365. Chong, W.P., et al., *NK-DC crosstalk controls the autopathogenic Th17 response through an innate IFN-γ-IL-27 axis.* Journal of Experimental Medicine, 2015. **212**(10): p. 1739-1752.
366. Wang, H., et al., *IL-27 induces the differentiation of Tr1-like cells from human naive CD4+ T cells via the phosphorylation of STAT1 and STAT3.* Immunol Lett, 2011. **136**(1): p. 21-8.

367. Neufert, C., et al., *IL-27 controls the development of inducible regulatory T cells and Th17 cells via differential effects on STAT1.* Eur J Immunol, 2007. **37**(7): p. 1809-16.
368. Villarino, A.V., et al., *IL-27 limits IL-2 production during Th1 differentiation.* Journal of Immunology, 2006. **176**(1): p. 237-247.
369. Murugaiyan, G., et al., *IL-27 is a key regulator of IL-10 and IL-17 production by human CD4 + T cells.* Journal of Immunology, 2009. **183**(4): p. 2435-2443.
370. Zander, R.A., et al., *PD-1 Co-inhibitory and OX40 Co-stimulatory Crosstalk Regulates Helper T Cell Differentiation and Anti-Plasmodium Humoral Immunity.* Cell Host Microbe, 2015. **17**(5): p. 628-41.
371. Witsch, E.J., et al., *ICOS and CD28 reversely regulate IL-10 on re-activation of human effector T cells with mature dendritic cells.* Eur J Immunol, 2002. **32**(9): p. 2680-6.
372. Lal, N., et al., *An immunogenomic stratification of colorectal cancer: Implications for development of targeted immunotherapy.* Oncoimmunology, 2015. **4**(3): p. e976052.
373. Dennis, K.L., et al., *Current status of interleukin-10 and regulatory T-cells in cancer.* Current Opinion in Oncology, 2013. **25**(6): p. 637-645.
374. Torisu-Itakura, H., et al., *Monocyte-derived IL-10 expression predicts prognosis of stage IV melanoma patients.* J Immunother, 2007. **30**(8): p. 831-8.
375. Zhao, S., et al., *Serum IL-10 predicts worse outcome in cancer patients: A meta-analysis.* PLoS ONE, 2015. **10**(10).
376. Nemunaitis, J., et al., *Comparison of serum interleukin-10 (il-10) levels between normal volunteers and patients with advanced melanoma.* Cancer Investigation, 2001. **19**(3): p. 239-247.
377. Adris, S.K., et al., *IL-10 expression by CT26 colon carcinoma cells inhibits their malignant phenotype and induces a T cell-mediated tumor rejection in the context of a systemic Th2 response.* Gene Therapy, 1999. **6**(10): p. 1705-1712.
378. Chen, D.S. and I. Mellman, *Elements of cancer immunity and the cancer-immune set point.* Nature, 2017. **541**(7637): p. 321-330.
379. Robert, C., et al., *Pembrolizumab versus ipilimumab in advanced melanoma.* New England Journal of Medicine, 2015. **372**(26): p. 2521-2532.
380. Page, D.B., et al., *Immune modulation in cancer with antibodies*, in *Annual Review of Medicine*. 2014. p. 185-202.
381. Sharma, P., et al., *Primary, Adaptive, and Acquired Resistance to Cancer Immunotherapy.* Cell, 2017. **168**(4): p. 707-723.
382. McLane, L.M., M.S. Abdel-Hakeem, and E.J. Wherry, *CD8 T Cell Exhaustion During Chronic Viral Infection and Cancer*, in *Annual Review of Immunology*. 2019. p. 457-495.
383. Thommen, D.S. and T.N. Schumacher, *T Cell Dysfunction in Cancer.* Cancer Cell, 2018. **33**(4): p. 547-562.
384. Chen, J., et al., *NR4A transcription factors limit CAR T cell function in solid tumours.* Nature, 2019. **567**(7749): p. 530-534.
385. Pauken, K.E., et al., *Epigenetic stability of exhausted T cells limits durability of reinvigoration by PD-1 blockade.* Science, 2016. **354**(6316): p. 1160-1165.
386. Wherry, E.J. and M. Kurachi, *Molecular and cellular insights into T cell exhaustion.* Nature Reviews Immunology, 2015. **15**(8): p. 486-499.

387. Ayers, M., et al., *IFN-γ-related mRNA profile predicts clinical response to PD-1 blockade.* Journal of Clinical Investigation, 2017. **127**(8): p. 2930-2940.
388. LaFleur, M.W., et al., *PTPN2 regulates the generation of exhausted CD8+ T cell subpopulations and restrains tumor immunity.* Nature Immunology, 2019. **20**(10): p. 1335-1347.
389. Kurtulus, S., et al., *Checkpoint Blockade Immunotherapy Induces Dynamic Changes in PD-1 − CD8 + Tumor-Infiltrating T Cells.* Immunity, 2019. **50**(1): p. 181-194.e6.
390. Siddiqui, I., et al., *Intratumoral Tcf1 + PD-1 + CD8 + T Cells with Stem-like Properties Promote Tumor Control in Response to Vaccination and Checkpoint Blockade Immunotherapy.* Immunity, 2019. **50**(1): p. 195-211.e10.
391. Miller, B.C., et al., *Subsets of exhausted CD8+ T cells differentially mediate tumor control and respond to checkpoint blockade.* Nature Immunology, 2019. **20**(3): p. 326-336.
392. Im, S.J., et al., *Defining CD8+ T cells that provide the proliferative burst after PD-1 therapy.* Nature, 2016. **537**(7620): p. 417-421.
393. Paley, M.A., et al., *Progenitor and terminal subsets of CD8+ T cells cooperate to contain chronic viral infection.* Science, 2012. **338**(6111): p. 1220-1225.
394. He, R., et al., *Follicular CXCR5-expressing CD8+ T cells curtail chronic viral infection.* Nature, 2016. **537**(7620): p. 412-416.
395. Sun, Z., et al., *IL10 and PD-1 cooperate to limit the activity of tumor-specific CD8+ T cells.* Cancer Research, 2015. **75**(8): p. 1635-1644.
396. Hanna, B.S., et al., *Interleukin-10 receptor signaling promotes the maintenance of a PD-1(int) TCF-1(+) CD8(+) T cell population that sustains anti-tumor immunity.* Immunity, 2021. **54**(12): p. 2825-2841 e10.
397. Giunta, E.F., et al., *Baseline IFN-gamma and IL-10 expression in PBMCs could predict response to PD-1 checkpoint inhibitors in advanced melanoma patients.* Sci Rep, 2020. **10**(1): p. 17626.
398. Qureshi, O.S., et al., *Trans-endocytosis of CD80 and CD86: a molecular basis for the cell-extrinsic function of CTLA-4.* Science, 2011. **332**(6029): p. 600-3.
399. Hall, A.O., et al., *The cytokines interleukin 27 and interferon-gamma promote distinct Treg cell populations required to limit infection-induced pathology.* Immunity, 2012. **37**(3): p. 511-23.
400. Bergmann, C., et al., *T regulatory type 1 cells in squamous cell carcinoma of the head and neck: Mechanisms of suppression and expansion in advanced disease.* Clinical Cancer Research, 2008. **14**(12): p. 3706-3715.
401. Scurr, M., et al., *Highly prevalent colorectal cancer-infiltrating LAP⁺ Foxp3⁻ T cells exhibit more potent immunosuppressive activity than Foxp3⁺ regulatory T cells.* Mucosal Immunology, 2014. **7**(2): p. 428-439.
402. Yan, H., et al., *Primary Tr1 cells from metastatic melanoma eliminate tumor-promoting macrophages through granzyme B- and perforin-dependent mechanisms.* Tumour Biol, 2017. **39**(4): p. 1010428317697554.
403. Ferber, I.A., et al., *Mice with a disrupted IFN-γ gene are susceptible to the induction of experimental autoimmune encephalomyelitis (EAE).* Journal of Immunology, 1996. **156**(1): p. 5-7.

404. Tichauer, J.E., et al., *Interferon-gamma ameliorates experimental autoimmune encephalomyelitis by inducing homeostatic adaptation of microglia.* Front Immunol, 2023. **14**: p. 1191838.
405. Gabrysova, L. and D.C. Wraith, *Antigenic strength controls the generation of antigen-specific IL-10-secreting T regulatory cells.* Eur J Immunol, 2010. **40**(5): p. 1386-95.
406. Bevington, S.L., P. Cauchy, and P.N. Cockerill, *Chromatin priming elements establish immunological memory in T cells without activating transcription: T cell memory is maintained by DNA elements which stably prime inducible genes without activating steady state transcription.* Bioessays, 2017. **39**(2).
407. Bevington, S.L., et al., *Inducible chromatin priming is associated with the establishment of immunological memory in T cells.* EMBO J, 2016. **35**(5): p. 515-35.
408. Chataway, J., et al., *Effects of ATX-MS-1467 immunotherapy over 16 weeks in relapsing multiple sclerosis.* Neurology, 2018. **90**(11): p. e955-e962.
409. De Souza, A.L.S., et al., *ATX-MS-1467 Induces Long-Term Tolerance to Myelin Basic Protein in (DR2 × Ob1)F1 Mice by Induction of IL-10-Secreting iTregs.* Neurology and Therapy, 2018. **7**(1): p. 103-128.